A Comparative Immunohistochemical Study of the Neuromuscular Organization of *Haliclystus 'sanjuanensis'* and *Manania handi* (Cnidaria: Staurozoa)

by

Hannah Westlake
Bachelor of Science, University of Victoria, 2012

A Thesis Submitted in Partial Fulfillment
of the Requirements for the Degree of

MASTER OF SCIENCE

in the Department of Biology

© Hannah Westlake, 2015
University of Victoria

All rights reserved. This thesis may not be reproduced in whole or in part, by photocopy or other means, without the permission of the author.

Supervisory Committee

A Comparative Immunohistochemical Study of the Neuromuscular Organization of *Haliclystus 'sanjuanensis'* and *Manania handi* (Cnidaria: Staurozoa)

by

Hannah Westlake
Bachelor of Science, University of Victoria, 2012

Supervisory Committee

Dr. Louise Page (Department of Biology)
Supervisor

Dr. Robert Chow (Department of Biology)
Departmental Member

Dr. Rana El-Sabaawi (Department of Biology)
Departmental Member

Dr. John Taylor (Department of Biology)
Departmental Member

Abstract

Supervisory Committee
Dr. Louise Page (Department of Biology)
Supervisor
Dr. Robert Chow (Department of Biology)
Departmental Member
Dr. Rana El-Sabaawi (Department of Biology)
Departmental Member
Dr. John Taylor (Department of Biology)
Departmental Member

Recent molecular evidence suggests staurozoans are medusozoans that diverged from Medusozoa before the medusa stage emerged. Morphological studies are needed to determine whether this framework can provide insight into medusa evolution. I studied the neuromuscular morphology of two staurozoans, *Haliclystus 'sanjuanensis'* and *Manania handi* using FMRFamide and α-tubulin antibodies to label neurons, and phalloidin to label muscles. Results indicate that similar to polyps, staurozoans possess one regionally differentiated FMRFamide and α-tubulin immunoreactive (IR) nerve net, and smooth muscles only. Comparisons with other cnidarians indicate that ancestral medusozoans had a marginal circular muscle and muscular manubrium, but lacked the parallel conducting nerve nets, striated muscle, and pacemaker required to coordinate medusa swimming. A possibly light-sensitive concentration of neurons at the base of the primary tentacles suggests that staurozoan primary tentacles are homologous to medusozoan rhopalia. The unique neuromusculature of nematocyst clusters suggests a defensive or predatory function for these staurozoan synapomorphies.

Table of Contents

Supervisory Committee ii
Abstract iii
Table of Contents iv
List of Tables vi
List of Figures vii
Acknowledgments ix
1.0 Introduction 1
1.1 Introduction to Cnidaria 1
1.1.1 Staurozoa 3
1.2 Cnidarian Taxonomy and Phylogeny 7
1.2.1 Phylogeny of Staurozoa 9
1.3 Cnidarian Life Cycles and Development 15
1.3.1 Anthozoa 17
1.3.2 Scyphozoa 17
1.3.3 Cubozoa 19
1.3.4 Hydrozoa 19
1.3.5 Staurozoa 20
1.4 Cnidarian Locomotion 21
1.4.1 Staurozoan Locomotion 22
1.5 Cnidarian Nervous and Muscular Systems 23
1.5.1 Sensory Organs 23
1.5.2 Nervous Systems 26
1.5.3 Musculature 30
1.6 Taxonomy of study species 32
1.6.1 *Haliclystus 'sanjuanensis'* 32
1.6.2 *Manania handi* 33
1.7 Objectives 35
2.0 Methods 37
2.1 Animal collection, care and live observation 37
2.2 Immunolabelling and phalloidin staining 37
2.3 Histology 39
2.4 Nematocyst observations 39
3.0 Results 40
3.1 General Morphology 40
3.1.1 General Morphology of *Haliclystus 'sanjuanensis'* 40
3.1.2 General Morphology of *Manania handi* 46
3.2 Musculature: Phalloidin labelling 51
3.2.1 Musculature of *Haliclystus 'sanjuanensis'* 51
3.2.2 Musculature of *Manania handi* 57
3.2.3 Musculature of *Aurelia* sp. life stages 64
3.3 Nematocysts 67
3.3.1 Nematocysts of *Haliclystus 'sanjuanensis'* 68

3.3.2 Nematocysts of *Manania handi* 74
3.4 Behaviour 80
3.4.1 Behaviour of *Haliclystus 'sanjuanensis'* 80
3.4.2 Behaviour of *Manania handi* 90
3.5 Nervous System 95
3.5.1 Nervous system of *Haliclystus 'sanjuanensis'* and *Manania handi* 95
3.5.2 Nervous system of *Aurelia* sp. life stages 121
4.0 Discussion 126
4.1 Musculature 126
4.1.1 Possible homology of staurozoan and medusa subumbrellar musculature 126
4.1.2 Functional hypotheses about muscular features 129
4.1.2.1 Synchronous contraction of the marginal muscle in *Manania handi* 129
4.2. Nervous system 135
4.2.1 Net-like organization of nervous system 136
4.2.2 One or two nerve nets? Comparison to other medusozoans 137
4.2.3 Sensory neurons and structures 140
4.2.4 Gastrodermal innervation 144
4.2.5 Possible significance of features of staurozoan neuromorphology 146
4.2.6 Behavioural corroboration of nerve net properties 147
4.2.7 Direct association of neurites with nematocysts 149
4.3. Morphological Features of Interest 150
4.3.1. Nematocyst Clusters 150
4.3.2 Other features of nematocysts 154
4.3.3 Periderm 156
4.3.4 Anchors 157
4.3.5 Basal disc 160
4.4 Notes on the neuromusculature of *Aurelia* sp. 160
4.5 Conclusions 162
5.0 Literature Cited 165
6.0 Appendix 181
6.1 Additional behavioural and morphological notes 181
6.2 Description of *Manania handi* 182
6.3 Age-specific substrate selection in *H. 'sanjuanensis'* 182
6.4 Dispersal 183
6.5 Reproduction and Development 184

List of Tables

Table 1. Shape and size data for the nematocysts of *H. 'sanjuanensis'* and *M. handi*..... 67

List of Figures

Figure 1. Diagrammatic guide to symmetry in Staurozoa and Schyphozoa. 1
Figure 2. Current phylogeny of cnidarian clades from Collins *et al*. (2006) 3
Figure 3. Staurozoan diversity 6
Figure 4. Anatomical features of *Haliclystus 'sanjuanensis'* and *Manania handi* 7
Figure 5. Key phylogenetic hypotheses for Cnidaria adapted from Collins (2002) and Marques and Collins (2004) 12
Figure 6. Comparison of simplified life cycles of cnidarian classes 18
Figure 7. Variation in *H. 'sanjuanensis'* specimens 42
Figure 8. Detailed anatomical features of *H. 'sanjuanensis'* 43
Figure 9. Features of juvenile *H. 'sanjuanensis'* 45
Figure 10. Variation in *M. handi* specimens 49
Figure 11. Detailed anatomical features of *M. handi* 50
Figure 12. Diagrammatic illustrations of the musculature of *H. 'sanjuanensis'* 52
Figure 13. Fluorophore-tagged phalloidin labelling of the arms, margin, tentacles, anchors, and calyx and stalk portions of the longitudinal muscles in *H. 'sanjuanensis'* . 55
Figure 14. Fluorophore-tagged phalloidin labelling of the manubrium and perradial musculature of *H. 'sanjuanensis'* 56
Figure 15. Diagrammatic illustrations of the musculature of *M. handi* 58
Figure 16. Fluorophore-tagged phalloidin labelling of the marginal and tentacle musculature of *M. handi* 59
Figure 17. Fluorophore-tagged phalloidin labelling of the longitudinal musculature of *M. handi* 62
Figure 18. Fluorophore-tagged phalloidin labelling of the perradial musculature and nematocyst clusters of *M. handi*. 63
Figure 19. Diagrammatic illustrations of the musculature of *Aurelia* sp. ephyra and adult medusa 64
Figure 20. Fluorophore-tagged phalloidin labelling of muscles in developmental stages of *Aurelia* sp. 66
Figure 21. Tentacle nematocysts of *H. 'sanjuanensis'* 70
Figure 22. Nematocysts of the muscles, gonads and nematocyst clusters of *H. 'sanjuanensis'* 71
Figure 23. Nematocysts of the gastric filaments and exumbrella of *H. 'sanjuanensis'* ... 73
Figure 24. Nematocysts of the tentacles and muscle bands in *M. handi* 76
Figure 25. Nematocysts of the clusters and manubrium in *M. handi* 78
Figure 26. Nematocysts of the exumbrella and adhesive pads in *M. handi* 79
Figure 27. Spawning in *H. 'sanjuanensis'* 82
Figure 28. Adhesion of the basal disc in *H. 'sanjuanensis*' 84
Figure 29. Behaviours of *H. 'sanjuanensis'* including tentacle contraction, interaction with isopods, arm bending and protective contraction 87
Figure 30. Use of the anchors in *H. 'sanjuanensis'* 89
Figure 31. Behaviours of *M. handi* including arm bending, calyx contraction and protective contraction 92

Figure 32. Behaviours of *M. handi* including arm bending, synchronous contraction of the margin, partial contraction of the margin, and contraction of the infundibular muscles 94
Figure 33. Innervation of the marginal muscle in *H. 'sanjuanensis'* 96
Figure 34. Innervation of the marginal muscle and arms in *M. handi* 97
Figure 35. Double-labelling of the margin in *H. 'sanjuanensis'* with FMRFamide and α-tubulin antibodies 99
Figure 36. CLSM images of FMRFamide and α-tubulin immunoreactive neurites in the tentacles of *M. handi* and *H. 'sanjuanensis'* 102
Figure 37. FMRFamide immunoreactivity of transformed tentacles 103
Figure 38. CLSM images of FMRFamide and α-tubulin immunoreactivity of the pigment spot in *M. handi* and corresponding region in *H. 'sanjuanensis'* 104
Figure 39. Innervation of the longitudinal muscles in the calyx and stalk of *H. 'sanjuanensis'* 108
Figure 40. FMRFamide immunoreactivity of neurites associated with the longitudinal muscles in the calyx and stalk of *M. handi* 110
Figure 41. Innervation of the manubrium in *H. 'sanjuanensis* and *M. handi* 112
Figure 42. Innervation of the subumbrellar perradius in *H. 'sanjuanensis'*, including perradial muscle and nematocyst clusters 115
Figure 43. Innervation of the subumbrellar perradius in *M. handi*, including perradial muscle and nematocyst clusters 117
Figure 44. Innervation of the gastrodermis 118
Figure 45. Innervation of the exumbrella and basal disc 119
Figure 46. Nervous system of *Aurelia* sp. ephyra as revealed by FMRFamide, glutamate, and tyrosinated tubulin antibodies 124
Figure 47. FMRFamide immunolabelling in *Aurelia* sp. polyps and strobila 125
Figure 48. Hypothesized characteristics suggested by comparative neuromusculature of staurozoans mapped at phylogenetic nodes 162

Acknowledgments

I would like to thank Louise Page for her enthusiasm and depth of knowledge which helped me cultivate an interest in and excitement for the study of marine invertebrates. Louise's knowledge of techniques and literature and her support has been invaluable throughout my research program.

I also thank all those who helped by teaching me techniques, allowing me use of their equipment, and funding my research. I thank Brent Gowen for sharing his knowledge and expertise on immunolabelling, histology and microscopy. I thank Heather Down for her help with imaging and microscopy techniques. I thank Dorothy Paul, Brian Christie, and Bob Chow for the use of their microscopes. I would also like to acknowledge funding for my research through the NSERC Discovery Grant awarded to Dr. Louise Page, and the UVic Fellowship program.

Thanks to all members of the lab, most of all to Sam Ferguson, Brenda Hookham, Alicia Donaldson, Amelia Hesketh, and Erick Jantzen, for their friendship, support and feedback throughout the research process.

Without the upbringing and support given to me by my family, I may never have had the desire to pursue knowledge nor the determination to persevere when its pursuit became difficult. I therefore give thanks and love to Larry Westlake, Alice Westlake, Laurie Rolland and Steve Weatherill, who believed in me when I forgot to. Thanks also to Mark Hanson, who was a frequent voice of reason and enemy of despair.

1.0 Introduction

1.1 Introduction to Cnidaria

Cnidarians are gelatinous diploblastic aquatic animals united by the ability to synthesize cnidae: complex cellular organelles used in prey capture, defense and locomotion. These animals have apparent radial symmetry (see Kayal *et al*., 2013) (Fig. 1), typically have a ciliated, sausage shaped planula larva, and may be colonial or solitary. They have a single internal compartment, the gastric cavity, which communicates with the exterior via the mouth and is used for digestion and circulation; in all cnidarians except members of the Hydrozoa the epithelial lining of the gastric cavity (gastrodermis) gives rise to gametes. Movement is accomplished through contraction of striated or smooth epitheliomuscular cells and behaviour is typically controlled by one or more diffuse nerve nets which may be regionally concentrated and respond to a range of neuropeptides (Grimmelikhuijzen *et al.*, 2002; Satterlie, 2002).

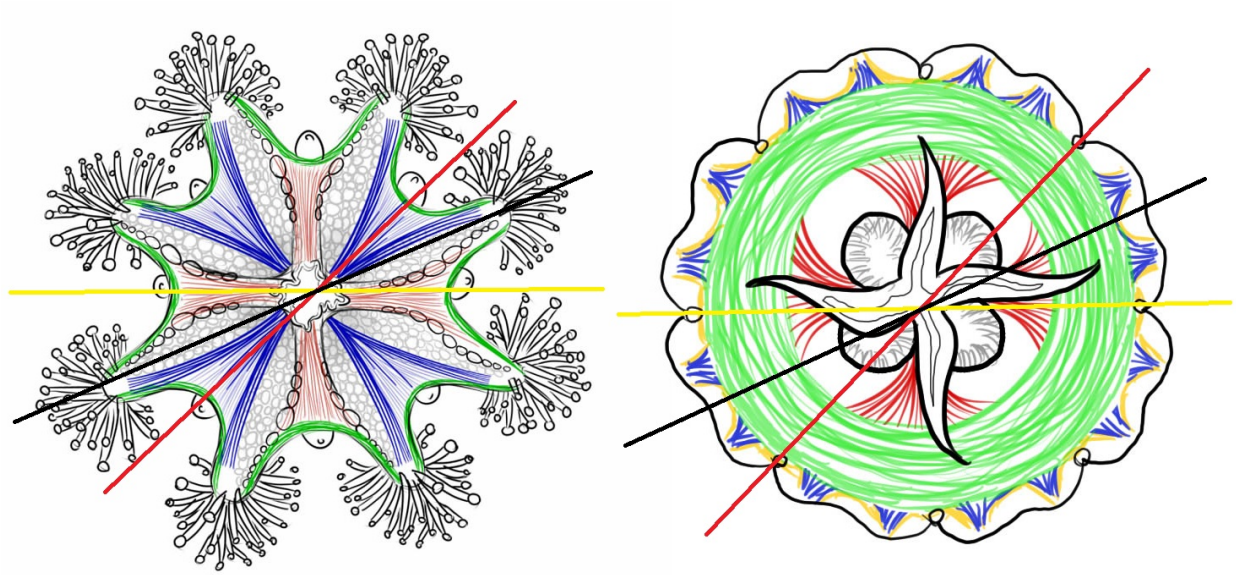


Figure 1. Staurozoa (left) and Scyphozoa (right) usually have tetraradial symmetry with four copies of most of their major organs, and appendages in multiples of four. In both Staurozoa and Scyphozoa the **interradial plane** (red line) is in line with the gastric filament bundles, flat sides of the quadrate manubrium, and a pair of marginal bodies (primary tentacles or rhopalia, respectively). The interradial plane also passes through the midline of the longitudinal muscles and infundibulae in Staurozoa. The **perradial plane**

(yellow line) passes through the corners of the quadrate manubrium, the midline of the radial muscles supplying the manubrium, and a pair of marginal bodies. The four gastric pockets of Staurozoa are also perradial. The **adradial plane** (black line) is a "radius of the 3rd order" (Schwab, 1977) situated between each pair of perradial and interradial planes. This plane corresponds to the arms in Staurozoa and the lappets (remnants of the ephyral arms) in Scyphozoa. There are two interradial and two perradial planes, and four adradial planes. In Staurozoa, the gonads are derived from the interradial septa and are located in the perradial pockets (Miranda *et al*., 2013), and may be four or eight in number. In *Haliclystu*s, there are eight leaf-shaped adradial gonads composed of spherical vesicles in the perradial pockets (Eckelbarger and Larson, 1993; Miranda *et al.*, 2013). *Manania* has four perradial gonads arising from the interradial septa arranged in a series of lobes. In *Aurelia* sp., the horseshoe-shaped gonads are interradial.

The cnidarian phylum includes two major clades: Anthozoa (*e.g.* corals, anemones, sea pens), whose members are characterized by a sessile or sedentary polyp body plan, and Medusozoa (*e.g.* jellyfish, hydroids, siphonophores), most of which are characterized by a lifecycle exhibiting alternation of generations between polyp and free-living medusa body plans (see Fautin [2002], Daly *et al.* [2007] or Mills *et al.* [2007] for reviews of cnidarian groups and characteristics, and their use in systematics). Medusozoa includes four classes: Staurozoa, Cubozoa, Scyphozoa, and Hydrozoa (Fig. 2). The polyp is usually sessile and produces additional polyps or medusae asexually (see Fautin, 2002). Asexual reproduction by polyps can be prolific and can contribute to blooms of cnidarians that disrupt human activities (Arai, 2009; Miranda *et al.*, 2012). Medusae reproduce sexually to produce larvae and function in dispersal, allowing genetic mixing between populations and colonization of new habitats (Muller and Leitz, 2002).

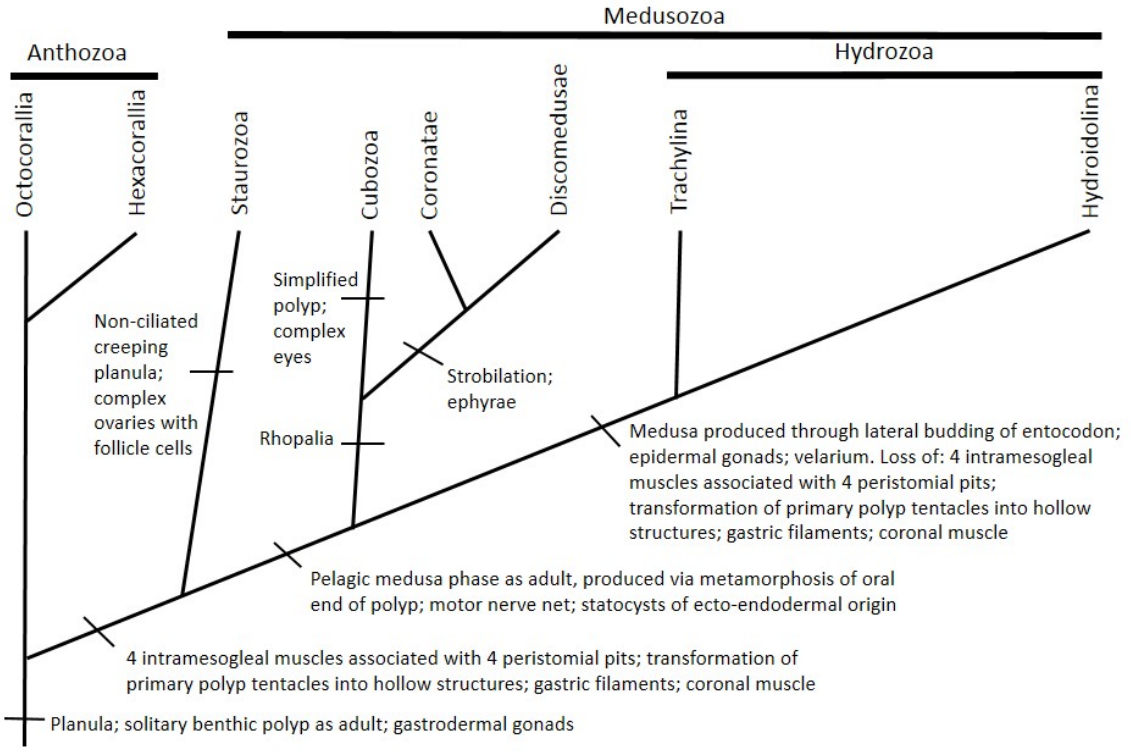


Figure 2. A working hypothesis for relationships among cnidarian taxa with selected hypothesized characteristics mapped at nodes. Adapted from Collins *et al*., 2006.

1.1.1 Staurozoa

Class Staurozoa contains only a single recognized Order, the Order Stauromedusae (Van Iten *et al.,* 2006).

Staurozoans are marine, goblet-shaped animals with four-part radial symmetry (Fig. 1), although symmetry is variable in some species (Naumov, 1961; Pisani *et al.*, 2007; Zagal, 2008; Falconer, 2013). They have a sedentary lifestyle, living attached by their stalk to various species-specific substrates (seaweed, rock, gravel, seagrass, shell) (Wieterzykowsky, 1912; Kikinger and Salvini-Plawen, 1995; Miranda *et al*., 2010). Staurozoans are generally small; all species larger than 40 mm in diameter are of the genus *Lucernaria* (Kramp, 1961), the largest of which is the deep sea *Lucernaria janetae* which may reach up to 100 mm in diameter (Collins and Daly, 2005). Of the approximately 50 known staurozoan species, most (40) are found in the Northern Hemisphere (Mills and Hirano, 2007). Most staurozoans live in coastal or intertidal waters, but the recent discovery of a deep sea hydrothermal vent staurozoan (Lutz *et al.*,

1998; Collins and Daly, 2005), two possibly new Australian species (Zagal *et al.* 2011), a cave-dwelling New Zealand species (Cairns *et al.*, 2009), and new records of species that show they occur in larger ranges than previously known (*e.g*. Larson and Fautin, 1989; McInnes, 1989) suggest that geographical distribution and habitat diversity may be greater than is currently appreciated, particularly in the Southern Hemisphere (see Grohmann *et al.*, 1999; Zagal *et al.*, 2011). Staurozoans have no economic importance and are easily overlooked due to their small and cryptic forms, and have received little attention from zoologists as a result.

Adult staurozoans comprise a basal, narrow conical or cylindrical stalk with a terminal adhesive basal disc, similar to anthozoan and other medusozoan polyps, and an apical calyx with features reminiscent of medusae (Fig. 3), including marginal structures derived from primary tentacles, gastric filaments, a circular muscle and manubrium, and gonads (Collins, 2002; Collins *et al.,* 2006). The proportional length of the stalk and calyx varies greatly among species. The margin of the calyx is elaborated into eight short or long adradial arms or lobes, each bearing hollow capitate secondary tentacles tipped with nematocysts that are used in prey capture (Figs. 1, 4). In members of some genera (*i.e. Kishinouyea, Sasakiella, Halimocyathus, Thaumatoscyphus,* some *Lucernaria*), the eight arms are grouped into four interradial pairs (Fig. 3F, G). Slight pairing of arms is often noted in other genera, but is variable among specimens and is probably due to differential contraction of marginal muscle segments (Gwilliam, 1956). The primary tentacles are the first set of eight tentacles, one in each per- and interradius, to develop at the margin of the calyx during metamorphosis from larva to polyp (Figs. 1A; 4A, C, D). These tentacles are variously modified in adult staurozoans: those that develop large adhesive glandular swellings that envelop the capitum of the primary tentacles are called anchors[i] (Fig. 4A, B); those that have a pad of adhesive glandular cells on the abaxial side of the tentacle only are termed adhesive pads (Fig. 4C, D); in some genera the primary tentacles persist to the adult stage unmodified, degenerate, or become incorporated into the secondary tentacle bunches at the ends of the arms. The calyx is usually conical, but may be open and flattened to narrow and tubular (Fig. 3). The calyx subumbrella (oral surface) has four interradial infundibulae, indentations of varying depth separated by the raised perradial pockets extending from the four corners of the

manubrium (Fig. 4B, C). In mature specimens, there are 4 gonads composed of globular saccules (Fig. 4A, B) or folded bands of tissue (Figs. 4C, D); in some species each gonad is divided into two distinct halves, giving the appearance of 8 gonads (Fig. 1; 4A, B). The manubrium in the center of the calyx is used to ingest food and expel wastes and gametes (Wietrzykowsky, 1912; Otto, 1976) (Figs. 1; 4B, C) as it is in other cnidarians. White nematocyst clusters[ii] are usually present on the subumbrellar surface, and typically form a distinctive species-specific pattern (Figs. 1; 4B, C). Some authors have erroneously called these structures 'batteries' (Berrill, 1962; Kikinger and Salvini-Plawen, 1995). While the nematocyst clusters of staurozoans are invaginations of the subumbrellar epithelium containing loose nematocysts of a single kind, 'battery' describes arrays of several nematocyst types embedded in the epithelial surface that discharge in concert when stimulated (Slautterback, 1967; Ostman and Hydman, 1997). Batteries are particularly abundant on the tentacles, but are found on both the subumbrellar and exumbrellar surfaces (Ostman and Hydman, 1997).

Ecological data on staurozoans are scarce: little is known about the distribution, abundance and niche of most species. Some are either very rare, or we are only aware of small populations, while other species are hugely abundant in certain locations. Populations may vary in density throughout the year (Zagal, 2004a; Miranda *et al.*, 2012) and experience boom and bust cycles (Corbin, 1979; Miranda *et al.*, 2012). Zagal (2004a) reported a Chilean population of *H. auricula* with a peak average density of 1405 individuals/m^2; in contrast, members of genera such as *Lipkea* are scarce. *Lipkea rusopoliana* was described from a single damaged specimen (Vogt, 1886; Vogt, 1887), and not reported again until over 100 years later, when specimens were found in an aquarium in Monaco (Pisani *et al.*, 2007).

Staurozoans are predators of small invertebrates such as small crustaceans, rotifers, and nematodes (Wieterzykowsky, 1912; Hyman, 1940; Jarms and Tiemann, 1966; Uchida and Hanaoka, 1933; Bouillon & Deroux, 1967; Larson, 1980; Larson and Fautin, 1989; Davenport, 1998; Zagal, 2004b; Collins and Daly, 2005; Falconer, 2013) and there is one report of a staurozoan preying on a ctenophore (Falconer, 2013). In turn, staurozoans are eaten by small fish (Davenport, 1998), aeolid nudibranchs (Mills and Hirano, 2007) and pycnogonids (Prell, 1909; Uchida and Hanaoka, 1933). A deep sea

hydrothermal vent staurozoan is the dominant organism in the communities where it occurs (Lutz *et al.*, 1998; Collins and Daly 2005), but the role of most species in their communities is not known.

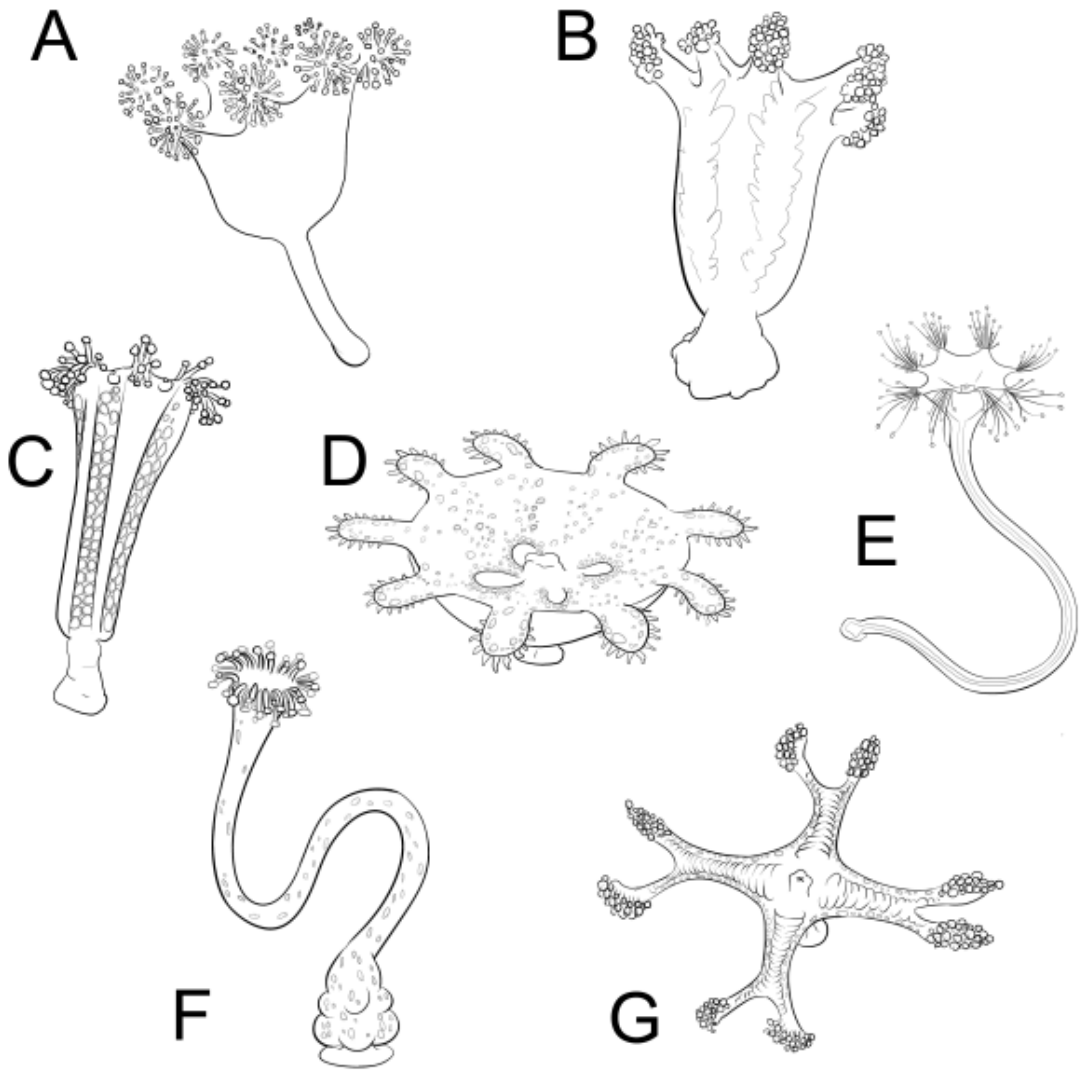


Figure 3. Drawings of body plans of diverse staurozoan genera. **A:** *Lucernaria janetae* **B:** *Craterolophus convolvulus* **C:** *Depastromorpha africana* **D:** *Lipkea* sp. **E:** *Stylocoronella reidlii* **F:** *Kyopoda lamberti* **G:** *Kishinouye* sp.

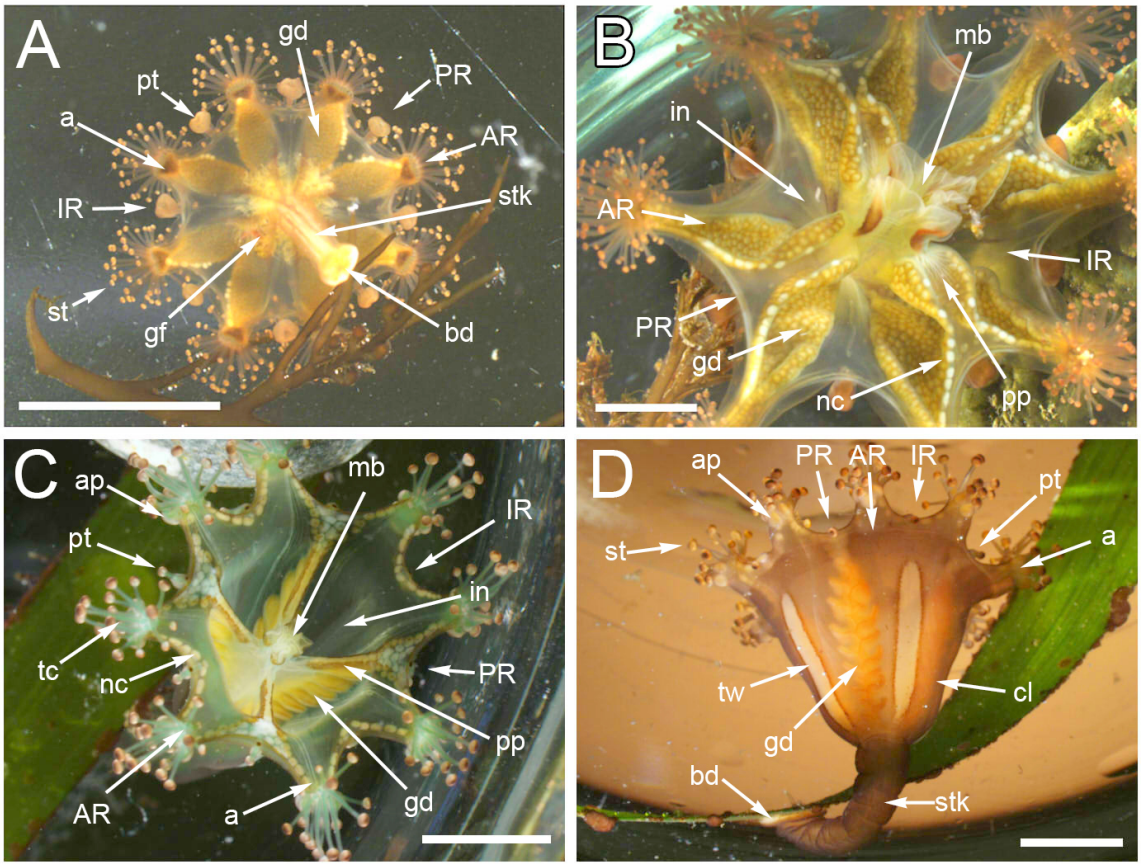


Figure 4. Anatomical features of *Haliclystus 'sanjuanensis'* (**A, B**) and *Manania handi* (**C, D**). **A:** Aboral view. **B, C:** Oral view. **D:** Lateral view. **Abbreviations:** a, arm; pt, primary tentacle; ap, adhesive pad; AR, adradii; cl, calyx; gd, gonad; gf, gastric filaments; in, infundibulum; IR, interradii; mb, manubrium; stk, stalk; pp, perradial pocket; PR, perradii; st, secondary tentacle; tc, tentacles; bd, basal disc; nc, nematocyst cluster; tw, transparent window. Scale bars, 4 mm.

1.2 Cnidarian Taxonomy and Phylogeny

Aspects of the cnidarian phylogeny have long been contentious (see Collins, 2002). Simply identifying and classifying cnidarians can be difficult; early literature often placed different life stages (polyps, ephyrae, medusae) of the same species in different genera as a result of lack of knowledge of ontogeny and alternation of generations (*e.g.* Vogt, 1887; Clark, 1878). Further knowledge of ontogeny has clarified some of these

cases, but other groups are still cryptic (see Dawson and Jacobs, 2011; Miranda *et al*., 2010).

Traditionally, Phylum Cnidaria consisted of three classes: Anthozoa, Scyphozoa, and Hydrozoa (Fig. 5A). Cubozoa and Staurozoa have been removed from the Scyphozoa in recent years, based on developmental features of these clades and predictions from molecular phylogenies (Werner, 1973; Marques and Collins, 2004; Collins and Daly, 2005). While there is a consensus that Anthozoa and Medusozoa (the latter consisting of Staurozoa, Scyphozoa, Cubozoa, and Hydrozoa) are sister groups (Werner 1973; Salvini-Plawen 1978; Schuchert, 1993; Bridge *et al*., 1992, 1995, 2004; Collins 2002), which of these incorporates characters that are more ancestral within the Cnidaria, and by extension whether the polyp or the medusa (or both) is the ancestral body plan, is still debated. A polypoid body form for the original cnidarians is most widely supported (Werner, 1973; Salvini-Plawen, 1978; Bridge *et al*., 1992, 1995, 2004; Collins, 2002; Marques and Collins, 2004), but arguments exist for the alternative (Schuchert, 1993; Seipel and Schmid, 2005, 2006) and further comparative and molecular studies are needed to clarify the issue.

Based on his study of cubozoan metamorphosis (see below) Werner (1973) regarded the medusa body plan as a detached polyp that had acquired the necessary adaptations for a free-swimming lifestyle. Some of the most convincing evidence for the polyp-first hypothesis is that medusozoans have linear mitochondrial DNA (mtDNA) while anthozoans and nearly all other metazoans have a circular mtDNA molecule (Bridge *et al*., 1992; Kayal *et al.*, 2012; see Seipel and Schmid, 2005 for a differing opinion). This suggests that a circular mtDNA molecule is an ancestral characteristic of Metazoa retained in Anthozoa, which likely diverged from the cnidarian line before the linear mtDNA molecule arose in Medusozoa. Schuchert (1993) argued that the medusa was the ancestral form, claiming that it would be more difficult for the complex medusa to develop from the simple polyp than *vice versa*, and that the presumed close relationship of Cnidaria with the pelagic Ctenophora supported a pelagic origin of Cnidaria. The first assertion seems short-sighted as it would require the medusa to evolve *de novo* without a less complex polyp intermediate, or from a less complex planktonic ancestor, which recapitulates the initial issue. Further, analysis of gene families involved

in neurogenesis, immunity and development support Ctenophora as the earliest metazoan lineage rather than as a sister group to Cnidaria (Moroz *et al*., 2014), which weakens Schuchert's (1993) argument for a pelagic origin of Cnidaria. Seipel and Schmid (2005, 2006) interpreted tissues involved in striated muscle production as homologous to bilaterian mesoderm, and argued that cnidarians are secondarily simplified from triploblast ancestors. The medusa, possessing striated muscle, was considered most similar to the triploblast ancestor and was therefore held to represent the ancestral body plan for cnidarians, while the polyp, lacking striated muscle, was considered secondarily simplified (Seipel and Schmid, 2006; see below). However, recent evidence indicates that despite similar morphology, bilaterian and cnidarian striated muscle are not homologous (Steinmetz *et al.,* 2012). Therefore, the presence of striated muscle in medusae does not necessarily represent an ancestral characteristic. Collins (2002) notes that re-expression of the medusa might be expected to occur in some anthozoans if the ancestor of Anthozoa had a medusa stage, but this has not occurred.

It is uncertain which cnidarian characters are ancestral, and how synapomorphies of extant clades were derived from ancestral structures. Medusozoa is considered monophyletic, but some evidence indicates that the medusa evolved independently in Scyphozoa+Cubozoa and Hydrozoa (see Thiel, 1966; Salvini-Plawen, 1978; Werner *et al.* 1983; Bridge *et al*., 1995; Marques and Collins, 2004; Kayal *et al.*, 2013). Sister group relationships are contentious among the medusozoan classes (Werner, 1973; Schuchert, 1993; Collins, 2002; Marques and Collins, 2004); various researchers think that Hydrozoa, Scyphozoa, Cubozoa, or Scyphozoa+Cubozoa is ancestral within Medusozoa (Werner, 1973; Salvini-Plawen, 1978; Bridge *et al*., 1992, 1995; Collins, 2002). More recently, the monophyly of Anthozoa has been strongly questioned (*e.g.* Kayal *et al.*, 2013). Any data that contribute to clarifying these issues is therefore of use. New information continues to redefine our view of cnidarian phylogeny.

1.2.1 Phylogeny of Staurozoa

The position of Staurozoa within the cnidarian phylogeny has long been of interest, as staurozoans display features of both polyp and medusa body plans (see Clark, 1863b; Vogt, 1887; Uchida, 1929), and may provide information key to resolving the issues discussed above. Despite this, they represent a small group and have received little

attention in the literature, due in part to their traditional interpretation as a degenerate and minor subgroup of the Scyphozoa (*e.g.* Uchida, 1929). Staurozoans were traditionally classified as scyphozoans based on shared morphological characteristics of four intramesogleal muscles associated with 4 peristomial pits in the polyps, eight primary polyp tentacles, gastric filaments, and presence of a claustrum and coronal muscle (Salvini-Plawen, 1978; Collins and Daly, 2005) (Fig. 5A, B). Staurozoans were thought to be most closely allied with the Cubomedusae (Uchida, 1929) prior to formation of the class Cubozoa (Werner, 1975) (Fig. 5B).

The intermediate morphology of the members of Staurozoa has invited numerous interpretations concerning phyletic placement; some early hypotheses are discussed by Wietrzykowsky (1912) and Uchida (1929). Staurozoans were interpreted as degenerate scyphozoans that had lost the ability to strobilate (Wietrzykowsky, 1912; Uchida, 1929), or paedomorphic scyphozoans that had developed gonads (Hornell, 1893; Hurst, 1893; Mayer, 1910; Wietrzykowsky, 1912). Wietrzykowsky (1912) claimed there was no evidence of the simplification of features that would be expected if staurozoans were degenerate medusae (although Hornell [1893], Hurst [1893] and Mayer [1910] disagreed, and regarded the anchors and primary tentacles in particular as vestigial organs), and staurozoan development should be interpreted as divergent rather than arrested (paedomorphic). Wietrzykowsky (1912) hypothesized that staurozoans diverged from the scyphozoan lineage very early and have parallel but distinct development displaying both medusoid and polypoid features. Some thought the stalk was a secondarily acquired characteristic of an ancestral swimming medusa form, or that staurozoans were capable of casting off the stalk and swimming away as a medusa (Vogt, 1887). A popular view of staurozoans was as sexually mature scyphistomae closely related to the ancestral scyphomedusa (Clark, 1878; Uchida, 1929). Thiel (1966) stated that staurozoans were a combination of polyp and medusa produced by the fusion of a metagenic ancestor (having alternation of generations) into a hypogenic form (lacking alternation of generations); a hypothesis also proposed by Clark (1878). Although some of these hypotheses were discounted with further studies of staurozoans (*e.g.* staurozoans have never been observed to detach from the stalk and swim away), difficulty obtaining

developmental data and a paucity of detailed morphological information prevented a more robust phylogenetic hypothesis until the advent of molecular techniques.

The first modern study to indicate that staurozoans lay outside the scyphozoan Class came from a study designed to determine phylogenetic relationships among hydrozoan taxa using 18S mitochondrial DNA. Sequence data from staurozoans and scyphozoans were included as outgroups and results showed that the staurozoans did not group with scyphozoans as expected (Collins, 2000). A subsequent study using large and small subunit ribosomal sequence from a greater variety of cnidarian taxa suggested that a scyphozoan clade that included Staurozoa was paraphyletic. These data showed that the Staurozoa may be the sister group to either Cubozoa (Fig. 5C) or all other medusozoans (Fig. 5D) (Collins, 2002). A review of cnidarian morphological characteristics prompted Marques and Collins (2004) to establish Staurozoa (Stauromedusae + the extinct Conulatae) as an independent class-level group based on distinct morphological and developmental characteristics, including unique ovaries with complex follicle cells (Eckelbarger and Larson, 1993), structurally divergent ocelli (Blumer *et al.* 1995), nonciliated creeping planulae with an invariant 16 endodermal cells (Wietrzykowsky, 1912; Otto 1976, 1978), and development where metamorphosis at the oral end produces medusoid characteristics, while the stalk remains polypoid (Wietrzykowsky, 1912). A conservative reassessment of the characteristics used by Marques and Collins (2004) supported Staurozoa as sister group to the remaining medusozoan classes, but indicated that Conulatae were more closely related to coronate scyphozoans than to Stauromedusae, and Staurozoa was redefined as equivalent to Stauromedusae (Van Iten *et al.,* 2006) (Fig. 5D). Ribosomal and mitochondrial DNA data also supports Staurozoa as a class sister to all other medusozoans (Collins and Daly, 2005; Dawson, 2004), although some evidence suggests a sister group relationship between Staurozoa and Cubozoa (Fig. 5C) (Collins, 2002; Marques and Collins, 2004; Kayal *et al*., 2013). The removal of Staurozoa from Scyphozoa suggests that strobilation (see below) is a synapomorphy of Scyphozoa (Marques and Collins, 2004) and indicates that Cnidaria is more diverse at a fundamental level than previously thought (Marques and Collins, 2004).

Placement of Staurozoa as sister group to all other medusozoans suggests that staurozoans are descendants of the common ancestor of Medusozoa that diverged before the swimming medusa stage evolved. According to this interpretation, medusoid features of staurozoans are precursors of medusa morphology that may have been shared by the common ancestor of Medusozoa rather than degenerate remnants of a medusoid ancestor. This is similar to Wietrzykowsky's (1912) and Uchida's (1929) view of staurozoans as sexually mature scyphistomae with development divergent but parallel to that of other medusozoans. If Staurozoa is supported as the sister group to Cubozoa, then the medusa stage probably arose in the lineage leading to Medusozoa, and was subsequently lost at the base of Staurozoa and in some hydrozoan lineages (Kayal *et al.*, 2013). This would be consistent with the "degeneracy" hypotheses discussed by Uchida (1929) and Wietrzykowsky (1912).

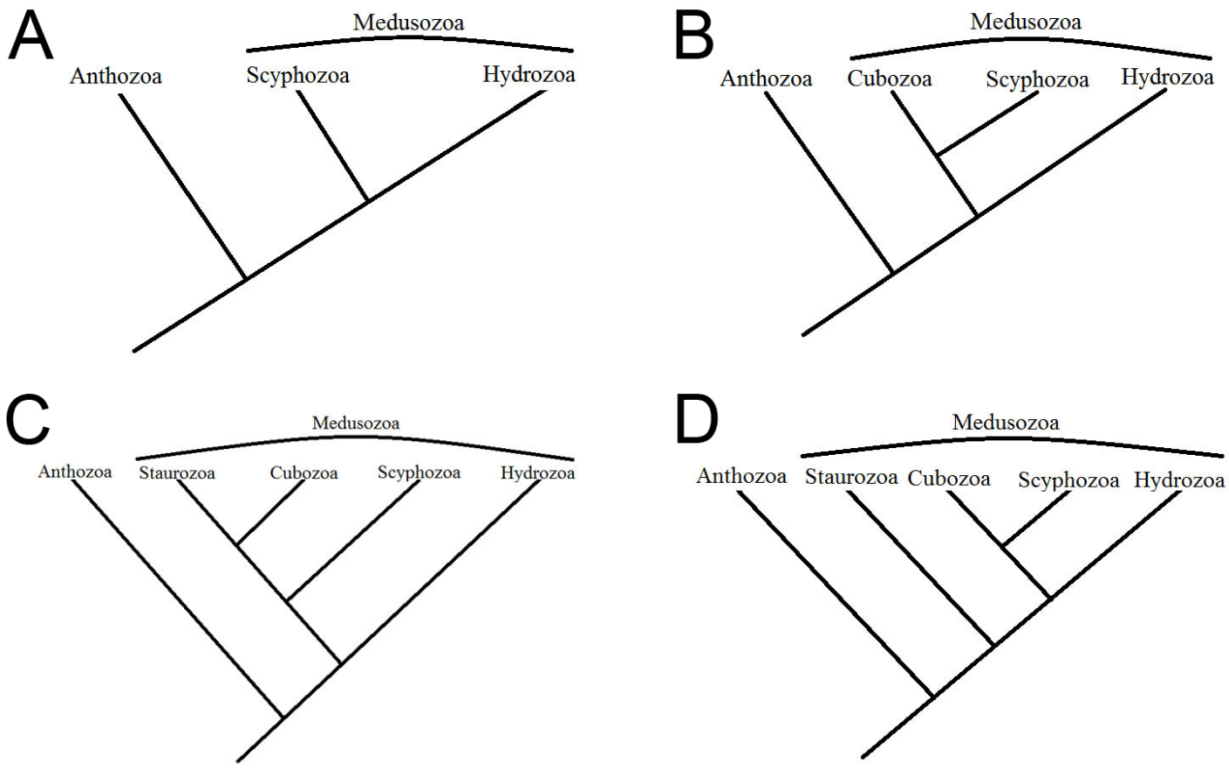


Figure 5. Key phylogenetic hypotheses for Cnidaria. **A:** Traditional hypothesis; Scyphozoa includes Stauromedusae and Cubomedusae. **B:** Hypothesis following Werner's (1973) separation of Cubozoa from Scyphozoa; Scyphozoa includes Stauromedusae. **C:** Alternate hypothesis for the placement of Staurozoa (Collins, 2002;

Marques and Collins, 2004; Kayal *et al.*, 2013). **D:** Most likely placement of Staurozoa within Cnidaria based on consensus of morphological cladistic analysis and ribosomal and mitochondrial DNA sequencing (Collins, 2002; Marques and Collins, 2004; Dawson, 2004; Collins and Daly, 2005; Van Iten *et al.*, 2006).

Collins and Daly (2005) suggested that potential synapomorphies for Staurozoa are: a nonciliated creeping planula with 16 rectangular endodermal cells, a four-chambered stalk with an adhesive basal disk, eight clusters of capitate tentacles, and complex ovaries involving follicle cells. They note that the nonciliated creeping planula, which has only been studied in three genera (Kowalevsky, 1884; Wietrzykowsky, 1912; Hanaoka, 1934; Otto, 1976, 1978), and the complex ovaries, which have only been studied in *Haliclystus* (Eckelbarger and Larson, 1993; Miranda *et al.*, 2013), require further investigation before they are accepted as characteristics of the Class (Collins and Daly, 2005). This is particularly tentative as the gonads of other genera of staurozoans differ greatly in form from those of *Haliclystus*; while the gonads of *Haliclystus* are composed of globular vesicles, those of most other genera are composed of lobes or ribbons of gametogenic tissue (Miranda, pers. comm.). It is possible that uniquely structured ocelli are also a characteristic of the class, but as they have only been studied in one species (Blumer *et al.* 1995), and ocelli have not been identified in most staurozoans, this is also very tentative. Features shared by Staurozoa, Cubozoa and Scyphozoa are likely symplesiomorphies that were lost in the lineage leading to Hydrozoa (Collins and Daly, 2005).

The inclusion of Staurozoa within Medusozoa is supported by several other lines of evidence. Like other medusozoans, staurozoans have linear mitochondrial DNA whereas anthozoans and most other metazoans have circular mtDNA (Bridge *et al.*, 1992). Staurozoans also lack any of the Anthozoa-specific nematocyst types. All staurozoans investigated have only two types of nematocysts: euryteles, and isorhizas (Gwilliam, 1956; Calder, 1983; Zagal *et al.*, 2011). Euryteles are common within Medusozoa but not found in Anthozoa (Kass-Simon and Scappaticci, 2002; Ostman, 2002). The nematocysts of staurozoans also have opercula, which is a medusozoan feature not present in anthozoan nematocysts (Schuchert, 1993; Reft, 2012).

Although evidence now indicates that Staurozoa is the sister group of the remaining Medusozoa, the phylogenetic relationships among staurozoans are poorly characterized. Staurozoans were traditionally divided into the families Eleutherocarpidae and Cleistocarpidae based on whether they lack or possess (respectively) a claustrum: a transverse membrane dividing the four perradial gastric pouches into eight (Kramp, 1961). A similar structure is also present in all Cubomedusae (Collins and Daly, 2005).

However, molecular investigations indicate that the claustrum is a more labile feature than previously thought, and does not reflect true phyletic groupings (Collins and Daly, 2005). Collins and Daly (2005) speculated that the claustrum was an ancestral medusozoan feature lost in some staurozoans and all scyphozoans and hydrozoans. Though the investigation of Collins and Daly (2005) included only four of the 14 accepted staurozoan genera (Mills, 1999), they found that Cleistocarpidae and Eleutherocarpidae were paraphyletic. A more extensive analysis including multiple representatives of ten genera (Collins and Miranda, unpublished) supported this finding. Collins and Miranda (unpublished) proposed a new classification based on ribosomal and mitochondrial sequence data (16S, 18S, 28S, CO1, ITS) that divided Staurozoa into two new clades: the Amyostaurida (staurozoans with no muscles in the stalk) and Myostaurida (staurozoans with muscles in the stalk). This study also synonymized members of several genera (*e.g. Lucernariopsis, Sasakiella,* and *Kishinouyea* probably represent a single genus, *Calvadosia*), indicating that finer divisions based on morphological features have not reflected phylogenetic groupings.

The problem of phylogenetic relationships within Staurozoa is twofold. First, there is a lack of distinctive morphological characteristics that can be used to distinguish groups within Staurozoa. Second, due to the fact that many species descriptions are incorrect (see Miranda *et al.*, 2013), or incomplete as a result of being described from few specimens a very long time ago (Gwilliam, 1956; Miranda *et al.*, 2013), it is difficult to positively identify species, such that any paper on staurozoans must be accompanied by clarification and review of the species being studied. Collins and Daly (2005) remarked, "Comparatively little effort has been put into determining the systematic relationships within Stauromedusae. As a result, families and genera are recognized by a mosaic of features, many of which are not exclusive, or which suggest contradictory groupings."

Intraspecific characters traditionally used for identification such as tentacle number, number of gonadal vesicles, unity of arm pairs, and anchor shape vary extensively with geographic location and development (Uchida, 1929; Gwilliam, 1956; Miranda *et al.* 2009; Miranda *et al.*, 2013). Many species look very similar and have been misidentified, renamed, grouped, and split (see Hirano, 1997) such that the validity of any species identification must be questioned. For example, members of the largest staurozoan genus, *Haliclystus* (Mills, 1999), are morphologically homogeneous, and some are distinguished outwardly only by the pattern of white nematocyst clusters on the subumbrellar surface (Hirano, 1997). Positive identification may require the use of histological characters (Miranda *et al.*, 2009).

When other techniques fail to provide a definitive species identification for cnidarians, nematocysts are often used, as their types and distribution vary with species (Ostman, 1987). However, all staurozoans studied to date possess only two (*e.g.* Gwilliam 1956; Gwilliam 1960; Larson and Fautin 1989; Fautin 2009; Collins and Daly 2005; Zagal *et al*., 2011) of the 25 known types (Kass-Simon and Scappaticci, 2002) of nematocyst, making nematocysts a poor criterion for identification of staurozoan species. Similarly, members of the Scyphozoa have only four major types of nematocyst, none of which are exclusive to the class (Ostman, 2000), and they usually do not differ enough to aid in identification between similar species (Calder, 1977). Distribution of the nematocyst types within the body may be of some value in identification, but sufficient data are not available to determine this.

There is need for a work that carefully describes all known staurozoan species and provides image references that show intraspecific variability. Molecular techniques may prove invaluable in clarifying inter- and intraspecific variability.

1.3 Cnidarian Life Cycles and Development

Compounding the problem of identification and classification of staurozoans is that very little is known about their development, and how features vary through ontogeny. Development varies significantly between cnidarian classes and differences have proven useful to determining taxonomic placement, as when it was used to

distinguish Cubozoa from Scyphozoa (Werner, 1975). Lack of knowledge of ontogeny is a prevalent problem in Cnidarian taxonomy as characteristics vary extensively with ontogeny and cnidarians are often difficult to culture in laboratory conditions. Although many clarifications have been made in recent years, alternation of generations and presence of several larval stages led early biologists to identify life stages of a single species as completely different species. Early researchers believed that adult medusa, ephyra, and scyphistoma were all different classes of organism (*e.g.* Vogt, 1887). Molecular data, particularly from fast-evolving markers (Miranda *et al.* 2010) are invaluable in clarifying these cases as they can be used to definitively match two disparate life stages to the same species without necessitating rearing and observation of the animal throughout its development.

Typical cnidarian life cycles include a planula larva that settles and develops into a polyp (Fig. 6). Medusozoan lifecycles, except for those of staurozoans and some hydrozoans, are characterized by alternation of generations between polyp and medusa forms. The medusa is typically the sexual stage, while the polyp reproduces asexually. Secondary loss of the medusa stage is relatively common, particularly in hydrozoans (Govindarajan *et al.*, 2006); loss of the polyp stage has also occurred, but is less common. In cases where the medusa is lost, the polyp stage reproduces sexually. Asexual reproduction in Cnidaria is closely linked to regeneration, and involves some of the same processes (Fautin, 2002). This is evident in the incredible flexibility displayed in cnidarian development. Reverse development, in which medusae or ephyrae transform back into polyps under unfavorable conditions is well known in Hydrozoa and Scyphozoa, as well as myriad forms of asexual reproduction and resting stages in all cnidarian classes (Boero *et al*. 2002; Piraino *et al.* 2004). These studies illustrate the close and interchangeable relationship between polyp and medusa stages, and indicate, as the existence of Staurozoa does, that the relationship between polyp and medusa may be graded rather than absolute (see Collins *et al.*, 2006). Staurozoans, like other cnidarians, are known to have impressive regenerative capabilities (Hanaoka, 1935) and are often found regenerating from damage in the wild (*e.g*. Gwilliam, 1956; Falconer, 2013).

1.3.1 Anthozoa

Anthozoan development is relatively simple among cnidarians. Fertilization may be internal or external, and resulting planulae, which are often brooded, develop into polyps that grow into sexually mature adults (Fig. 6A) (Bocharova and Kosevich, 2011). Anthozoans display many forms of asexual reproduction including longitudinal and transverse fission, and several forms of budding (Fautin, 2002; Bocharova and Kosevich, 2011).

1.3.2 Scyphozoa

With the exclusion of Staurozoa and Cubozoa from Scyphozoa, it appears that development characterized by strobilation (transverse fission of the oral end of the polyp to produce juvenile medusae called ephyrae) is a synapomorphy of Scyphozoa (Fig. 6B) (Marques and Collins, 2004; Collins *et al*., 2006; Van Iten *et al.*, 2006). Some scyphozoans exhibit monodisk strobilation, where each polyp produces a single medusa, while others undergo polydisk strobilation, where a stack of ephyrae develop and are released sequentially (Collins, 2002). The number of ephyrae produced varies according to species and environmental conditions; numbers of 2-40 have been reported (Arai, 1997). During strobilation, the polyp tentacles are resorbed, and then regrown after the ephyrae are released, so that the polyp may feed and strobilate again (Arai, 1997; Collins, 2002). While strobilation is considered characteristic of Scyphozoa, asexual reproduction by transverse fission is known in members of Anthozoa, Cubozoa, and Hydrozoa (Fautin, 2002; Straehlr-Pohl and Jarms, 2005; Bocharova and Kozevich, 2011).

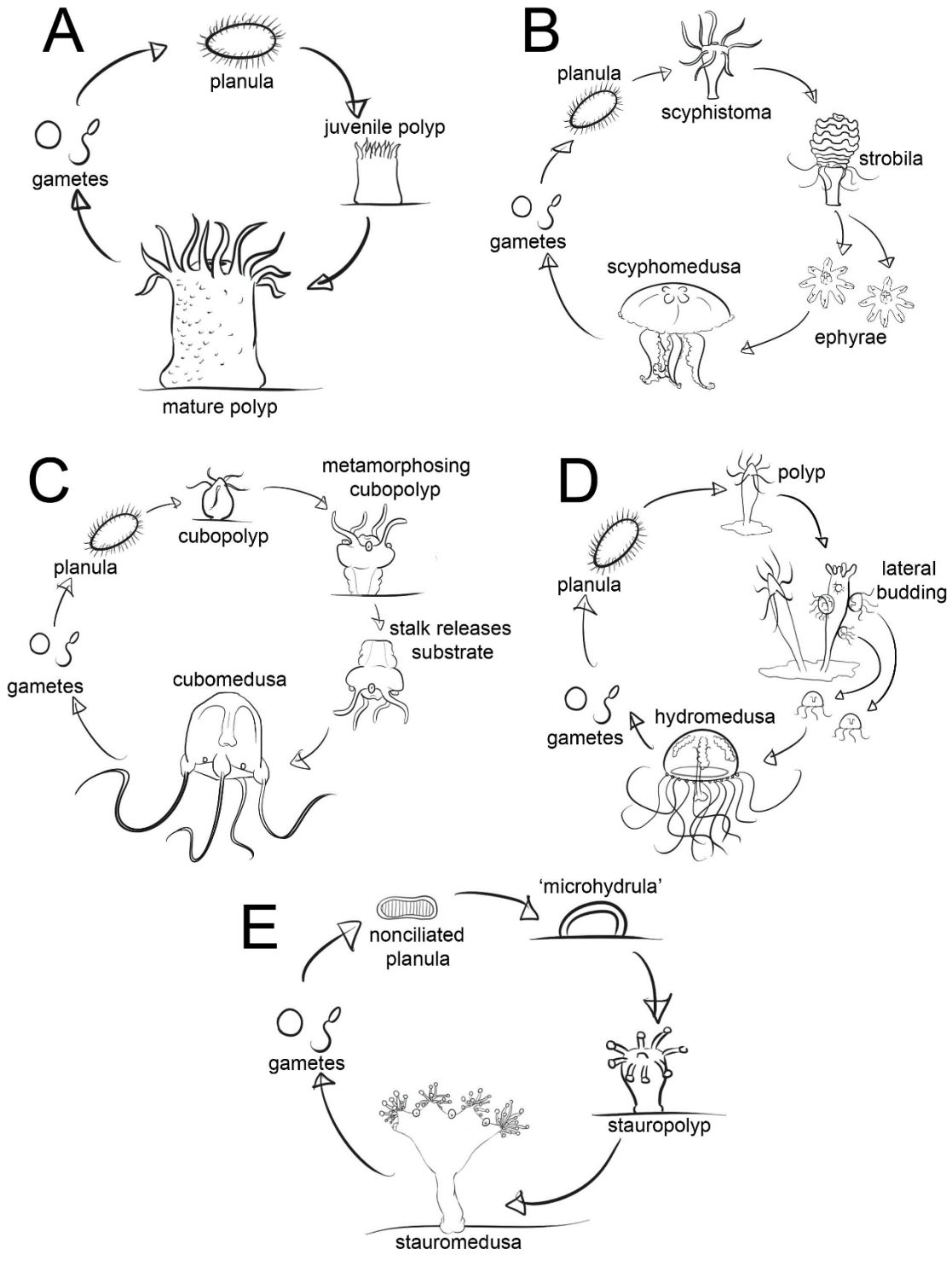


Figure 6. Comparison of simplified life cycles of cnidarian classes. **A:** Anthozoa (after Bocharova and Kosevich, 2011). **B:** Scyphozoa (after Vagelli, 2007). **C:** Cubozoa (after Werner, 1973). D: Hydrozoa (after Tardent, 1978). E: Staurozoa (after Miranda *et al.* 2010).

1.3.3 Cubozoa

Cubozoan development is unique in that the entire polyp transforms into a single reproductive medusa (Fig. 6C) (Werner, 1973; Werner, 1975; Strahler-Pohl and Jarms, 2005). Transformation to the medusa is concentrated at the oral end, while the stalk atrophies and is eventually completely resorbed after the stalk releases the substrate and the medusa swims away (Werner, 1973; Werner, 1975). Werner (1973) found that in 2% of cases during the metamorphosis of *Carybdea marsupialis* the remaining polyp stalk remained attached to the substrate while the medusa broke off and swam away, leaving a remnant which regenerated into a polyp and was in turn able to metamorphose. Werner (1973) interpreted this as an accidental or atavistic phenomenon. However, Strahler-Pohl and Jarms (2005), using polyps from the same laboratory-maintained culture, found that 45% of metamorphosing polyps left a residuum (stalk remnant) which regenerated into a polyp in 56% of cases. This phenomenon further emphasizes the link between regeneration and asexual reproduction (Fautin, 2002). The fact that the proportion of polyps in the population displaying this trait increased over time (~30 y) suggests a genetic component or aspect of the environment influencing the population. The increase in polyps displaying this trait may have been exaggerated by the increased frequency of asexual reproduction observed in this culture (Straehlr-Pohl and Jarms, 2005). Straehlr-Pohl and Jarms (2005) emphasize the similarity between this apparently anomalous cubozoan development and monodisc strobilation in scyphozoans, while Stangl *et al*. (2002) stress the similarity of cubozoan metamorphosis to that of members of Staurozoa. Total metamorphosis where a single polyp results in a single medusa is present in some species of all medusozoan classes (Schuchert, 1993), but is typical in Cubozoa only. Schuchert (1993) hypothesized that total metamorphosis was the original form of medusa production from which others developed, and cites this as support for a single origin for the medusa.

1.3.4 Hydrozoa

While the other medusozoan classes produce medusae through some form of apical transformation of the polyp, hydrozoan polyps that produce medusae usually do so through lateral budding of the entocodon, a tissue between the gastrodermis and epidermis (Fig. 6D) (Boero *et al.*, 2002; Marques and Collins, 2004; Collins *et al.* 2006;

Seipel and Schmid, 2006). In hydrozoans that lack a polyp stage the medusa develops directly from the planula or various intermediate larval stages (Boero *et al.*, 2002).

1.3.5 Staurozoa

Development has been studied in very few staurozoans, as they are difficult to maintain (*e.g*. Clark, 1878; Hyman, 1940; Gwilliam, 1956) and inducing metamorphosis in the lab has not been reliably achieved (Wietrzykowsky, 1912; Otto 1976, 1978). Figure 6E summarizes what is known of staurozoan development, but it is unknown whether this is true of all staurozoans (Miranda *et al.*, 2010). Early development has been studied in only three genera: *Haliclystus* (Wietrzykowsky, 1912; Otto 1976, 1978), *Lucernariopsis* (as '*Lucernaria'*) (Kowalevsky, 1884) and *Manania* (=*Thaumatoscyphus*) (Hanaoka, 1934), and observations for all but the first of these are rudimentary. What we know of development in other genera is from discovering juveniles at various stages of development in the wild (Hirano, 1986; McInnes, 1989; Kikinger and Salvini-Plawen, 1995); these observations do not include larval stages prior to the polyp.

Staurozoan development corresponds in several important respects to that of other cnidarians. As with all cnidarians, sexual reproduction by mature adults produces planulae, which settle and metamorphose into polyps capable of asexual reproduction. Metamorphosis at the oral end of the polyp produces the sexually mature adult and features typically associated with the medusa body plan (marginal structures derived from tentacles, gastric filaments, a circular marginal muscle and manubrium) as it does in Cubozoa and Scyphozoa. In contrast to other medusozoan classes, staurozoan development never produces free-living medusae.

Wietrzykowsky (1910, 1911, 1912) is the only researcher to successfully observe the development of a staurozoan, *Haliclystus octoradiatus,* in the lab; all other attempts have resulted in arrested development at the settled planula, or 'microhydrula' stage (Kowalevsky, 1884; Hanaoka, 1934; Otto, 1976, 1978; see Miranda *et al.*, 2010). Staurozoans are dioecious, but the sexes are indistinguishable in most cases except by spawning (Clark, 1878; Wietrzykowsky, 1912; Otto, 1976; Kikinger and Salvini-Plawen, 1995). Fertilization and cleavage produce odd, non-ciliated planulae with an invariant 16 endodermal cells (Kowalewsky 1884; Wietrzykowsky 1910, 1912; Hanaoka, 1934; Otto 1976). As they are sticky and lack ciliation, staurozoan planulae are incapable of

swimming as cnidarian planulae typically do (Stake and Sammarco, 2003), and instead crawl by alternating anterior and posterior adhesion (Wietrzykowsky, 1910; Otto, 1976; Hanaoka, 1934).

Planulae settle in aggregates (Wietrzykowsky 1912; Hanaoka, 1934; Otto, 1976, 1978), which feed co-operatively using apical nematocysts to capture prey such as nematodes, nauplii or rotifers that are much larger (20-30x) than an individual settled planula (~35um) (Wietrzykowsky, 1910, 1912). The prey is engulfed by the settled larvae, although no mouth or internal cavity is apparent prior to ingestion (Wietrzykowsky, 1912; Bouillon and Deroux, 1967; Spoon and Blanquet, 1978). Only a few larvae in the aggregate benefit from the initial prey; these few capture subsequent prey more easily and outcompete the remaining larvae, which degenerate (Wietrzykowsky, 1912). Similar to other cnidarian groups, the settled larvae reproduce asexually, giving off crawling planuliform buds which settle in turn (Wietrzykowsky, 1912; Jarms and Tiemann, 1966; Bouillon and Deroux 1967; Spoon and Blanquet, 1978).

Several days after settlement, fed larvae elongate and begin to differentiate the hypostome, calyx, stalk, basal disc, and finally tentacles. As the staurozoan grows differentiation progresses at the oral end: secondary tentacles are progressively added to the arms, the primary tentacles are modified, and the gonads develop (Wietrzykowsky, 1912).

1.4 Cnidarian Locomotion

Medusae are planktonic and usually swim actively with rhythmic contractions of striated subumbrellar musculature which decrease the internal volume of the bell, resulting in propulsion (Satterlie, 2002). Cubomedusae (Petie *et al.*, 2013) and hydromedusae (Dabiri *et al.*, 2006) possess a thin flap of muscular tissue which narrows the bell opening and greatly increases swimming speed and agility. Although most polyps are largely sessile, many have developed a variety of locomotory methods: they may move slowly through various creeping behaviours involving muscular contraction of the basal disc, mucociliary gliding, or adhesive crawling (McFarlane, 1969; Collins *et al.,* 2000; Toshino *et al.*, 2014); polyps may detach the basal disc and be carried passively by

currents (McFarlane, 1969; Mandal, 2012), burrow (Magnum, 1970) and some can even swim for a short time by flexing the body (Ellis, 1969) or tentacles (Josephson, 1966).

1.4.1 Staurozoan Locomotion

Staurozoans are thought to have limited potential for dispersal due to their lack of free-swimming planula and medusa stages (Wietrzykowsky, 1912; Otto 1976, 1978; Lutz *et al.,* 1998). Nevertheless, although staurozoans are largely sessile, some are capable of moving from place to place. Wietrzykowsky (1912) noted that staurozoan polyps *must* move, as the larvae and small juveniles are predominantly found on filamentous algae, whereas larger juveniles and adults are present on a greater range of substrates.

Though the apical end of adult staurozoans has features similar to that of a free-living medusa, they are not capable of swimming or swim-like pulsations similar to those of medusae (Kishinouye, 1902, Mayer, 1910; Gwilliam, 1960). A very early source claimed that *Lucernaria (=Haliclystus) auricula* swam frequently and easily by sweeping the arms to the manubrium (Johnston, 1835); Couch (1878) indicated that the same species moved distances by wafting along with "various and active contortions"; Guberlet (1936) asserts that staurozoans are capable of swimming; and Lamouroux (1815) goes so far as to say that *Lucernaria campanulata* actively pursues prey. However, these assertions have not been widely accepted. Clark (1878) looked for swimming behaviour in *H. auricula* during his exhaustive investigations, but never observed it. Current accounts never associate swimming with staurozoans, and describe them as sessile save the adhesive locomotion described below (*e.g.* Mills and Hirano, 2007). Based on neuromuscular data, they are considered to be incapable of coordinated contractions similar to swimming contractions in free-living medusae (Gwilliam, 1960). Evidence indicates that the assertions above were either misinterpretations or fabrications. Haeckel (1882) also claimed the Tesseridae were swimming staurozoans, but they are in fact planktonic larval anthozoans mistakenly identified as free-swimming staurozoans (Rodriguez *et al.*, 2011).

A somersaulting kind of movement similar to that of *Hydra* has been observed in many staurozoans (Couch, 1878; Clark, 1878; Kassianow, 1901; Kishinouye, 1902; Mayer, 1910; Berrill, 1962; Larson, 1980; Kikinger and Salvini-Plawen, 1995). This form

of locomotion involves alternate adhesion of the tentacles or marginal adhesive structures and the basal disc.

1.5 Cnidarian Nervous and Muscular Systems

Neuromusculature provides an excellent basis for morphological comparison of cnidarians as it varies between life stages and Classes. Neuropeptides are present from very early developmental stages (Yuan *et al.*, 2008) and a nervous system is present in all life stages from planula (Nakanishi *et al*., 2008) to medusa (Horridge, 1956b). Kass-Simon and Pierobon (2007) review chemical neurotransmission in cnidarians. Neuropeptides with the C-terminal sequence RFamide (Arg-Phe-amide) appear to be ubiquitous in members of the Cnidaria (Grimmelikhuijzen *et al.*, 2002; Satterlie, 2002; Plickert and Schneider, 2004) and may act as neurotransmitters or neurohormones (which control development) (Grimmelikhuijzen *et al.*, 2002). All cnidarians make use of bidirectional chemical synapses, which may be necessary to coordinate a radial body plan (Satterlie, 2002). Medusae typically have multiple parallel conducting systems, which may take the form of nerve nets or condensed rings or tracts of nerves and allow an increase in behavioural complexity (Satterlie, 2002) over polyps, which typically have a single nerve net (Schwab, 1977).

1.5.1 Sensory Organs

Sensory structures in cnidarians are usually associated with the tentacles. The main sensory organs of cubomedusae and scyphomedusae are rhopalia. Rhopalia are hollow structures ontogenetically derived from primary tentacles that incorporate statocyst and ocellus components (Marques and Collins, 2004). Some hydromedusae have statocyst-bearing structures that are similarly derived from tentacles, but these are not considered homologous to rhopalia as they lack an ocellus (Marques and Collins, 2004). Ocelli are often present near the tentacle bases or bell margin of hydromedusae (Martin, 2002), but are separate from the statocyst structures (Jacobs *et al.* 2007). Sensory structures are associated with increased density of neurites and neuronal cell bodies, and label strongly with antibodies against known cnidarian neuropeptides (*e.g.* Nakanishi *et al*., 2009; Satterlie and Eichinger, 2014). When present, cnidarian

photoreceptive organs are always associated with RFamide immunoreactive neurons (Plickert and Schneider, 2004). Orienting behaviour can be disrupted by administering micromolar concentrations of RFamide, suggesting that RFamides are involved in transmission of photic stimuli to muscle fibers (Plickert and Schneider, 2004). Polyps generally lack specialized sensory structures such as photoreceptors and ocelli, although many polyps and medusae lacking ocelli have extraocular sensitivity to light (Martin, 2002). Jacobs *et al.* (2007) argues that the clusters of light-sensitive cells on and around the tentacles of some eyeless polyps and medusae merit status as sense "organs". The young polyps of the staurozoan *Stylocoronella reidlii* are considered the only polyp with distinct ocelli (Blumer *et al.* 1995).

The anchors of staurozoans have long been considered homologous to the rhopalia of scyphozoans (Clark, 1863b, 1878; Hornell, 1893; Hurst, 1893; Kassianow, 1901; Thiel, 1966; Marques and Collins, 2004; Nakanishi *et al*., 2009) due to their similar derivation from primary tentacles during metamorphosis (Hurst, 1893; Wietrzykowsky 1910, 1912; Thiel, 1966). Rhopalia and anchors are usually 8 in number, with one in each per- and interradius at the margin of the bell or calyx (Fig. 1). Cubozoans have four perradial rhopalia which incorporate complex lensed eyes, simple ocelli, and statocysts (Piatigorsky and Kozmik, 2004); the interradial corners bear fleshy pads called pedalia from which the tentacles arise. Researchers have suggested that the anchors of staurozoans may have a similar integrative or sensory function as rhopalia in the nervous system (Clark, 1878; Schlater, 1891; Kassianow, 1901; Thiel, 1966). Nakanishi *et al.* (1999) refer to the structures derived from tentacles (including staurozoan anchors) collectively as "sensory structures" and note that comparative data are needed to determine the relationship among them. The anchors have been alternately interpreted as independently derived from the tentacles (Thiel, 1966) or secondarily simplified from more complex rhopalia (Mayer, 1910; Marques and Collins, 2004). It is unclear why hydrozoan statocyst-bearing structures derived from tentacles are not considered homologous to rhopalia due to their lack of ocelli (Marques and Collins, 2004), while the various adhesive structures derived from staurozoan primary tentacles (collectively called "rhopalioids" by Marques and Collins [2004]) are considered homologous to rhopalia despite apparently lacking both statocyst and ocellus.

When present, the anchors of staurozoans function as adhesive organs and are used in locomotion (Clark, 1878; Berrill, 1962; Larson, 1980) or may be used to prevent being swept away if the animal becomes detached (Larson, 1988). They are not, as some authors have suggested (*e.g.* Hornell, 1893) used directly in prey capture as secondary tentacles are. If the anchors do have a sensory or integrative function, it is odd that only three of the 14 recognized genera of Staurozoa have anchors as adults: *Haliclystus, Stenoscyphus* and *Halimocyathus* (Mills, 1999; Collins and Daly, 2005). Further, data indicate that *Halimocyathus* and *Stenoscyphus*, each of which is represented by one species, are probably synonymous with *Haliclystus* (Miranda and Collins, pers. comm.). It is probable, then, that only one staurozoan genus possesses true anchors.

Manania (Larson and Fautin, 1989)*, Depastromorpha* (Carlgren, 1935) and *Kyopoda* (Larson, 1988) have modified primary tentacles as adults that have small glandular swellings on the adaxial sides, while *Lucernaria, Stylocoronella* (Kikinger and Salvini-Plawen, 1995)*, Kishinouyea* (Larson, 1980)*, Lucernariopsis, Lipkea and Craterolophus* have no primary tentacles as adults (Kramp, 1961) and *Sasakiella* and *Depastrum* have unmodified primary tentacles (Kramp, 1961). Kikinger and Salvini-Plawen (1995) indicate that the primary tentacles of *Stylocoronella* migrate to join the adradial tentacle bunches during development and that this is unique among staurozoans. However, as detailed developmental information is not available for most staurozoan genera, it is unknown whether this occurs in other groups. Wietrzykowsky (1912) notes that *L. campanulata* and *C. tethys* have basal swellings on the primary tentacles as juveniles, though the adults of these species lack marginal bodies. This may indicate that adhesive structures have been secondarily lost in some staurozoan groups.

Many staurozoan genera have adhesive structures associated with the base of the secondary tentacles which are used for locomotion or adhesion in the same manner as adhesive primary tentacles. *Manania* (Kishinouye, 1910; Uchida and Hanaoka, 1933; Berrill, 1962; Larson and Fautin, 1989; Miranda *et al.*, unpublished), *Depastromorpha* (Carlgren, 1935; Zagal *et al.,* 2011), *Craterolophus* (Carlgren, 1935; Miranda *et al.*, unpublished), some *Lucernariopsis* (Browne, 1910; Eales, 1938; Panikkar, 1944; Zagal *et al.,* 2011; Miranda *et al.*, unpublished), *Kyopoda* (Larson, 1988), some *Haliclystus* (Clark, 1878; Gwilliam, 1956; Kahn *et al.*, 2010), and *Halimocyathus* (*=Haliclystus?*

Clark, 1863b) have individual adhesive pads on the outermost (adaxial) secondary tentacles. Of these, *Manania, Depastromorpha, Kyopoda, Haliclystus,* and *Halimocyathus* also have adhesive pads on primary tentacles, while *Lucernariopsis* and *Craterolophus* have no primary tentacles as adults. *Kishinouyea* (Larson, 1980; Miranda *et al.*, unpublished) and some *Lucernariopsis* (Carlgren, 1938; Corbin, 1978; Zagal *et al.*, 2011; Miranda *et al.*, 2012) have broad cushions of adhesive material on the ends of the arms below the outer row of secondary tentacles; these may be formed through fusion of individual adhesive pads during development (Corbin, 1978; Larson, 1980). As *Lucernariopsis, Kishinouyea* and *Sasakiella* likely represent a single genus (*Calvadosia*), the broad cushions may be a synapomorphy of that genus (Miranda *et al.*, unpublished). *Stylocoronella* (Kikinger and Salvini-Plawen, 1995; Salvini-Plawen, 2006), *Lucernaria* (Collins and Daly, 2005; Miranda *et al.*, unpublished) and *Lipkea* (Pisani *et al.*, 2007; Zagal *et al.*, 2011) do not have adhesive structures associated with the tentacles or arms. However, members of the former two genera are known to move about actively using their highly adhesive unmodified secondary tentacles (Berrill, 1962; Kikinger and Salvini-Plawen, 1995).

1.5.2 Nervous Systems

1.5.2.1 Scyphozoa

Much of the fundamental work on scyphozoan nervous systems has been performed on species within the genus *Aurelia*. *Aurelia* sp. ephyrae (young juvenile medusae) display three principle behaviours: the feeding response, where a touch on an arm causes the animal to bring that arm and the manubrium towards each other; the swim response, where the circular and radial muscles contract synchronously and spontaneously to produce propulsion; and spasm, a protective response initiated by strong stimulation where all the arms are brought to the mouth in a prolonged contraction (Horridge, 1956a). These behaviours can all occur independently. Using vivisection techniques to selectively sever and paralyze portions of the neuromuscular system, Horridge (1956a) demonstrated that two distinct nerve nets were required to produce the behaviours displayed by *Aurelia* sp. ephyra and adults. The swim response was disrupted or modified by severing the circular muscle or removing rhopalia, while spasm and feeding were unaffected by extensive mutilation. The ectodermal nerve nets are termed

the giant fibre nerve net (GFNN) or motor nerve net (MNN; Anderson and Schwab 1981) and the diffuse nerve net (DNN) (Horridge, 1956a). The presence of these two nerve nets is characteristic of scyphomedusae (Horridge, 1956b; Satterlie, 2002).

The GFNN of *Aurelia* sp. is a subumbrellar net composed of bipolar neurons that closely overlie the radial and circular muscles (Horridge, 1956a). Deviation from the muscle occurs only where the neurons take a short cut between the arms, and where neurons extend to the rhopalia (Horridge, 1956a). Physiological evidence suggested that these neurons innervated the muscle (Horridge, 1956a); this was later confirmed by Westfall (1973) who provided histological evidence of neuromuscular synapses in several cnidarians. The GFNN is through conducting and nonpolar; that is, an impulse generated in one part of the net is transmitted to the entire system in any direction (Satterlie, 2002). Action potentials can propagate in any direction between interconnected neurites of the GFNN because the net incorporates bidirectional chemical synapses (Anderson and Schwab, 1983). The GFNN is immunoreactive to α- and β-tubulin and anti-taurine antibodies (Satterlie, 2002; Nakanishi *et al.*, 2009; Satterlie and Eichinger, 2014).

The rhopalia contain pacemakers which regulate the swim response: a nerve impulse from a pacemaker propagates through the GFNN and initiates a swim beat. This impulse resets all of the other pacemakers, such that the pacemaker with the fastest rhythm at a given time (as the rhythm of each pacemaker is modified by sensory input) controls the periodicity of the swim pulsations (Satterlie, 2002). Removal of all rhopalia arrests the swim response; one rhopalium is sufficient to maintain it (Horridge, 1956a). Each rhopalium includes an ocellus and statocyst, the sensory input from which can modify swim responses (Passano, 1982). The arrangement of the rhopalia around the margin of the bell distributes the sensory structures in a way that best suits these radial animals (Satterlie, 2002).

The DNN is composed of multipolar and bipolar cells, which form a diffuse net over the exumbrellar and subumbrellar epithelium in ephyrae (Horridge, 1956a) and adult medusae (Anderson *et al.*, 1992). Fibers from this net also contact the rhopalia (Horridge, 1956a; Satterlie and Eichinger, 2014). The DNN is sensory (Horridge, 1956a; Satterlie and Eichinger, 2014), and coordinates the spasm and feeding behaviours; the spasm is interpreted as a feeding response which is propagated to all arms and the circular muscle

by interneural facilitation (Horridge, 1956a). In adult medusae, the DNN appears to be involved in waves of tentacular activity, feeding responses of the lappets (when present), and movements of the manubrium and oral arms (Horridge, 1956b). Interaction of the two nets at the rhopalia allows sensory information from the DNN to modify the rate and asymmetry of the swim response effected by the GFNN (Horridge, 1956b). The DNN is FMRFamide immunoreactive (Anderson *et al.*, 1992; Satterlie, 2002; Nakanishi *et al.*, 2009; Satterlie and Eichinger, 2014).

Scyphopolyps have a less complex nervous system than their medusa counterparts, possessing only a single nerve net homologous to the DNN of medusae (Schwab, 1977). The DNN has been described as "the primitive general purpose net of the Scyphozoa" (Passano, 1982). Similar to ephyrae and medusae, the DNN of polyps is not through-conducting: interneural facilitation is required to transmit impulses between sectors of the polyp (Chapman, 1965; Schwab, 1977). Scyphopolyp behaviour is generally limited to feeding responses involving the tentacles and a protective spasm response where the column and tentacles are contracted (Chapman, 1965; Arai, 1997). These responses are regarded as homologous to the feeding and spasm responses of the ephyra: the behaviours originate in the scyphopolyp and are retained in the ephyra (Schwab, 1977).). The GFNN develops during medusa formation to coordinate the more complex behaviours and sensory input of medusae (Schwab, 1977).

1.5.2.2 Cubozoa

Cubomedusae modify their behaviour in response to photic and visual stimuli received by four rhopalia that incorporate complex lensed eyes and a statolith (Satterlie, 1979). As in scyphomedusae, removal of the rhopalia arrests the swim response, and the pacemaker mechanism controlling swim beat is similar in scyphomedusae and cubomedusae (Satterlie, 1979). A nerve ring connects the four rhopalia and four tentacle bases, providing a rapid conducting route that may aid in pacemaker coordination (Satterlie, 1979). The circular musculature is innervated by a dense network similar to that of scyphomedusae, and is labelled with α- and β-tubulin antibodies (Eichinger and Satterlie, 2014). The nerve ring, rhopalia and a diffuse network of nerves on the subumbrella are FMRFamide immunoreactive; these neurons are distinct from those that label with tubulin antibodies. The nervous system of cubomedusae is interpreted as

similar to that of scyphomedusae, but more condensed (Satterie, 1979; Eichinger and Satterlie, 2014).

1.5.2.3 Hydrozoa

The nervous system of hydromedusae is also more condensed than that of scyphomedusae, comprising an exumbrellar and a subumbrellar nerve ring located at the junction of the bell edge and velum (Lin *et al.*, 2001; Satterlie, 2002). Each electrically-coupled neuron of the subumbrellar nerve ring appears to act as a pacemaker to control the swim response, such that removal of the entire margin is needed to paralyze hydromedusae; if even a tiny piece is remaining, swim contractions will continue (Romanes, 1885). Some hydromedusae also have diffuse nets associated with the subumbrellar musculature (*e.g.* Mackie and Meech, 2008; Satterlie, 2008). Hydromedusae are unique among cnidarians in having electrically coupled epithelial and myoepithelial cells; that is, impulses can be conducted through the epithelium independent of neurons to produce muscle contraction (Mackie and Passano, 1968). Exumbrellar epithelial conduction is common in hydromedusae and may modify responses of the neurons (Mackie and Passano, 1968).

1.5.2.4 Staurozoa

Little is known about the nervous system of staurozoans. Early investigators reasoned that there must be a nervous system due to the presence of structures interpreted as ocelli (Clark, 1878; Kassianow, 1901).

Schlater (1891) stated that staurozoans have a simple nervous system concentrated in the heads of the tentacles and the anchors, and considered the anchors homologous to rhopalia in development and function. Kassianow (1901) performed exhaustive studies of muscle and nerve cells using maceration and staining techniques on *Lucernaria campanulata, Craterolophus tethys,* and *Haliclystus octoradiatus* and found evidence of gastrodermal and epidermal nerve nets consisting of bipolar and tripolar neurons, with plexuses occurring on the subumbrella and exumbrella. Sensory cells were concentrated in the capita of the secondary tentacles, but not in fully-formed anchors. Kassianow (1901) found a very high concentration of neurons at the ends of the arms,

which led to his interpretation that these sites acted as nervous centers that co-ordinated activity in staurozoans.

Gwilliam (1960), who thought that the sedentary state of staurozoans was secondarily acquired, wondered whether staurozoans retained the neuromuscular characteristics of scyphozoans, which were then considered their closest relatives, or if their sedentary habit had led to convergent similarity to Anthozoa. Gwilliam (1960) hypothesized that staurozoans were incapable of swimming contractions only because they lack a pacemaker, and he attempted to artificially induce a swimming pulse in *Haliclystus 'sanjuanensis'* (as *H. auricula* – see Hirano [1997]). He applied electrical stimulation to whole and vivisected animals in experiments similar to those of Horridge (1956a). Gwilliam's (1960) experiments suggested that diffuse exumbrellar and subumbrellar nerve nets were present, but there was no evidence of neural centers. He hypothesized that every nerve cell had the potential to contribute to spontaneous activity. Gwilliam (1960) concluded that *H. 'sanjuanensis'* had a single through-conducting system, and that staurozoans had lost the specialized through-conduction and pacemakers needed to produce swim contractions typical of scyphozoans. The nerve net of *H. 'sanjuanensis'* displayed characteristics of a through-conducting net with interneural facilitation (Gwilliam, 1960), similar to the DNN of scyphozoans (Horridge, 1956a; Chapman, 1965; Schwab, 1977). Westfall (1973) demonstrated the presence of neuromuscular synapses in *H. auricula* using transmission electron microscopy.

Passano (1982) in a review of the neuromusculature of Scyphozoa and Cubozoa, briefly addresses staurozoans. He claimed that the only purpose of the GFNN is to innervate striated effector muscles, and the absence of these effectors in staurozoans explained why Gwilliam (1960) did not find evidence of a GFNN in his experiments on *H. 'sanjuanensis'*. It is unclear from where Passano (1982) derived the claim that staurozoans lack striated muscles, as I can find no description of the composition of staurozoan muscle fibers in the literature prior to his claim.

1.5.3 Musculature

Muscle takes several forms in cnidarians, and varies extensively with life stage. Muscle in cnidarians is generally derived from the ectoderm, although some muscle fibers may arise from the mesoderm-like entocodon tissue in hydrozoans (Seipel and

Schmid, 2005) and from the endoderm of hydrozoan and anthozoan polyps only (Jahnel *et al.*, 2014). Muscle derived from the ectoderm or endoderm consists of epitheliomuscular (or myoepithelial) cells, which have an apical epithelial soma and basal muscle component (Chapman *et al*., 1962; Quaglia, 1981; Arai, 1997). The apical part of the cell may be further specialized for other functions, such as secretion (Singla, 1976). The polyp body plan is characterized by smooth musculature; anthozoan, scyphozoan, cubozoan and hydrozoan polyps lack striated muscle (Chapman *et al.*, 1962; Fautin and Mariscal, 1991; Thomas and Edwards, 1991; Schuchert, 1993; Seipel and Schmid, 2005, 2006). Although striated muscle fibers have been reported in some scyphopolyps (Chia *et al.*, 1984; Arai, 1997) and cubopolyps (Chapman, 1978), Arai (1997) explains that these fibers do not constitute true striated muscle as the thick and thin filaments are not separated into sarcomeres by Z-discs (Chia *et al.*, 1984); the thick filaments are simply aligned such that they give the appearance of the regular sarcomeres of striated muscle. True striated muscle in cnidarians is only present in the circular and radial swim muscle of medusae (Arai, 1997; Seipel and Schmid, 2005). The circular swim muscle is a two-dimensional sheet (Satterlie and Eichinger, 2014) that may be continuous (*e.g.* Horridge, 1956b) or divided into several circularly-oriented segments (Gladfelter, 1972, 1973; Anderson *et al.*, 1992), and may form a more or less narrow band or cover the entire subumbrella (Seipel and Schmid, 2006; Satterlie and Eichinger, 2014). Some scyphomedusae have lappets with radial musculature retained from the ephyra stage, while in others the radial musculature is completely lost during the ephyra to medusa transformation (Passano, 1973).

Descriptions of basic muscle layout are available for most described species of staurozoans, usually based on brightfield observations of muscle fibers. Major muscle groups of staurozoans include: a marginal muscle band at the edge of the calyx; four longitudinal muscles which run up the stalk and fan out to insert at the margin; and radial muscles extending from each corner of the manubrium to the margin (Kramp, 1961; Miranda *et al.*, 2009). I cannot find any reports that address muscle composition (striated or smooth) in members of the Staurozoa.

There are some major intergeneric variations in staurozoan musculature. The form of the marginal muscle varies: in *Stenoscyphus, Lipkea, Kyopoda, Manania,*

Depastromorpha, Depastrum, and *Halimocyathus* it is a continuous band, while in *Craterolophus*, *Haliclystus, Lucernaria, Kishinouyea, Lucernariopsis (Calvadosia),* and *Sasakiella* it is divided into eight segments corresponding to the perradii and interradii (Kramp, 1961; Larson, 1988; Miranda *et al.*, unpublished). The marginal muscle is reported to be absent in *Stylocoronella;* serial sectioning of *S. riedli* showed no evidence of a marginal muscle (Kikinger and Salvini-Plawen, 1995), suggesting that it is vestigial or absent in this genus.

Although all genera have longitudinal muscles in the calyx, not all have four intramesogleal muscles extending the length of the stalk. Genera lacking stalk muscles comprise *Craterolophus, Kishinouyea, Lucernariopsis/Calvadosia,* and *Sasakiella* (Kramp 1961; Miranda *et al.* 2013). More detailed differences in musculature between groups are not known.

1.6 Taxonomy of study species

1.6.1 *Haliclystus 'sanjuanensis'*

As is typical of staurozoans, the taxonomy of *Haliclystus* is uncertain and complicated by poor descriptions, synonymizations, redescriptions and misidentifications. Hirano (1997) and Miranda *et al.* (2009) have reviewed and clarified some of the taxonomy of *Haliclystus*.

Although *H. 'sanjuanensis'* has been discussed several times in the literature, it has never been formally described and was considered by many to be synonymous with *H. auricula*. The first use of the species designation in the literature was by Gellerman (1926) in her MSc thesis performed at Friday Harbor Laboratories, University of Washington; the name subsequently made its way into common use at the Friday Harbor Laboratories and was used in a guide book by Guberlet (1936) and in a physiological investigation by Hyman (1940). These authors were apparently unaware that it was not a formally described species. Gwilliam (1956) and Kramp (1961) considered *H. 'sanjuanensis'* and other similar species synonymous with *H. auricula*. Hirano (1997) made a survey of populations considered synonymous with *H. auricula* and distinguished four distinct species based on morphological characteristics including intertentacular lobules and position of nematocyst clusters: *H. 'sanjuanensis', H. tenuis, H. auricula,*

and H. octoradiatus. Haliclystus tenuis, H. octoradiatus and *H. 'sanjuanensis'* have since been borne out as distinct species through genetic investigations (Collins and Daly, 2005; Miranda and Collins, pers. comm.) but samples of *H. auricula* have not yet been included in such an analysis. A formal description of *H. 'sanjuanensis'* is pending (Mills and Miranda, pers. comm.).

According to Hirano (1997) *H. 'sanjuanensis'* may be distinguished from closely related species by having the widest calyx and largest gonads with the greatest number of gonadal vesicles. *Haliclystus 'sanjuanensis'* has intertentacular lobules and many closely spaced nematocyst clusters along the perradial edges of the gonads. Each species also has a distinct geographical distribution (see Hirano [1997] for a full comparison).

1.6.2 *Manania handi*

Manania handi was described by Larson and Fautin (1989) after an original unpublished description by Gwilliam (1956) (as *M. prasinus*). *Manania gwilliami* is a similar species which was also described by Gwilliam (1956; *M. enereuthes*) and Larson and Fautin (1989).

Major morphological and histological features are identical for *M. handi* and *M. gwilliami*: both species have a stalk that is four-chambered along its entire length, nematocyst clusters along the margin and on the top of the perradial pockets, and a stalk of variable length (Gwilliam, 1956; Larson and Fautin, 1989). Larson and Fautin (1989) describe the stalk of *M. handi* as shorter than the calyx, whereas Gwilliam (1956) describes it as equally long or longer than the calyx. The uncontracted stalk of *M. gwilliami* is described as ½ - 4 times as long as the calyx (Larson and Fautin, 1989; Gwilliam, 1956). The main distinguishing features between these species are in colour and pigmentation patterns. Although colour is variable in staurozoans and is not a reliable distinguishing feature, distinctive patterns and bands of pigment are generally constant (Gwilliam, 1956). *Manania handi* is described as translucent yellow green, nearly identical to the colour of the *Zostera* it was found on (Gwilliam, 1956). The outside of the calyx has a semitransparent 'window' in each interradius outlined in brown pigment, and the gonads are cream-coloured (Larson and Fautin, 1989; Gwilliam, 1956). The colour range of my specimens was greater than that described for *M. handi* to date, but pigment bands were consistent with those previously described. *Manania gwilliami* is described as

dark red in the type locality but may be tan to magenta with cream or tan gonads; distinctive brown radial pigment bands extend over the perradial pockets, and the herringbone pattern of the gonads is visible from the exumbrella (Larson and Fautin, 1989). Gwilliam (1956) described the same species as "mottled reddish or brownish on white" with red or white tentacles, and no distinctive pigment bands.

The known range of *M. handi* is restricted in comparison to *M. gwilliami* (Larson and Fautin 1989); the two forms have apparently never been found in the same location. *Manania handi* is known only from San Juan Island and Vancouver Island in intertidal habitats on *Zostera* (Gwilliam, 1956; Larson and Fautin, 1989). Gwilliam (1956) found only two live specimens, and records indicate that only a handful of other specimens have been found (Larson and Fautin, 1989). My two years of collection yielding 30 specimens probably represent more *M. handi* than all other findings recorded to date. *Manania gwilliami* is more common, and is found in deeper subtidal habitats (>10m depth) or occasionally tide pools with coralline algae along the west coast of North America from British Columbia to Mexico (Gwilliam, 1956; Larson and Fautin, 1989). My specimens were found in a habitat consistent with that known for *M. handi* – on *Phyllospadix* in the mid-intertidal where the seagrass would not be fully exposed at low tide. Gwilliam (1956) suggested that the fact that very few *M. handi* specimens have been found in the intertidal may indicate that these individiuals represent the edges of the population rather than the centre, and hypothesizes that the centre of the population is subtidal.

Manania handi is easily distinguished from the one other recognized species of *Manania* from the west coast of North America, *M. distincta,* which is cream coloured and has dark brown pigmentation over the herringbone pattern produced by the gonads on the outside of the calyx and interradial stripes extending down the stalk. *Manania* species from the west coast of North America are frequently misidentified; although the windows should clearly distinguish *M. handi* from *M. gwilliami*, specimens that are red in colour have been identified as *M. gwilliami* despite the presence of interradial windows. Other evidence suggests that there are as many as five species of *Manania* along the west coast of North America, and that four of these are commonly identified as *M. handi* or *M. gwilliami*. Further studies are needed to clarify the diversity of *Manania.*

1.7 Objectives

The purpose of this study was to characterize staurozoan neuromuscular morphology, and examine and interpret the results in the context of functional morphology and phylogeny.

Staurozoa are of interest due to their newly revised phylogenetic position as sister group to the remaining Medusozoa, which are groups that produce medusae. This puts them in a position of key interest, and requires morphological studies to determine whether this new framework can provide insight into when and how features associated with the medusa body plan evolved. Although molecular genetic data are useful in providing a phylogenetic framework, comparative anatomical data increase the value of phylogenetic studies by allowing us to make inferences about character evolution and ancestral forms (Mayorova *et al.,* 2012). I performed a comparative neuromuscular study of the staurozoans *Haliclystus 'sanjuanensis'* and *Manania handi* using immunolabelling of neurons and fluorophore-tagged phalloidin to label the F-actin of muscle fibers to compare them to other cnidarian groups and examine character evolution within cnidaria. Immunolabelling is an effective tool with which to examine morphology, and neuromusculature provides an excellent basis for comparison as it differs between cnidarian classes. As the gross morphology of staurozoans appears intermediate between polyp and medusa, I expected to find muscular features associated with both body plans. Staurozoans were expected to have neural characteristics similar to those of polyps, as previous investigations have suggested that a single nerve net is sufficient to produce observed behaviours, and there is no evidence of swim behaviors that would require a pacemaker.

Polyps and ephyrae of the scyphozoan *Aurelia* sp. were investigated for comparative purposes. *Haliclystus 'sanjuanensis'* and *M. handi* co-occur at intertidal sites along southern Vancouver Island, British Columbia, and provide an interesting neuromuscular comparison as the morphology of these genera differs in key respects (Kramp, 1961). Immunolabelling of nervous system components have been performed for representatives of all other classes of Cnidaria (see Satterlie, 2002); however, this represents the first study of its kind for members of the Staurozoa. *Aurelia* sp. is an excellent comparative species as Staurozoa was until recently included in Scyphozoa, and

the two classes are known to share key characteristics. The polyps, ephyrae and medusae of *Aurelia* sp. have been the subject of extensive studies, providing a wealth of research to draw from, and life stages are readily available. Behaviour was investigated so that hypotheses on functional morphology could be drawn.

The distribution of neuroactive substances was investigated as they provide information on the organization of the nervous system; if studied over developmental stages, it can illuminate how ontogenesis is regulated (Mayorova *et al.,* 2012). Study of neuromuscular functional morphology illuminates how behaviour is controlled, effected and limited by the physiological infrastructure, and how those behaviours act to increase survival. Variation between closely related species provides insight into how ancestral forms have diversified to suit the peculiarities of their habitats.

The neuromusculature of cnidarians is of particular interest as Cnidaria is one of the earliest diverging metazoan groups to possess a nervous system (Watanabe, 2009) and smooth and striated musculature (Burton, 2008; Steinmetz *et al.*, 2012). Study of cnidarians may therefore provide a window into how these key components evolved and how they coordinated early animal behaviour.

---

[i] Anchors and various marginal structures derived from the primary tentacles in staurozoans have alternately been called auricles (Clark, 1863a), rhopalioids (Nakanishi *et al.*, 2009; Thiel, 1966), marginal tubercles (Couch 1878), and collectocystophores (Clark 1878).

[ii] The nematocyst clusters have alternately been called vesicles filled with nematocysts (Larson, 1980), white spots of nematocysts (Hirano, 1986; Miranda *et al.*, 2013), nematocyst sacs (Uchida and Hanaoka, 1933), batteries (erroneously: Berrill, 1962; Kikinger and Salvini-Plawen, 1995), and nematocyst vesicles (Miranda *et al.*, 2012).

2.0 Methods

2.1 Animal collection, care and live observation

Haliclystus "sanjuanensis" and *Manania handi* were collected by hand at low tide in the bay near Chinese Cemetery in Victoria, BC (Vancouver Island, latitude: 48°24'22.88"N longitude: 123°19'24.48"W) between May and September of 2013-2015. Live animals were maintained in groups of 2-4 in 100 mL glass bowls set in a circulating seawater system maintained at 12°C. Fresh unfiltered seawater was provided at least every two days, and animals were fed with freshly hatched *Artemia* nauplii weekly unless they were processed for immunolabelling immediately after collection. *H. 'sanjuanensis'* were also collected at Cattle Point, San Juan Island, Washington, in May 2015. Live observations were made from this population, but they were not used for immunolabelling or histology.

Aurelia sp. polyps that were immunolabeled in this study were obtained from populations that had become established in aquaria within the University of Victoria recirculating seawater system from field-collected animals obtained from sites around southern Vancouver Island. Rocks with attached polyps were maintained in buckets set in running sea water and fed twice weekly with *Artemia* nauplii; water was changed daily. Ephyrae were collected daily from strobilating polyps and maintained in small glass bowls set in running seawater. Ephyrae were fed twice weekly with Artemia nauplii; water was changed after feeding.

Photos and videos of live animals were taken with an Olympus SZX9 dissecting microscope with Olympus DP72 camera attachment and DP2-BSW software (Version 2.2, Build 6212) with a framerate of 10 fps.

2.2 Immunolabelling and phalloidin staining

Only staurozoans that had developed major adult features (gonads, nematocyst clusters, transformed primary tentacles) were used in immunolabelling experiments. Major neuromuscular features did not differ between stages and specimens used. Four specimens of each species were labelled with α-glutamate and tyrosinated tubulin

antibodies; four to ten specimens of each species were labelled with each of FMRFamide and α-tubulin antibodies plus fluorophore-tagged phalloidin; four specimens of each species were double-labelled with FMRFamide and α-tubulin antibodies.

Animals were anaesthetized at 12°C by gradually substituting local seawater with artificial seawater containing an elevated concentration of magnesium ions and reduced concentration of calcium ions (Audesirk & Audesirk, 1980); salinity of the artificial seawater was adjusted to match that of local seawater. Anaesthetized animals were fixed for 1 h at room temperature in 4% paraformaldehyde (PFA) and 0.1 M phosphate buffer and 0.085 M sodium chloride for labelling with anti-FMRFamide or anti-α-tubulin antibodies. For labeling with anti-tyrosinated tubulin and anti-glutamate antibodies, 0.05% glutaraldehyde was added to the PFA fixative. Fixed specimens were rinsed 3x at 30 min intervals in PBA (phosphate buffered saline with 0.1% sodium azide) with agitation at room temperature and refrigerated overnight at 4^0C. Subsequent steps were carried out at 4^0C with agitation. Specimens were rinsed 4x at 15 min intervals in PBT (PBA with 0.1% Triton-X) and incubated in blocking medium (1:33 heat inactivated goat serum in PBT) for 1h. Antibodies were diluted in blocking medium and specimens incubated for at least 20 h in 1:1000 anti-FMRFamide antibodies (ImmunoStar, polyclonal rabbit), 1:200 anti-alpha tubulin antibodies (Developmental Studies Hybridoma Bank, mouse monoclonal), 1:800 anti-tyrosinated tubulin antibodies (Sigma Aldrich, monoclonal mouse), or 1:200 α-glutamate antibodies (Chemicon, polyclonal rabbit). For double labelling experiments, specimens were incubated in antibodies mixed together at appropriate dilutions. Specimens were rinsed 4x at 30 min intervals in PBT and 1h in blocking solution before incubation in secondary antibody (goat anti-rabbit or goat anti-mouse Alexa 488, 546 or 568, 1:300; Invitrogen) for at least 20 h. They were subsequently rinsed 3x at 30 min intervals in PBT and incubated 3h in 1:40 Phalloidin-Alexa 568 or Phalloidin-Alexa 488 (Molecular Probes). Finally specimens were rinsed 3x at 20 min intervals in PBA and mounted on glass slides in glycerol for imaging with a Zeiss Axioskop compound microscope with an epifluorescence attachment and a Retiga 2000R digital camera with QCapture Pro software (version 6.0.0.412) or a Leitz Aristoplan compound microscope with an epifluorescence attachment and a Leica MC170 HD camera and Leica Application Suite V4.4 software. Specimens were also

imaged with a Nikon confocal laser scanning microscope (CLSM) with EZ-Cl 3.60 software or Olympus BX 61 WI CLSM with Olympus FluoView FV10-ASW version 1.7c software.

An attempt to improve tissue clarity in *Aurelia* sp. polyps and strobila was made using the clearing method described by Tsai *et al.* (2009), using reduced (3h rather than 6h) incubation times for equilibrating the increasing concentrations of sucrose. Clarity was not improved and the specimens disintegrated when a coverslip was applied.

Photographs were adjusted for brightness and contrast and colourized for immunolabel overlay using Paint Tool SAI (Version 1.2.0). Picasa 3 image editing software (version 3.9, Google) was used to invert some fluorescence images to improve contrast and clarity.

2.3 Histology

Animals were anaesthetized as described above and fixed in 2.5% glutaraldehyde fixative (5:4:1 mixture of 0.4 M Millonig's phosphate buffer at pH 7.6, 0.34 M sodium chloride solution, and 25% glutaraldehyde) at 4^0C for 20 h. Specimens were rinsed 4x at 10 minute intervals in 2.5% sodium bicarbonate solution at pH 7.2 and post-fixed in 2% osmium tetroxide in 1.25% bicarbonate buffer for 1 h, then dehydrated in an acetone series from 30% to 100%. Specimens were then embedded in epoxy resin (Electron Microscopy Sciences). Sections (800 nm) were cut with an MT 5000 Sorvall ® UltraMicrotome, stained with Richardson's stain (Richardson *et al.*, 1960) and photographed with the Zeiss Axioskop setup. Colour balance and brightness were adjusted in Picasa 3.

2.4 Nematocyst observations

Nematocysts were observed and photographed using brightfield (Zeiss Axioskop) and Nomarski differential interference contrast (DIC) (Leitz Aristoplan) microscopy and identified according to Marsical (1974). Measurements of capsules were made using ImageJ software (Version 1.48).

3.0 Results

3.1 General Morphology

3.1.1 General Morphology of *Haliclystus 'sanjuanensis'*

Haliclystus 'sanjuanensis' were found in abundance in the bay opposite Chinese Cemetery, a small bay sheltered by large, low rock formations that partially occlude the mouth. These barriers were submerged at high tide, while at low tide they funneled water to produce a surge channel effect in some areas of the bay while others were sheltered. *Haliclystus 'sanjuanensis'* were common on *Ulva, Mazzaella splendens*, *Odonthalia floccosa*, and *Phyllospadix*, while they were not present on large brown algae such as *Laminaria*, *Alaria* or *Egrigia menziesii*. The habitat was densely populated; a single frond of *Odonthallia floccosa* was often inhabited by a dozen or more staurozoans. No staurozans were found attached to rock or gravel. At low tide, some of the population near shore was left exposed for several hours. A range of developmental stages of *H. 'sanjuanensis'* was found at Chinese Cemetery. Despite an extensive search, larval stages were not found.

Adult *H. 'sanjuanensis'* were chartreuse or olive green, red-orange or rarely wine red (Fig. 7A-H). Colour was usually uniform over the body, but some green specimens had red-orange tentacles. The gonads, manubrium and capita were more pigmented than other areas. Juveniles were beige or peach coloured (Fig. 7I, J); arm tips and developing gonads were somewhat darker than the rest of the body. Adult colouration does not appear to develop until juveniles are greater than 10 mm in diameter.

Haliclystus 'sanjuanensis' reached a maximum diameter (arm tip to arm tip) and height of approximately 40 mm. The calyx and stalk each constituted half this height and both of these regions had a smooth surface. The calyx had an open flattened shape that was clearly demarcated from the stalk, which gave an overall impression of a flared martini glass. The infundibulae were shallow. The eight distinct adradial arms were equidistant and tipped with a variable number of capitate tentacles of approximately equal length that created a pom-pom effect around the end of the arm (Fig. 8A). Anchors (developed primary tentacles) were located at the margin of the calyx at each inter- and

per- radius (Fig. 8B). The manubrium was quadrate with dark-pigmented corners and frilled lips (Fig. 8C).

The stalk was quadrate with longitudinal indentations at each interradius, and flared slightly towards the basal disc; it contained four white interradial longitudinal muscle bands and four darkly pigmented perradial extensions of the gastric cavity (also called taenioles or perradial chambers [Miranda *et al*., 2013]) (Fig. 8D). The basal disc was also indented at the interradii (Fig 8E). Gently undulating bunches of gastric filaments were visible through the semitransparent exumbrella. In adults, the pigmented lanceolate gonads composed of globular gonadal vesicles were clearly visible when viewed through the sub- and exumbrellar surfaces (Fig. 8F). While the subumbrella of young *H. 'sanjuanensis'* was smooth, the edges of adult gonads formed pronounced ridges at the perradii and adradii (Fig. 4B).

White nematocyst clusters were present in a single row along the perradial edges of the lanceolate gonad halves from the tips of the arms to the widest point of the gonads (Fig. 8F, G). These nematocyst clusters were more numerous in larger animals; in some of the largest adults (greater than 30 mm in diameter and height) clusters deviated from single file and were occasionally present nearer the center of the perradius, along the perradial margin, and very rarely along the interradial margins (Fig. 8H). The clusters appeared granulated and had a slightly darker spot near the center of each cluster. The subumbrellar epidermis was raised in slight bulges over each cluster (Fig. 8G).

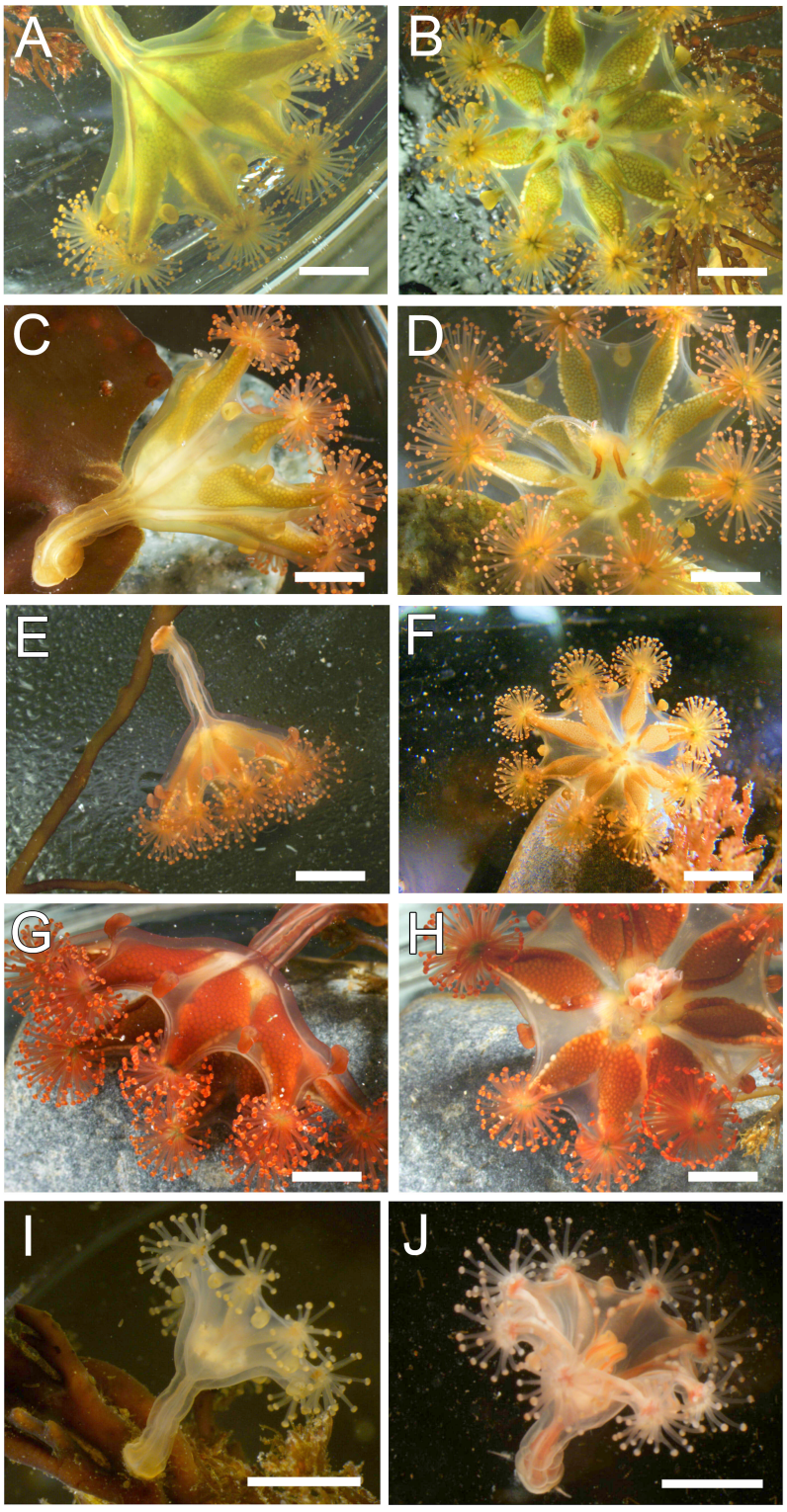


Figure 7. Photographs showing variation in *H. 'sanjuanensis'* specimens. **A-H:** adults; **I, J:** juveniles. **A, B:** Green/olive. **C, D:** Green/olive with red tentacles. **E, F:** Orange. **G, H:** Wine red. **I:** Beige. **J:** Peach. Scale bars 4 mm.

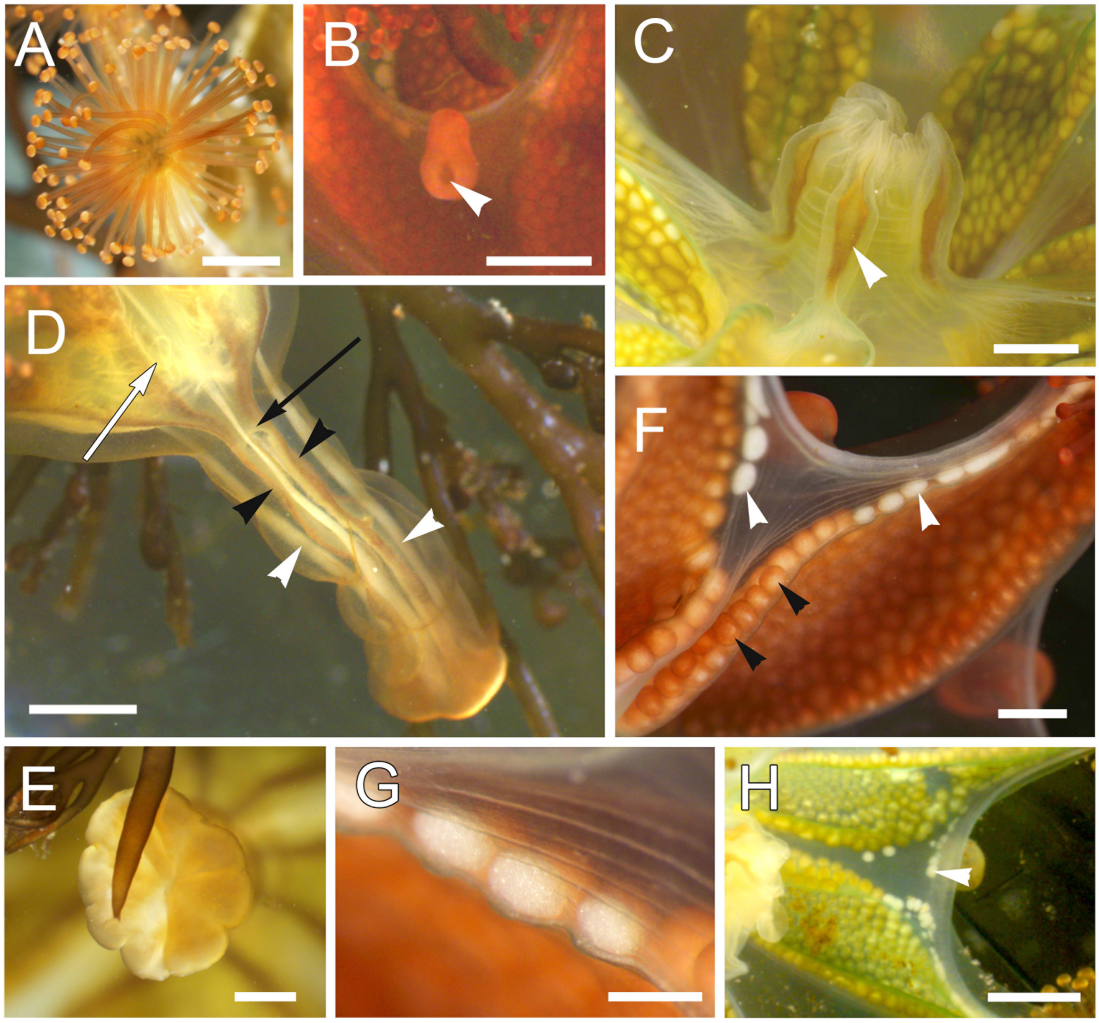


Figure 8. Anatomical features of *H. 'sanjuanensis'*. **A:** Bunch of capitate secondary tentacles. Scale bar, 2 mm. **B:** Anchor with remnant of primary tentacle (arrow). Scale bar, 2 mm. **C:** Manubrium with dark pigmented corners (arrowhead). Scale bar, 1 mm. **D:** Stalk showing longitudinal muscle bands (white arrowheads) and gastric filaments (black arrowheads). The gastric cavity divides at the base of the calyx (arrow) into four perradial extensions in the stalk (black arrowheads). Scale bar, 2 mm. **E:** Basal disc. Scale bar, 1 mm. **F:** Gonad with gonadal vesicles (black arrowheads) and nematocyst clusters along perradial edges (white arrowheads); ridges are formed in the perradius by the gonads. Scale bar, 1 mm. **G:** Tangential view of nematocyst clusters with raised bump over apex. Scale bar, 400 µm. **H:** Abnormally arranged nematocyst clusters in the perradius, including nematocyst clusters along the margin (arrowhead). Scale bar, 2 mm.

Of the juveniles found at Chinese Cemetery, the smallest was 200 μm in diameter and 400 μm in height, with 8 primary tentacles, no distinct separation of calyx and stalk, and a hypostome that had not yet developed elaborations of the manubrium. Some tentacles had a tiny bump where the glandular swelling of the anchor was beginning to develop (Fig. 9A). This polyp was capable of twisting and bending the body, but the primary tentacles were not mobile. Several 1 mm long polyps were found with groups of 1-3 secondary tentacles and larger glandular swellings on the primary tentacles (Fig. 9B-E). These polyps were capable of swifter and a greater range of motion, and their tentacles (including the primary tentacles) were independently mobile. Juveniles measuring 3-10 mm in height and diameter were easily found; these had primary tentacles surrounded by glandular tissue and rudimentary gonads (Fig. 9F). I was not able to follow the development of these small individuals as they did not survive in the lab.

Several abnormal animals were found. One had perfect hexaradiate symmetry. Many animals were found in the process of regenerating part of the margin that had duplicate or twinned anchors and arms.

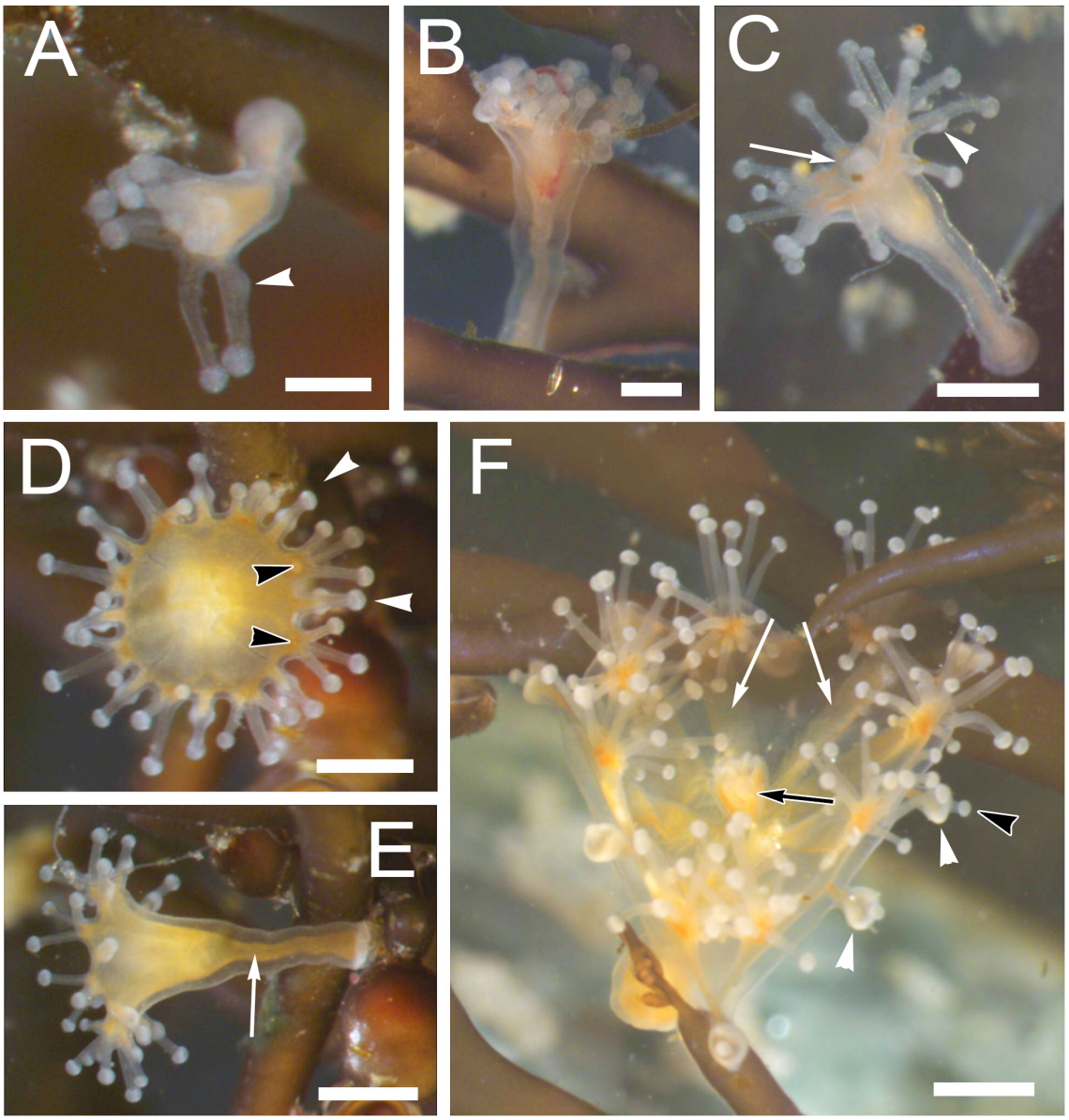


Figure 9. Features of juvenile *H. 'sanjuanensis'* collected at Chinese Cemetery on *Odonthalia floccosa.* **A:** Lateral view of smallest stauropolyp found, with 8 primary tentacles. The adhesive glandular tissue of the anchor had begun to develop (arrowhead). Scale bar, 200 µm. **B:** Lateral view of stauropolyp with 1 secondary tentacle in each adradius. Scale bar, 200 µm. **C:** Lateral view of stauropolyp with differentiated hypostome (arrow) and 2 secondary tentacles per adradius. A patch of adhesive glandular material is present on the distal side of each primary tentacle (arrowhead). Scale bar, 500 µm. **D:** Oral view of a stauropolyp with 3 secondary tentacles per adradius (black arrowheads) between perradial and interradial primary tentacles (white arrowheads).

Scale bars, 500 µm. **E:** Lateral view of (**D**); at this point in development there is a single extension of the gastric cavity in the stalk (arrow). Scale bars, 500 µm. **F:** Oral view of 4 mm stauropolyp with distinct manubrium (black arrow), tentacle bunches, anchors (white arrowheads) with a distinct tentacle remnant (black arrowhead), and developing gonads (white arrows). Scale bar, 1 mm.

3.1.2 General Morphology of *Manania handi*

Manania handi were much rarer than *H. 'sanjuanensis'* within the intertidal zone bordering Chinese Cemetery. Extensive searching over two seasons (2014, 2015) turned up only 30 individuals. *M. handi* were found exclusively on *Phyllospadix,* much of which had the red alga *Smithora naiadum* growing on it. They could only be collected at extreme low tides, as they were found only on seagrass that remained in at least 60 cm of water at low tide. Specimens were usually found on healthy *Phyllospadix* with small amounts of new S*mithora naiadum* growth. The habitats of *M. handi* and *H. 'sanjuanensis'* overlapped only a little; although they were only a few feet away from each other, few *H. 'sanjuanensis'* were found at the depths preferred by *M. handi.*

The *M. handi* specimens fell into one of three colour categories: green, purple-green, or orange-brown. As shown in Figure 10, the tentacle heads and gonads were usually of a different colour to the rest of the animal. Four exumbrellar interradial white stripes, which were in fact transparent "windows" that displayed the lighter internal colour of the animal, extended from near the margin to the base of the calyx near the stalk (Fig. 4D). These windows were surrounded by a border of brown pigment. The gonads produced a distinctive herringbone pattern when viewed through the exumbrellar surface (Fig. 4D), and appeared brightly coloured when viewed from the subumbrellar surface (Fig. 4C). Green individuals were a solid emerald green exactly matching the *Phyllospadix* on which they live. The calyx, stalk and tentacle stalks were green; the tentacle heads and adhesive pads were golden- or purple-brown. The gonads were chartreuse or bright yellow (Fig. 10A, B). The purple-green specimens varied widely in colour. Generally, the mesoglea and subumbrella of purple-green specimens appeared green while the exumbrellar epidermis was purple. Due to these layers of semitransparent colours and degree of pigmentation in each, the animals appeared green-yellow to light

purple or dark purple-brown depending on degree of illumination and angle of viewing. The gonads appeared brown from the exumbrellar surface but were bright yellow from the subumbrella, and the tentacle heads were purple-brown. The anchors were yellowish or cream (Fig. 10C, D). Orange-brown individuals had a dark red-brown calyx and stalk, golden brown tentacle stalks and heads, cream or yellowish anchors, and bright orange gonads (Fig. 10E, F). The smallest *M. handi* lacking distinct gonads were either light purple with green tints and lavender capita, or beige-peach all over, similar to the smallest *H. 'sanjuanensis'* (Fig. 10G, H).

No *M. handi* with abnormal symmetries or obviously regenerated tissues were found. One 30 mm specimen was found that had apparently been recently preyed upon; half of the calyx from margin to stalk was missing, leaving the gastric cavity open to the exterior. This animal survived four days in the lab without marked deterioration until fixed, and spawned on three successive days.

The colouration of *M. handi* was good camouflage: under the diffuse light found *in situ* they are very similar in colour to the algae with which they predominantly co-occur, *Phyllospadix* and *Smithora*. Partial transparency further camouflaged these animals. The largest specimen was a female 40 mm long and 20 mm in diameter. Most of the specimens found were 15-25 mm long. Three small (<10 mm) juveniles without differentiated gonads were also found (Fig. 10G, H). Half of the total length of the animal was calyx and half stalk, although the stalk was relatively longer in smaller individuals. The calyx widened abruptly above the stalk in adults; in some specimens there was a slight constriction between stalk and calyx (Fig. 10B, D). The calyx had deep infundibulae and flared slightly at the margin, giving the adult animal an overall shape similar to a hand bell. The calyx transitioned smoothly into the stalk with no constriction or abrupt widening of the calyx in small specimens, which were vuvuzela-shaped (Fig. 10G). In adults, the calyx was smooth while the stalk was textured like crushed silk (Fig. 11A). The stalk, which was cylindrical or tapered distally, ended abruptly in a thin, flat basal disc twice the diameter of the stalk surrounded by a thin transparent sheath (Fig. 11A).

The eight short arms were roughly equidistant; in some specimens pairs of arms were slightly closer to the perradii, but in others there were slight interradial pairings. The

number of tentacles per arm varied, but was invariably far fewer than that found on *H. 'sanjuanensis'*. The capita were larger in relation to the stalk and were somewhat depressed at the apex rather than spherical as they were in *H. 'sanjuanensis'*. Capita of younger individuals were less depressed. Several long tentacles occupied the center of the bunch; those on the periphery were shorter (Fig. 11B, C). Primary tentacles and the outermost secondary tentacles had adhesive glandular swellings on the exumbrellar base of the shaft (Fig. 11B, C, G, H). The number of secondary tentacles with adhesive pads varied depending on the size of the specimen. The smallest specimen had one large central pad and a small one on either side beginning to develop. The mid-sized specimens either had three (Fig. 11B) (a larger central one plus a smaller one on either side) or three plus two new outer ones developing. The largest specimen had five adhesive pads. The central pad was always the largest, while the flanking pairs were successively smaller (Fig. 11B). The pad of the primary tentacles was smaller than the smallest pair of secondary pads (Fig. 11B). Each primary tentacle had a distinct oval brown pigment spot at the subumbrellar base of the shaft where tentacle joined the margin (Fig. 11E, F, H). The size of these pigment spots did not vary within individuals, and the location was consistent between individuals.

A row of white nematocyst clusters followed the margin in each interradius and perradius (Fig. 11E, F), extending to the arms. The top of the wedge-shaped perradial pockets that divide the infundibulae were also covered in nematocyst clusters (Fig. 11F). The nematocyst clusters each produced a bulge in the surface of the subumbrella. There was often a ring of brown pigmentation in the center of the clusters at the apex of the bulge (Fig. 11F). The edges of the nematocyst clusters in the perradii were partially covered by borders of brown pigmentation. The clusters were similar in appearance to those of *H. 'sanjuanensis'*.

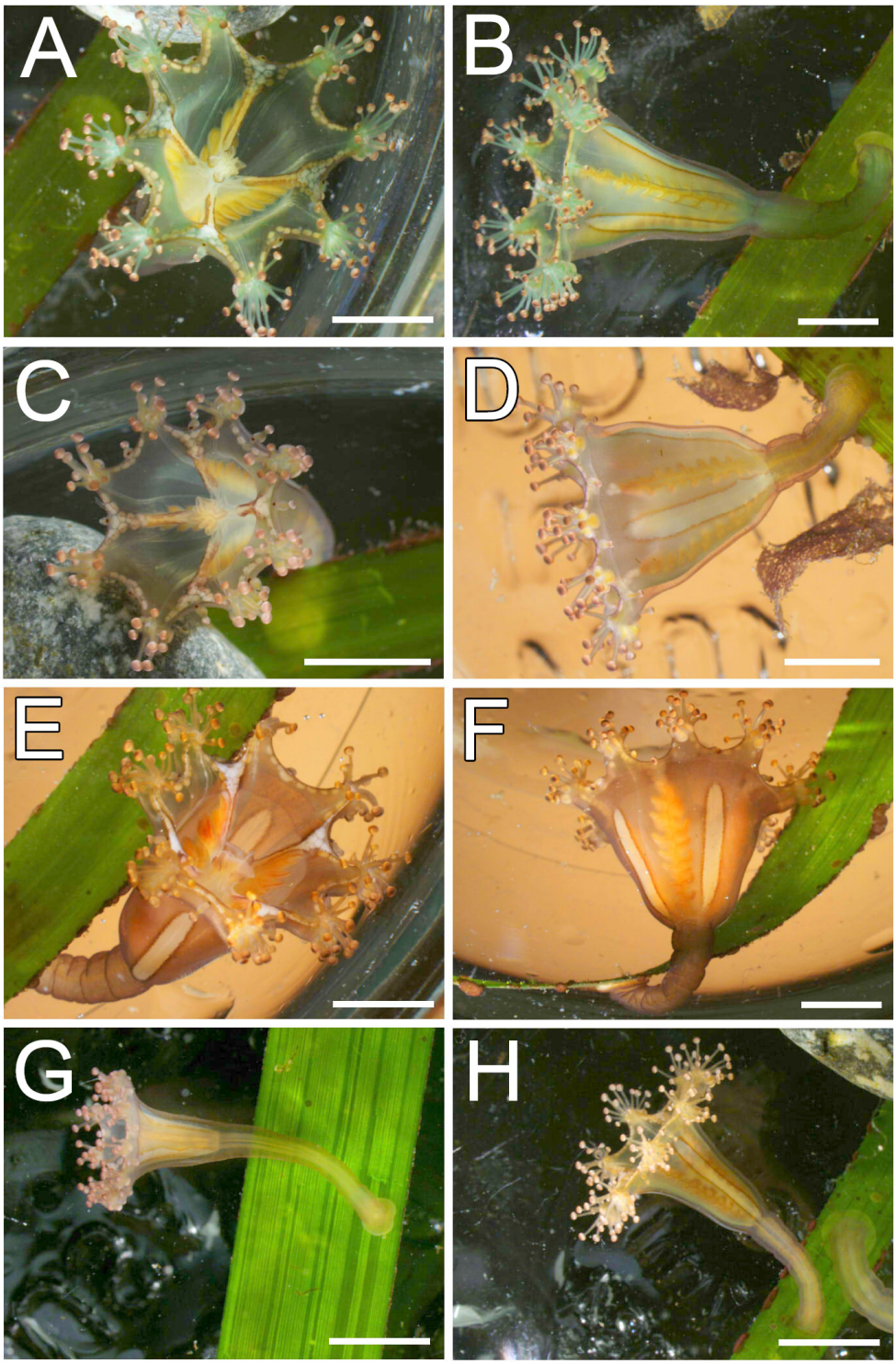


Figure 10. Variation in *M. handi* specimens found on *Phyllospadix*. **A-F:** Adults. **G, H:** Juveniles. **A, B:** Green. **C, D:** Purple-green. **E, F:** Orange-brown. **G:** Purple-green juvenile. **H:** Beige-peach juvenile. Scale bars, 4 mm.

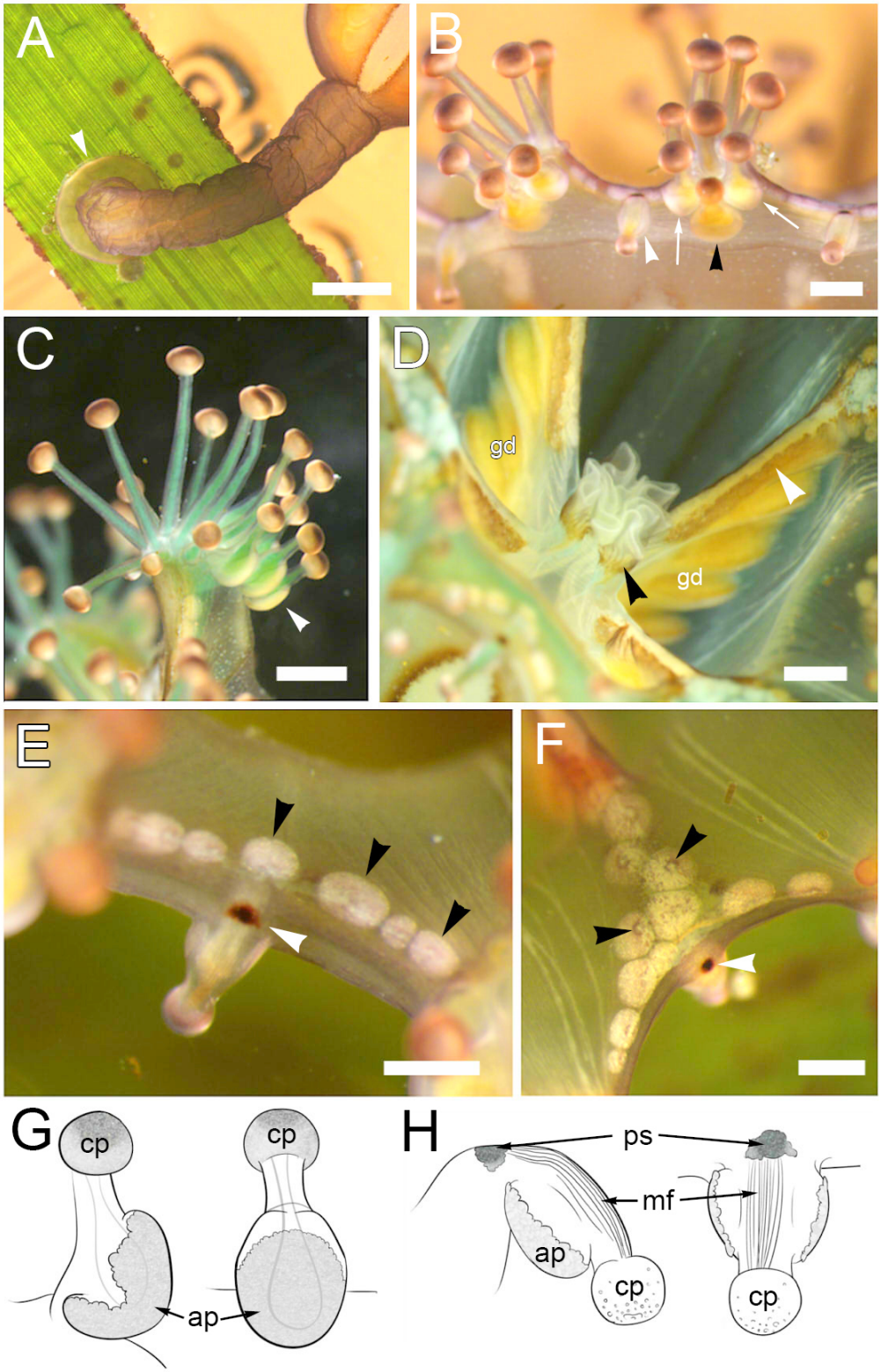


Figure 11. Anatomical features of *M. handi.* **A:** The stalk has a texture like crushed silk and a flat basal disc surrounded by a thin, transparent sheath (arrowhead), scale bar 2 mm. **B:** Exumbrellar view of primary and secondary tentacles. Adhesive pads are present

on the primary (white arrowheads) and outer secondary tentacles (black arrowhead, white arrows). Note size of lateral adhesive pads (white arrows) compared to the central one (black arrowhead). Scale bar 500 µm. **C:** Lateral view of arm showing arrangement of secondary tentacles and their adhesive pads (black arrowheads). Scale bar 1mm. **D:** Oral view showing frilled manubrial lips, brightly coloured gonads and distinctive bands of pigmentation on the manubrium (black arrowhead) and the sides of the perradial pockets (white arrowhead). Scale bar, 500 µm. **E:** Primary tentacle with pigment spot (white arrowhead) and nematocyst clusters (black arrowheads) along interradial margin. Scale bar, 200 µm. **F:** Primary tentacle with pigment spot (white arrowhead) and nematocyst clusters in the perradius. Note ring of pigmentation near the center of each cluster (black arrowheads). Scale bar, 400 µm. **G:** Lateral (left) and abaxial (right) diagrams of a secondary tentacle with adhesive pad. Gray outline shows gastrodermal cavity of tentacle. **H:** Lateral (left) and oral (right) diagrams of a primary tentacle with adhesive pad, pigment spot and musculature. **Abbreviations:** ap, adhesive pad; cp, capitum; gd, gonad; mf, muscle fibers; ps, pigment spot.

3.2 Musculature: Phalloidin labelling

3.2.1 Musculature of *Haliclystus 'sanjuanensis'*

All muscles were composed of smooth fibers; muscle bands labeled with fluorophore-tagged phalloidin and exposed by cuts showed no evidence of striations like those evident in *Aurelia* sp. ephyrae that were labelled with fluorophore-tagged phalloidin. Figure 12 shows the musculature of *H. 'sanjuanensis'* as revealed by fluorophore-tagged phalloidin labelling.

3.2.1.1 Marginal Muscles

The marginal muscles lay beneath the peripheral subumbrellar epidermis, and comprised four perradial and four interradial segments, each of which extended along the margin between two adjacent adradial arms and were discontinuous at the ends of the arms (Figs. 12A, B; 13A). The marginal muscle segments were proximal to the anchors (Figs. 12A, B; 13B), uniform in width, and muscle fibers were more densely packed nearer the outer rim of the calyx (Fig. 13B). The marginal muscle fibers extending up the

sides of the adjacent arms appeared to intermingle with the muscle fibers of the secondary tentacles. The marginal muscles labelled more intensely with fluorphore-tagged phalloidin than other muscle groups. Focus series indicated that these muscles were folded and occurred at a variety of depths.

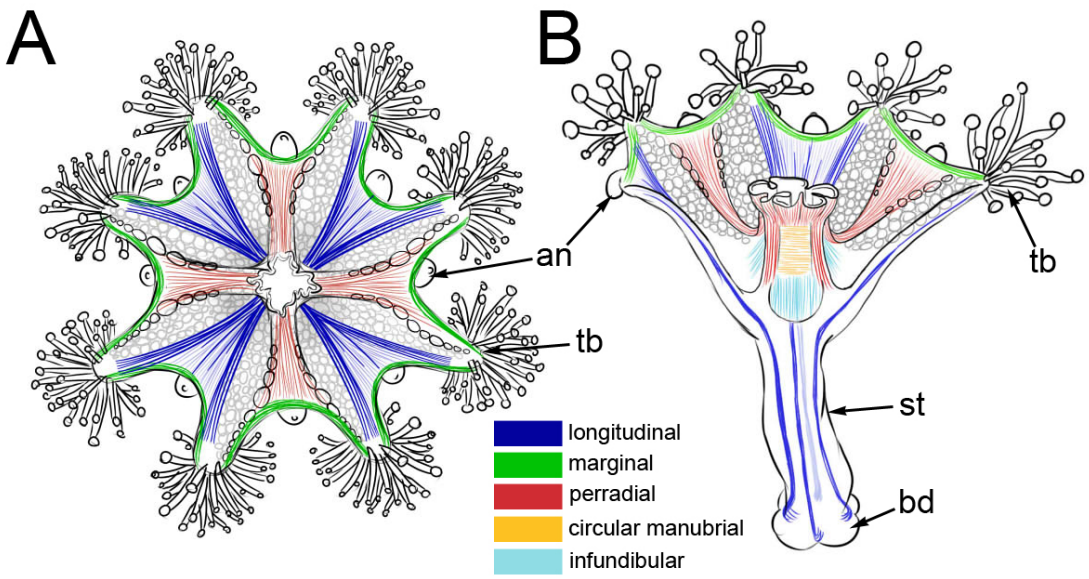


Figure 12. Diagrammatic representation of the musculature of *H. 'sanjuanensis'* in **A:** oral view and **B:** lateral view with half the calyx removed. Interradial longitudinal muscles are in dark blue; the marginal muscles are in green; radial and manubrial lip muscles are in red; circular muscles of the manubrium are in orange; muscle sheets of the infundibula are in light blue. **Abbreviations:** an, anchor; bd, basal disc; st, stalk; tb, tentacle bunch.

3.2.1.2 Tentacles

Each secondary tentacle had a set of epidermal longitudinal muscles that evenly ensheathed the stalk of the tentacle and terminated inside the capitum (Fig. 13C). Fluorophore-tagged phalloidin also labelled short, thin protrusions extending from the epithelium of the capita (Fig. 13C).

When primary tentacles of juveniles first developed, they were morphologically similar to secondary tentacles of older animals (Fig. 9); however, the adhesive glandular cells which eventually form the anchors began to develop before secondary tentacles

appeared (Fig. 9A). The muscle fibers of each primary tentacle were apparently destroyed by the swelling glandular patch. In small adults in which the anchors retained a clear tentacle remnant, a few superficial muscle fibers extended along the midline of the anchor from its insertion point at the distal edge of the marginal muscle to the remnant of the primary tentacle's capitum (Fig. 13D). In adults where the tentacle remnant of the anchor had been subsumed, the anchor no longer had any musculature (Fig. 13B).

3.2.1.3 Longitudinal Muscles

The four interradial longitudinal muscles extended from the base of the stalk to the margin of the calyx. In the stalk, the fibers of each muscle formed a tightly bundled, radially flattened band embedded in the mesoglea (Figs. 8D; 13E). At the base of the stalk, the fibers turned at right angles to project slightly towards the center point of the basal disc (Fig. 13E). In the calyx, the longitudinal muscle fibers lay beneath the subumbrellar epidermis and were flattened in the subumbrellar-exumbrellar direction from the base of the infundibulum. As the fibers extended towards the margin, they fanned out towards the two adjacent adradial arms to fill the region beneath the subumbrellar epidermis, bounded by a leaf-shaped half of a perradial gonad on either side (Fig. 13F). The longitudinal muscle fibers ran directly beside the gonad tissue, but never overlapped it. Towards the margin, each longitudinal muscle had three distinct regions: two strong peripheral bands that extended into the adradial arms and abruptly terminate at the base of the arm below the tentacles (Fig. 13A), and a central interradial sheet of continuous but sparser muscle fibers (Fig. 13B, F). The strong peripheral bands were folded as the margin was, while the middle section was a thin, superficial sheet. In some specimens there was a strongly labelled narrow central band following the midline of the interradial space which tapered towards the margin, terminating before reaching the marginal muscle. The fibers of the longitudinal muscles terminated before merging with the marginal muscle (Fig. 13B).

3.2.1.4 Radial Muscles

Radial musculature extended down each of the four perradial corners of the manubrium. At the base, a portion of this muscle extended along the top of the corresponding perradial pocket to the calyx margin, while other fibers continued towards

the base of the calyx to line the infundibula (Figs. 12A, B; 14A). The radial muscle fibers were subumbrellar, epidermal, and fanned out between the two perradial leaves of a single gonad as they extended towards the margin (Fig. 12A, B). This fan had a uniform density of fibers similar to that of the weaker central portion of the longitudinal muscles (Fig. 14B) and terminated before contacting the marginal muscle (Figs. 12A, B; 13B; 14C). Similar to the longitudinal muscles, the radial muscle fibers ran directly adjacent to the gonads without overlapping them. The radial muscle fibers overlaid the halves of the nematocyst clusters that protruded into the perradial space (Fig. 14D). The nematocyst clusters in the perradii labelled much more strongly with fluorophore-tagged phalloidin than other non-muscle tissue. Each cluster was highlighted by phalloidin, and a spot corresponding to the raised central portion of each cluster was labeled particularly intensely (Fig. 14B, D).

3.2.1.5 Manubrium

The four flat interradial sides of the manubrium bore fibers that ran perpendicular to the radial muscles of the manubrium corners (Fig. 14A). These fibers did not label strongly with fluorphore-tagged phalloidin, but they formed thin muscle sheets which extended a short distance into the infundibula before they were replaced with the longitudinal fibers that lined the infundibula (Fig. 14E). The frilled lips of the manubrium were also muscular. Sparse muscle fibers ran from the base of the lips to their peripheral edge, fanning out as they did so. These fibers were continuous with those of the perradial corners of the manubrium (Fig. 14A).

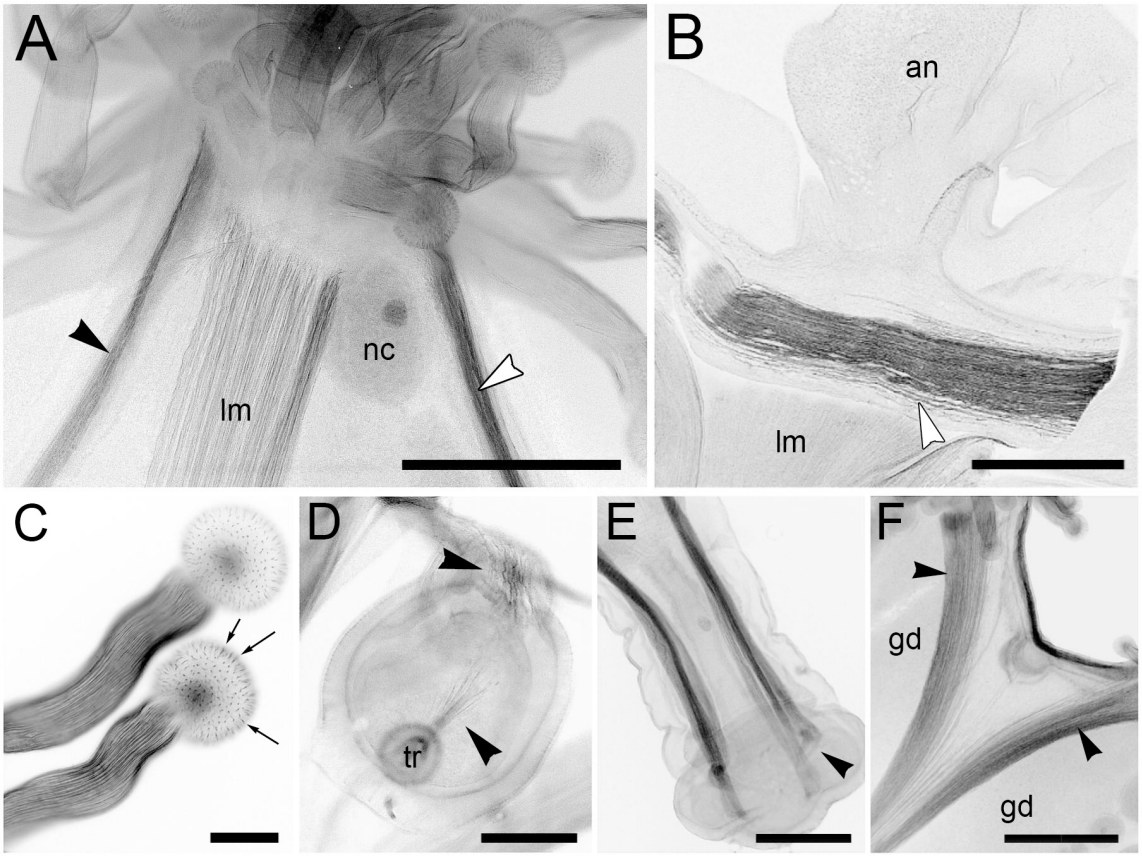


Figure 13. Fluorophore-tagged phalloidin labelling of muscles in *H. 'sanjuanensis'*. **A:** An interradial (black arrowhead) and perradial (white arrowhead) segment of marginal muscle runs up the sides of an arm to the tentacles. A longitudinal muscle band terminates abruptly at the base of the tentacles. Scale bar, 400 μm. **B:** Interradial margin at a developed anchor lacking muscle fibers. Muscle fibers were less densely packed on the proximal side of the marginal muscle (arrowhead). The sparse sheet of muscle fibers occupying the centre of the interradius terminated short of the marginal muscle. Scale bar, 400 μm. **C:** Tentacles were ensheathed by longitudinal muscles and short, phalloidin-labelled projections extended from the surface of the capita (arrows). Scale bar, 100 μm. **D:** An incompletely transformed primary tentacle had muscle fibers extending from the marginal muscle along the midline to the tentacle remnant (arrowheads). Scale bar, 200 μm. **E:** The stalk had four interradial longitudinal muscle bands terminating at right angles (arrowhead) at the base of the basal disc. Scale bar, 500 μm. **F:** Each interradial longitudinal muscle diverged near the base of the calyx to form two strongly labelled bands running into adjacent arms and a middle area within the interradius consisting of a

much more diffuse sheet of muscle. Scale bar, 600 µm. **Abbreviations:** an, anchor; gd, gonad; lm, longitudinal muscle; nc, nematocyst cluster; tr, tentacle remnant.

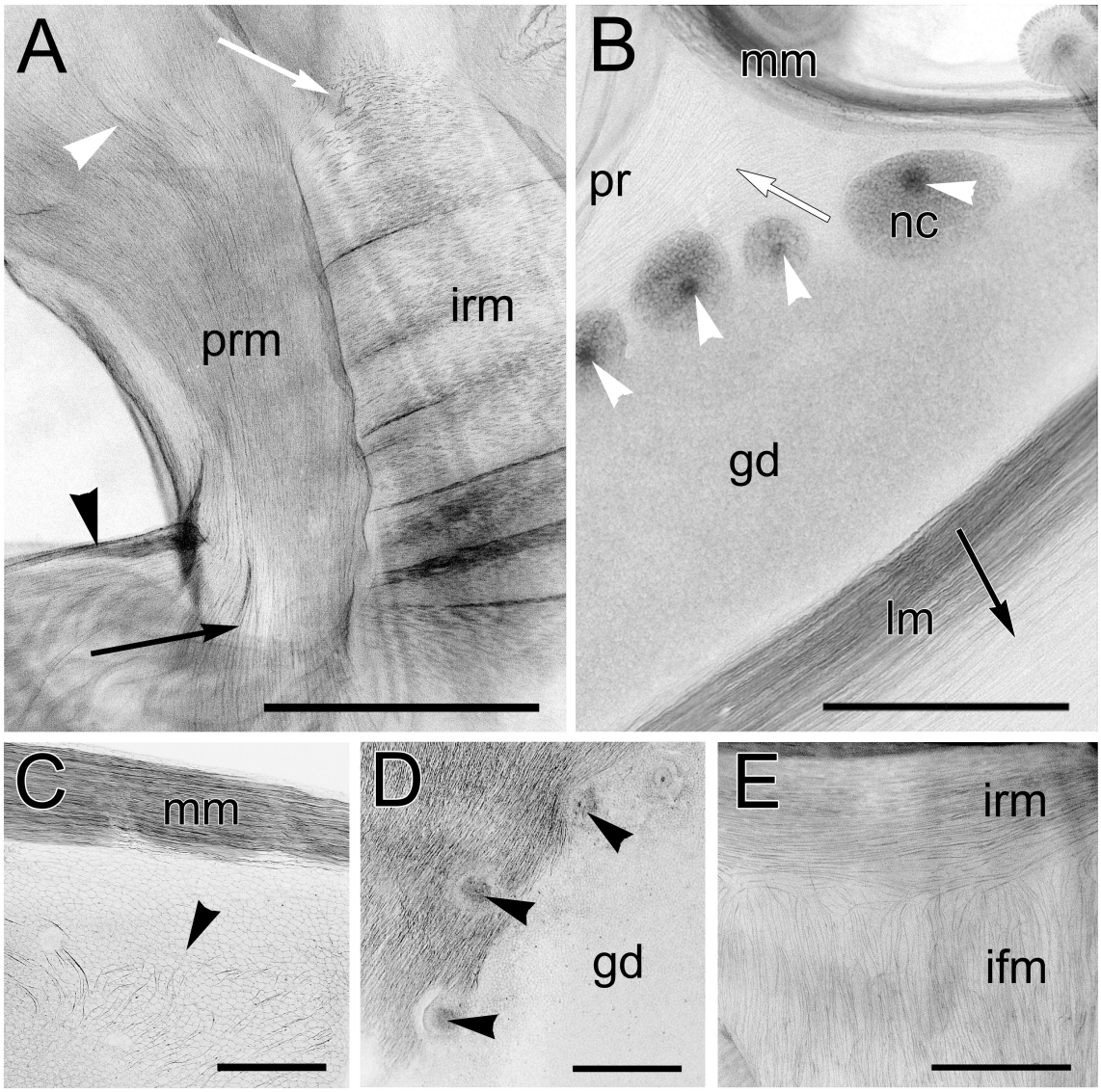


Figure 14. Fluorophore-tagged phalloidin labelling of the manubrium and perradial musculature of *H. 'sanjuanensis'*. **A:** Perradial bands of muscle extended from the lips (white arrowhead) to the base of the manubrium. Fibers turned at a right angle to extend along the perradius to the margin (black arrowhead) and continued below the manubrium to line the infundibula (black arrow). Circularly oriented fibers occupied the interradial face from the lips to the base of the manubrium (white arrow). Scale bar, 40 µm. **B:** Density of perradial muscle fibers (white arrow) compared to fibers in the middle of an

interradius (black arrow). The nematocyst clusters labelled strongly with fluorophore-tagged phalloidin; a strongly labelled central spot corresponded to the apex of each cluster (arrowheads). Scale bar, 400 μm. **C:** Fibers of the perradial muscle terminated short of the margin (arrowhead). Scale bar, 100 μm. **D:** Fibers of the perradial muscle extended over one half of each perradial nematocyst cluster lining the edge of a gonad. Fibers do not extend over the apices of the clusters (arrowheads) or the gonad tissue. Scale bar, 200 μm. **E:** Interradial face of the manubrium at the base, where circularly oriented fibers of the interradial manubrial muscles were replaced by the longitudinal sheets of muscle lining the infundibula. Scale bar, 20 μm. **Abbreviations:** gd, gonad; ifm, infundibular muscles; irm, interradial muscles of manubrium; lm, longitudinal muscle; mm, marginal muscle; nc, nematocyst cluster; pr, perradius; prm, perradial face of manubrium**.**

3.2.2 Musculature of *Manania handi*

Similar to *H. 'sanjuanensis'*, *M. handi* muscles were composed exclusively of smooth muscle fibers. Many aspects of the musculature were similar between these two species, but they also differed in several important respects. Figure 15 shows the musculature of *M. handi* as revealed by fluorophore-tagged phalloidin labelling.

3.2.2.1 Marginal muscle

As in *H. 'sanjuanensis',* the marginal muscle of *M. handi* was subepidermal and folded. However, in *M. handi* the marginal muscle was exumbrellar in location, rather than subumbrellar as in *H. 'sanjuanensis'*, and it formed a continuous band along the margin of the calyx outside of the tentacles. The lower border of this muscle was straight around the circumference of the calyx, while the upper border of the muscle was scalloped to cover the exumbrellar surface of each arm (Figs. 15B; 16A, B). A thin band of marginal muscle remained inside the lip of the calyx, proximal to the attachment point of the primary tentacles, and distal to the nematocyst clusters; this thin band was interrupted at the end of each arm (Figs. 15A; 16B-D).

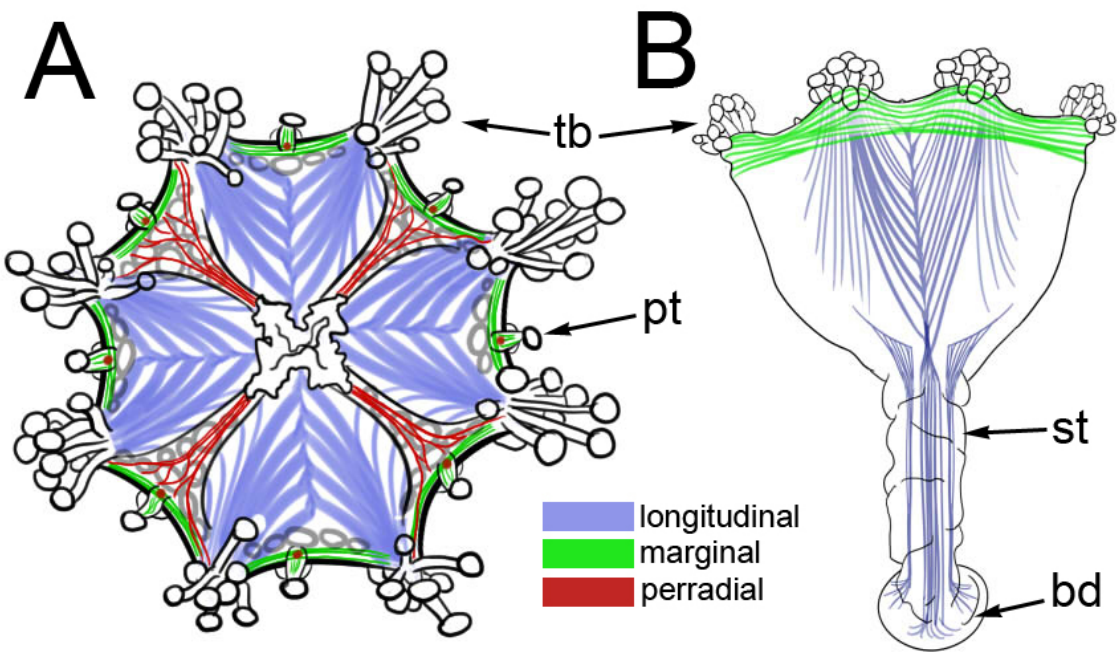


Figure 15. Diagrammatic representation of the musculature of *M. handi* in **A:** oral view and **B:** lateral exumbrellar view. Interradial longitudinal muscles are in dark blue; the marginal muscles are in green; radial and manubrial lip muscles are in red; pigment spots are indicated at the base of each tentacle. **Abbreviations:** bd, basal disc; pt, primary tentacle; st, stalk; tb, tentacle bunch.

3.2.2.2 Tentacles

Tentacle musculature was similar to that of *H. 'sanjuanensis'*, although the longitudinal muscle fibers were more densely packed. The muscle fibers of the tentacles were not continuous with the longitudinal or radial fibers, but did appear to interdigitate with fibers of the marginal muscle (Fig. 15A; 16D). Primary and outer secondary tentacles did not have musculature in areas occupied by glandular swellings (Fig. 16E). The muscle fibers of the primary tentacle stalks were continuous with the thin band of marginal muscle inside the calyx lip (Fig. 15A; 16C).

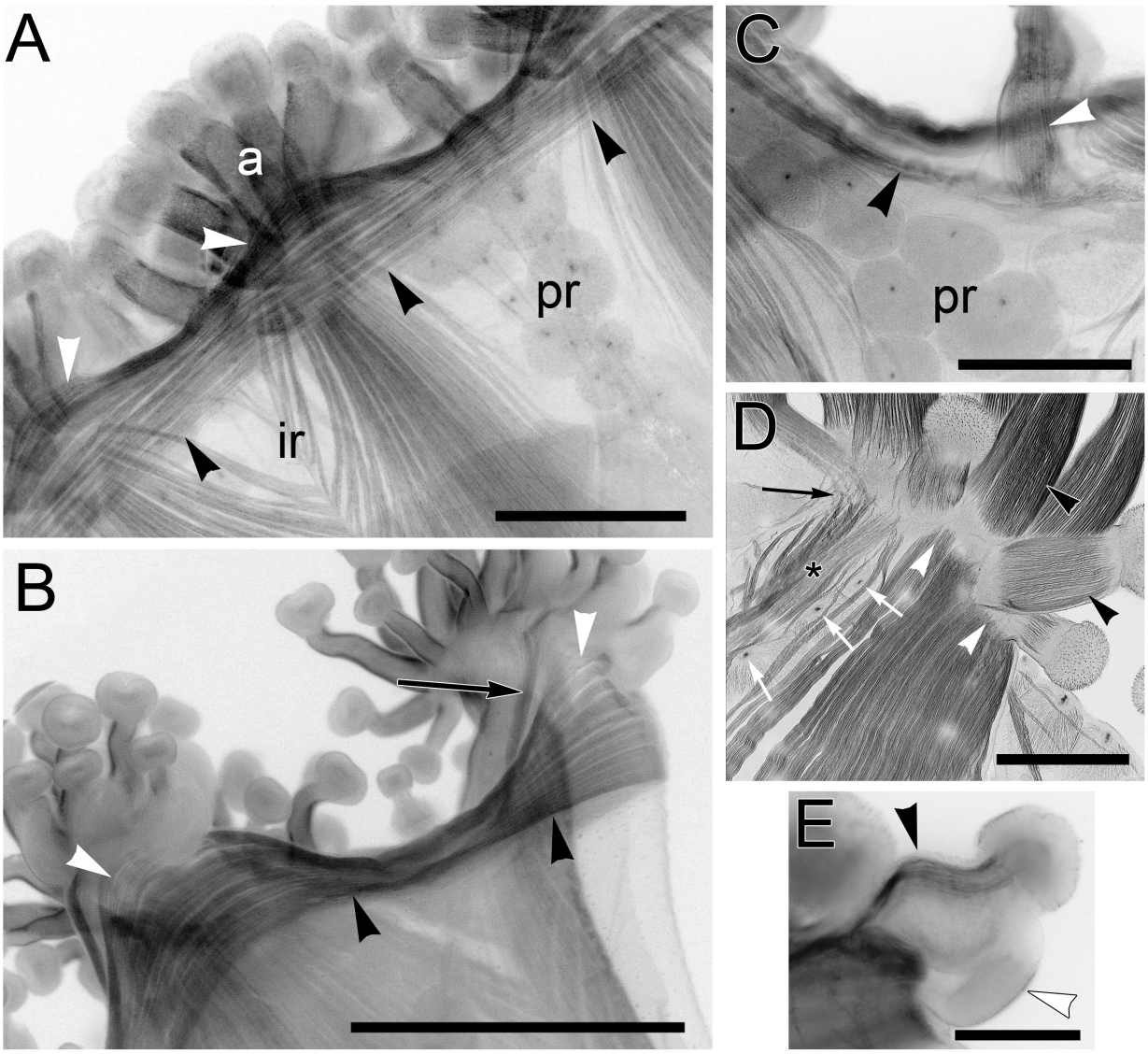


Figure 16. Fluorophore-tagged phalloidin labelling of the marginal and tentacle musculature of *M. handi*. **A, B:** Exumbrellar views of the marginal circular muscle. The lower border of the muscle was straight around the circumference of the calyx (black arrowheads) and the upper border was scalloped to cover the arms (white arrowheads). **A:** The relationship of the marginal muscle to the longitudinal and radial muscles of the interradius and perradius, respectively, and perradial nematocysts of the subumbrella are visible through the calyx. Scale bar, 500 μm. **B:** The exumbrellar muscle was on the opposite side of the mesoglea from the subumbrellar musculature, and a thin band of marginal muscle inside the lip of the subumbrella was interrupted at the arms (arrow). Scale bar, 2 mm. **C:** Perradial margin; the musculature of the primary tentacle (white

arrowhead) was continuous with the thin band of subumbrellar marginal muscle (black arrowhead). Scale bar, 100 μm. **D:** Subumbrellar view of the end of an arm. The musculature of the unmodified secondary tentacles (black arrowheads) was similar to that of *H. 'sanjuanensis'*. The longitudinal muscle terminated at the end of the arm below the tentacles (white arrowheads). The muscle fibers of the tentacles (black arrow) were continuous with the thin band of marginal muscle inside the subumbrella (asterisk). The apices of the nematocyst clusters (white arrows) occupied a gap between the marginal and longitudinal muscle. Scale bar, 400 μm. **E:** Lateral view of a transformed primary tentacle; musculature was present along the subumbrellar midline (black arrowhead) but absent in the region of the adhesive pad (white arrowhead). Scale bar, 200 μm. **Abbreviations:** a, arm; ir, interradius; pr, perradius.

3.2.2.3 Longitudinal muscles

In the calyx, each longitudinal muscle had a central interradial axis from which multiple side-branches extended at an acute angle to the central axis on either side (creating a herringbone pattern) (Fig. 15A,B; 17A, B). These branches were folded as the marginal muscle was. The distal tips of these branches extended to the base of the tentacles in the adjacent arm and terminated there (Figs. 15A,B; 16D; 17A), as did the distal fibers of the longitudinal muscles in *H. 'sanjuanensis'*. The final branches of the longitudinal muscle framed a triangular segment of tissue occupied by nematocyst clusters near the margin in each interradius (Fig. 17A). Muscle branches always deviated around the apices of the nematocyst clusters (Figs. 16D; 17A). The central interradial axis of each longitudinal muscle was deeply embedded in the mesoglea, while the branches emanating from the central axis projected towards the subumbrella to assume a position closer to the epidermis. Similar to *H. 'sanjuanensis'*, the longitudinal muscle fibers were grouped into four bundles within the stalk and fanned out within the calyx (Figs. 15A, B; 17 A, C). In the basal disc, the muscle fibers bent at right angles to project towards the periphery of the basal disc rather than the centre, as seen in *H. 'sanjuanensis'* (Figs. 15B; 17C). Bundles of fibers that appeared to be extensions of the longitudinal muscle projected back from the arm tip towards the wall of the adjacent perradial pocket (Figs. 15A, B; 17D) (which contained the gonads and formed the deep infundibulae of *M.*

handi). These bundles were smaller than those projecting from the main interradial axis and they anastomosed as they extended towards the manubrium, terminating shortly before they reached the gonad tissue embedded in the perradial pockets (Fig. 17D).

3.2.2.4 Radial muscles and manubrial musculature

The manubrial muscles of *M. handi* were very similar to those of *H. 'sanjuanensis'*. Radial muscles ran down each corner of the manubrium, sheets of circular muscle occupied the flat sides of the manubrium and extended a short distance into the infundibulae, and the manubrial lips were muscular (Figs. 13B; 14A, E). Unlike the diffuse fans of *H. 'sanjuanensis'*, the radial muscles of *M. handi* ran in a tight band along the top of each perradial pocket, overlying the nematocyst clusters that also occupied the top (Figs. 15A; 18A). The apices of the clusters along the top of the pocket lay to either side of the muscle band (Fig. 18A). Near the edge of the calyx, the bundled perradial muscles branched out and anastomosed as they extended to the margin (Figs. 15A; 18A-C). Branches of perradial muscle either deviated around the apices of the nematocyst clusters or terminated on one side of the apex to begin on the other side, leaving a gap where the cluster was connected to the subumbrella (Fig. 18B, C). Some branches of the perradial muscles ended near the calyx margin, while others extended to the base of the tentacles in adjacent arms (Fig. 15A). The walls of the infundibula were uniformly covered in thin epidermal sheets of muscle running longitudinally, as in *H. 'sanjuanensis'*.

3.2.2.5 Nematocyst clusters

The nematocyst clusters were labelled with fluorophore-tagged phalloidin similar to those of *H. 'sanjuanensis'* (Fig. 18A). CSLM images revealed that each cluster was surrounded by muscle fibers which ran meridionally from the apical central spot towards the opposing pole of the cluster (Fig. 18B, C). The central spot was brightly labelled (Fig. 18A-C); tangential views revealed what looked like a short, twisted tube leading from the cluster to the subumbrellar surface (Fig. 18A, inset).

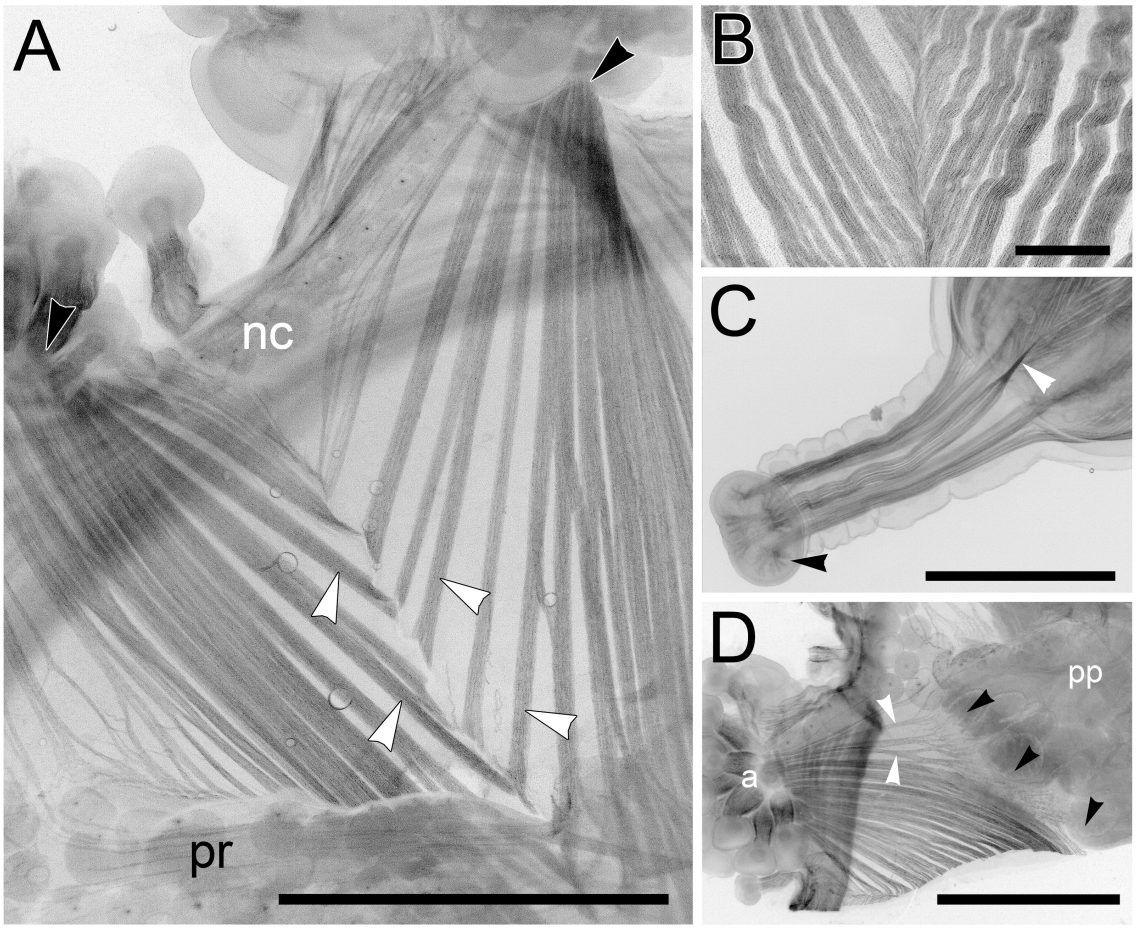


Figure 17. Fluorophore-tagged phalloidin labelling of the longitudinal musculature of *M. handi*. **A:** The longitudinal muscle was herringbone-shaped; oblique bands of muscle extended from a central interradial axis (white arrowheads). The final branches of the muscle framed nematocyst clusters situated between the longitudinal muscle and margin. The longitudinal muscle bands terminated at the end of the adjacent adradial arms (black arrowheads). Scale bar, 2 mm. **B:** Detail of oblique bands of muscle issuing from the central interradial axis of the longitudinal muscle. Scale bar, 250 μm. **C:** The longitudinal muscles were grouped into four bundles in the stalk. At the base of the basal disk, the fibers projected towards the periphery of the disc (black arrowhead). Where the muscle bands entered the calyx, they abruptly fanned out to occupy the calyx walls (white arrowhead). Scale bar, 2 mm. **D:** Anastomosing bands of muscle (white arrowheads) extended back from the end of the arm towards the gonads (black arrowheads) on the perradial pocket, where they terminated. Scale bar, 2 mm. **Abbreviations:** a, arm; nc, nematocyst clusters; pp; perradial pocket; pr, perradius.

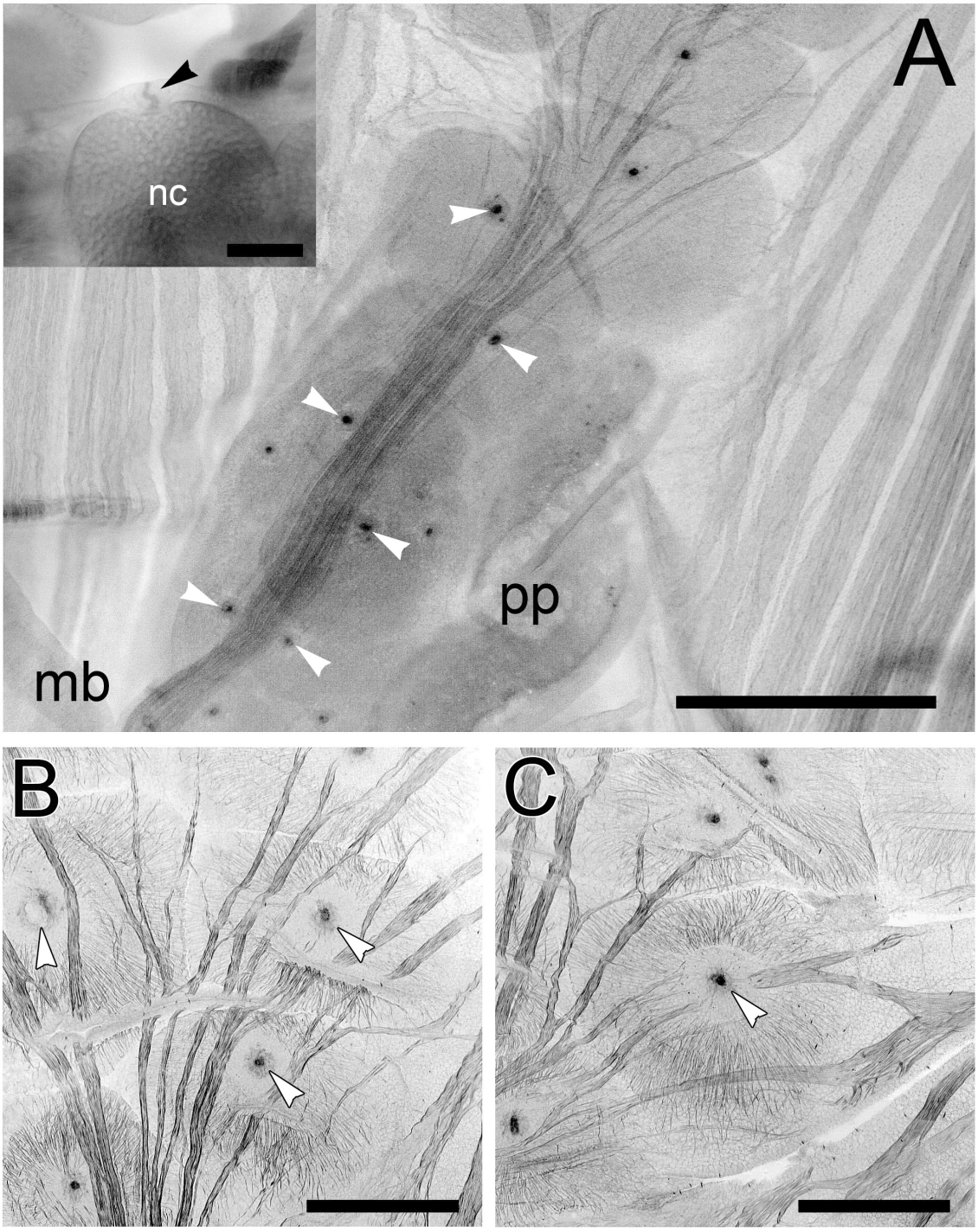


Figure 18. Fluorophore-tagged phalloidin labelling of the radial musculature and nematocyst clusters of *M. handi*. **A:** The tightly bundled radial muscle ran along the top

of the perradial pocket; where the pocket joined the calyx wall, the muscle began to branch, fan out and anastomose. Along the top of the perradial pocket, the apices of the nematocyst clusters (white arrowheads) labelled with phalloidin lay to either side of the muscle band. Scale bar, 500 µm. **Inset** shows tangential view of cluster apex with what appears to be a short tubular structure (black arrowhead) connecting the cluster to the subumbrellar surface. Scale bar, 100 µm. **B, C:** CLSM images of perradial muscle branches that anastomosed around (**B**) and left gaps (**C**) for the apices of the nematocyst clusters (white arrowheads) near the margin. Meridional muscle fibers wrapped around each cluster from the apices. Scale bars, 200 µm. **Abbreviations:** mb, manubrium; nc, nematocyst clusters; pp, perradial pocket.

3.2.3 Musculature of *Aurelia* sp. life stages

3.2.3.1 *Aurelia* sp. ephyra

Figure 19 shows the overall layout of muscles in *Aurelia* sp. ephyrae and adults, as shown by phalloidin labelling.

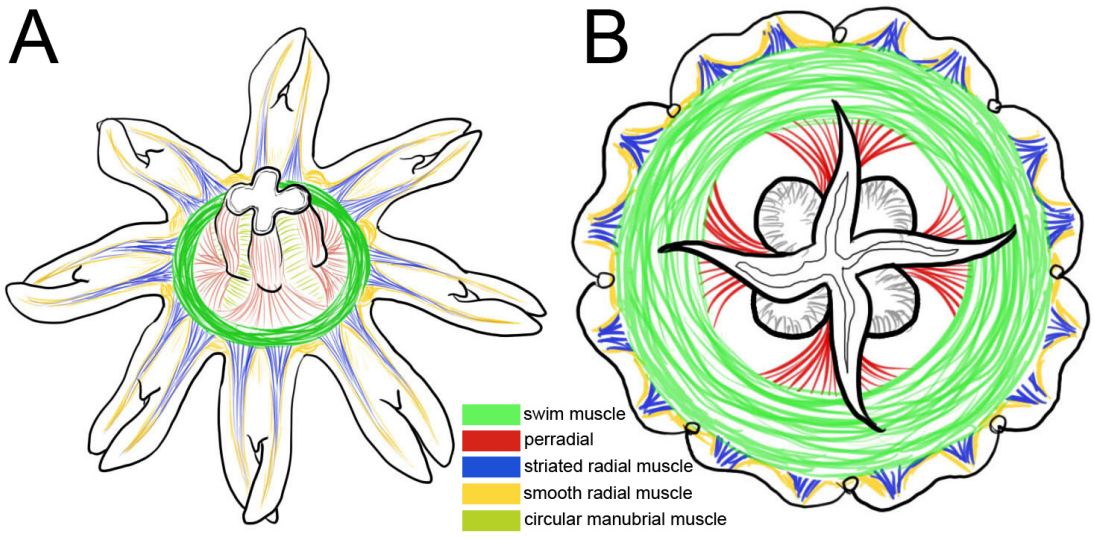


Figure 19. Diagrammatic representation of the musculature of *Aurelia* sp. **A:** ephyra and **B:** young medusa. Striated radial muscles of the arms are in dark blue; smooth muscle bordering the radial arm muscles and forming knots at the apices between the arms is in

orange; the striated circular swim muscle is in green; smooth radial muscles are in red; smooth circular muscles of the manubrium are in olive.

The circular muscle of *Aurelia* sp. ephyrae was continuous, subumbrellar, epidermal, and composed of cross-striated fibers. The striated muscle band was bordered on the distal (outer) edge by smooth fibers; this was best seen in young ephyrae (Figs. 19A; 20A-C). The circular muscle extended toward the edge of the bell as the ephyral arms became less prominently demarcated during development (Fig. 19B); this muscle performs swimming contractions in adult jellyfish. Each arm had two distinct bands of radial muscle that inserted exumbrellar to the circular muscle and projected into the two lappets (Figs. 19A; 20A). Each band had a central portion composed of striated muscle, and smooth peripheral fibers (Figs. 19A; 20B). These muscles are used for swimming in young ephyrae. These arm muscles were reduced in the adult (Fig. 19B) but function in adult paddling motions involving the lappets. Early ephyrae had distinct bundles of smooth fibers at the apex of each adradial cleft between the arms (Figs. 19A; 20C). These gradually disappeared during development. The smooth fibers may be precursors to the definitive striated ones.

Similar to the two staurozoans, *Aurelia* sp. ephyrae had bands of radial muscles that ran down the four perradial corners of the manubrium, fanned out at the base, and inserted into the circular muscle. These fibers were exclusively smooth. There were also four regions of circularly oriented fibers between the corners of the manubrium (Figs. 19A; 20D). No distinct lip musculature was observed in the ephyra, but as very young ephyrae were examined, it is probable that additional musculature would develop in that area as the oral arms form. For adult musculature, see Chapman (1999).

3.2.3.2 Musculature of *Aurelia* sp. polyps and strobila

Fluorophore-tagged phalloidin labeling of muscle in polyps and strobila was often not strong or clear; tissue thickness or pigmentation made imaging difficult.

Aurelia sp. polyps had four longitudinal muscles running from oral disc to basal disc which were funnel shaped where they joined the oral disc at the peristomial pits (Fig. 20E). Imaging of the oral disc and hypostome was unclear, but the fibers of the longitudinal muscles seemed to be continuous with muscles that covered the oral disc and

radiated into the tentacles. Tentacles were supplied by flat sheets of muscle. The hypostome had uniform radial muscles that ran from the edge of the oral disc up the hypostome to the lip. Muscle fibers were evenly distributed and not concentrated in bands as in the ephyra. All muscle fibers were smooth.

The four longitudinal muscles of the strobila were bundled into the central column of the animal and ran through the stack of developing ephyrae, terminating at the most distal ephyra (Fig. 20F). The developing arm muscles of the ephyrae were also visible.

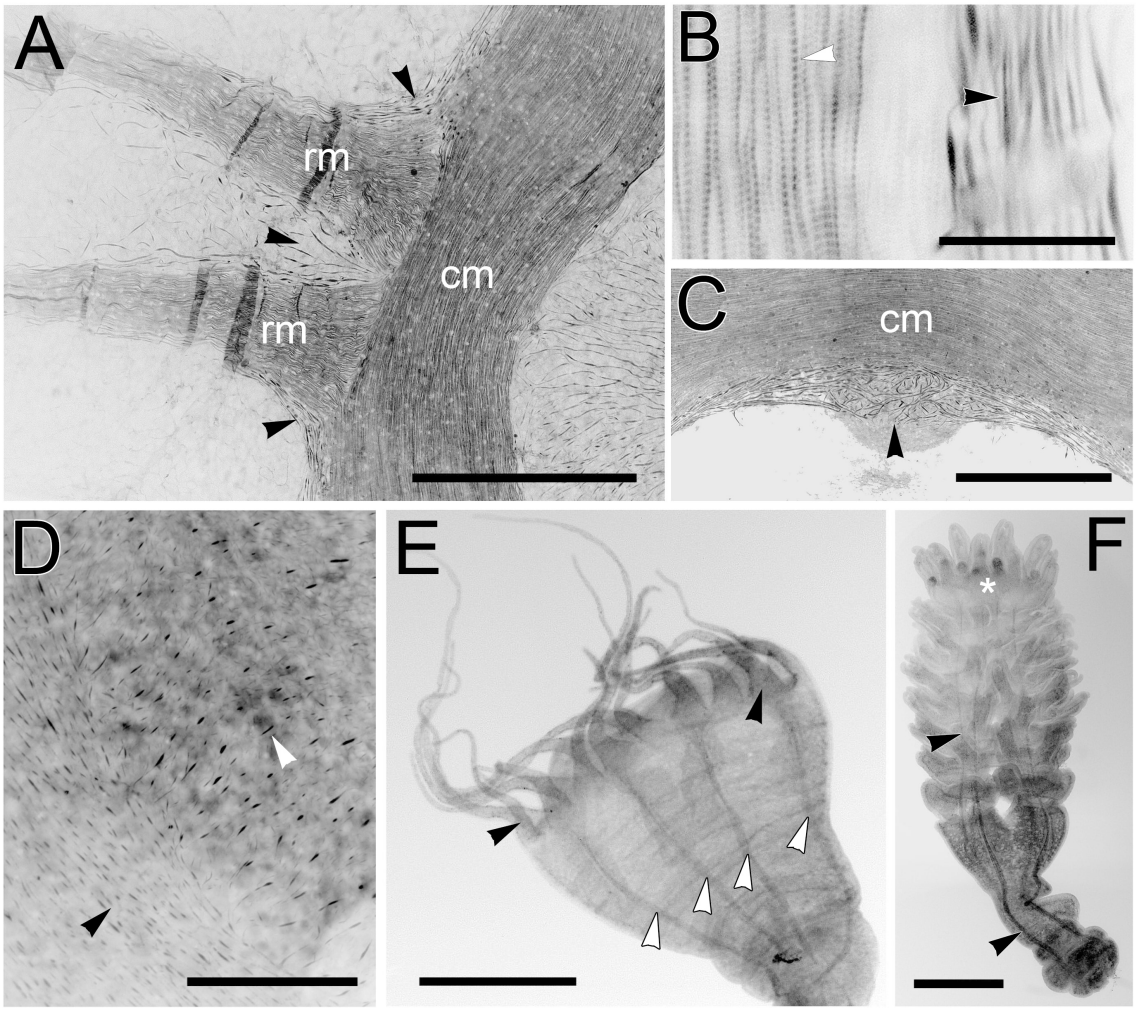


Figure 20. Fluorophore-tagged phalloidin labelling in developmental stages of *Aurelia* sp. **A-D:** ephyra; **E:** polyp; **F:** strobila. **A:** Portion of the circular muscle and two radial muscle bands of a single arm. Smooth fibers bordered the striated swimming muscle fibers (arrowheads). Scale bar, 200 µm. **B:** Detail of the distal edge of the circular

muscle. Striated muscle fibers (white arrowhead) were bordered by smooth muscle fibers (black arrowhead). Scale bar, 20 μm. **C:** Distal margin of the circular muscle at the apex between two arms, showing the distinct knot of smooth muscle that bordered the striated fibers (arrowhead). Scale bar, 200 μm. **D:** Portion of the manubrium; smooth muscle fibers ran up the perradial corner of the manubrium (black arrowhead) and circularly oriented fibers occupied the interradial flat side (white arrowhead). Scale bar, 100 μm. **E:** Four longitudinal muscles ran from the oral disc to the basal disc (white arrowheads) of a polyp, and flat sheets of muscle supplied the tentacles (black arrowheads). Scale bar, 1 mm. **F:** *Aurelia* sp. strobila that has not yet released any ephyra; longitudinal muscle bands (black arrowheads) ran from the apical ephyra (asterisk), through the strobila to the basal disc. Scale bar, 1 mm. **Abbreviations:** cm, circular muscle; rm, radial muscle.

3.3 Nematocysts

Several animals of both *Manania handi* and *Haliclystus 'sanjuanensis'* were examined to determine nematocyst distribution and shape, but measurements of nematocyst dimensions recorded in Table 1 were taken from only a single adult of each species. Size of nematocysts varied with specimen size, but the length-to-width ratio (lwr) of the various nematocyst types was consistent. The closer an lwr score was to 1, the rounder was the nematocyst type.

On the subumbrellar surface, nematocysts were concentrated in the tentacle capita and ends of the arms at the base of the tentacles. Nematocysts were also embedded in the marginal muscle, over the gonads, and along the longitudinal muscles and radial muscles. Nematocysts were contained in the nematocyst clusters, and batteries were embedded in the exumbrellar epidermis. Both species had two kinds of nematocyst: heterotrichous microbasic euryteles and atrichous isorhizas.

Table 1. Shape and size data for the nematocysts of *H. 'sanjuanensis'* and *M. handi.* Measurements were taken from a single adult specimen for each species; the *H. 'sanjuanensis'* specimen was 27 mm in diameter, and the *M. handi* specimen was 30 mm long. Measurements taken from specimens of a variety of sizes indicated that although nematocyst size varied with the size of the animal, the length to width ratio (lwr) metric was relatively constant; scaling of nematocysts was isometric.

Species	Body Part	Type	Length (µm)	Width (µm)	N	LWR	Shape
Haliclystus	Tentacles	Isorhiza	12.78 +/- 0.72	3.77 +/- 0.40	12	3.8	Sausage
'sanjuanensis'		Eurytele	19.07 +/- 0.78	9.06 +/- 0.30	14	2.1	Oval
	Gonad	Isorhiza	11.65 +/- 0.65	2.89 +/- 0.24	7	4	Sausage
		Eurytele	15.98 +/- 0.74	7.94 +/- 0.56	11	2	Oval
	Clusters	Eurytele	16.61 +/- 0.52	11.08 +/- 0.31	22	1.5	Lemon
	Manubrium	Eurytele	9.17 +/- 0.60	7.25 +/- 0.49	6	1.3	Round
	Gastric Filaments	Eurytele	10.70 to 7.10	6.80 to 4.13	11	1.5	Lemon
	Exumbrella	Eurytele (?)	11.04 +/- 0.67	4.46 +/- 0.37	13	2.5	Eggplant
Manania	Tentacles	Isorhiza	20.03 +/- 1.03	3.14 +/- 0.23	16	6.4	Sausage
handi		Eurytele	16.20 +/- 0.59	6.15 +/- 0.17	10	2.6	Ellipse
	Clusters	Eurytele	15.07 +/- 0.76	10.76 +/- 0.53	20	1.4	Lemon
	Manubrium	Eurytele	9.99 +/-0.52	6.55 +/- 0.44	16	1.5	Lemon
	Gastric Filaments	Eurytele	7.59 +/- 0.17	5.17 +/- 0.36	3	1.5	Lemon
	Exumbrella	Eurytele (?)	15.05 +/- 0.66	5.79 +/- 0.37	24	2.6	Ellipse

3.3.1 Nematocysts of *Haliclystus 'sanjuanensis'*

The tentacle capita had two types of nematocysts (Fig. 21): sausage shaped isorhizas were tightly packed to cover most of the capitum (Fig. 21A, C-E), and less common large oval euryteles were more abundant towards the tip of the capitum, but were nearly absent at the base (Fig. 21A, F, G). The isorhizas were curved in one plane and straight in the other (Fig. 21C). These nematocysts were also found in tracts embedded in the muscle fibers running longitudinally up the stalks of the tentacles. The long axis of these nematocysts was parallel to the muscle fibers, and the non-discharging

end of the capsules pointed towards the capitum (Fig. 21B). The isorhizas occasionally discharged incorrectly, leaving the filament coiled (Fig. 21E).

The nematocysts along the marginal muscle, longitudinal muscles and around the base of the tentacles were the same types and sizes as those found in the tentacle capita. Most nematocysts along the marginal and longitudinal muscles were oriented with their long axis parallel to the muscle fibers, but were pointed in either direction along the fibers (Fig. 22A). Those around the base of the tentacles were disorganized. The density of nematocysts embedded in various muscle bands was highly variable within and between animals.

The subumbrellar gastrodermis composing the gonadal vesicles contained pigment granules, through which the developing gametes were visible. Large oval euryteles and sausage shaped isorhizas were embedded in the tissue subumbrellar to the gonadal vesicles (Fig. 22B). These were similar in shape and appearance to those on the tentacles, but were smaller (Table 1). These nematocysts did not appear to be oriented in any particular direction; most lay with their long axis roughly parallel to the subumbrellar surface. There were no nematocysts on the gonadal vesicles themselves.

Sectioning showed that the nematocyst clusters were ovoid invaginations of the subumbrellar epidermis that were packed with nematocytes. The central patch that labelled strongly with fluorophore-tagged phalloidin corresponded to a solid pack of cells at the apex of the cluster that connected it to the subumbrellar surface (Fig. 22C). Nematocysts within clusters showed variable orientations (Fig. 22D), and when a cluster was cut open, the nematocytes spilled freely from the pocket. The nematocysts within these nematocytes were large, lemon-shaped euryteles (Fig 22E).

The pigmented perradial corners of the manubrium and lips had a few nematocysts of one size, but the interradial faces of the manubrium bore no or very few nematocysts.

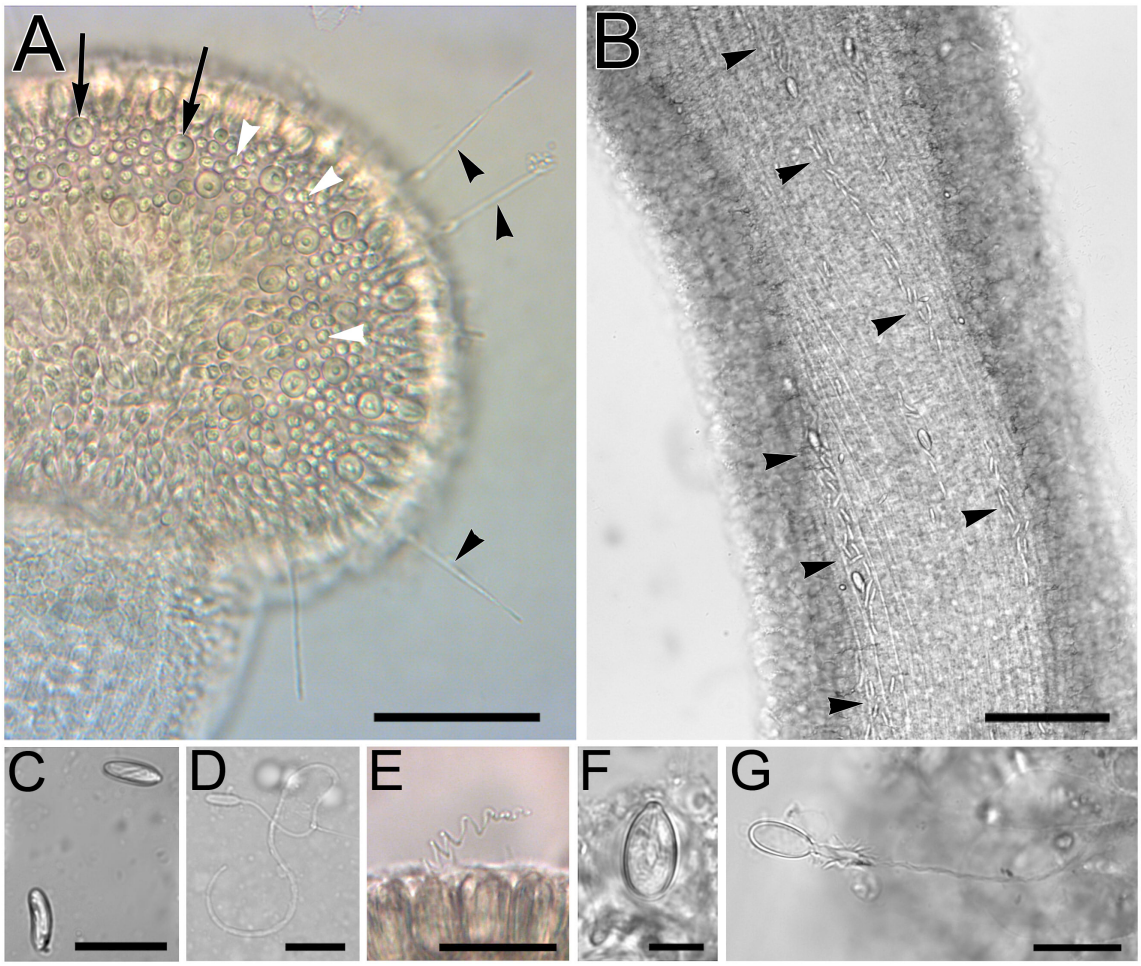


Figure 21. Brightfield images of the tentacle nematocysts of *H. 'sanjuanensis'*. **A:** The tentacle capitum was covered in isorhizas (white arrowheads) and occasional larger euryteles (black arrows), which were more abundant near the tip. Some nematocysts were discharged (black arrowheads). Scale bar, 50 mm. **B:** Tentacle stalk; capitum is towards the top of the photo. Tracts of nematocysts (arrowheads) ran parallel to the muscle fibers. Scale bar, 100 µm. **C:** Undischarged sausage-shaped isorhiza capsules. Scale bar, 20 µm. **D:** Discharged atrichous isorhiza with characteristic smooth non-tapering filament. Scale bar, 20 µm. **E:** Isorhizas occasionally did not discharge fully and produced a spiral filament. Scale bar, 25 µm. **F:** Large oval eurytele of the tentacle capita; note dark core indicating the bulbed base of the inverted filament. Scale bar, 10 µm. **G:** Discharged eurytele showing barbed bulbed base and filament characteristic of heterotrichous microbasic euryteles. Scale bar 20 µm.

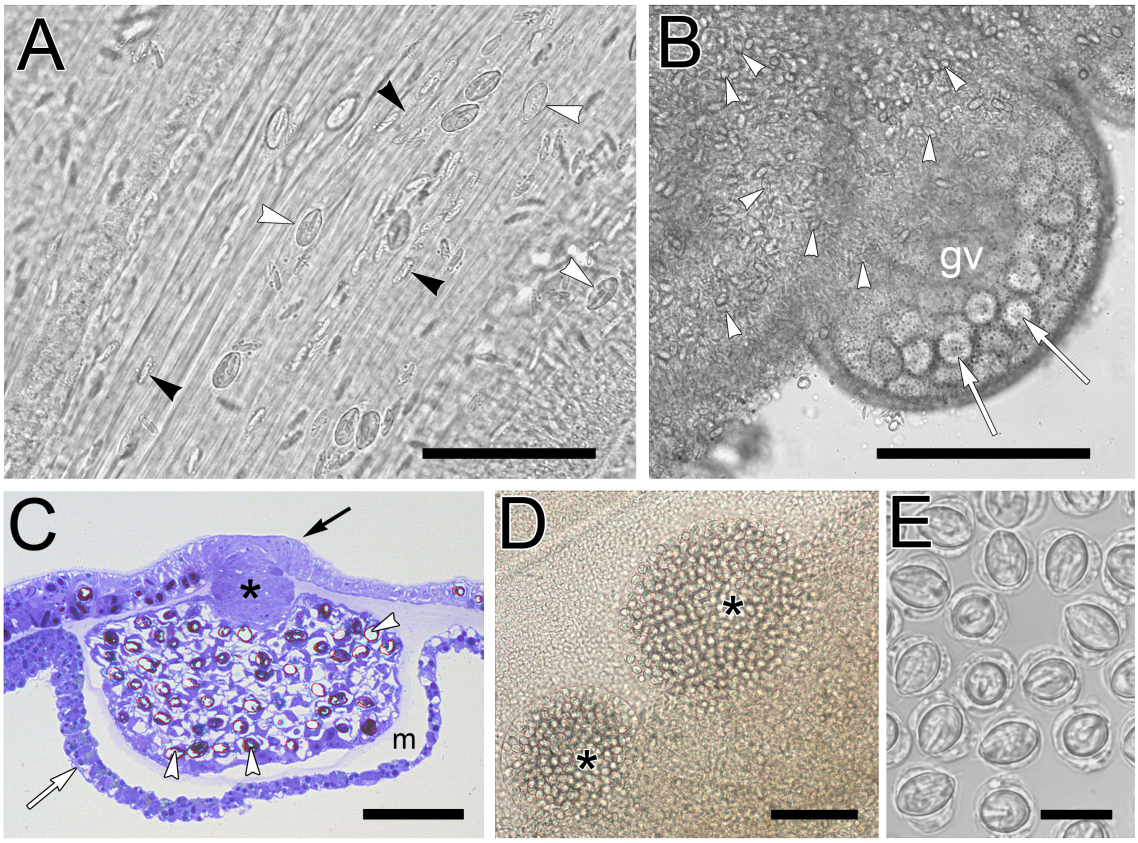


Figure 22. Brightfield images of whole mounted (**A, B, D, E**) and sectioned (**C**) tissues of *H. 'sanjuanensis'* showing nematocyst distributions in muscle, gonad and nematocyst clusters. **A:** Euryteles (white arrowheads) and isorhizas (black arrowheads) embedded in the marginal muscle; note that the eurytele capsules point in both directions along the muscle fibers. Scale bar, 80 µm. **B:** Gonadal vesicle with nematocysts (arrowheads) embedded in the epithelium from which it hangs. Eggs (arrows) are visible through the vesicle wall. Scale bar, 200 µm. **C:** Histological section of a subumbrellar nematocyst cluster. Note bump in the subumbrellar epidermis (black arrow) corresponding to the apex of the cluster, ball of cells connecting the cluster to the subumbrellar epidermis (asterisk), gastrodermis surrounding the cluster (white arrow), and solid ball of nematocytes with nematocysts (arrowheads) within the pocket. Scale bar, 50 µm. **D:** Whole mount of clusters seen through subumbrellar surface. Asterisks indicate the apices of the clusters. Scale bar, 200 µm. **E:** Nematocytes containing eurytele nematocysts that spilled from a cut cluster. Scale bar, 20 µm. **Abbreviations:** gv, gonadal vesicle; m, mesoglea.

The gastric filaments were densely ciliated and arranged in fanlike clusters, where many filaments were joined at the base. The cells on one side of the gastric filaments contained granular material that flowed out in spherical globules when the filaments were squashed. The epithelium of the gastric filaments had scattered euryteles, which were more abundant at the tips of the filaments than the bases (Fig. 23A). These nematocysts were similar in shape to those in the nematocyst clusters, but were highly variable in size (Fig. 23B).

Small patches (batteries) of nematocysts were distributed evenly over the exumbrellar surface of the calyx and stalk: patches of 1-10 were common (Fig. 23C). Patches tended to consist of fewer nematocysts on smaller animals. The ectodermal nematocysts were eggplant-shaped: slightly curved, and pointed at one end (Fig. 23C, inset). I was not able to resolve the filament of these nematocysts or induce discharge; although many of them had a slightly darker core, it was not distinct like the inverted shaft of the subumbrellar euryteles.

Nematocysts were absent or nearly so on the anchors and pedal disc. The tentacle remnant bore nematocysts similar to the secondary tentacles. Large, lucent glandular cells of the anchors and basal disc were apparent with light microscopy. On the anchors, a strip of glandular cells surrounded the tentacle remnant and extended along the subumbrellar midline of stalk. Scattered glandular cells surrounded this main strip (Fig. 23D, E).

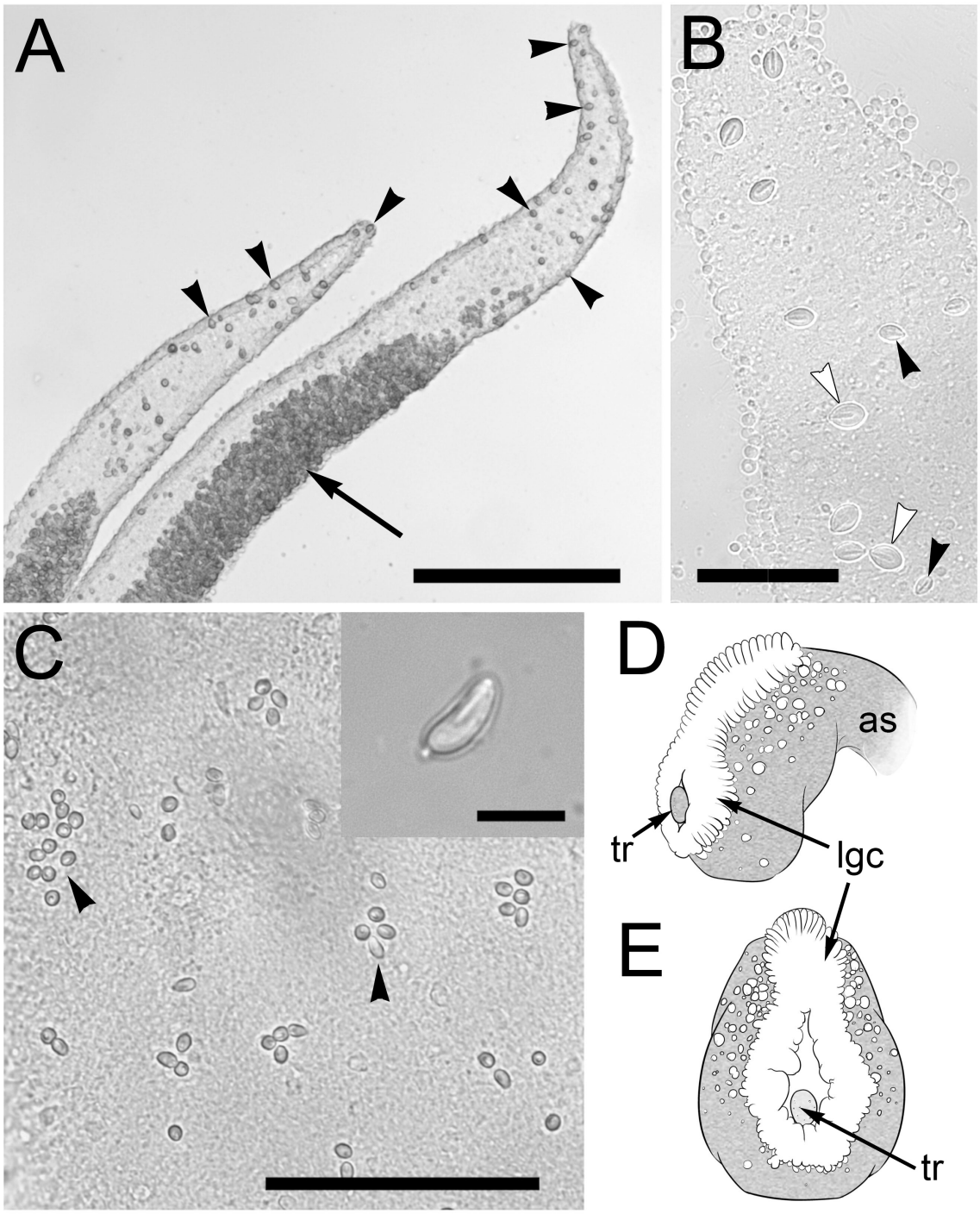


Figure 23. Brightfield images of whole mounted *H. 'sanjuanensis'* specimens showing nematocyst distributions in the gastric filaments and exumbrella. **A:** Nematocysts were studded along the gastric filaments (arrowheads), and concentrated towards the tip of the filaments. One side of each filament was composed of cells containing granular material (arrow). Scale bar, 200 μm. **B:** Squashed gastric filament tip showing large (white

arrowheads) and small (black arrowheads) euryteles. Scale bar, 40 um. **C:** Large and small nematocyst batteries (arrowheads) were embedded in the epithelium of the exumbrella. Scale bar, 100 um. **Inset:** exumbrellar nematocysts were eggplant-shaped. Scale bar, 10 μm. **D:** Diagrammatic representation of lateral and frontal views of a well-developed anchor showing distribution of lucent glandular cells (white) and tentacle remnant. **Abbreviations:** as, anchor stalk; lgc, lucent glandular cells; tr, tentacle remnant.

3.3.2 Nematocysts of *Manania handi*

Similar nematocysts were found in similar locations in both *Manania handi* and *Haliclystus* '*sanjuanensis*'.

The epidermis of the tentacle capita in *M. handi* was covered with sausage shaped isorhizas (Fig. 24A-C). These were longer than the corresponding nematocysts of *H. 'sanjuanensis'*, and were arranged such that their curves fit against the adjacent nematocysts to form a tightly packed, uninterrupted layer on the surface of the tentacle (Fig. 24A). Below this layer were unevenly staggered layers of nematocysts, presumably waiting to take the place of surface nematocysts when they are spent (Fig. 24A). Euryteles studded the distal tentacle capita, but were much fewer than in *H. 'sanjuanensis'* tentacles (Fig. 24B). Similar to *H. 'sanjuanensis'*, nematocysts with the long axis oriented parallel to the longitudinal muscle fibers and non-discharging end pointing towards the capitum were present in streams in the epidermis of the tentacle stalk.

The surface of each tentacle capitum had short projections that extended from the nematocyst layer (Fig. 24A). There were far fewer projections than nematocysts, so if these were sensory triggers for nematocyst capsules it is doubtful that there is a one-to-one correspondence between trigger and nematocyst. These projections extended about 4.5 μm away from the tentacle surface.

Manania handi did not appear to have nematocysts associated with the gonads, and few nematocysts were embedded in the marginal muscle. Portions of the longitudinal muscles and more superficial perradial muscles were packed with nematocysts like those of the tentacle capita, and nematocysts were abundant around the bases of the tentacles.

Those nematocysts embedded in the muscle fibers were generally parallel to them (Fig. 24D).

The nematocysts of the clusters were large euryteles. They were disorganized within the cluster, and spilled freely from it when it was pierced (Fig. 25A-D).

Lemon-shaped euryteles were concentrated on the lips of the manubrium (Fig. 25D) and scattered along the perradial corners, but the interradial faces bore very few nematocysts.

Nematocysts of the gastric filaments were distributed similarly to those of *H. 'sanjuanensis'* but varied less in size. These nematocysts were similar in shape to those of the nematocyst clusters and manubrium, but much smaller (Fig. 26A).

The exumbrellar ectodermal nematocyst patches of *M. handi* were not distributed as evenly as those of *H. 'sanjuanensis'*, and tended to be much larger (Fig. 26B). Each battery was borne on a tubercle or raised portion of epidermis. The patches were smaller and further apart where they directly overlaid the marginal circular muscle, and most concentrated in a band directly below the marginal muscle. Spacing between patches was slightly wider and patches were smaller from mid-calyx to the peduncle base. These nematocysts were ellipsoid, and did not have the typical eggplant shape of the exumbrellar nematocysts of *H. 'sanjuanensis'* (Fig. 26C).

A very few ellipsoid euryteles were embedded in the epidermis of the adhesive pads (Fig. 24D); where the glandular tissue connects to the unmodified tentacle tissue, there were more nematocysts, including sausage shaped isorhizas and ellipsoid euryteles. These nematocysts were similar to those occupying the tentacle capita. No nematocysts were found on the pedal disc.

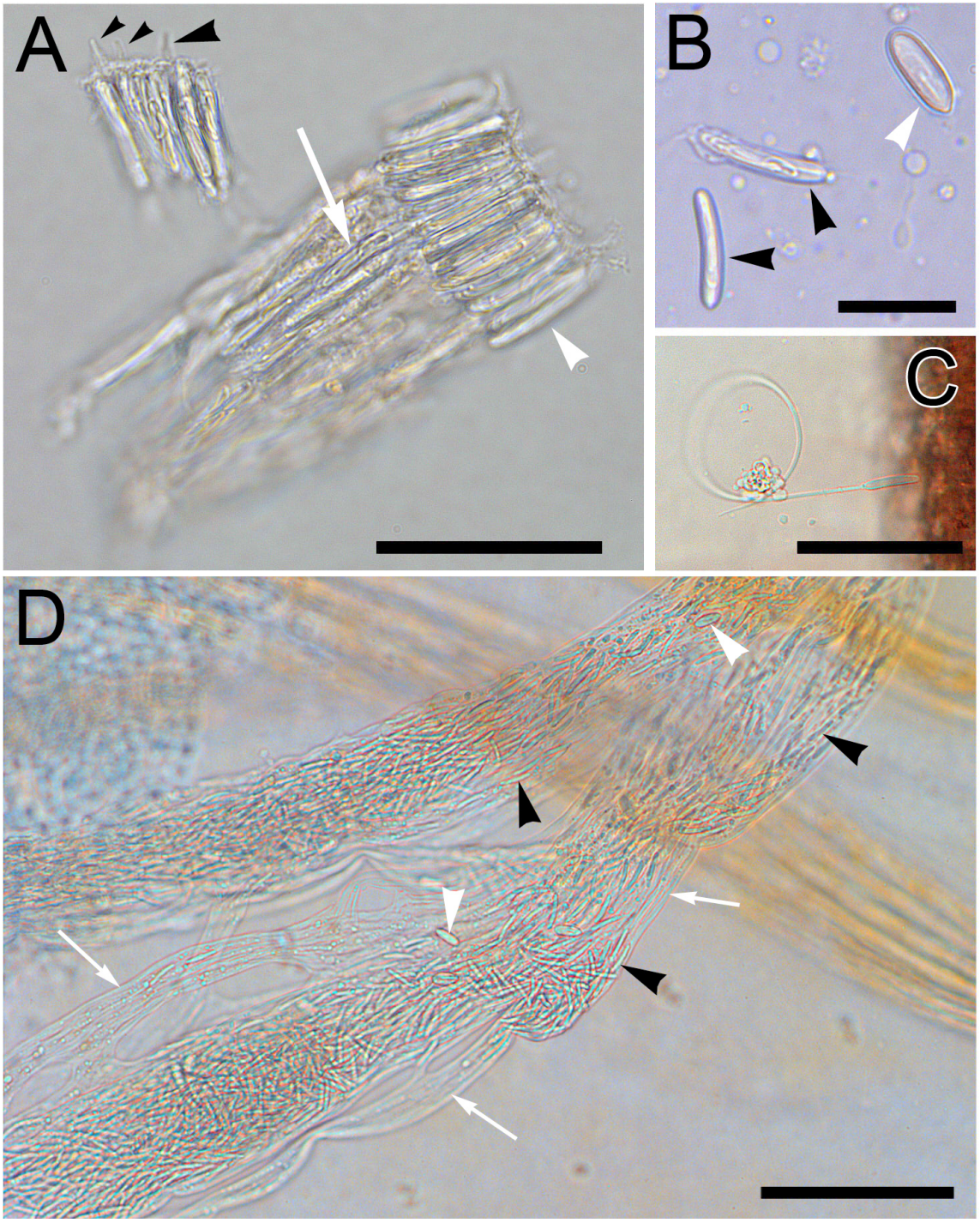


Figure 24. Brightfield images of whole mounted *M. handi* specimens showing nematocyst distributions in the tentacles and muscle bands. **A:** Portion of the epithelium of the tentacle capita showing tightly packed nematocysts in the apical layer (white arrowhead) and disorganized nematocysts in layers beneath that (arrow). Projections extended from the surface of the tentacles (black arrowheads), corresponding to the

projections labelled with fluorophore-tagged phalloidin. Scale bar, 40 μm. **B:** Undischarged isorhizas (black arrowheads) and a eurytele (white arrowhead) from a tentacle capitum. Scale bar, 20 μm. **C:** Discharged tentacle isorhiza. Scale bar, 50 μm. **D:** Many isorhizas (black arrowheads) and euryteles (white arrowheads) were embedded in the perradial muscle fibers (arrows); note parallel orientation of many nematocysts. Scale bar, 100 μm.

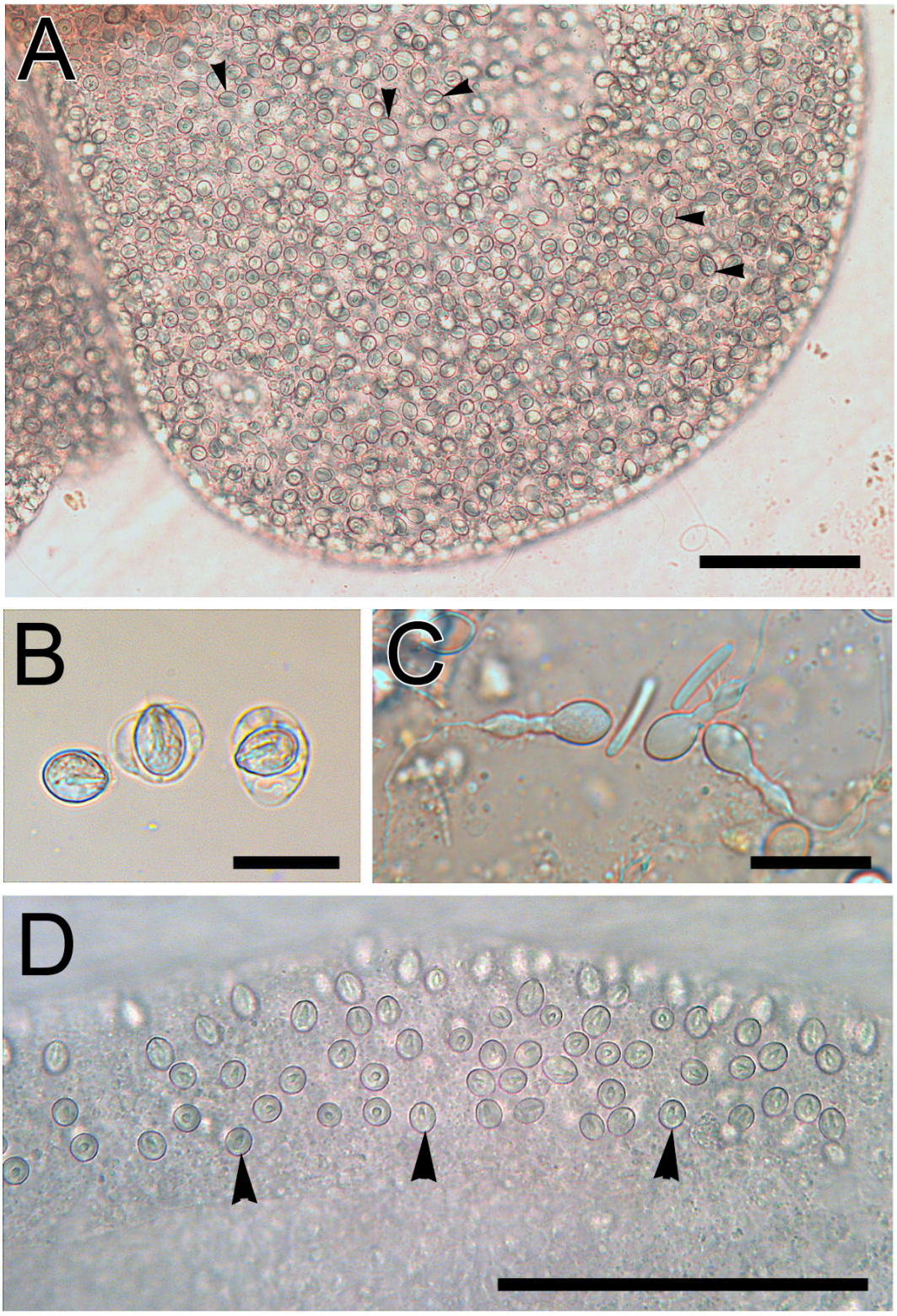


Figure 25. Brightfield images of whole mounted *M. handi* specimens showing nematocyst of the clusters and manubrium. **A:** Whole mount of a cluster exposed by

peeling away the gastrodermis. Each cluster contained a huge number of nematocysts which were disorganized. Scale bar, 100 µm. **B:** Isolated cluster nematocytes with nematocysts that spilled from a pierced nematocyst cluster. Scale bar, 25 µm. **C:** Discharged cluster nematocysts had the barbed bulb and filament characteristic of microbasic heterotrichous euryteles. Scale bar, 25 um. **D:** Euryteles (arrowheads) were concentrated on the lip of the manubrium. Scale bar, 100 µm.

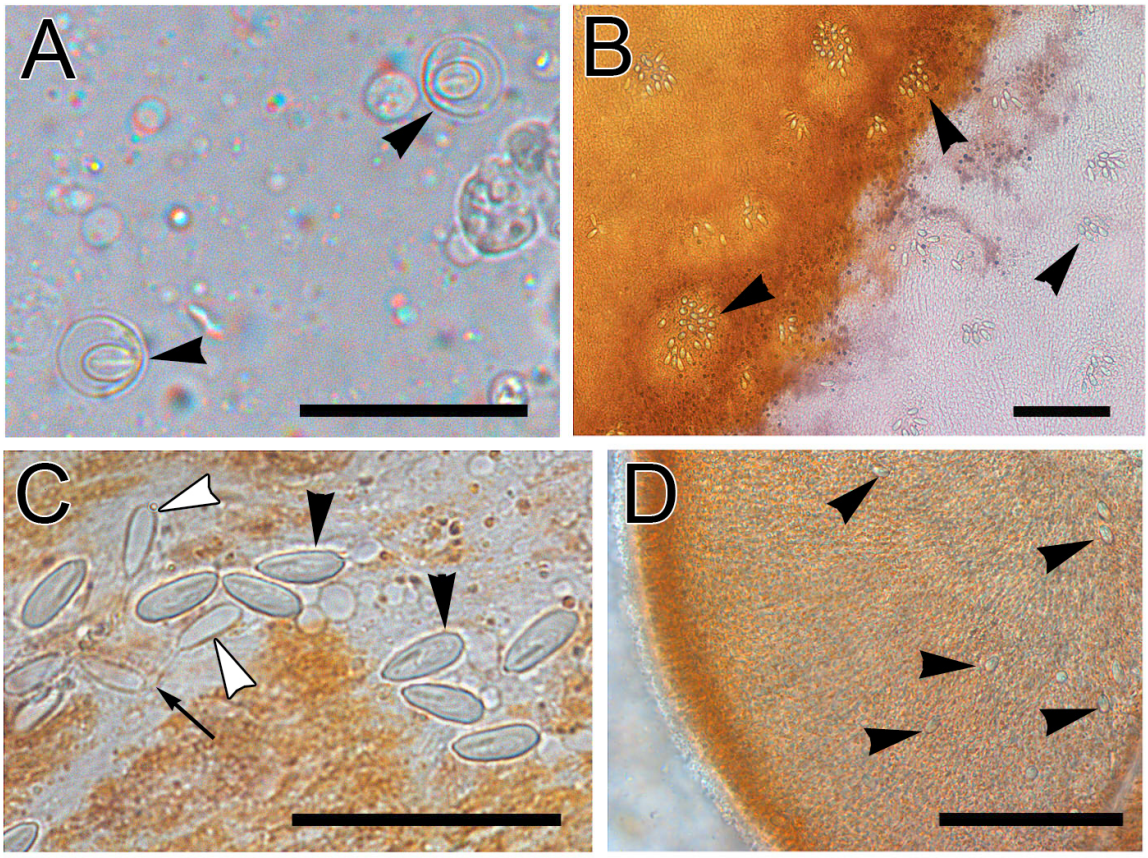


Figure 26. Brightfield images of whole mounted *M. handi* specimens showing nematocysts of the gastric filaments, exumbrella and adhesive pads. **A:** Nematocysts of the gastric filaments were similar in shape to those of the clusters (arrowheads). Scale bar, 25 µm. **B:** Patches of exumbrellar nematocysts studded the exumbrellar epidermis (arrowheads). Scale bar, 100 µm. **C:** Isolated exumbrellar nematocysts, discharged (white arrowheads) and undischarged (black arrowheads). A slight swelling in the filament (arrow) indicates that the exumbrellar nematocysts may be euryteles. These nematocysts lack the distinct eggplant shape of the exumbrellar nematocysts of *H. 'sanjuanensis'*.

Scale bar, 50 μm. **D:** The adhesive pads were studded with a few euryteles (arrowheads). Scale bar, 50 μm.

3.4 Behaviour

3.4.1 Behaviour of *Haliclystus 'sanjuanensis'*

3.4.1.1 Behavioural Observations in the Field

Haliclystus 'sanjuanensis' in the wild were always attached by the basal disk. Some use of anchors for anchorage was additionally observed. The posture of specimens was relaxed, with arms extended and offering no resistance to movement by the water. Even very vigorous agitation by waves did not appear to perturb *H. 'sanjuanensis'*. Frequent contact with conspecifics and environmental factors such as seaweed or rock produced no response.

Differential habitat use was observed for size classes of *H. 'sanjuanensis'*. Small individuals were only found in more sheltered locations with less wave action, and were highly abundant on the filamentous red alga *Odonthalia floccosa.* Juveniles larger than approximately 10 mm in diameter were found on a greater variety of algae, and the largest specimens (adults with developed gonads) were the only size class abundant in flow channels and rocky shore locations that received more water agitation. The adults were also the only size class commonly found on *Phyllospadix*.

The smallest *H. 'sanjuanensis'* polyps observed in this study were found near Cattle Point on San Juan Island WA, exclusively on the epiphytic filamentous brown alga *Ectocarpus* growing on *Desmerestia.* Several polyps with no distinct tentacles or mouth were found; the smallest of these was 100 μm long and was little more than an oblong with four equally spaced bumps at the apex indicating development of the first tentacles. Larger *H. 'sanjuanensis'* were also present at the Cattle Point site on a variety of algae, as they were at Chinese Cemetery. *Ectocarpus* and *Desmerestia* were not present at Chinese Cemetery, and the only other filamentous alga present at Chinese Cemetery, *Acrosiphonia*, was never inhabited by staurozoans, although it was densely inhabited by appropriate food sources such as copepods, nematodes and small amphipods.

3.4.1.2 Laboratory Observations of Behaviour

Health and Animal Maintenance

Specimens were maintained in custard bowls, where they usually lay on their sides with the stalk attached. The condition of laboratory-held animals soon deteriorated; none survived longer than six weeks and no growth was observed. This may be due in part to the lack of wave agitation in the lab, and unnatural stresses imposed on the animals by resting on a hard surface. Larger animals were particularly susceptible to laboratory conditions and often began to deteriorate after only two to three days. Two attempts were made to provide the larger animals with a more natural setting. First, animals were placed in a mesh basket filled with algae in the flow-through sea table, providing them with a constant supply of fresh seawater and gentle agitation; however, this did not slow degeneration. Second, specimens (~10 per bowl) attached to small pieces of the seaweed they were collected on were placed in large glass bowls of seawater agitated with automated paddles (Plexiglas, approximately 50x75 mm and 5 mm thick) and incubated at 13°C; survival was extended to several weeks using this method. Water was changed every two days. Large specimens maintained in this way were frequently observed to change their place of attachment using their anchors for temporary adhesion. When left undisturbed overnight on pieces of seaweed, 2-4 individuals were usually attached to the paddle by their basal disc in the morning. If these were removed, the paddle would again be colonized by the following day.

Attempts were made to induce spawning in *H. 'sanjuanensis'*. In mid-September 2014, 10 bowls each containing a pair of adults were illuminated with lamps to increase brightness and to gradually raise the temperature of the seawater to 20°C over 5 h. Although the animals began to show signs of distress and contracted into a protective posture, no spawning was observed, and the experiment was terminated. One animal collected in May 2015 spawned spontaneously in the laboratory; the eggs were 35 µm in diameter and were released from the manubrium in sticky strands (Fig. 27A). Patches of ruptured gonadal vesicles from which the eggs had been released were apparent (Fig. 27B).

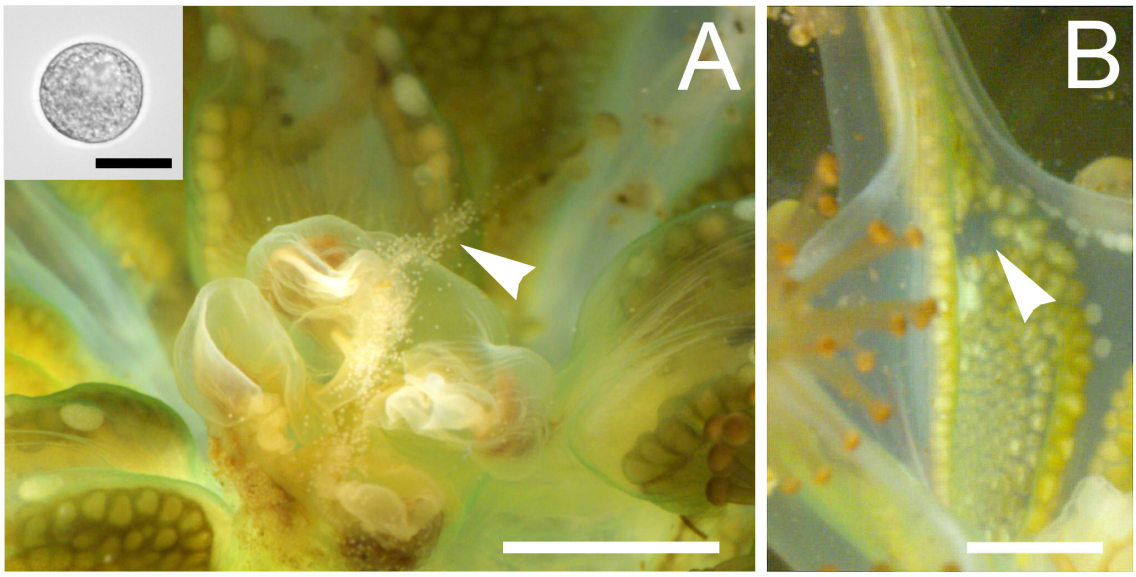


Figure 27. Spawning in *H. 'sanjuanensis'*. **A:** Eggs were released from the manubrium in strands held together by mucus (arrowhead). Scale bar, 2 mm. **Inset**, whole mounted egg. Scale bar, 25 µm. **B:** A patch of gonadal vesicles was left empty after the spawning episode (arrowhead). Scale bar, 2 mm.

Spontaneous Movement and Response to Inorganic Stimuli

Movement in the lab included abrupt rolling to one side or the other, with no apparent initiating stimulus and no associated retraction of arms or tentacles. No directional preference for this behaviour was noted. This may represent a 'searching' behaviour used to sample the environment for prey. Other spontaneous behaviours included partial or complete bending of an arm or arms to the manubrium, and intermittent flexing of tentacles.

Metal and glass probes were used to stimulate the tentacle bunches, manubrium and subumbrellar surface of freshly caught animals. Animals usually did not respond beyond a slight twitch of an arm or tentacles unless the prodding was strong enough to displace or injure the animal. Glass and metal probes dragged repeatedly through tentacle bunches produced no response.

Adhesion of the Basal Disc

Effective adhesion by the basal disc was maintained even when only a small portion of the basal disc was in contact with the substrate (Fig. 28A), and could be maintained after death or dismemberment; animals that were fixed while adhered by the basal disc maintained attachment until manually detached. Reattachment did not occur after death. Tensile adhesive strength of the basal disc was very high; pulling on the animal while it was attached by the basal disc would often damage the animal before adhesion failed. However, shear adhesive strength was low; gentle pressure applied laterally to an attached basal disc easily disrupted adhesion. Animals that had adhered to objects smaller than the diameter of their basal disc molded the disc around the object in question to increase contact with the substrate. When an animal was removed from the substrate it was collected on, the basal disc peeled out of a putative periderm: a small, stiff, semitransparent cup, which consisted of a flat disc on the substrate and walls that reached a short distance up to embrace the basal disc (Fig. 28B). The outside of the cup was often encrusted with algae and diatoms (Fig. 28B). Once the animal attached to a new substrate, it produced a new cup after several hours (Fig. 28C). All *H. 'sanjuanensis'* that were examined produced these cups, from the smallest juveniles to the largest adults.

Tentacles and Feeding Behaviour

The tentacles of *H. 'sanjuanensis'* never shorten when contracted as most cnidarian tentacles do; staurozoan tentacles always bend (flex) without shortening. Tentacles flexed with or without associated arm movement, and all tentacles in the bunch, a small section of the bunch, or individual tentacles could flex independently. Flexing was spontaneous or in response to a stimulus. Individual tentacle flexing was frequent in relaxed, apparently unstimulated animals. During an individual tentacle flexion the capitum described a circle (Fig. 29A). The circle varied in size depending on the degree of tentacle flexion, and both clockwise and counter-clockwise circling was observed. The tentacles were highly sensitive: contact with anything that was a possible food source caused strong adhesion of the tentacles and retraction of the associated arm.

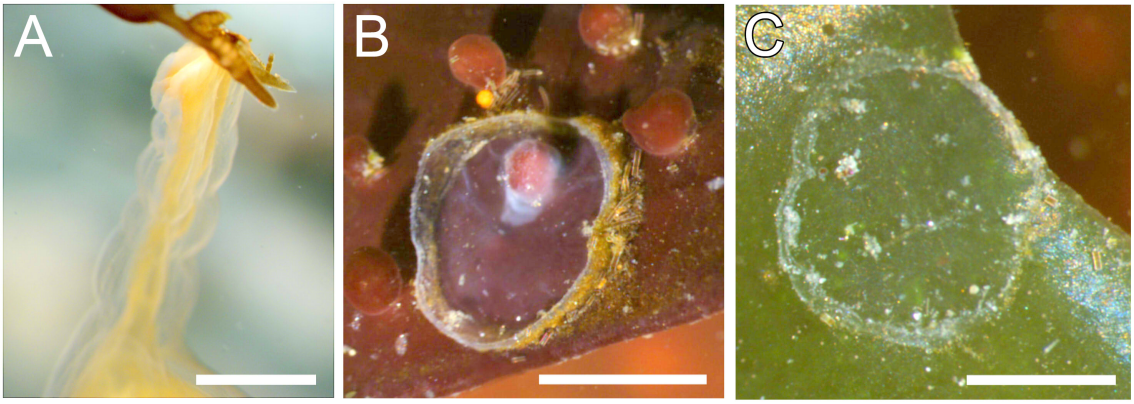


Figure 28. Adhesion of the basal disc in *H. 'sanjuanensis'*. **A:** Effective adhesion was maintained even when only a small portion of the basal disc was in contact with the substrate. Scale bar, 1 mm. **B:** A putative periderm that surrounded the basal disc of a specimen when it was collected. The short walls were encrusted with algae and diatoms. Scale bar, 2 mm. **C:** Putative periderm produced by an animal detached from its place of adhesion and then left 3 h to produce a new one. The walls were much shorter than those found on animals that had been attached for an extended period of time, and it was not encrusted with diatoms or algae. Scale bar, 1 mm.

Adhesion to a potential prey item was strong enough that the animal could be pulled to the air-water interface when attached to a finger by one tentacle bunch, and out of the water if attached by more than one. Adhesion by the tentacles was not prolonged, strong or commonly initiated unless it was to a potential food item. *H. 'sanjuanensis'* tentacles adhered strongly to glass, plastic or metal, but only did so if handled roughly or prodded extensively with a probe. Tentacles were sometimes torn off if an effort was made to remove the animal from the substrate it had adhered to. Tentacle bunches could be pulled off of human skin without any apparent damage to the animal, but a 15 mm *H. 'sanjuanensis'* presented with an 8 mm amphipod had many of its tentacles ripped off as the prey struggled and escaped.

Haliclystus 'sanjuanensis' were selective of their potential food sources. *Haliclystus 'sanjuanensis'* always adhered to *Artemia* nauplii, fingertips, or to small (5-10 mm) amphipods regardless of relative size. However, 10-15mm isopods that were collected with *H. 'sanjuanensis'* were able to crawl all over the body and tentacles of the

animal with no response (Fig. 29B). One isopod appeared to attack the *H. 'sanjuanensis'* it was crawling on; a brief bout of thrashing dislodged the isopod and the staurozoan appeared undamaged. Protist-like animals crawling over *H. 'sanjuanensis'*, were also ignored. Small nematodes sometimes elicited a feeding response and were ingested, but I also observed thrashing nematodes captured by distal tentacle nematocysts, while no effort was made to ingest it. Dense ciliate communities dominated by *Euplotes* were present in the infundibula of *H. 'sanjuanensis'* collected in May 2015, but it is unknown whether this is common in the wild or was introduced by lab conditions.

Once the tentacles captured a prey item, the arm was immediately bent in to the manubrium. If the prey was large, or there were several prey items, several or all of the arms were often bent in to the manubrium. Bending of an arm or arms was often accompanied by bending or twisting of the stalk. Full bending of one arm to the manubrium caused the stalk to bend towards the substrate in the direction of the bending arm. If multiple arms bent successively, the calyx tilted successively as each arm produced directional bending.

When provided with a large food item or many small prey, *H. 'sanjuanensis'* sometimes performed a 'faceplanting' behaviour. The animals bent the stalk to bring the calyx rim in contact with the substrate while folding in some of the arms, adhered to the substrate with an anchor, and then detached the basal disc so that the subumbrella was pressed against the substrate, over the food item (Fig. 29C).

Spontaneous bending of single and multiple arms was observed in all specimens. Adjacent arms often folded inward in quick succession; these were perradial pairs (adjacent arms supplied by different longitudinal muscles) as often as interradial pairs (adjacent arms supplied by same longitudinal muscle) (Fig. 29D). Asymmetrical configurations of bent arms such as a perradial pair and interradial pair on opposite sides of the bell plus an additional arm adjacent to neither of them were common. When all arms were folded to the manubrium, they were never folded in synchrony, but rather in quick succession. Some arms often unfolded while others continued to periodically contract. No regular patterns were observed. A strong stimulus (such as food or damage) caused bending of all the arms such that the tentacles were largely or completely concealed by the exumbrellar surface of the arms pressing together at the center, usually

accompanied by strong retraction of the stalk (Fig. 29E). Arm bending was not an all-or nothing response: bending was sometimes swift and accompanied by a jerk of the body in the direction of the folding arm, and sometimes slow and gradual. Arm movement in *H. 'sanjuanensis'* always appeared languid due to the thickness of the arm mesoglea and the large distance from arm tip to manubrium. After a stimulus was applied, the arms were often held to the manubrium for an extended period, usually accompanied by periodic contractions of the arms and stalk that result in "scrunching" motions, bringing the arms closer to the manubrium and the animal closer to the substrate. Even after the stimulus was no longer present, the animal often remained agitated for 15-30 minutes.

Anchors

The anchors did not participate in feeding behaviours as the secondary tentacles did; their sole purpose appeared to be as adhesive organs. Although the anchors allowed pivoting and bending during adhesion, they did not have independent movement. As they do not have muscle fibers when fully developed (see above) this is unsurprising.

Although the large, lucent cells that presumably produce glandular secretions involved in adhesion were concentrated along the subumbrellar midline of the anchor and around the tentacle rudiment (Fig. 23D), adhesion occurred via any part of the large swelling that constitutes the anchor. A single anchor appeared to hold the animal in place as securely as did the basal disc; adhesion by anchors to glass or seaweed was secure enough that vigorous and jerky agitation did not dislodge the animal. Several anchors were often used simultaneously (Fig. 30). Adhesion of the basal disc and anchors was similar in that the adhesion had high tensile strength but low shear strength. All size classes of *H. 'sanjuanensis'* used anchors extensively. Anchor adhesion in juveniles was not hindered by the fact that their adhesive pads were not fully developed. I observed effective adhesion of a tiny 1 mm long juvenile with just three secondary tentacles per bunch by a single anchor that had barely started to develop glandular swelling.

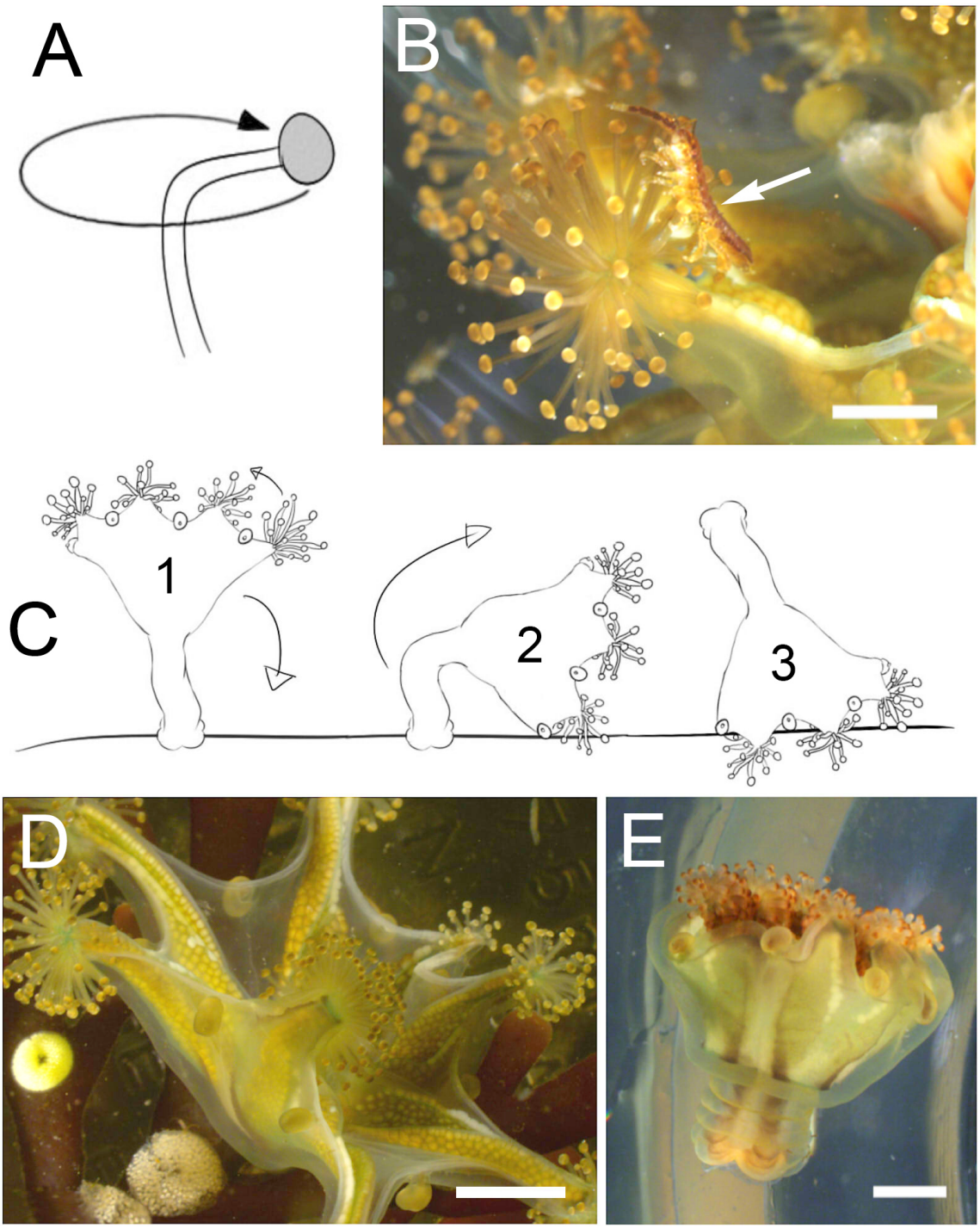


Figure 29. Various behaviours observed in *H. 'sanjuanensis'*. **A:** Characteristic circular contraction of a tentacle. The tentacle could bend at any point along the shaft prior to describing a circle. **B:** Small isopod (arrow) crawling on a tentacle bunch without eliciting a response from the staurozoan. Scale bar, 2 mm. **C:** Progression of the 'faceplanting' behaviour exhibited during feeding. 1) Prey is caught on a tentacle bunch;

2) the tentacle bunch or bunches are folded in to the manubrium. At the same time, the stalk bends to the substrate in the direction of the bending arm. 3) Anchors attach the animal to the substrate and the stalk is released such that the oral surface is pressed against the substrate. **D:** A single arm is bent to the manubrium. Scale bar, 4 mm. **E:** Full contraction of the stalk and arms as observed during protective behaviours or when large prey is provided. Scale bar, 2 mm.

Anchors readily adhered to any available substrate (glass, metal, seaweed, plastic) when the animal or its substrate was agitated. If basal disc adhesion was disrupted and the animal was allowed to float freely, the animal would without fail adhere to the first thing an anchor came in contact with, however brief the contact. If the anchors of a relaxed animal were prodded with the same substances, adhesion usually did not occur. However, if a probe was used to press an anchor firmly against a substrate, adhesion usually occurred, and the animal may thus be pinned out using its anchors.

Animals adhering by anchors alone eventually bent the calyx and stalk to bring the basal disc in contact with the substrate for adhesion. Once the basal disc was secure, the anchors were eventually released. Animals were observed to maintain anchoring for tens of minutes, but usually anchors were released shortly (a few seconds) after jostling ceased.

Manubrium, Subumbrella and Exumbrella

The manubrium was active independent of the arms. Movements included shifting of the whole manubrium within the subumbrella, and gaping and ruffling of the lips. The manubrium usually shifted along the perradial axes (where the radial muscles are positioned) but could also move towards an interradius through simultaneous contraction of two radial muscles. During feeding, the manubrium moved towards the arm or arms that captured prey.

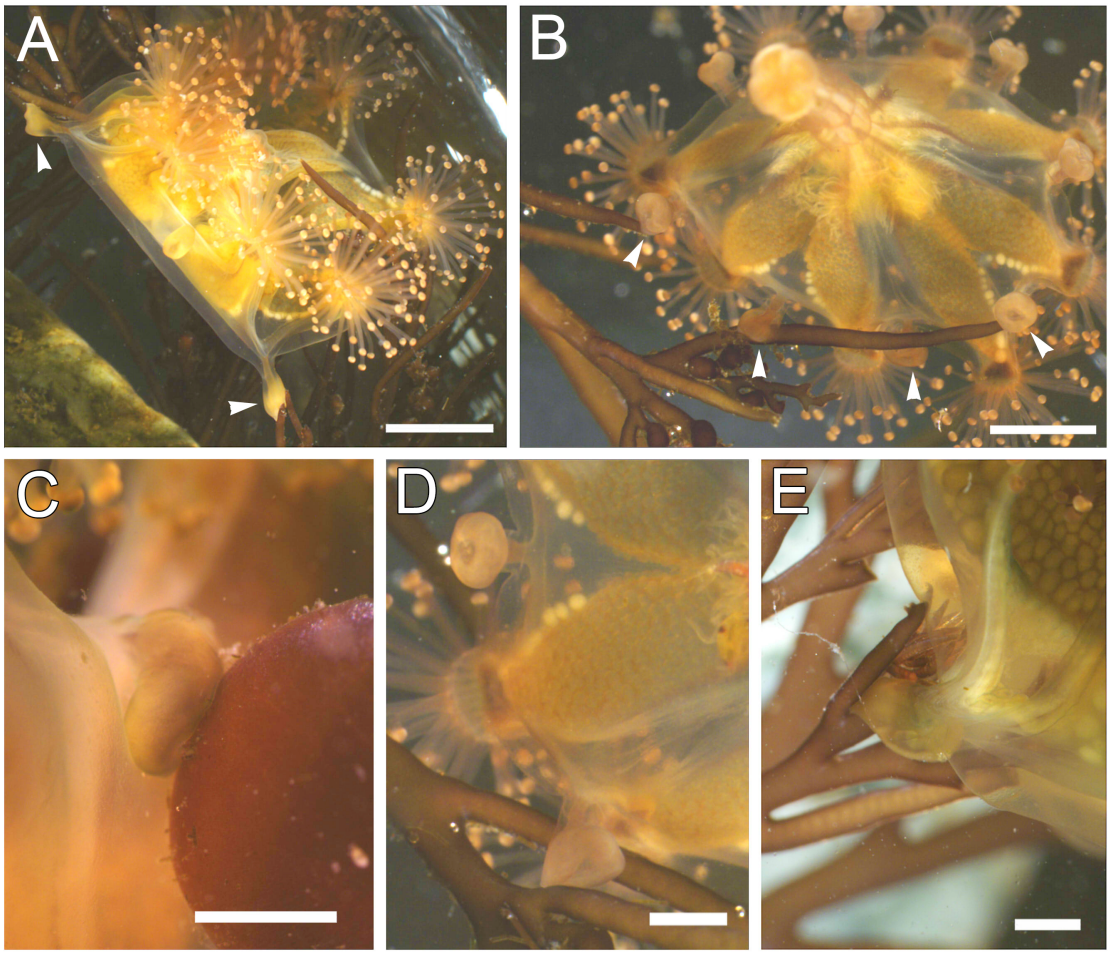


Figure 30. Anchoring in *H. 'sanjuanensis'*. **A:** Staurozoan stretched between two anchors (arrowheads). Scale bar, 4 mm. **B:** Staurozoan using four anchors (arrowheads) to adhere to the algal substrate; the basal disc is not adhered. Scale bar, 4 mm. **C:** Anchor attached by area surrounding the tentacle remnant. Scale bar, 1 mm. **D:** Two attached anchors, one attached by the extreme subumbrellar surface of the anchor, the other by a portion of the side of the anchor. Scale bar, 1 mm. **E:** Anchor attached by its distal tip. Scale bar, 1 mm.

The subumbrellar surface was not sensitive to stimulation; a response was only elicited when stimulation with a blunt probe deformed or shifted the animal. This response usually took the form of the animal twisting away from the probe or folding in one or more arms to the site being stimulated.

The exumbrella was insensitive to stimulation: sustained, vigorous prodding rarely resulted in a response of any kind. The basal disc was more sensitive and prodding usually caused some contraction of the calyx.

3.4.2 Behaviour of *Manania handi*

3.4.2.1 Behavioural Observations in the Field

M. handi were found in relaxed postures hanging from wave-swept *Phyllospadix*. Most animals found were adults over 20 mm long with developed gonads. Juveniles with incomplete gonads that were observed in the field did not behave differently from adults.

3.4.2.2 Laboratory Observations of Behaviour

Animal Health and Maintenance

Pieces of *Phyllospadix* that the specimens were collected on were arranged in beakers so that the animals were suspended in the water beneath the grass frond. *M. handi* were not maintained in the lab as long as *H. 'sanjuanensis'*. *M. handi* did not accept *Artemia* nauplii as a food item. Although *Artemia* that came into contact with the tentacles were killed, *M. handi* made no apparent effort to ingest them and the dead nauplii fell to the bottom of the beaker. Although feeding attempts were unsuccessful, three 2014 specimens were maintained for 2-3 weeks. Of these, one deteriorated and died, one did not show any signs of deterioration, and the largest 30mm long specimen spawned eggs during several successive days. Five of the largest specimens (25-40mm long) collected in 2015 were maintained in the lab for 1 week; all of these spawned eggs daily for five days, at which point the animals began to deteriorate. As the animals were suspended above the substrate, the eggs formed a small white mound underneath each animal every morning. Spawning was never observed, and must have occurred overnight between 5 pm and 9 am. The eggs were about 30 μm in diameter (Fig. 31A).

Arm Movements

The arms of *M. handi* were shorter and had thinner mesoglea than those of *H. 'sanjuanensis'*, and the arm movements of these two species were very different. As the arms of *M. handi* are so short, they are less dextrous than those of *H. 'sanjuanensis'*. Contractions and rebound of *M. handi* arms were very swift, giving the animals a "twitchy" appearance. Most spontaneous arm movement consisted of arms twitching

towards each other (from side to side around the rim) rather than bending towards the manubrium. When arm bending towards the manubrium did occur, the short arm rotated around the calyx rim towards the manubrium. Due to the depth of the calyx and length of the arms, this action did not result in the arm contacting the manubrium. To contact the manubrium, several or all of the arms bent together (Fig. 31B). These arms were pressed together and down into the calyx such that the side of the calyx bearing the contracting arms became longitudinally crumpled (Fig. 31C). Quadrants of the calyx wall were also periodically contracted and compressed independent of arm bending. When all arms bent simultaneously, the calyx accordioned and became compressed longitudinally. This could be accompanied by or independent of stalk contraction (Fig. 31D).

Arm bending was not coupled to stalk contraction as it was in *H. 'sanjuanensis'*. When arm and stalk contractions did occur simultaneously, it resulted in a swift motion that oriented the axis of the calyx parallel to or slightly pointing towards the substrate. Bending of multiple arms usually involved multiple arms on one side of the bell which contracted successively or in concert. If prodded or stressed (*e.g.* by a sudden temperature change) *M. handi* contracted instantaneously and completely; the arms drew in and calyx and stalk contracted like an accordion, flattening longitudinally (Fig. 31D). Three adjacent arms often folded together in a specific pattern: the central arm bent to the manubrium while the two peripheral ones bent towards each other and the center, pleating the margin (Fig. 32A).

Manania handi also displayed occasional synchronous contraction of the margin, such that the arms met in the center with all the tentacles pointing straight up (Fig. 32B). Occasionally one or several arms were partially folded in during this type of contraction. These contractions were brief, coordinated, and apparently spontaneous. Water was expelled from the calyx during these contractions and the calyx was pushed back slightly against the stalk. Contraction of the marginal circular muscle was not all-or-nothing; animals were frequently observed to partially contract the marginal muscle and maintain that contraction (Fig. 32C), such that the edge of the calyx was narrowed or pursed, but not completely closed.

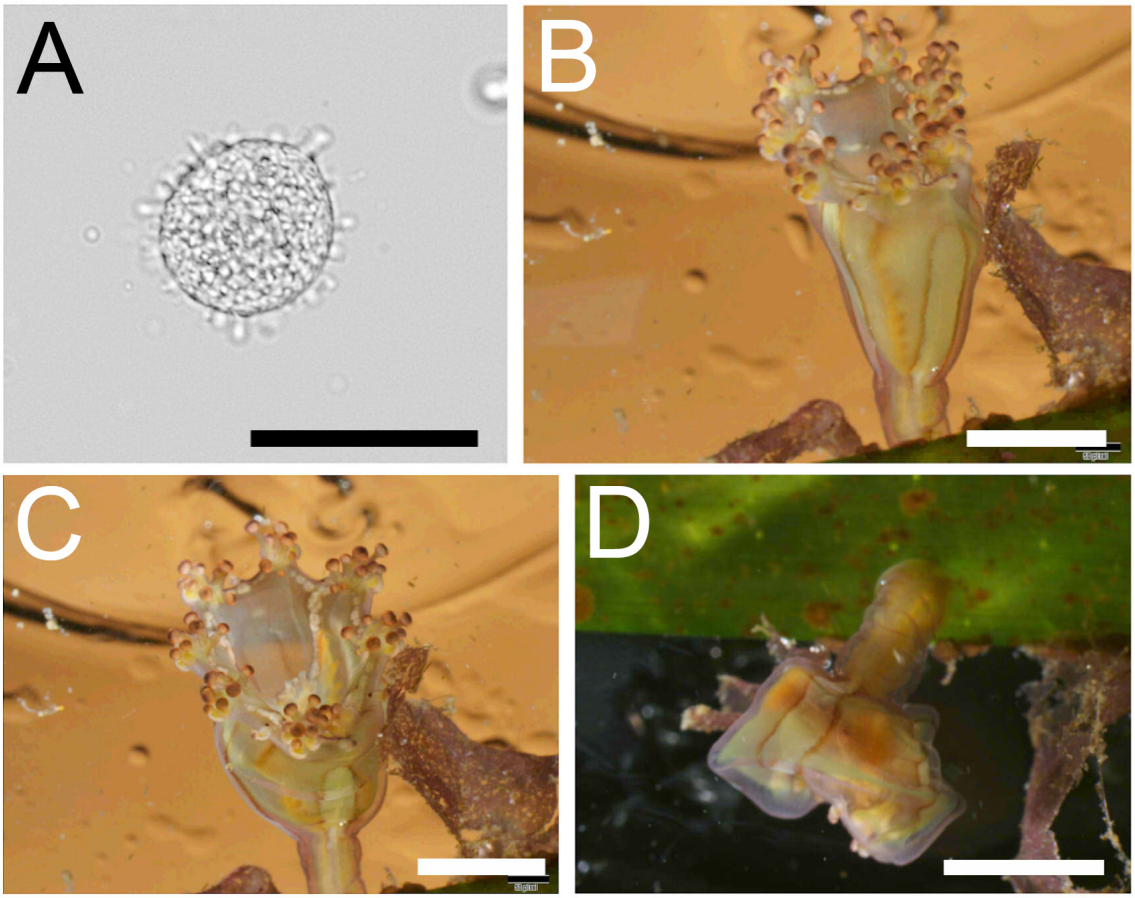


Figure 31. Behaviours of *M. handi*. **A:** Whole mount of *M. handi* egg. Scale bar, 40 um. **B:** Three arms are bent towards the manubrium together. Scale bar, 4 mm. **C:** Contraction of one interradial quadrant of the calyx wall. Scale bar, 4 mm. **D:** Complete contraction of stalk and calyx during protective response. Scale bar, 4 mm.

Stalk

Manania handi was not observed to voluntarily detach its basal disc from the substrate in the lab. Algal and diatom growth around the basal disc further suggested that *M. handi* does not move as much or as willingly as *H. 'sanjuanensis'*. If manually removed from the substrate, however, *M. handi* was able to reattach. Similar to *H. 'sanjuanensis'*, the basal disc was surrounded by a putative periderm.

The stalk was very flexible and offered little resistance to movement; when jostled, the stalk relaxed completely, allowing the animal to wave around very loosely as though the calyx was dangling from a string. If jostled for an extended period or particularly violently, the stalk and calyx retracted uniformly (Fig. 31D). Once jostling

stopped, the animal recovered within a few seconds, relaxing and extending stalk and calyx. Recall that in *H. 'sanjuanensis'* relaxation following stimulation was slow and often involved frequent re-contraction. Spontaneous shortening of the stalk with no associated calyx contraction was also frequently observed, such that the relaxed calyx was jerked back as though on a string.

The relaxed stalk of *M. handi* appeared to contribute to behavioural camouflage of these animals; when the stalk was fully relaxed, movement of the animal by currents and wave action is passive, like a piece of seaweed. As gentle jostling of the animal caused full relaxation of the stalk, this appeared to be an active behavioural camouflage. All *M. handi* displayed this relaxed posture when found in the wild.

Adhesive pads

Manania handi did not appear to use adhesive pads as extensively as *H. 'sanjuanensis'* used anchors. When adhering, more than one pad was usually used as they are tightly clustered. Adhesion by a single cluster allowed the animal to be pulled out of the water. Once attached, *M. handi* would maintain adhesion for extended periods (tens of minutes) with no further stimulation. The anchors of *M. handi* did not reflexively adhere to substrates when the stalk was detached as did those of *H. 'sanjuanensis'*. Jostling or prodding generally caused the animal to initiate adhesion.

Manubrium

The manubrium moved constantly and independently of the arms. Manubrium movements were quick and jerky, similar to other *M. handi* movements. When arms were bent, the manubrium did move towards those arms, but most movements were independent. The lips were also mobile and ruffled periodically. When pulled in one of the four cardinal directions (perradial, in line with the partitions), the lips on the side it was pulled towards gaped open. The manubrium could also contract strongly so that the whole structure plunged deep into the calyx with very little corresponding contraction of the calyx walls, in what resembled a swallowing motion (Fig. 32D). No obvious stimulus initiated this behaviour.

Tentacles

The tentacles moved independently, but less frequently and with less dexterity than those of *H. 'sanjuanensis'*, and usually one at a time rather than in concert. Although the tentacles were shorter and thicker than those of *H. 'sanjuanensis',* they appeared to move in a similar circling motion when contracted individually. *M. handi* performed "searching" behaviours such as rolling much less frequently than did *H. 'sanjuanensis'*.

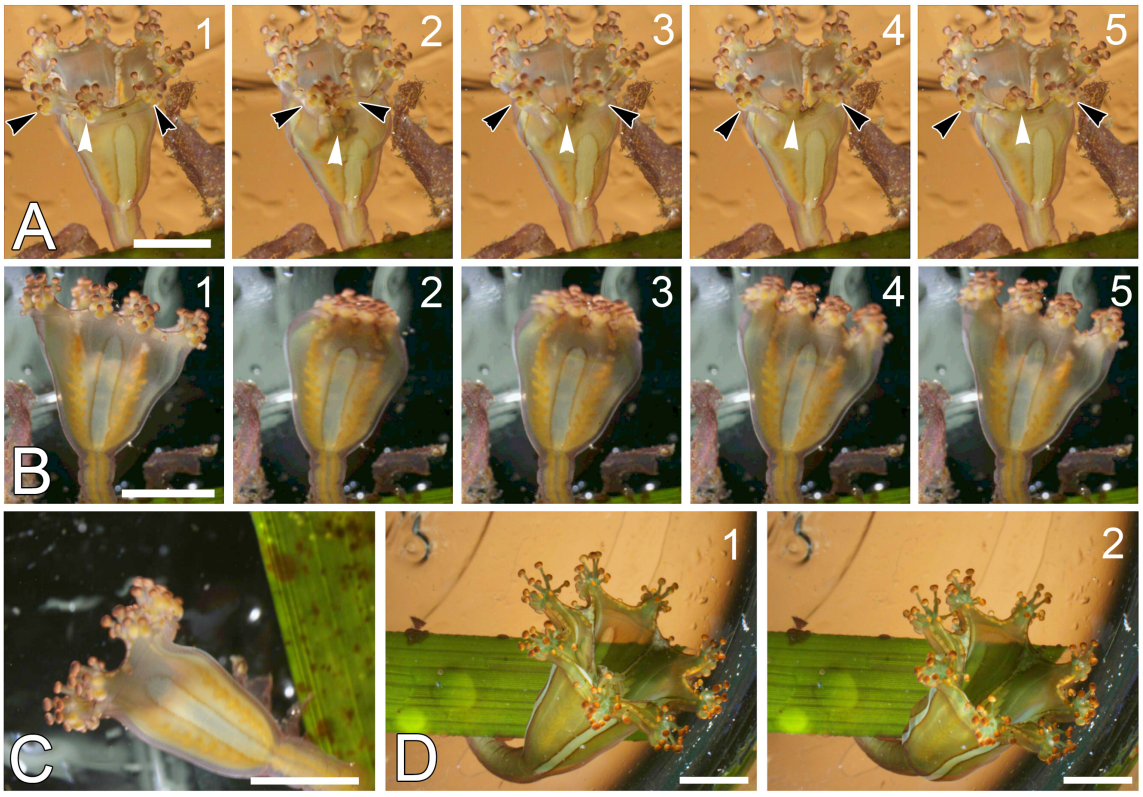


Figure 32. Spontaneous behaviours in *M. handi*. Images are stills from video recordings. **A:** Characteristic arm folding behaviour; the central arm (white arrowhead) is folded towards the manubrium while the two arms on either side of it (black arrowheads) bend towards each other. Stills are at 0.5 s intervals. **B:** Synchronous contraction of the margin. Stills are at 0.5 s intervals. **C:** Animal with partially contracted margin resulting in a pursed calyx opening. **D:** Contraction resulting in a withdrawal of the manubrium deep into the calyx. 1) Relaxed, 2) contracted. Scale bars, 4 mm.

3.5 Nervous System

3.5.1 Nervous system of *Haliclystus 'sanjuanensis'* and *Manania handi*

Paraformaldehyde fixed *H. 'sanjuanensis'* and *M. handi* were incubated in antibodies against glutamate, tyrosinated tubulin, FMRFamide and α-tubulin, but only the latter two produced neuron-specific labelling.

Subumbrellar, exumbrellar and gastrodermal neural components of both staurozoan species were immunoreactive to antibodies against FMRFamide and α-tubulin. Immunoreactivity was similar in many respects between the two species. While FMRFamide and α-tubulin antibodies each uniquely labelled some aspects of the nervous system, many neurites of the subumbrellar network co-labelled with both antibodies. FMRFamide antibodies strongly labelled a subset of the more extensive but less strongly labelled α-tubulin-immunoreactive (IR) neurites of the tentacles, calyx margin, longitudinal and radial muscles, manubrium and exumbrella. FMRFamide antibodies revealed neuronal cell bodies, neurites and putative sensory cells. Sensory neurons and cell bodies were not strongly labelled by α-tubulin antibodies. In addition to neurites, α-tubulin antibodies labelled non-neural components including nematocysts, cytoskeletal elements and cilia; this often made neurite labelling by α-tubulin antibodies more difficult to distinguish. In general, α-tubulin-IR neurites were more numerous, less frequently oriented along the muscles, and more highly interconnected than those labelled by FMRFamide antibodies. FMRFamide antibodies produced punctate labelling of most neurites, while labelling by α-tubulin antibodies usually did not. Neurite density was greatest in the calyx margin and manubrial lips.

3.5.1.1 Marginal muscle

A network of neurons associated with the marginal muscle labelled strongly with FMRFamide and α-tubulin antibodies in both *H. 'sanjuanensis'* and *M. handi*; neurite density within this region was higher than in other regions. The epidermal network of neurons closely followed the marginal circular muscle, and ended abruptly at its lower margin (Figs. 33A; 34A, B). The network incorporated both superficial and deeply embedded neurites, indicating that some neurites lay between the apical epithelial components of the myoepithelial cells, while others were located between the basal

muscle extensions, or within the folds of muscle that extended more deeply into the mesoglea. In *H. 'sanjuanensis'* these neurites were largely parallel to the fibers of the subumbrellar marginal muscle, and were continuous with neurites around the base of the tentacles (Figs. 33A, B; Fig 35). In *M. handi* neurites of the marginal muscle formed an interconnected network with no apparent preferred orientation (Fig. 34A, B, D), save for a few neurites that paralleled the scalloped bands of muscle which loop up to cover the arms (Fig. 34A, C). The exumbrellar and subumbrellar networks were continuous at the margin and tentacles (Figs. 33B; 34E, F). In *M. handi*, neurites of the exumbrellar marginal muscle were continuous with a dense band of neurites proximal to the subumbrellar strip of marginal muscle inside the lip of the margin. This dense band ended abruptly at the line of nematocyst clusters along the edge of the calyx. The more diffusely distributed neurites of the subumbrella lay proximal to the line of nematocyst clusters (Fig. 34F).

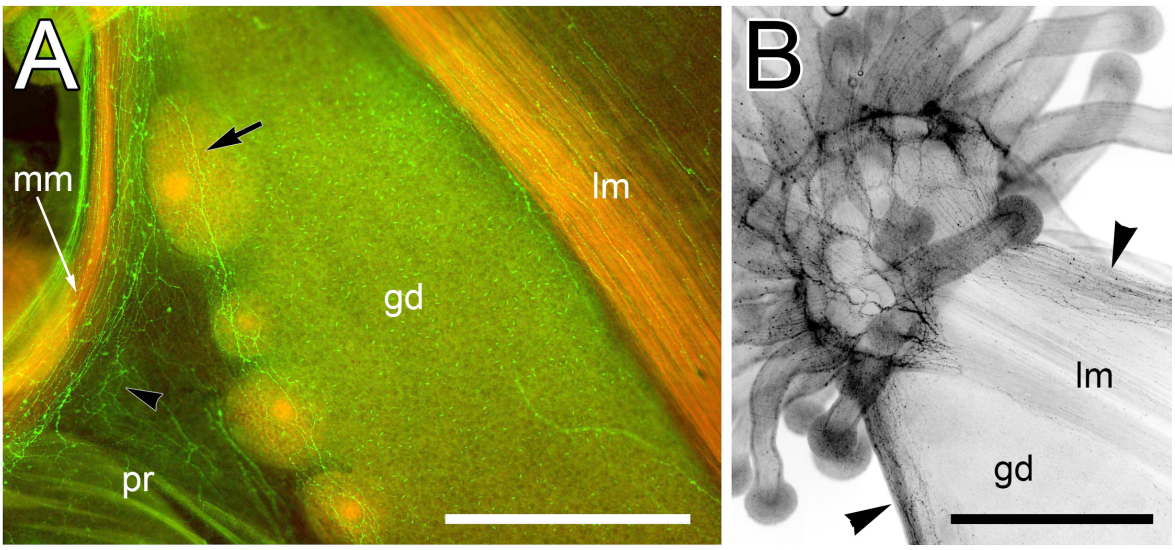


Figure 33. Innervation of the marginal muscle in *H. 'sanjuanensis'*. **A:** A network of FMRFamide-IR neurites (green) closely coincided with the phalloidin-labelled (red) marginal muscle. Neurites of the perradius (arrowhead) and nematocyst clusters (black arrow) were continuous with those of the margin. Scale bar, 400 µm. **B:** FMRFamide-IR neurites of the margin (arrowheads) were continuous with those at the ends of the arms, where neurites formed a honeycomb pattern around the base of the tentacles. Scale bar,

100 µm. **Abbreviations:** gd, gonad; lm, longitudinal muscle; mm, marginal muscle; pr, perradius.

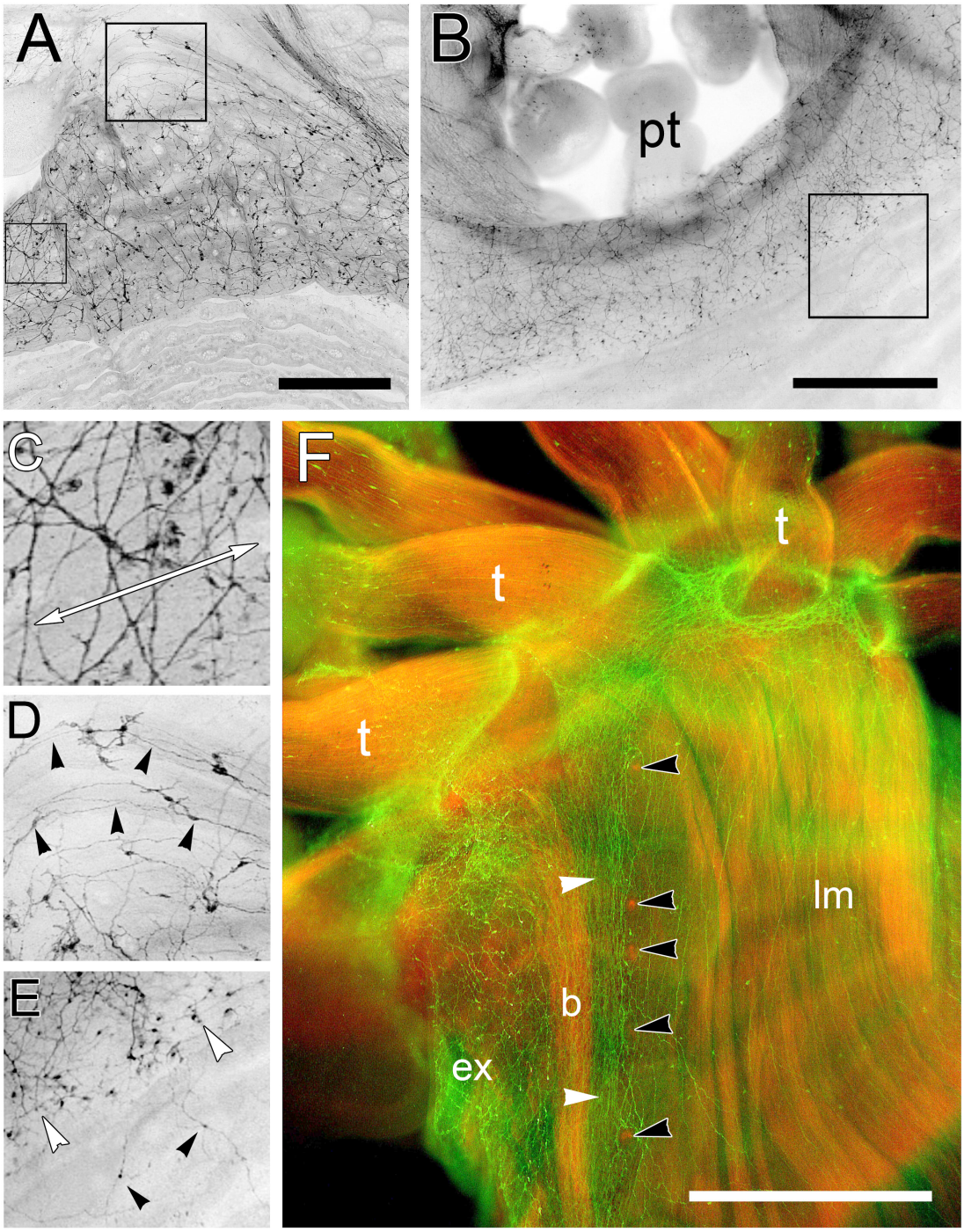


Figure 34. Innervation of the marginal muscle and arms in *M. handi*. **A:** A continuous network of FMRFamide-IR neurites closely overlaid the exumbrellar marginal muscle,

extending up onto the arms and **B:** running outside the primary tentacles. **C:** Enlargement of small box indicated in (**A**). Neurites overlying the marginal muscle (muscle fiber orientation indicated by arrow) were randomly oriented. **D:** Enlargement of large box indicated in (**A**). Only the muscle fibers that loop up to the ends of the arms are paralleled by neurites (arrowheads). **E:** Enlargement of box indicated in (**B**). The network of neurites overlying the marginal muscle ended abruptly at its lower border (white arrowheads); neurites of the marginal network were continuous with neurites of the exumbrella (black arrowheads). Scale bars, 500 μm. **F:** FMRFamide (green) and phalloidin (red) labelling of the subumbrella and margin at an arm. Neurites overlying subumbrellar structures were continuous with those of the exumbrella at the margin. A dense network of neurites (white arrowheads) overlaid the thin band of marginal muscle (b) inside the the calyx. This band of neurites terminated distal to the apices of the nematocyst clusters (black arrowheads) which lined the edge of the calyx. Neurites were concentrated around the base of the tentacles and formed a honeycomb pattern. Scale bar, 350 μm. **Abbreviations:** b, band of marginal muscle inside the calyx; ex, exumbrella; lm, longitudinal muscle; pt; primary tentacle; t, secondary tentacle.

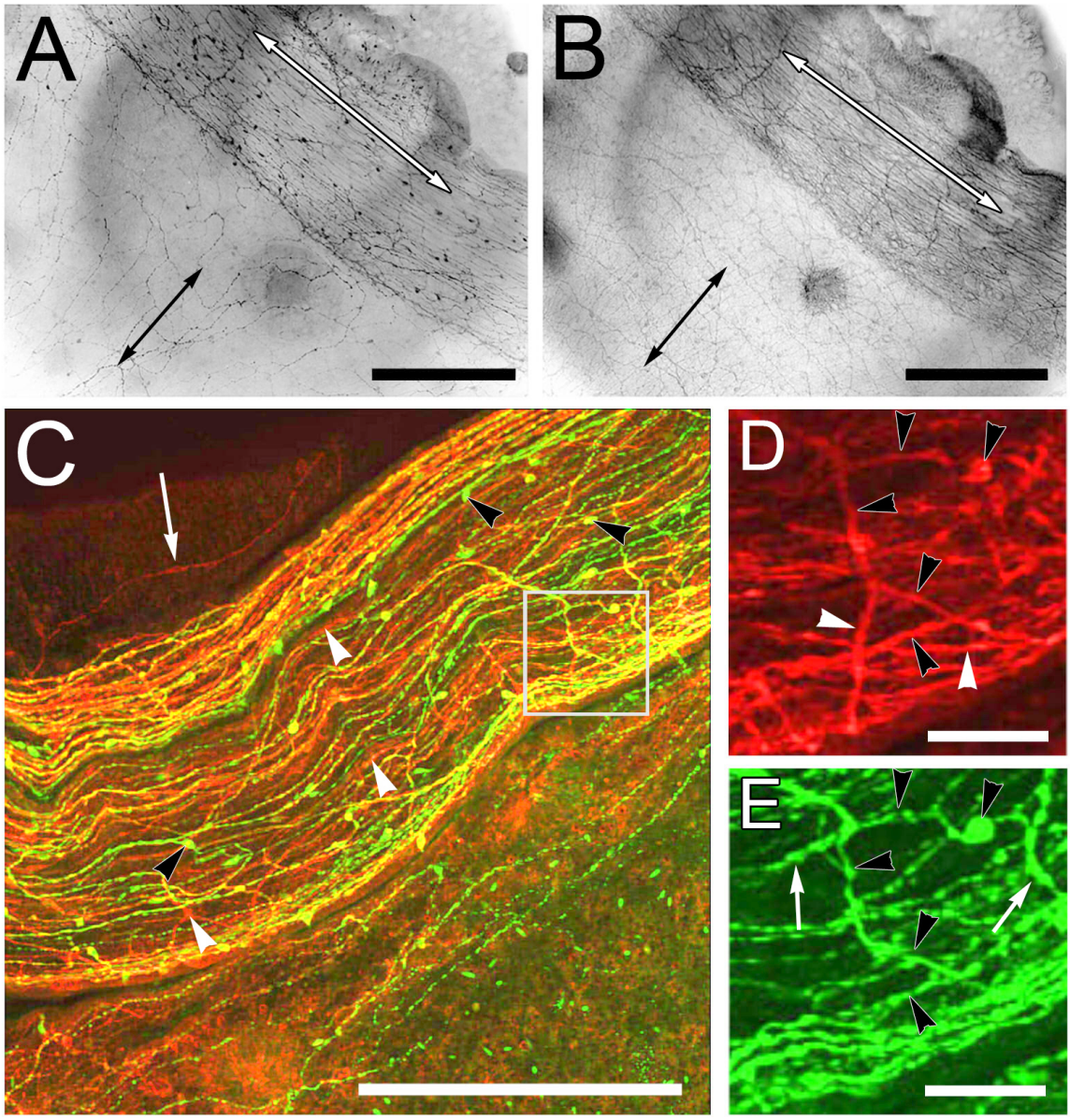


Figure 35. Double-labelling of the margin in *H. 'sanjuanensis';* results were similar in *M. handi.* **A, B:** Perradial margin double-labelled with FMRFamide (**A**) and α-tubulin (**B**) antibodies. Arrows indicate muscle fiber direction in the perradius (black arrows) and margin (white arrows). **A:** FMRFamide-IR neurites in the perradius were largely parallel to the muscle fibers. Focus series shows neurites along the marginal muscle were also largely parallel to muscle fibers, as in (**C**). **B:** Alpha-tubulin-IR neurons were more numerous, more highly interconnected and were apparently randomly oriented. Scale bars, 20 µm. **C:** CLSM image shows that FMRFamide-IR neurites (green) were predominantly parallel to muscle fibers of the margin. Many neurites of the margin co-

labelled with α-tubulin (red) and FMRFamide (green) antibodies; orange neurites represent those labelled strongly by both antibodies. Alpha-tubulin antibodies exclusively labelled many neurites (white arrowheads). Cell bodies labelled strongly with FMRFamide antibodies (black arrowheads). Arrow indicates α-tubulin-IR neurite of the exumbrella that is continuous with neurites of the margin. Scale bar, 200 μm. **D, E:** Detail of the area outlined in (**C**) but showing separate immunoreactivity to α-tubulin (**D**) and FMRFamide (**E**) antibodies. Black arrowheads indicate neurites strongly co-labelled by both antibodies; white arrowheads indicate neurites labelled exclusively by α-tubulin antibodies; white arrows indicate FMRFamide-IR neurites very weakly co-labelled by α-tubulin antibodies. Scale bars, 25 μm.

Alpha-tubulin antibodies labelled a denser, more highly interconnected network than that labelled by FMRFamide (Fig. 35A, B). Double-labelling showed that few neurites were exclusively FMRFamide-IR; most FMRFamide-IR neurites co-labelled with α-tubulin antibodies (Fig. 35C-E), and many neurites were exclusively α-tubulin-IR (Fig. 35C-E).

3.5.1.2 Tentacles, Adhesive Bodies and Pigment Spots

The secondary tentacles were similarly innervated in both species. Neurons sheathed the tentacles as muscle fibers did. While neurites formed parallel tracts that rarely interconnected along the tentacles of *M. handi* (Fig. 36A), innervation of *H. 'sanjuanensis'* tentacles included lateral neurites that connected neurites running parallel to muscle fibers (Fig. 36B-D). FMRFamide antibodies labelled only a subset of tentacle neurites labelled by α-tubulin antibodies; exclusively α-tubulin-IR neurites were predominantly longitudinal (Fig. 36B-D). In the tentacle capita, FMRF-amide-IR sensory neurons radiated from the base of the nematocyst-packed epithelium to the surface (Fig. 36E), while α-tubulin antibodies labelled the short projections extending from the surface of the tentacle capita that were also labelled by phalloidin and found in brightfield images (Figs. 13C; 24A; 36F). Bundles of exclusively FMRFamide-IR neurites surrounded the bases of the tentacles where they met the arm (Fig. 36G), producing a honeycomb-like pattern (Figs. 33B; 34F).

Tentacles with adhesive glandular swellings lacked innervation in the regions where development of the adhesive cells had subsumed the muscle fibers. As they retained much of the original tentacle structure, adhesive primary and secondary tentacles of *M. handi* were innervated as unmodified tentacles were, except that they lacked neurons where glandular tissue was present (Fig. 37A). Sensory neurons were not found in the adhesive pads. Neurites of the primary tentacles were continuous with those of the margin at their base (Fig. 38A, B, D, E). In *H. 'sanjuanensis'*, if a tentacle remnant was present, it was innervated as secondary tentacles were, and a few neurites extended along subumbrellar midline of the anchor from the margin to capitum (Fig. 37B) as muscle fibers did (Fig. 13D). If there was no tentacle remnant, neurites projected onto the stalk of the anchor and terminated a short distance from the margin (Fig. 38D). Sensory neurons were occasionally found in the thickened pad at the tip of the anchor, distal to the tentacle remnant (Fig. 37B). Alpha-tubulin antibodies labelled thin projections which appeared to form a basket around each large, lucent glandular cell included in the adhesive pads and anchors (Fig. 38C).

The pigment spot of *M. handi* was associated with a distinct knot of neurites and greatly increased concentration of cell bodies relative to other areas (Fig. 38A, B). These neurites and cell bodies were concentrated beneath the epithelium where the tentacle stalk joined the margin, such that neurites of the margin and primary tentacle were superficial to them. A similar aggregation of cell bodies and neurites was found in the same area in *H. 'sanjuanensis'* (Fig. 38D, E), although this was not associated with any externally visible structure.

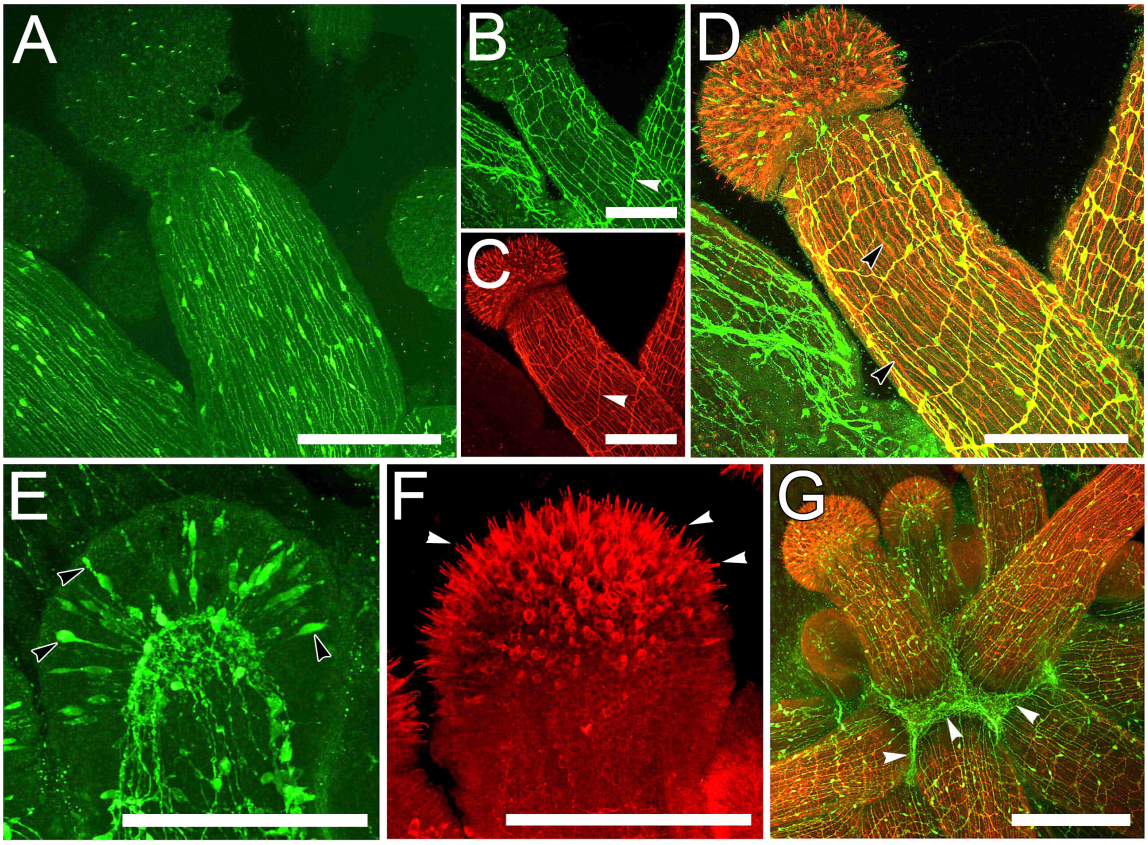


Figure 36. CLSM images of FMRFamide (green) and α-tubulin (red) immunoreactive neurites in the tentacles of *M. handi* (**A**) and *H. 'sanjuanensis'* (**B-G**). **A:** Long, parallel neurites followed the muscle fibers in the tentacles of *M. handi*. Scale bar, 200 µm. **B, C:** *H. 'sanjuanensis'* tentacles included many lateral neurites (white arrowheads) in addition to those running longitudinally. Scale bars, 200 µm. **D:** Overlay of (**B**) and (**C**). Alpha-tubulin antibodies labelled longitudinal neurites (black arrowheads) that were not co-labelled by FMRFamide antibodies. Scale bar, 200 µm. **E:** Capitum of a tentacle showing FMRFamide-IR sensory neurons (black arrowheads) radiating from the base to the surface of the epithelium. **F:** Capitum of same tentacle as in (**E**) showing α-tubulin-IR nematocysts and short projections extending from the epithelial surface (white arrowheads). Scale bars, 100 µm. **G:** Exclusively FMRFamide-IR neurites surround the base of tentacles (arrowheads). Scale bar, 200 µm.

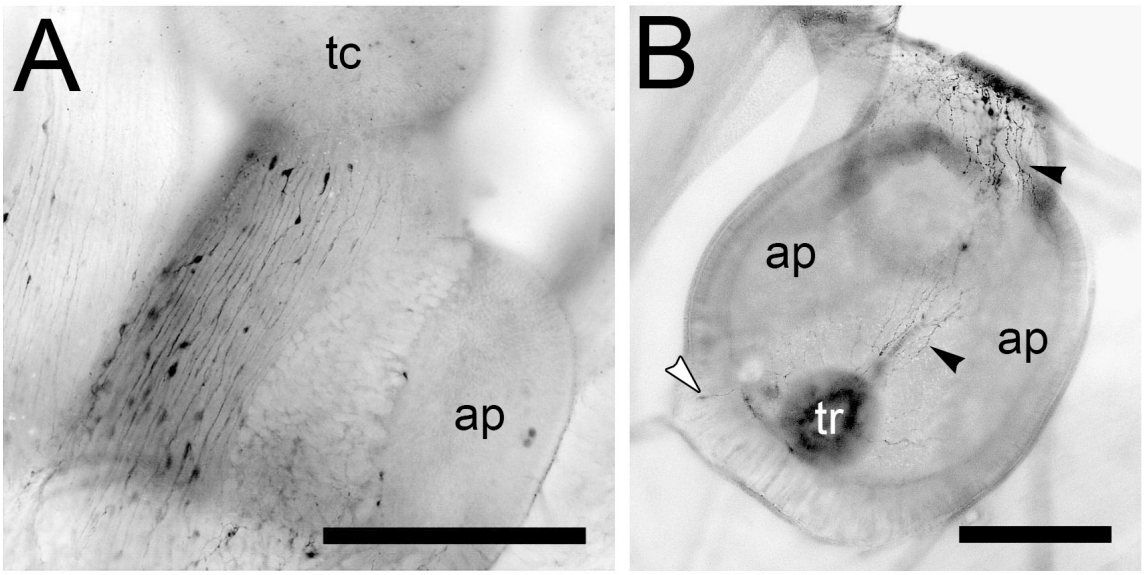


Figure 37. FMRFamide immunoreactivity of transformed tentacles. **A:** CLSM image shows neurites were absent on the distal side of transformed secondary tentacles in *M. handi* where the glandular cells of the adhesive pad had developed. Scale bar, 40 μm. **B:** Anchors of *H. 'sanjuanensis'* that had not yet fully transformed retained a few neurites (black arrowheads) that extended from the margin along the midline of the anchor to the tentacle remnant; these followed muscle fibers occupying the same region. Putative sensory neurons were found in the thickened pad distal to the tentacle remnant (white arrowhead). Scale bar, 200 μm. **Abberviations:** ap, adhesive pad; tc, tentacle capitum; tr, tentacle remanant.

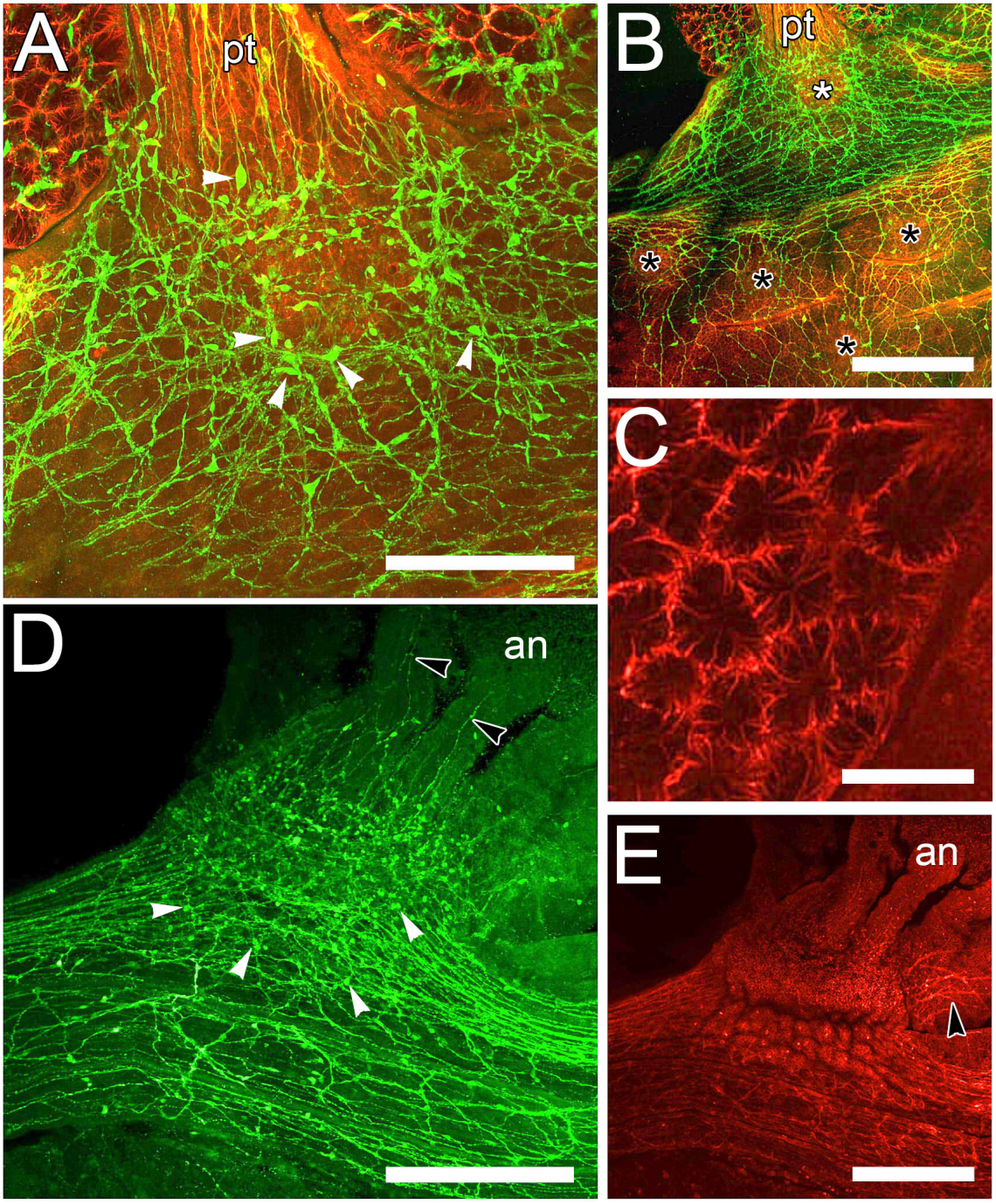


Figure 38. CLSM images of FMRFamide (green) and α-tubulin (red) immunoreactivity of the pigment spot in *M. handi* (**A, B**) and corresponding region in *H. 'sanjuanensis'* (**D, E**). **A:** Base of the primary tentacle; note FMRFamide-IR neurites that encircle the central spot corresponding to the pigmented area. This knot of neurites had an increased concentration of cell bodies (arrowheads) in comparison to surrounding areas and was not

co-labelled by α-tubulin antibodies, whereas some neurites extending onto the primary tentacle were α-tubulin-IR. Scale bar, 100 μm. **B:** Lower magnification of (**A**) showing context with the margin and perradial nematocyst clusters (black asterisks) below the pigment spot (white asterisk). Note increased concentration of FMRFamide-IR neurites and decreased α-tubulin immunoreactivity in area surrounding the pigment spot. Scale bar, 200 μm. **C:** Alpha-tubulin antibodies label projections which appear to form a basket around each large glandular cell of an adhesive pad. Scale bar, 25 μm. **D, E:** FMRFamide (**D**) and α-tubulin (**E**) immunoreactivity at the base of the anchor in *H. 'sanjuanensis'*. Scale bars, 200 μm. **D:** Increased concentration of cell bodies (white arrowheads) and neurites at the base of the anchor. Some neurites extended a short distance up the fully transformed anchor (black arrowheads), but terminated without extending along the midline. **E:** No α-tubulin-IR neurites were present in the location corresponding to the knot of neurites in (**D**), although some α-tubulin-IR neurites extended up the stalk of the anchor (arrowhead). **Abbreviations:** an, anchor; pt, primary tentacle.

3.5.1.3 Longitudinal muscles

In *H. 'sanjuanensis',* neurites ran parallel to the muscle fibers of the two main bands of longitudinal muscle and rarely branched to contact each other (Fig. 39A). These neurites occurred at a variety of depths, embedded in the folds of longitudinal muscle. Tracts of FMRFamide-IR neurites occasionally extended from this interradial network to project over the gonads (Fig. 39A); α-tubulin-IR neurites did not deviate from the muscle. Near the center of the interradius, where muscle fibres formed a sparse superficial sheet, FMRFamide-IR neurites formed a loose, superficial network as they extended towards the margin (Fig. 39B, C). Alpha-tubulin-IR neurites near the center of the interradius were no less dense but were more randomly oriented than those overlying the strong muscle bands (Fig. 39D). Neurites following the longitudinal muscles extended from the base of the infundibula to the margin where they merged with those along the marginal muscle and around the base of the tentacles (Fig. 39E). The portions of the longitudinal muscles embedded in the stalk were innervated by sparse α-tubulin-IR neurites (Fig. 39F).

In *M. handi*, subumbrellar epidermal neurites formed two distinct networks associated with the interradial longitudinal muscles. First, FMRFamide-IR neurites were embedded in the muscle and oriented parallel to the fibers (Fig. 40A) as they were in *H. 'sanjuanensis'*. A thick bundle of neurites followed the central axis of each longitudinal muscle; neurites extended from this bundle to follow the oblique bands of muscle extending from the central axis (Fig. 40A, B). It is likely that these fibers were also α-tubulin-IR, but labelling was obscured by immunoreactivity of epithelial components. Second, a superficial network of longitudinally oriented neurites ran from the base of the calyx to the margin (Fig. 40C); this network co-labelled with FMRFamide and α-tubulin antibodies. The subset of this network that labelled with FMRFamide antibodies comprised very long bipolar neurites with small cell bodies and infrequent lateral components (Fig. 40C, D). Alpha-tubulin antibodies co-labelled these FMRFamide-IR neurites and also labelled many neurites running transversely. This network increased abruptly in density and became more interconnected near the margin, at the level of the calyx where the top of the perradial pockets merged with the calyx wall (Fig. 40C). Neurites of these two longitudinal networks were continuous with those of the margin and adjacent arms (Fig. 34F). Sparse FMRFamide-IR neurites were embedded between the muscle fibers of the portions of the longitudinal muscles in the stalk (Fig. 40E).

3.5.1.4 Manubrium, Radial Muscles and Nematocyst Clusters

Innervation of the manubrium was entirely similar between species. A dense, highly interconnected FMRFamide and α-tubulin-IR network was associated with the radial muscles of the manubrium and muscles of the frilled manubrial lips. Many neurites were oriented in a similar direction to the muscle fibers. This network increased in density towards the edge of the manubrial lip, which was provided with many putative FMRFamide-IR sensory neurons (Fig. 41A, B). As in other areas, FMRFamide antibodies labelled a subset of the more highly interconnected α-tubulin-IR network (Fig. 41B). The flat, interradial faces of the manubrium that were provided with circular muscle fibers were nearly devoid of neurons; a few neurites from the radial corners turned to extend along the circular fibers, but terminated shortly (Fig. 41C, D). At the base of the manubrium neurites extended basally along the muscle sheets lining the infundibulae. In *M. handi*, the network spread radially from the base of the manubrium

into the infundibula and towards the gonads embedded in the perradial pockets. Neurons did not overlie regions of the perradial pockets in which the gonads were embedded, and decreased in density near the gonads and towards the base of the calyx (Fig. 41E).

Neurites extended from the corners of the manubrium along the top of the perradial pockets to the margin, following the radial musculature. Innervation of the weak perradial muscles in *H. 'sanjuanensis'* comprised a loose network (Fig. 42A) similar in form and density to that innervating the sparse musculature in the center of the interradii (Fig. 39B). Tracts of strongly FMRFamide-IR neurons framed the nematocyst clusters along the gonads on either side of the perradius (Fig. 42B). These tracts ran along the line of clusters and circumvented the central (phalloidin-labelled) spot, wrapping around it in a ring (Fig. 42B, C). Neuronal cell bodies were more numerous in this ring than in other areas and may be sensory (Fig. 42C). Alpha-tubulin antibodies co-labelled many neurites of the tracts, but did not co-label those FMRFamide-IR neurites that extended over the gonads to wrap around the nematocyst clusters (Fig. 42D, E). Alpha-tubulin antibodies labelled the apex of the clusters as phalloidin did (Fig. 42D, E). Near the margin, the neurites innervating the perradius and nematocyst clusters were continuous with neurites of the marginal muscle (Figs. 33A; 42A, B).

The neurites overlying the radial muscles of *M. handi* were generally parallel to the muscle fibers (Fig. 43A, B). Neurites of this network also innervated the many nematocyst clusters that occupied the top of the perradial pocket (Fig. 43A-E). Neurites did not extend down the sides of the perradial pocket, which were occupied by the gonads (Fig. 43B). Each nematocyst cluster apex was α-tubulin-IR and was encircled by FMRFamide-IR neurons. These neurites did not form a distinct tract extending from cluster to cluster as they did in *H. 'sanjuanensis'* (Fig. 43B-E). The network of the perradius deviated around the apex of the nematocyst clusters and a ring of putative sensory neurons encircled the apex (Fig. 43D, E). The nematocyst clusters along the interradial margin were similarly innervated.

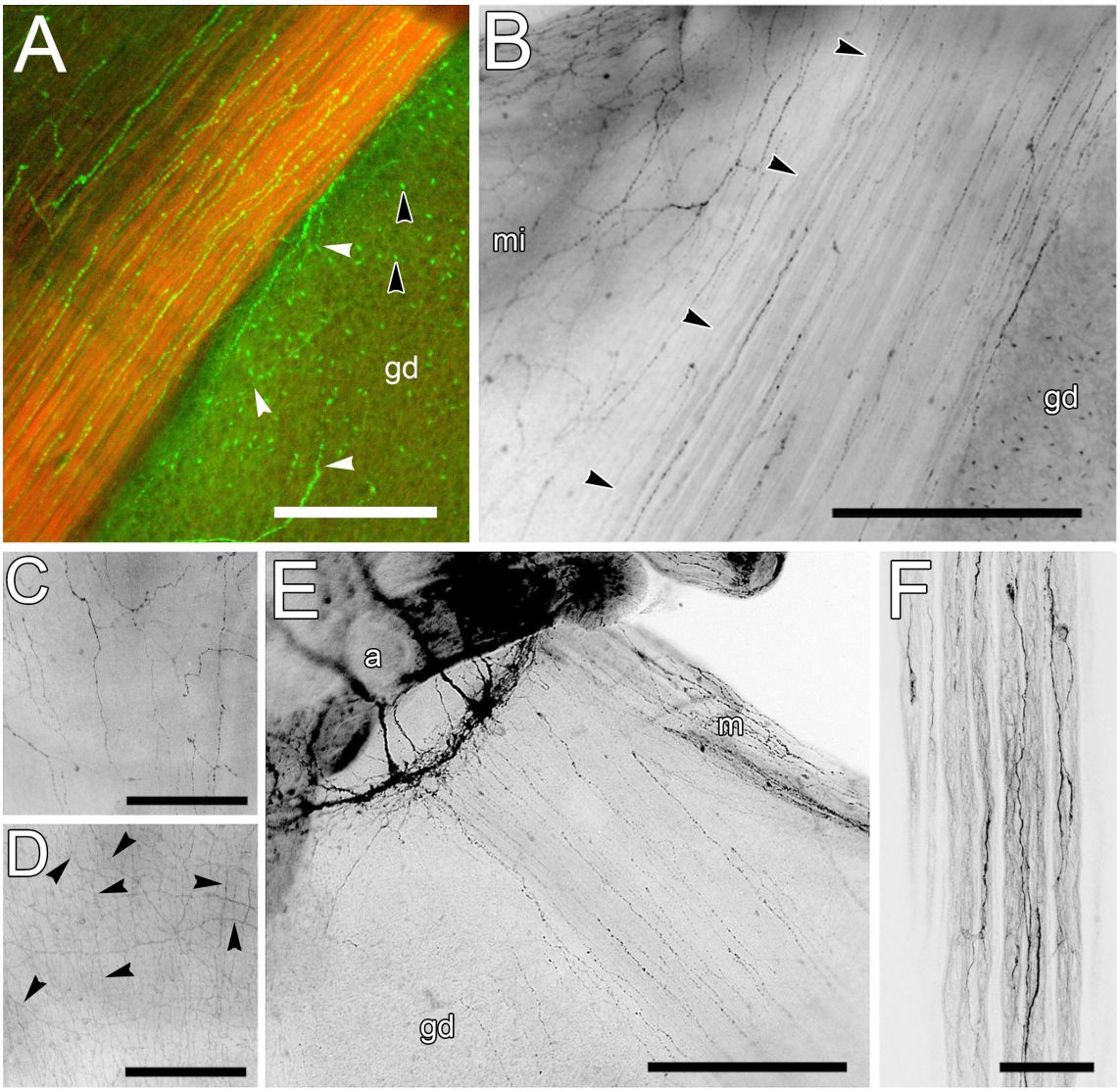


Figure 39. Innervation of the longitudinal muscles in the calyx and stalk of *H. 'sanjuanensis'*. **A:** CLSM image of long FMRFamide-IR neurites (green) running parallel to the band of longitudinal muscle fibres strongly-labelled by phalloidin (red). Note FMRFamide-IR neurites extending over the gonad (white arrowheads), and FMRFamide-IR flecks (black arrowheads) overlaying the gonad tissue Scale bar, 200 µm. **B:** Orientation of FMRFamide-IR neurites overlaying the longitudinal muscle bands compared to those overlaying the sparse muscle sheet in the middle of the interradius. Black arrowheads indicate the boundary between the longitudinal muscle band and the sparse muscle sheet in the middle of the interradius. Scale bar, 40 µm. **C, D:** Neurites of the middle of interradius double-labelled with antibodies against FMRFamide (**C**) and α-

tubulin (**D**). Note increased density of α-tubulin-IR neurites compared to FMRFamide-IR neurites. Arrows in (**D**) indicate α-tubulin-IR neurites that co-label with FMRFamide antibodies in (**C**). Scale bars, 20 μm. **E:** FMRFamide-IR neurites of the longitudinal muscle merge with neurites of the arm and margin. Scale bar, 200 μm. **F:** CLSM image of α-tubulin-IR neurites embedded in the stalk portion of a longitudinal muscle. Scale bar, 100 μm. **Abbreviations:** a, arm; gd, gonad; m, margin; mi, middle of interradius.

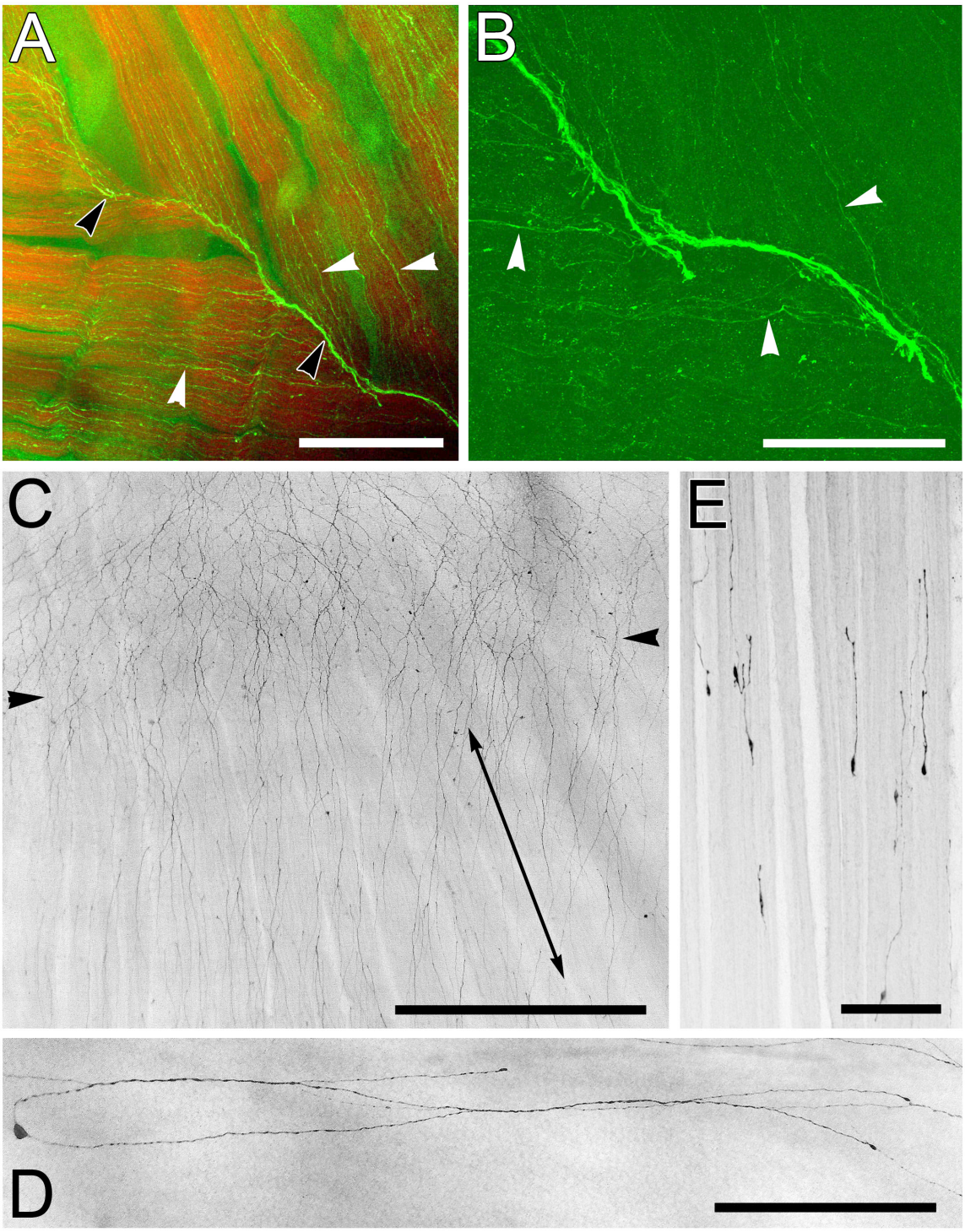


Figure 40. FMRFamide immunoreactivity of neurites associated with the longitudinal muscles in the calyx and stalk of *M. handi.* **A, B:** CLSM images of neurites embedded between the longitudinal muscle fibers of the calyx. **A:** FMRFamide-IR neurites (green) associated with the central axis and branches of a phalloidin-labelled longitudinal muscle in the calyx (red). A thick bundle of neurites (black arrowheads) ran along the central

axis of each longitudinal muscle; thin neurites extended from this bundle into branches of muscle issuing from the central axis (white arrowheads). Scale bar, 200 μm. **B:** Detail of neurite bundle along the central axis of a longitudinal muscle within the calyx. Neurites extended from the central bundle (arrowheads). Scale bar, 100 μm. **C:** Superficial FMRFamide-IR neurites extended from the base of the calyx to the margin. Their directionality was unrelated to that of the muscle bands, indicated by the black arrow. The network becomes more interconnected where the perradial pockets join the calyx (black arrowheads). Scale bar, 500 μm. **D:** Detail of a long bipolar neuron of the superficial network in (C). Scale bar, 20 μm. **E:** CLSM image of FMRFamide-IR neurites embedded in a band of longitudinal muscle within the stalk. Scale bar, 200 μm.

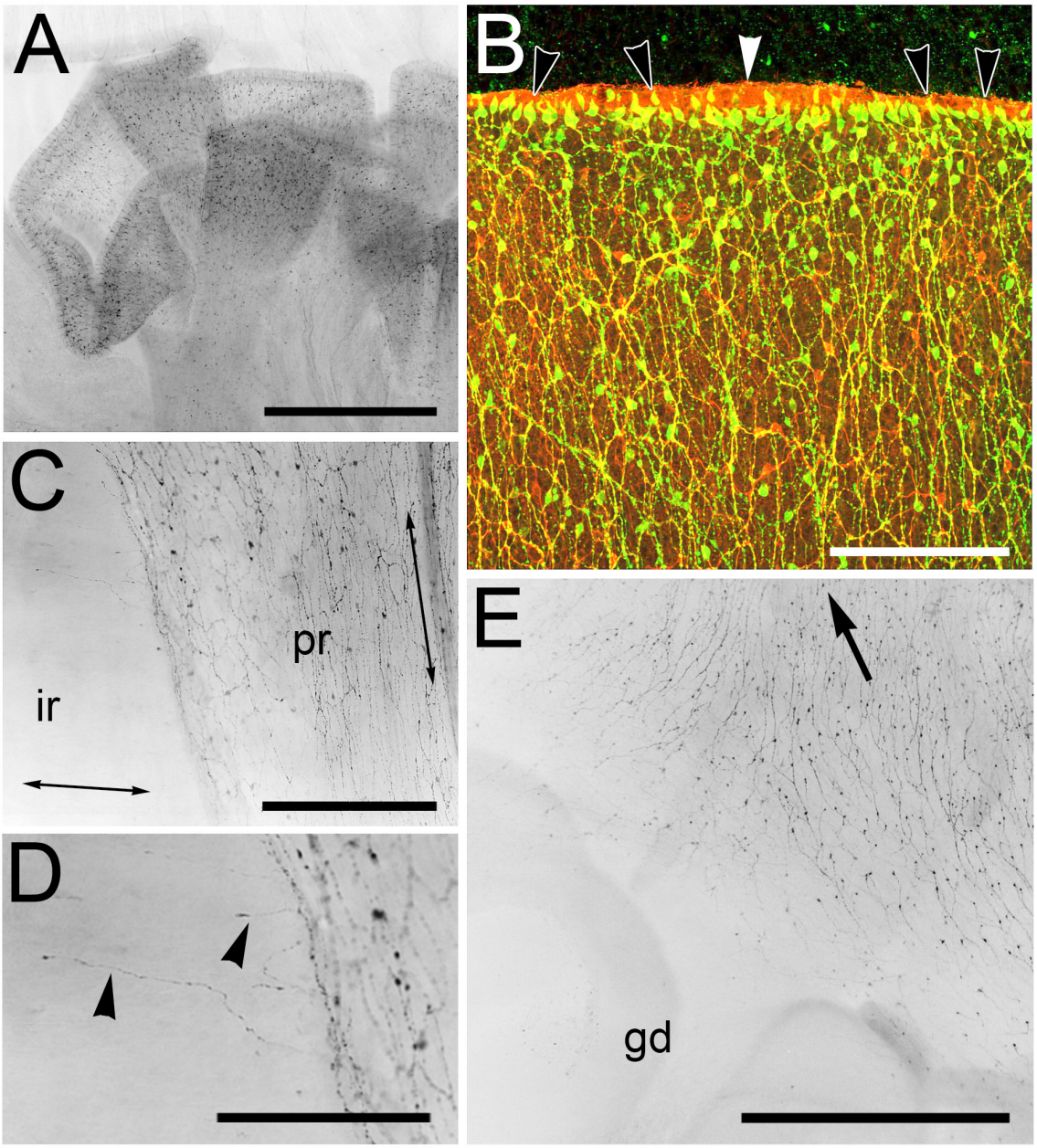


Figure 41. Innervation of the manubrium in *H. 'sanjuanensis* and *M. handi*. **A:** Perradial corner of the manubrium in *H. 'sanjuanensis'* showing increase in FMRFamide-IR neurite density towards the lips. Scale bar, 500 µm. **B:** CLSM image of the manubrial lip in *H. 'sanjuanensis'*. FMRFamide antibodies (green) labeled a dense band of sensory neurons (black arrowheads) on the lip. Alpha-tubulin antibodies (red) labeled the cilia (white arrowhead) lining the gastrodermis of the manubrium. Both antibodies labelled or co-labelled neurites and cell bodies of the manubrial epidermis. Scale bar, 100 µm. **C:** FMRFamide antibodies labeled a dense network on the perradial corners of the

manubrium, while interradial faces were nearly devoid of innervation. Arrows indicate directionality of muscle fibers in each region. Scale bar, 200 μm. **D:** Detail of (**C**); a few neurites (arrowheads) extended along the circularly oriented muscle fibers on the interradial faces of the manubrium. Scale bar, 100 μm. **E:** The infundibular network in *M. handi* decreased in density further away from the manubrium (position indicated by arrow) and terminated before extending on to the portion of the perradial pocket in which the gonads were embedded. Scale bar, 400 μm. **Abbreviations:** gd, gonad; ir, interradius; pr, perradius.

3.5.1.5 Gastrodermis

Gastrodermal innervation was entirely similar between species. The inner surface of the manubrium and subumbrellar gastrodermis were innervated with a highly interconnected FMRFamide-IR network of neurites (Fig. 44A). No α-tubulin-IR neurites were found in the gastrodermis. Alpha-tubulin antibodies labelled cilia covering the inner surface of the manubrium and gastric filaments. The gastrodermal network had a predominantly longitudinal orientation in the manubrium (Fig. 44B); at the base of the manubrium where the gastrodermis extended to form the perradial pockets and gastric filaments, the neurites formed a loose network (Fig. 44C). The gastric filaments were innervated by neurites oriented along the long axis of each filament (Fig. 44D). Putative sensory cells were present along the filaments (Fig 44D, inset). Neurites of the subumbrellar gastrodermis were continuous with those of the gastric filaments. The exumbrellar gastrodermis and taenioles were devoid of FMRFamide and α-tubulin-IR neurites, and did not appear to be ciliated. The gastrodermal network was continuous with the subumbrellar network at the manubrial lip.

3.5.1.6 Gonads

FMRFamide-IR flecks on the gonads of *H. 'sanjuanensis'* (Fig. 39A) were consistent in size within a specimen, and were oriented at varying angles below or within the subumbrellar epidermis over the gonads. Comparison with brightfield images revealed that these flecks correspond to the inverted shaft of eurytele nematocysts

embedded over the gonad tissue. In both species, neurons were largely absent in epithelia overlying gonad tissue.

3.5.1.7 Exumbrella and Pedal Disc

Alpha-tubulin antibodies labelled a dense, highly interconnected network of neurons extending over the exumbrella of both *H. 'sanjuanensis'* and *M. handi*. This network was diffuse and randomly oriented (Fig. 45A). Alpha-tubulin-IR neurites frequently intersected beneath the nematocyst batteries studding the exumbrella, which also labelled with α-tubulin antibodies (Fig. 45A). It was not clear whether the neurites innervated the nematocyst batteries. A very small subset of the α-tubulin-IR neurons co-labelled with FMRFamide antibodies (Fig. 45A). These neurons were usually bipolar, occasionally tripolar, and were usually isolated from other FMRFamide-IR neurons. There was a dense network of FMRFamide-IR neurites at the base of the thick glandular epidermis (Fig. 45B). Many putative sensory cells extended from this network to the surface of the glandular pad of the basal disc (Fig. 45B, C). No α-tubulin immunoreactivity was observed in the basal disc. The exumbrellar network was continuous with the subumbrellar network at the margin and arms (Fig. 34E, F; 35C).

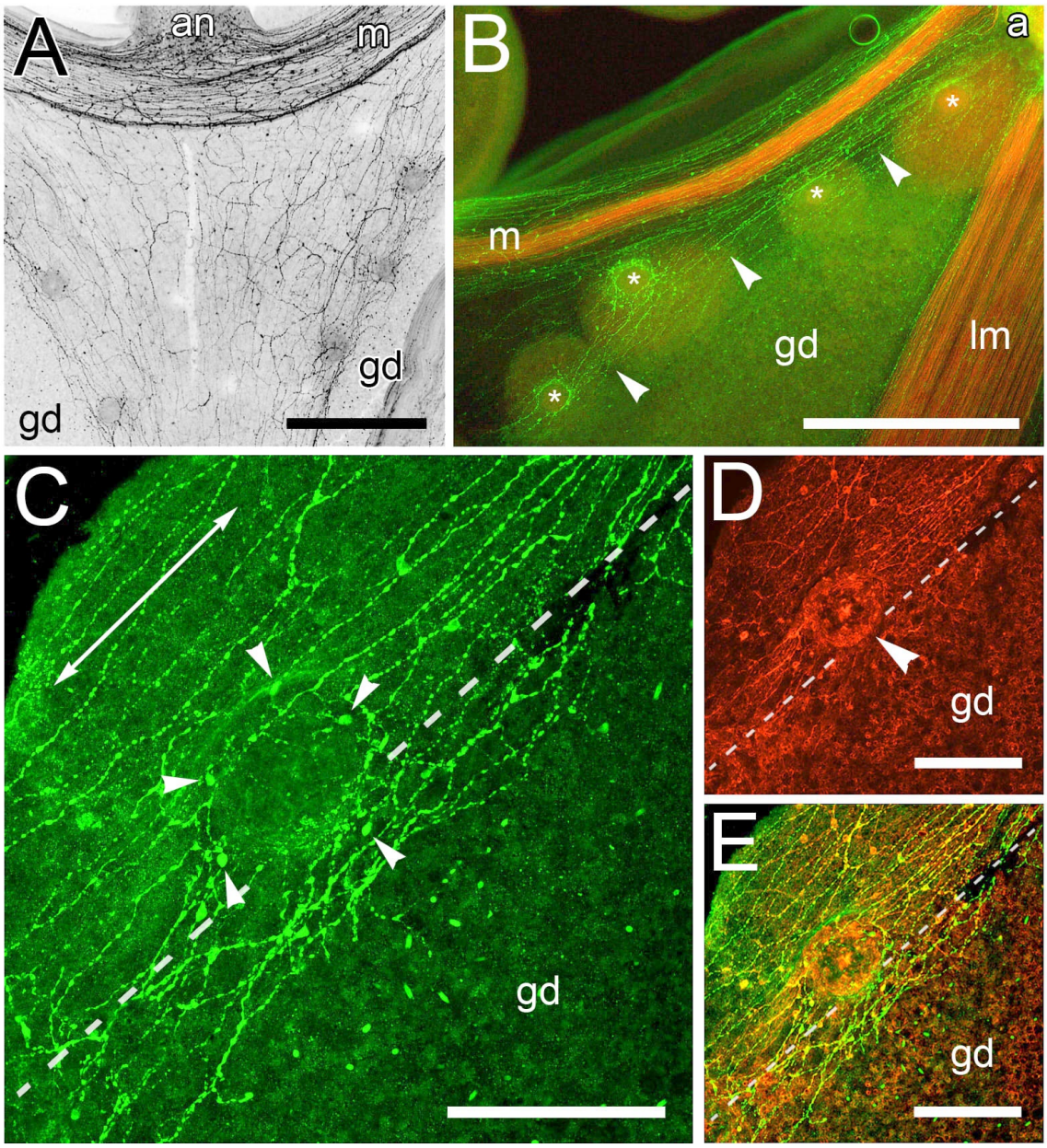


Figure 42. Innervation of the subumbrellar perradius in *H. 'sanjuanensis'*. **A, C-E:** CLSM images. **A:** The loose FMRFamide-IR network of the perradius was continuous with neurites of the margin. Scale bar, 400 µm. **B:** Tracts of strongly FMRFamide-IR neurites (green) (arrowheads) ran along the lines of nematocyst clusters and circumvented their apices; these neurites were continuous with those of the margin and tentacles. Phalloidin-labelled muscles and nematocyst clusters are in red. Scale bar, 400 µm. **C-D:** A single perradial cluster double-labelled with FMRFamide (green) and α-tubulin (red) antibodies. Dotted lines indicate extent of gonad tissue. Scale bars, 100 µm.

C: FMRFamide-IR neurons encircled the apex of the cluster. A ring of cell bodies surrounded the central spot (arrowheads), and neurites extended over the gonad tissue adjacent to the cluster. Neurites overlying the perradial musculature were largely parallel to the muscle fibers (arrow indicates direction of musculature). Note punctate labelling of neurites. **D:** Alpha-tubulin labelled neurites in the perradius around the cluster, and strongly labelled the apex of the cluster (arrowhead). Alpha-tubulin-IR neurites did not extend over the gonad tissue as FMRFamide-IR neurites did. **E:** Overlay of (C) and (D); the ring of FMRFamide-IR neurites and cell bodies encircles the α-tubulin-IR apex of the cluster. **Abbreviations:** a, arm; gd, gonad; lm, longitudinal muscle; m, margin.

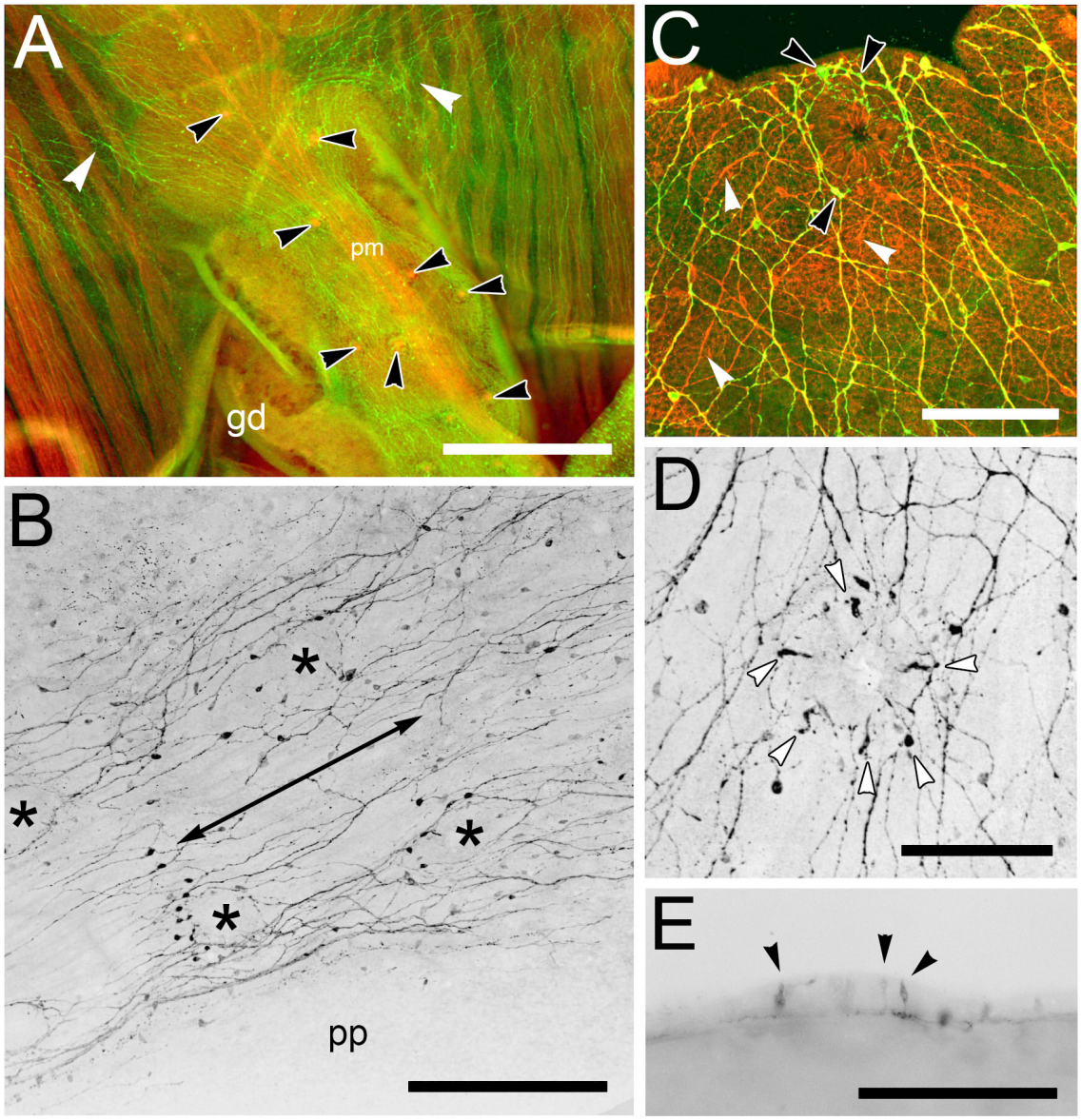


Figure 43. Innervation of the subumbrellar perradius in *M. handi*. **B-D:** CLSM images. **A:** FMRFamide-IR (green) neurites on the top of the perradial pocket were generally parallel to phalloidin-labelled muscles (red). The apices of the nematocyst clusters (black arrowheads) lie to either side of the perradial muscle band. Where the perradial pocket joins the calyx wall (white arrowheads), the neurites of the perradius fan out as they extend towards the margin. Scale bar, 500 µm. **B:** FMRFamide-IR neurons on the top of the perradial pocket; neurites were no more concentrated over the muscle band (directionality indicated by the arrow) than they were around the clusters on either side of it. Neurites do not overlie apices of the clusters (asterisks). Neurites do not extend down

on to the sides of the perradial pocket, in which the gonads are embedded. Scale bar, 200 µm. **C:** FMRFamide-IR neurites (green) were co-labelled by α-tubulin (red) antibodies, save for those neurites and cell bodies directly encircling the apex of the nematocyst cluster (black arrowheads). Many neurites were independently α-tubulin-IR (white arrowheads). Scale bar, 100 µm. **D:** Detail of FMRFamide immunoreactivity of the apex of a nematocyst cluster; putative sensory neurons (arrowheads) encircle the apex. Scale bar, 100 µm. **E:** Tangential view of FMRFamide labelling showing elongate putative sensory cell bodies (arrowheads) occupying the thickened epidermis of a nematocyst cluster apex. Scale bar, 20 µm. **Abbreviations:** gd, gonad; pm, perradial muscle; pp, perradial pocket.

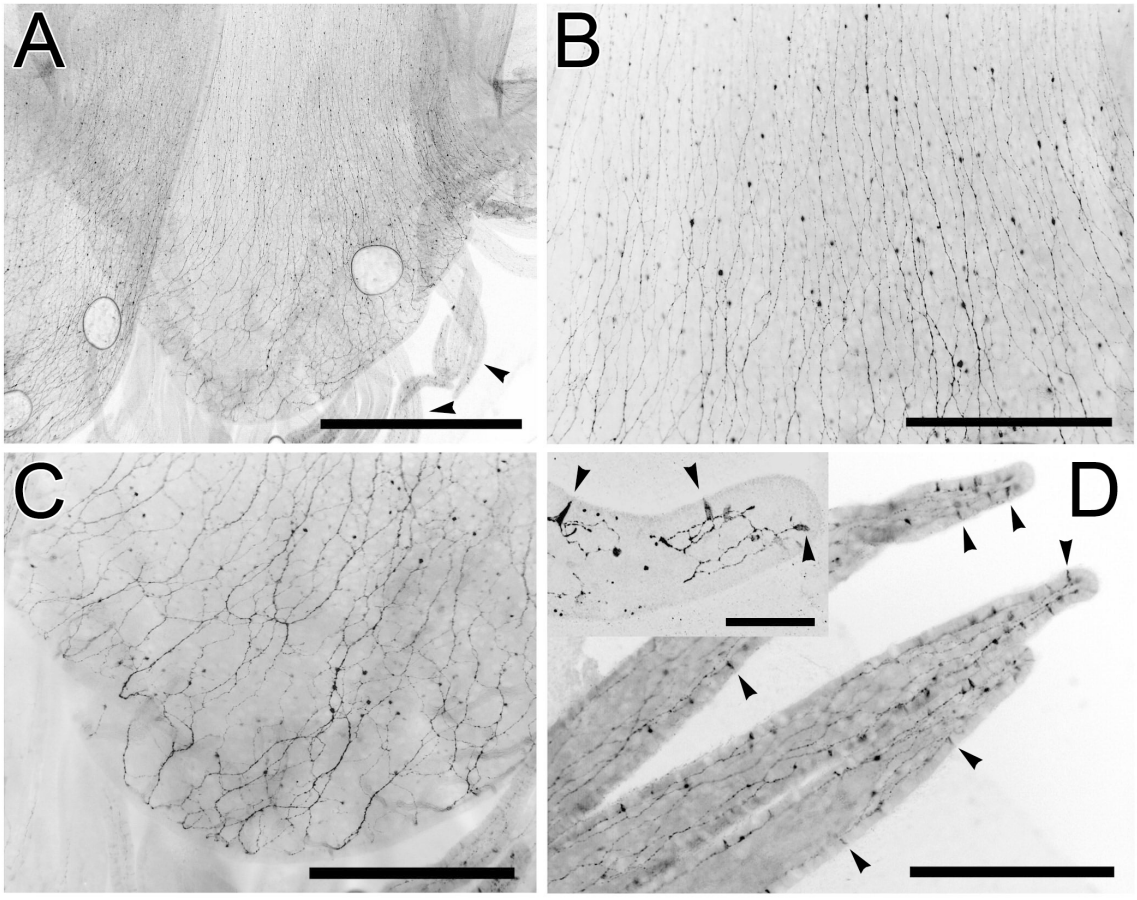


Figure 44. FMRFamide-IR neurons of the gastrodermis. Results are shown for *H. 'sanjuanensis'*; labelling in *M. handi* was similar. **A:** Manubrium sliced longitudinally to

expose the interior. The network was dense near the top of the manubrium and more diffuse at the base where it extended to innervate the stomach, perradial pockets and gastric filaments (arrowheads). Scale bar, 100 μm. **B:** Near the lips of the manubrium, gastrodermal neurites ran longitudinally. Scale bar, 40 μm. **C:** Near the base of the manubrium, the network was more loosely organized. Scale bar, 40 μm. **D:** Innervation of the gastric filaments. Putative sensory neurons (arrowheads) were present along the length of each filament, and were more concentrated towards the tips. Scale bar, 40 μm. Inset: CLSM image of sensory neurons (arrowheads) on the tip of a filament. Scale bar, 50 μm.

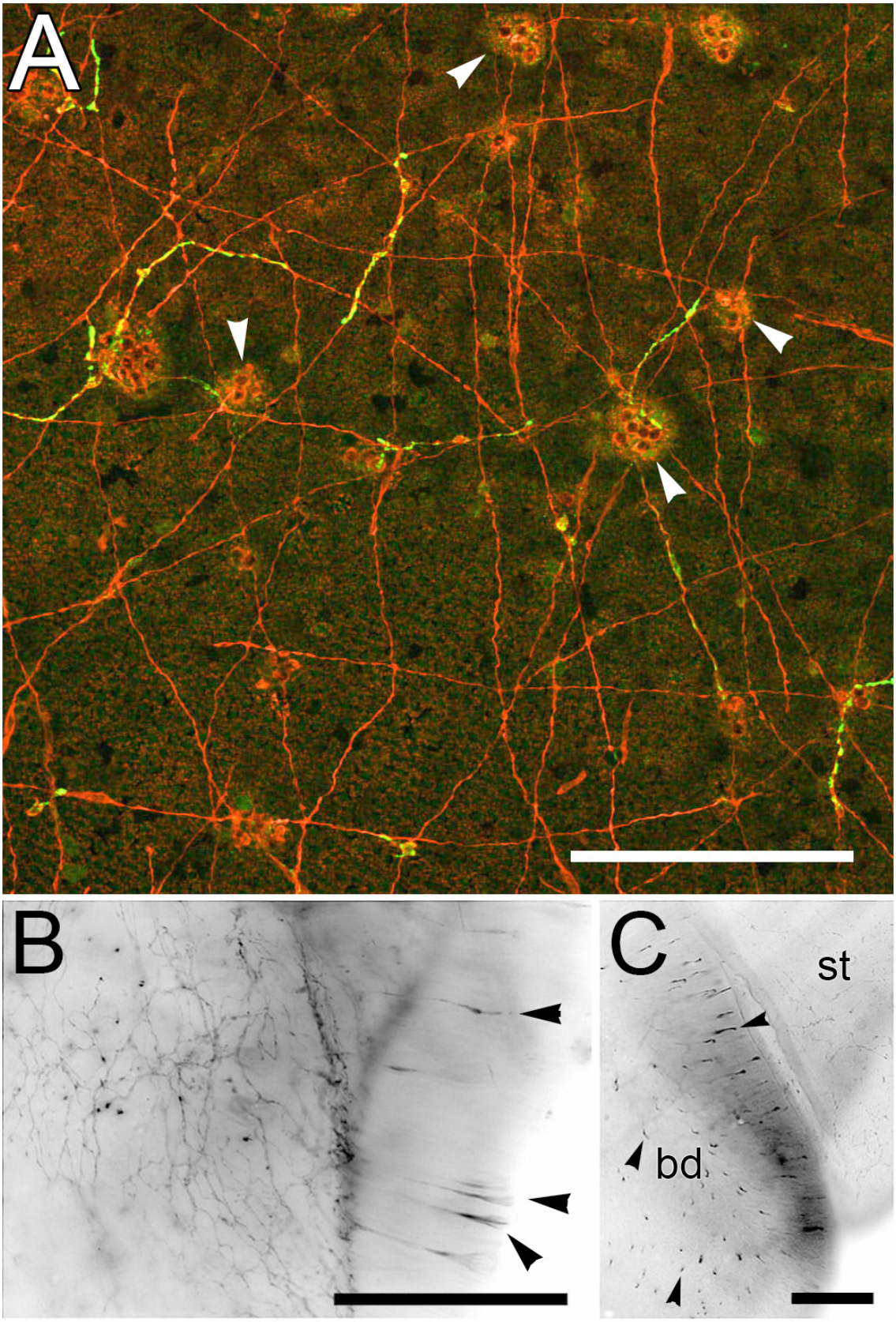

A
B
C
st
bd

Figure 45. Innervation of the exumbrella and basal disc. Results are shown for *H. 'sanjuanensis'*; similar results were obtained for *M. handi*. **A:** CLSM image shows the diffuse network of α-tubulin-IR neurites (red) covering the exumbrella. Neurites intersected beneath the small nematocyst batteries (arrowheads) embedded in the exumbrellar surface. A small subset of neurites was co-labelled by FMRFamide antibodies (green). **B:** A network of neurites lay at the base of the thick epidermis of the basal disc; long sensory neurons (arrowheads) extended from this network to the epidermal surface. **C:** Planar surface of the basal disc and adjacent area of the stalk showing sensory neurons (arrowheads) evenly distributed over the surface of the basal disc. Scale bars, 100 μm. **Abbreviations:** bd, basal disc; st, stalk.

3.5.2 Nervous system of *Aurelia* sp. life stages

3.5.2.1 Nervous system of *Aurelia* sp. ephyra

Antibodies against FMRFamide labelled a continuous network of neurons on the subumbrellar and exumbrellar epidermis corresponding to the Diffuse Nerve Net. FMRFamide antibodies strongly labelled cell bodies and neurites with many varicosities (Fig. 46A-C). The net was concentrated on the subumbrella in areas overlying smooth muscle fibers. Neurons were increasingly dense towards the lips of the manubrium (Fig. 46A), and concentrated over the knots of smooth muscle at the apices of the arm clefts (Fig. 46B). A few neurons in the rhopalium labelled brightly with antibodies against FMRFamide, and some neurites extended from the net to contact each rhopalium (Fig. 46C).

Antibodies against glutamate labelled neurites that corresponded to the Giant Fibre Nerve Net (GFNN). Glutamate-IR neurons overlaid the striated swim muscle of ephyra (Fig. 46D, E). Antibodies against glutamate also produced strong labelling in the rhopalium (Fig. 46E), and weakly labelled the nematocysts. Distinct neurites extended from the neurons overlying radial muscle bands to the rhopalium (Fig. 46E).

Antibodies against tyrosinated tubulin strongly labelled nematocyst capsules and neurons corresponding to the GFNN. Concentrations were found in the same areas labelled by glutamate. However, antibodies against tyrosinated tubulin labelled neurites, but not cell bodies (Fig. 46F, G). Antibodies against tyrosinated tubulin also labelled

neurites radiating out from the striated muscle which were not labelled by glutamate, including many neurites which appeared to contact nematocysts (Fig. 46G, inset). The rhopalia and neurites extending to them from the radial muscles were also strongly tyrosinated tubulin-IR (Fig. 46G).

3.5.2.2 Nervous system of *Aurelia* sp. polyps and strobila

Antibodies against FMRFamide labelled neurons concentrated over polyp muscles. Tentacle and oral disc musculature were innervated by an evenly distributed network of neurites, and neurons followed the longitudinal muscles embedded in the stalk. Neurons following longitudinal muscles were long, straight and rarely branched, and appeared to thin and terminate partway down the stalk (Fig. 47A). Neurons were most concentrated on the tentacles and oral disc (Fig. 47A, B). No FMRFamide-IR neurons were observed in the pedal disc.

FMRFamide-IR tracts of epidermal neurons issued from the oral disc between adjacent tentacles and ran down the body column. These epidermal tracts were composed of long, straight neurites with few visible cell bodies (Fig. 47C).

Developing ephyrae close to the apical end of a strobila labelled strongly with FMRFamide antibodies as did released ephyra. Those closer to the base of the stack which were less developed had weak, patchy FMRFamide labelling, with none of the distinctive patterning seen in fully formed ephyrae (Fig. 47D).

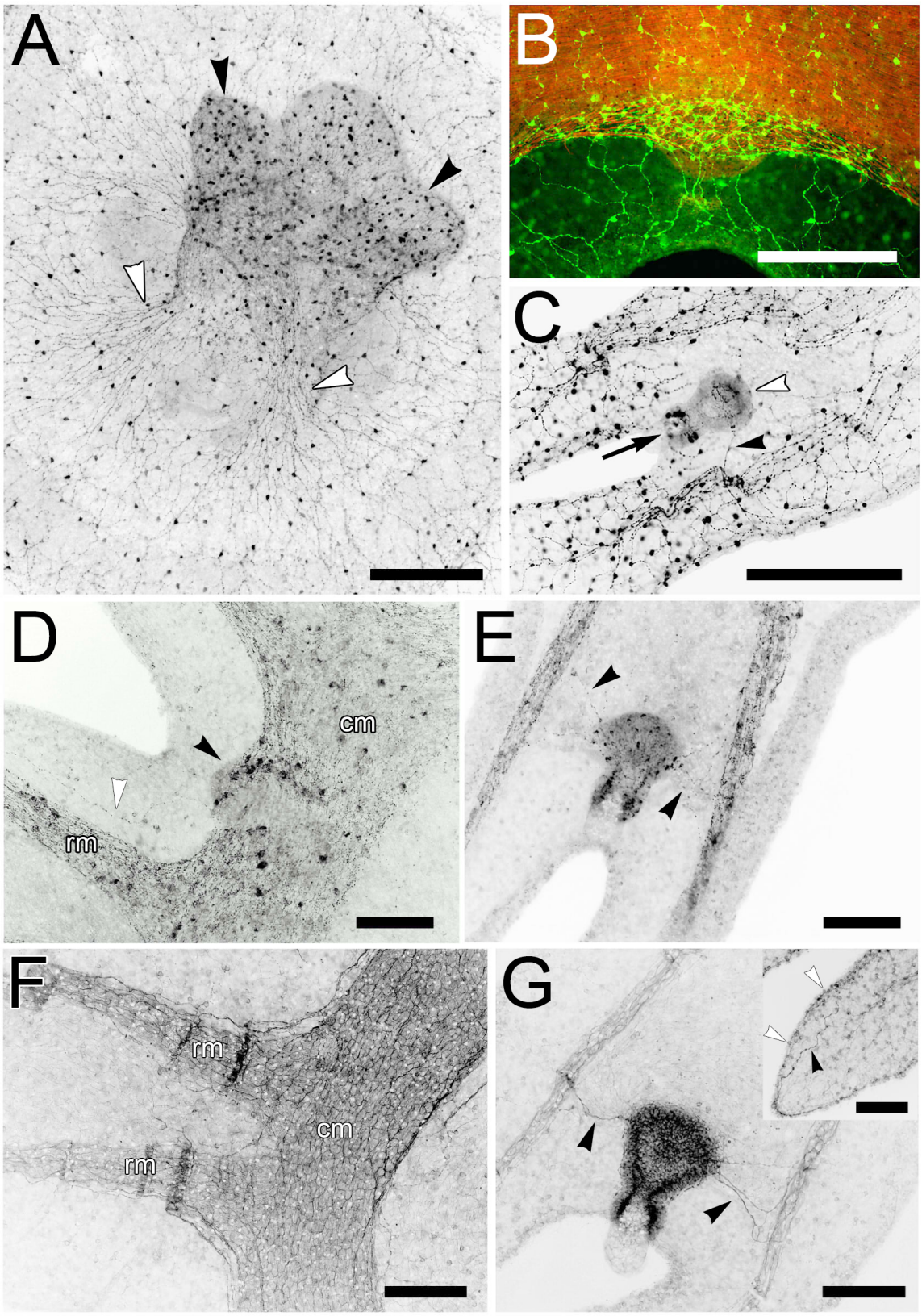

A
B
C
D
cm
rm
E
F
rm
cm
rm
G

Figure 46. Nervous system of *Aurelia* sp. as revealed by antibody-labeling. **A-C:** FMRFamide-IR; **D, E:** glutamate-IR; **F, G:** tyrosinated tubulin-IR. **A:** FMRFamide-IR neurons within the manubrium; neurites increased in concentration towards the manubrial lips (black arrowheads) and ran down the perradial corners of the manubrium (white arrowheads) to radiate over the subumbrella. Scale bar, 200 μm. **B:** FMRFamide-IR neurites were concentrated over the knot of smooth muscle fibers between each pair of arms. Scale bar, 200 μm. **C:** FMRFamide-IR neurites (black arrowhead) extended to the rhopalium (white arrowhead), which included some FMRFamide-IR cell bodies (arrow). Scale bar, 200 μm. **D:** Glutamate-IR neurons along the striated swim and arm musculature; cell bodies were concentrated over the smooth muscle between arms (black arrowhead). A few neurites extended over the subumbrellar surface away from areas overlying the striated muscle (white arrowhead). Scale bar, 50 μm. **E:** Glutamate-IR neurons in an arm; neurites (arrowheads) extended from the bands overlying the muscle fibers to join the rhopalium, which contained some glutamate-IR neurons. Scale bar, 50 μm. **F:** A highly interconnected net of tyrosinated tubulin-IR neurites closely followed the striated muscle fibers of the swim and arm musculature. Scale bar, 100 μm. **G:** Tyrosinated tubulin-IR neurites (arrowheads) extended from those overlying the radial muscle bands to contact the rhopalium, which labelled strongly. Scale bar, 100 μm. Inset; tyrosinated tubulin antibodies labelled nematocyst capsules (white arrowheads) and neurites which extended over the epithelium (black arrowhead) and appeared to contact the capsules. Scale bar, 100 μm. **Abbreviations:** cm, circular muscle; rm, radial muscle.

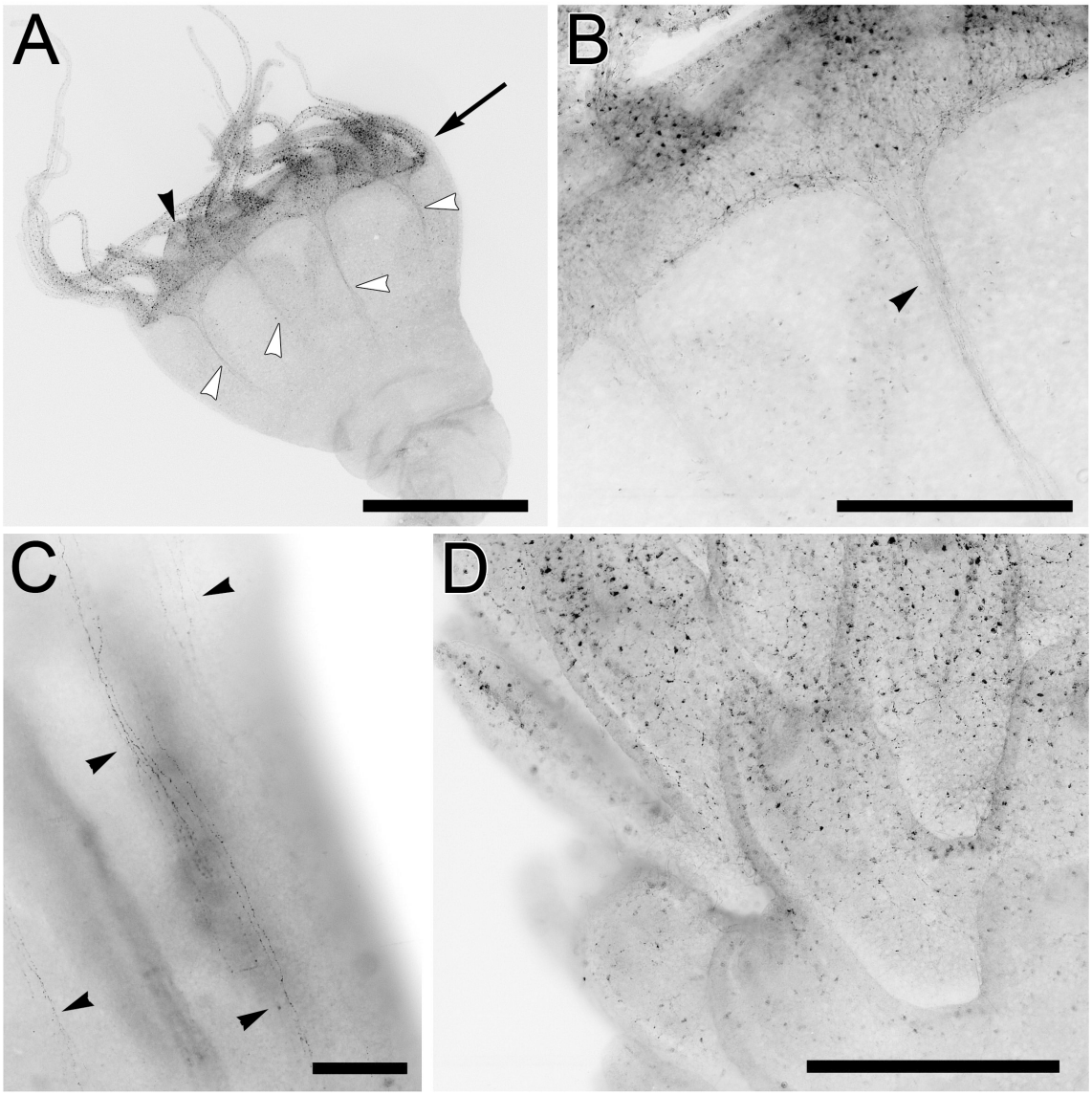


Figure 47. FMRFamide immunolabelling in *Aurelia* sp. polyps and strobila. **A:** FMRFamide-IR neurons were associated with tentacle and longitudinal musculature (white arrowheads). Neurons were concentrated around the periphery of the oral disc between the tentacles (arrow). Neurons were also concentrated at the lip of the hypostome (black arrowhead). Scale bar, 1 mm. **B:** Detail of (**A**). Neurites extended from the oral disc to run along the longitudinal muscles (arrowhead). Scale bar, 400 µm. **C:** Tracts of epidermal neurites (arrowheads) on the body column of a polyp. Scale bar, 100 µm. **D:** Ephyra nearer the apex (towards the top of the photo) of strobila had more advanced neurite development than those at the base (towards the bottom of the photo). Scale bar, 400 µm.

4.0 Discussion

Haliclystus 'sanjuanensis' and *Manania handi* both had marginal, longitudinal, perradial and manubrial muscle groups, and longitudinal musculature in the tentacles. The marginal muscle of *H. 'sanjuanensis'* was subumbrellar and divided into eight perradial and interradial segments at the ends of the arms, while that of *M. handi* was exumbrellar and undivided save a narrow band inside the lip of the calyx which was interrupted at the ends of the arms. The longitudinal muscles of *H. 'sanjuanensis'* are simple fan shapes while those of *M. handi* are pinnate and include branches which extend back from the ends of the arms on to the perradial pockets.

Neurons of *H. 'sanjuanensis'* and *M. handi* were immunoreactive to FMRFamide and α-tubulin antibodies and formed subumbrellar, exumbrellar and gastrodermal networks. FMRFamide antibodies co-labelled a subset of the more extensive network labelled by α-tubulin antibodies. FMRFamide-IR neurons were concentrated in sensory structures and over muscle bands. While the adhesive glandular swellings of the primary tentacles were lacking innervation, an intriguing concentration of cell bodies at the base of the primary tentacles was found.

Observations of general morphology and behaviour provide context with which to interpret the functional significance of neuromuscular features.

4.1 Musculature

4.1.1 Possible homology of staurozoan and medusa subumbrellar musculature

The form and position of the marginal circular muscle, perradial muscles and muscles of the manubrium in staurozoans (Figs. 12, 15) suggests that they are homologous to the swim, perradial and manubrial muscles of other medusozoans. As demonstrated by fluorophore-tagged phalloidin labelling, the manubrial muscles of both scyphomedusae and staurozoans comprise four smooth perradial muscles that extend from the manubrial lips along the corners of the manubrium and then fan out over the subumbrella and insert at the marginal muscle of staurozoans or at the circular swim muscle of scyphomedusae. Both scyphomedusae and staurozoans also have weak, circularly-oriented muscle fibers on the interradial faces of the manubrium. Information on manubrial musculature in Cubozoa and Hydrozoa is sparse, although Satterlie *et al.*

(2005) reported that the cubomedusa *Tripedalia cystophora* possesses perradial muscles that extend from the lips of the manubrium to the swim muscle. It is unknown whether this species also possesses circularly oriented fibers on the interradial faces of the manubrium; Satterlie *et al.* (2005) mentioned the possibility that their actin labelling had not shown some muscle groups, as the circular muscles of the tentacles were not shown in their preparations. Scemes and McNamara (1991) found that the hydromedusa *Liriope tetraphylla* also had four smooth perradial muscle bands extending from the manubrial lip to bell margin, but they did not mention circular muscles on the interradial faces of the manubrium.

All medusae possess striated, circular swim muscles. The staurozoan marginal muscle is composed of smooth fibers, but its position, its relationship to other muscle groups, and its ontogenetic derivation from subumbrellar ectoderm is consistent with a common origin to the swim muscles of other medusozoans (Fig. 48). This arrangement of muscles, which differs from that of anthozoan and medusozoan polyps (see Chapman, 1965; Chia *et al.,* 1982; Swain *et al*., 2015), suggests that the common ancestor of the Medusozoa incorporated a life stage that possessed a circular muscle, radial muscles associated with the four-cornered manubrium and extending to the margin of the calyx, and perhaps circularly oriented muscle fibers on the interradial faces of the manubrium. Regardless of whether the medusa arose once or twice (see Thiel, 1966; Salvini-Plawen, 1978; Werner *et al.* 1983; Bridge *et al.*, 1995; Marques and Collins, 2004; Kayal *et al.*, 2013) it is possible that these muscle groups have been conserved from the common ancestor of the Medusozoa before a planktonic medusa stage emerged.

If this arrangement of muscles was present in the putative sedentary ancestor of Medusozoa, an understanding of the function of these muscles in modern staurozoans may provide insight into how they eventually became modified to produce the behaviours, particularly the swim contractions, of modern medusae. The circular (marginal) muscle of a sedentary staurozoan-like ancestor, with a primary function in feeding, self-cleaning, or defense, may have been co-opted or repurposed for locomotion. Modifications including a transition from smooth to striated muscle fibers to allow swift, strong contractions, and introduction or refinement of a mechanism to initiate and

coordinate contraction of the marginal muscle (rhopalia), were probably required to facilitate swimming.

The lack of striated muscle fibers in staurozoans supports the hypothesis that the striated muscle characteristic of other medusozoans arose in the common ancestor of Cubozoa, Scyphozoa and Hydrozoa. Striated muscle is not found in Anthozoa save for in the deep sea swimming anemone group Boloceroididae (as stated by Burton, 2008) which is deeply nested in Anthozoa (Rodriguez *et al.,* 2014). Homology of medusozoan and anthozoan striated muscle would require at least five independent losses of striated muscle within Cnidaria (Burton, 2008). Given the recent strong evidence against homology of cnidarian and bilaterian striated muscle (Burton, 2008; Steinmetz *et al.*, 2012) the most parsimonious explanation is that striated muscle arose twice within Cnidaria: once in the lineage leading to Boloceroididae, and once in the lineage leading to Cubozoa, Scyphozoa and Hydrozoa. Unfortunately no molecular studies have compared the striated muscle of Boloceroididae to medusozoan striated muscle; further studies are needed to explore the origin of striated muscle in these groups. Further study is also needed to determine that Staurozoa as a group lacks striated muscle; the musculature of most groups has not been studied in detail, and it is yet possible that striated muscle is present in some groups.

The longitudinal muscles of staurozoans are most similar to those of scyphopolyps: both are four in number, embedded in the mesoglea of the stalk, of ectodermal origin, and are associated with peristomial pits (Wietrzykowsky, 1912; Collins, 2002; Eggers and Jarms, 2007). Cubopolyps have a variable number of longitudinal muscles arranged radially around the body, while hydropolyps have an epidermal layer of longitudinal muscle fibers that originates from the aboral ectoderm (as opposed to the oral ectoderm in Scyphozoa and Staurozoa) and a circular gastrodermal muscle layer (Werner *et al.*, 1976). Cubopolyps and hydropolyps tend to be radially symmetrical rather than tetraradial (Werner *et al.*, 1976). However, not all staurozoans have musculature in the stalk. It remains to be seen whether the similarity between the longitudinal musculature of some staurozoans and scyphopolyps is a result of common descent or convergent evolution between a subset of Staurozoa and Scyphozoa.

4.1.2 Functional hypotheses about muscular features

Several authors have previously investigated the musculature of *Haliclystus* species, using basic observational techniques or histology. The major muscle groups found in *H. 'sanjuanensis'* (longitudinal, perradial, marginal) are similar in form and position to those described by Clark (1878), Miranda *et al.* (2009) and Gwilliam (1960) of *H. auricula*, *H. antarcticus* and *H. 'sanjuanensis',* respectively. Clark (1878) and Gwilliam (1960) also discussed muscles in the tentacles, anchors and gastric filaments.

Although the exumbrellar position of the marginal muscle in *Manania* has been a source of interest, other muscle groups have not been the subject of much study. *M. handi* was described as having eight adradial muscles extending into the arms (Gwilliam, 1956; Larson and Fautin, 1989), and a highly contractile stalk. Gwilliam (1956) noted that the eight adradial muscles joined in interradial pairs near the base of the calyx and ran the length of the stalk in the interradius. Muscle descriptions for other members of the genus are similar. Berrill (1962) and Uchida and Hanaoka (1933) noted that the adradial muscles of *M. uchidai* and *M. atlantica* respectively extended laterally in the wall of the calyx, such that they occupied most of the infundibular wall. Kishinouye (1910) found that the longitudinal muscles in *M. distincta* divided to form two adradial bands only very near the margin, and also noted the presence of broad, weak perradial muscles. My results indicate that the longitudinal muscles form tight bands in the stalk and are pennate in the calyx, spreading out laterally to occupy the majority of the calyx wall. The longitudinal muscles do not diverge into adradial bands until very near the margin, and weak bands of perradial muscle are present.

4.1.2.1 Synchronous contraction of the marginal muscle in *Manania handi*

Manania handi has a complete marginal muscle and is capable of synchronous, pulse-like contractions (Fig. 32B) similar to swim contractions of medusae; this is the first reliable report of such a behaviour in a member of the Staurozoa. Swim-like contractions were not observed in *H. 'sanjuanensis'*, which has a divided marginal muscle. Divided musculature does not preclude synchronous contraction; many medusae have swim muscles divided by radial canals, muscle attachment points or gonad tissue (Cubomedusae: Satterlie *et al.*, 2005; Scyphomedusae: Gladfelter, 1972; Hydromedusae: Gladfelter, 1972; Scemes and McNamara, 1991; Satterlie 2008), but co-ordinated

contraction is possible due to neuronal conduction (Horridge, 1956b). As the nervous systems of *M. handi* and *H. 'sanjuanensis'* are very similar while their musculature differs, it is probably continuity of the muscle rather than specialization of the nervous system that makes synchronous contraction possible in *M. handi.* This hypothesis could be tested by isolating a portion of the marginal muscle of *M. handi* by pharmacologically paralyzing it without disrupting the marginal network of neurons. If disrupting the continuity of the muscle prevents synchronous contraction, then it is continuity of the muscle fibers rather than neural infrastructure that makes synchrony possible. My results support Gwilliam's (1960) conclusion that *H. 'sanjuanensis'* is incapable of swim-like contractions and does not possess an analogue of the GFNN, which coordinates swim behaviours in scyphomedusae.

The function of the pulse behaviour in *M. handi* is not clear. Observations indicate that the contractions do not produce much propulsive force, occur infrequently, and would be useless for locomotion. The contractions might be used to quickly close upon and trap prey, or to expel water from the calyx to remove debris such as exoskeletons of digested and regurgitated prey. Debris might accumulate in the long narrow calyx of *M. handi* and require active expulsion, while debris would probably be easily swept away from the open, flat calyx of *H. 'sanjuanensis'*. The marginal circular muscle can also be partially contracted for extended periods of time such that the calyx opening is pursed. As the tentacles are not folded in during this behaviour, it is unlikely that it serves a protective purpose.

Among staurozoans that have an undivided marginal muscle (*Stenoscyphus, Lipkea, Manania, Depastromorpha, Depastrum,* and *Halimocyathus*), nearly all have a long, narrow body shape with short arms that are little more than tentacles stuck to the edge of the calyx lip. In contrast, most genera that have a divided marginal muscle (*Haliclystus, Lucernaria, Kishinouyea, Lucernariopsis,* and *Sasakiella*) tend towards a flatter, more open calyx and long arms. All staurozoans that have a flat, cruciform shape or paired arms have a divided marginal muscle. This may indicate that a divided marginal muscle is supplementary to the longitudinal muscles and aids in coordinating the longer, more dextrous arms. Certainly in my own observations, *H. 'sanjuanensis'* was capable of a greater variety of arm movements than *M. handi*. It would be interesting to make a

survey of staurozoans that have a divided marginal muscle compared to those with an undivided muscle with respect to a variety of factors to gain a better understanding of how the muscle is used in these groups. Divided or undivided marginal muscles may be correlated with habitat, method of prey capture, prey type, dispersal, locomotion, or spawning behaviour.

4.1.2.2 Exumbrellar position of marginal muscle in *Manania handi*

The exumbrellar position of the marginal muscle of *M. handi*, outside the point of tentacle attachment (Fig. 16A, B), is extremely unusual among cnidarians; the exumbrellar epidermis of medusae does not produce contractile elements, and most polyps also have epidermal musculature derived exclusively from the oral surface (Hündgen, 1984). The oddity of this muscle was commented on by Kishinouye (1910), who described the first species of *Manania* and noted that exumbrellar musculature is not found in scyphomedusae. A single-cell layer of ectodermal origin termed the 'cellular lamella' morphologically separates the subumbrellar and exumbrellar tissue of cnidarians (Grassé, 1997). Sections of this lamella thus provide a line which separates structures derived from the exumbrella and subumbrella. In most staurozoans, the lamella runs just abaxial to the primary and secondary tentacles, which are structures derived from the subumbrella; in *Manania*, the lamella extends below the marginal circular muscle situated outside the tentacles (Uchida and Hanaoka, 1933; Hanaoka, 1935; Carlgren, 1935; Gwilliam, 1956). Muscle fibers are only found on the adaxial side of the cellular lamella in *Manania* (Uchida and Hanaoka, 1933; Hanaoka, 1935) and are therefore morphologically part of the subumbrella. Exumbrellar and subumbrellar epithelia also differ in structure and may be distinguished based on histological features of cell layers (Hündgen, 1984). A similar position has not been noted for the marginal muscle in other staurozoans, with either a divided or undivided marginal muscle. It is unknown if the peculiar position of this muscle confers some function or serves a purpose that is not possible in staurozoans where the muscle is in a typical subumbrellar position.

4.1.2.3 Longitudinal muscles and arm bending

The presence of longitudinal muscles in the calyx, and often in the stalk, of staurozoans has long been known (Clark, 1863b). Clark (1863b) noted that in the calyx of

'L. auricula' the longitudinal muscles filled the space between adjacent gonads. Clark (1878) thought that the muscles extended over the gonads as well but were obscured by pigmentation. Berrill (1963) noted that the expansion of muscle bands in several genera of staurozoans was limited by gonad tissue, and that the two did not overlap. My observations support the assertion that muscle fibers never overlie gonad tissue.

As other authors have noted, arm bending is mediated by the longitudinal muscles (*e.g.* Berrill, 1962, 1963). The marginal muscles probably also play a role in coordinating arm movements in *H. 'sanjuanensis'* and other staurozoans with a divided marginal muscle. Dexterity of the arms probably differs between species depending on calyx morphology and muscle arrangement. Berrill (1962) reported that in *H. salpinx*, all arms were bent simultaneously to the manubrium through contraction of the coronal muscle. However, as the muscles of *H. salpinx* do not differ significantly from those of *H. 'sanjuanensis'* (Berrill, 1963) there must be some other explanation for this behaviour, if Berrill's (1962) observations were accurate. Berrill (1962) reports independent and dextrous movement of arms in *L. quadricornis*, while Gwilliam (1960) claimed that in *H. 'sanjuanensis'* arms were usually bent in interradial, or less frequently perradial, pairs. My own observations indicated that there was no preference for paired arm bending in *H. 'sanjuanensis'*, so it is possible that behaviour within the same species differs depending on geographical region or environmental conditions.

4.1.2.4 Protective 'crumple' response

The protective contractions of *M. handi* and *H.'sanjuanensis'* in which the arms were folded to the manubrium and the longitudinal muscles were contracted to reduce the profile (Figs. 29E; 31D) are similar to the 'crumple' or 'spasm' behaviour common in polyps and medusae. In polyps the tentacles are drawn to the mouth and the longitudinal muscles contract, resulting in a reduced profile; in medusae, the tentacles are retracted, the bell margin is drawn in, and swimming ceases (Chapman, 1965; Mackie and Passano, 1968; Schwab, 1977; Arai, 1997; Scemes and McNamara, 1991; Satterlie, 2014). In medusae, this response is executed by the smooth musculature (Mackie and Passano, 1968; Scemes and McNamara, 1991), is mediated by a conduction pathway separate from that which co-ordinates the swim response (Horridge, 1956b; Mackie and Passano, 1965; Schwab, 1977; Satterlie, 2014) and results in passive sinking (Horridge, 1956b; Satterlie,

2014). In scyphomedusae, this nerve net is the DNN (Horridge, 1956b), which is considered homologous to the single nerve net in scyphopolyps where it also produces the crumple response (Chapman, 1965; Passano, 1982). In both polyps and medusae, the spasm is interpreted as a feeding response that has spread to all arms or tentacles through interneural facilitation (Horridge, 1956a). The similarity of the protective response in staurozoans and scyphozoans suggest that they may be similarly mediated and effected.

4.1.2.5 Pennate shape of longitudinal muscles in *Manania handi*

The flat, pennate shape of the longitudinal muscles of *M. handi* (Figs. 15; 17A, B) may be unique among cnidarians. Although many anthozoans have marginal sphincter muscles described as 'pennate' that are elaborated into folds and have a branching structure in cross section (Swain *et al.*, 2015; Daly, 2004), their structure is not comparable to the longitudinal muscles of *M. handi*.

Pennate muscles increase contraction force (Azizi *et al.*, 2008). *M. handi* may require strong pennate muscles to reduce its profile during protective contractions as it has a tubular calyx with a high profile. *H. 'sanjuanensis'* effectively reduces its profile by folding in its long arms and contracting the short stalk, but the arms of *M. handi* are short and folding them in does not reduce its profile significantly. Rather, during a protective contraction the entire calyx of *M. handi* collapses like an accordion. The pennate muscles may be required to generate the additional force needed to compress the mesoglea of the calyx during this behaviour. That the branches of the longitudinal muscle occupy most of the calyx wall area probably serves both to increase strength and to distribute the force of contraction throughout the calyx in order to reduce stresses on any single part of the calyx wall. During protective contractions, it is likely that the longitudinal muscles of the infundibula also contribute by pulling the manubrium to the base of the calyx. The folds in the longitudinal and marginal muscles of both *M. handi* and *H. 'sanjuanensis'* also have the potential to increase contraction force by increasing the number of contractile fibers per unit of calyx surface area; histology supports the presence of folded muscle bands in staurozoans (Westfall, 1973).

4.1.2.6 Perradial branches of longitudinal muscles in *Manania handi*

Unlike *H. 'sanjuanensis'*, *M. handi* possesses bands of muscle that are apparently offshoots of the longitudinal muscles, which extend back from the arms on to the walls of the perradial pockets (Figs. 15; 17D). The mesoglea of cnidarians functions as a hydrostatic skeleton. Contraction of muscles surrounding a hydrostat increases pressure within the hydrostat, which increases the tension experienced by the wall. Contraction of the longitudinal muscles in *M. handi* strongly compresses the mesoglea, increasing the stresses experienced by the epithelia that contain the mesoglea. The accessory longitudinal muscle bands in *M. handi* may provide structural stability and prevent expansion and rupture of the calyx as the mesoglea is compressed by the pennate longitudinal muscles.

4.1.2.7 Manubrial musculature

The presence of perradial muscles has been noted for several staurozoans (*e.g.* Clark, 1863a; Kishinouye, 1910; Miranda *et al.,* 2009) and is probably ubiquitous among members of Staurozoa. The perradial muscles allow movement of the manubrium independent of or in conjunction with arm movements.

The manubrium is usually pulled along the perradial axes in line with the perradial muscles, but can also move interradially as two perradial muscles contract simultaneously. Similar to scyphomedusae (Horridge, 1956b) and scyphopolyps (Schwab, 1977), the manubrium moves towards the arm or arms that have captured prey during the feeding response, indicating that the tentacles and manubrium are neuronally interconnected. In ephyrae, the perradial muscles at the corners of the manubrium are thought to open the mouth (Eggers and Jarms, 2007) and presumably serve a similar function in staurozoans. Although Berrill (1962) reported that the manubrium of *Lucernaria quadricornis* was actively used to guide suspended food particles into the mouth, and in the cubomedusa *Chironex fleckeri* the manubrium is prehensile and can capture and ingest prey independently (Hamner *et al.*, 1995), no such dextrous movements of the manubrium were observed in *M. handi* or *H. 'sanjuanensis'*. As the lips are muscular and capable of independent movement, they are likely used to grasp prey from the arms when it is brought to the mouth.

4.1.2.8 Lack of gastrodermal musculature

Muscle fibers were not found in the gastrodermis; this is unsurprising as endodermally derived muscles are known only in anthozoans and hydropolyps (Jahnel *et al.*, 2014). Clark (1878) and Gwilliam (1960) both claimed that the gastric filaments of *Haliclystus* were muscular, but I think it very likely they were mistaken. Clark's (1878) claim that the gastric filaments protruded out of the mouth to grasp prey in a prehensile fashion is extraordinary; neither *H. 'sanjuanensis'* nor *M. handi* had filaments long enough to reach the lips of the manubrium. Gwilliam (1960) used histological sections to confirm his observations of musculature, but his data are not shown, and I am again inclined to think him mistaken. The gastric filaments are very slender structures and muscle fibers, if present, should have labelled easily with fluorophore-tagged phalloidin and been clearly visible with confocal laser scanning microscopy. The sinuous movements of the filaments are driven by the dense ciliation along their length.

Descriptions of scyphozoans, cubozoans and staurozoans frequently detail the number and position of gastric filaments, but I can find no study on their function in any Class. As the filaments bear nematocysts and are located in the gastric cavity, we assume that they function in either subduing or envenomating prey for digestion. Schlesinger *et al.* (2009) demonstrated that the acontia (filaments loaded with nematocysts) of some anthozoans envenomate ingested prey with cytolytic substances that aid in digestion. Gastric filaments may perform a similar function in staurozoans. The cells filled with granular material (round globules all of a similar size) along one side of each gastric filament in staurozoans are similar to secretory cells described in the gastrodermis of *Hydra* (Sanyal and Mookerjee, 1960). Their function is not known, but they presumably have some role in digestion, such as releasing digestive enzymes.

4.2. Nervous system

FMRFamide and α-tubulin antibody labelling in *H. 'sanjuanensis'* and *M. handi* revealed that characteristics of innervation varied according to body region. On the subumbrella and exumbrella, α-tubulin antibodies labelled a highly interconnected and regionally concentrated nerve net, a subset of which was labelled by FMRFamide antibodies. On the subumbrella, neurons were concentrated over muscle bands.

FMRFamide-IR neurons of the subumbrella were generally oriented parallel to muscle fibers where they co-occurred. Although FMRFamide antibodies were more strongly immunoreactive than α-tubulin antibodies, the α-tubulin immunoreactivity was persistent; in contrast, Satterlie and Eichinger (2014) and Eichinger and Satterlie (2014) found that α-tubulin antibodies faintly co-labelled FMRFamide-IR neurons in *Aurelia* and *Carybdea*, but that this faded instantly upon illumination. Sensory cells abundant on the tentacles, apices of the nematocyst clusters, manubrial lips and basal disc and neuronal cell bodies labelled either exclusively or much more strongly with FMRFamide than with α-tubulin antibodies. FMRFamide antibody labelling was concentrated in the epithelium over prominent structures such as the tentacles, nematocyst clusters, muscle bands, and manubrium, whereas the α-tubulin-IR neurites were uniformly distributed over all subumbrellar structures save the gonads. The exumbrellar network was predominantly α-tubulin-IR and associated with the exumbrellar nematocyst batteries; a very small subset of exumbrellar neurons co-labelled with FMRFamide antibodies. The subumbrellar gastrodermis was provided with an exclusively FMRFamide-IR network while the exumbrellar gastrodermis was devoid of immunoreactivity.

Comparing characteristics of the staurozoan nervous system to those of polyps and medusae of other cnidarian classes may provide insights into evolution of cnidarian nervous systems. Comparisons to Scyphozoa and Cubozoa are particularly relevant as staurozoans were, until recently, classified as scyphozoans, and some molecular and developmental data suggest a close relationship between Staurozoa and Cubozoa. Since phylogenetic data support Staurozoa as the sister group to the remaining Medusozoa, and because staurozoans have features that are intermediate between polyps and medusae, it is also important to make comparisons to polyp forms, including anthozoans. Although RFamide distribution has been investigated in many polyps and medusae, tubulin distribution has only been cursorily studied. Some groups, such as cubopolyps, have been entirely overlooked in terms of immunolabelling.

4.2.1 Net-like organization of nervous system

The nervous system of both *H. 'sanjuanensis'* and *M. handi* comprised an interconnected network of neurons with regional variation in density and orientation of neurons, which is characteristic of cnidarian nervous systems in general (Satterlie, 2002).

Although the diffuse radial organization of cnidarian nerve nets is often considered primitive, the diffuse organization with non-polarized bidirectional synapses is admirably suited to their radial body plan, as stimuli can be received at any point and be transmitted quickly to the rest of the body (Satterlie, 2011; Eichinger and Satterlie, 2014). Other typical cnidarian characteristics displayed by the staurozoan nervous system are: subumbrellar, exumbrellar and gastrodermal innervation; increased neuronal density and orientation on the subumbrella over muscular regions (Chapman, 1965); concentration and specialization associated with the primary tentacles (Anderson *et al.,* 2004); FMRFamide immunoreactivity primarily associated with smooth muscle and sensory systems; concentrations of FMRFamide immunoreactivity in light-sensitive organs (Plickert and Schneider, 2004); concentrations of FMRFamide-IR sensory neurons on the manubrium and tentacles; punctate labelling of neurites (Parkefelt and Ekstrom, 2009); probable innervation of nematocysts (Anderson *et al.*, 2004); and increased density of innervation towards the oral disc (Grimmelikhuijzen *et al.*, 1985).

Where α-tubulin and FMRFamide immunoreactivity co-occur in cnidarians, the network of neurites labelled by α-tubulin antibodies tends to be much denser and more interconnected than that labelled by FMRFamide antibodies (Anthozoa: Girosi *et al.*, 2005; Staurozoa: present work; Scyphozoa: Satterlie, 2008; Satterlie and Eichinger, 2014; Cubozoa: Eichinger and Satterlie, 2014; Hydrozoa: Groger and Schmid, 2000). Tubulin antibodies label microtubules composed of tubulin, which are components of the cytoskeleton of all cells, and enriched in neurites (Martin, 1988), while RFamide antibodies label a specific neuropeptide (Grimmelikhuijzen *et al.*, 2002). Thus it is unsurprising that the network of neurites labelled by α-tubulin antibodies is more extensive than that labelled by RFamide antibodies.

Only three studies have previously investigated the nervous system of staurozoans; my observations agree in many respects with Kassianow's (1901) extensive morphological investigations using tissue masceration, staining and histology, Gwilliam's (1960) physiological experiments and Westfall's (1973) ultrastructural study.

4.2.2 One or two nerve nets? Comparison to other medusozoans

A single nerve net is considered characteristic of polyps (Horridge, 1956a; Schwab, 1977, Passano, 1982) while medusae have multiple parallel-conducting systems

that coordinate their more complex behaviours (Passano, 1982; Satterlie, 2002). However, it is not immediately clear what it means to have “single nerve nets” or “multiple parallel-conducting systems”.

In scyphomedusae, where a large body of neurophysiological and immunohistochemical work has been done on *Aurelia* sp., “parallel conducting systems” is used to describe two nets that label with different substances (the GFNN labels with α-tubulin antibodies, the DNN with FMRFamide antibodies) and although they overlap, their neurites are not continuous and do not co-label. The two nets are continuous only at the rhopalia. Each nerve net independently innervates the musculature and has a different primary function (Satterlie and Eichinger, 2014; Satterlie, 2011; Horridge, 1956a, 1956b; Passano, 1973).

The nervous system of cubomedusae is similar to that of scyphomedusae in many respects: physically distinct but overlapping RFamide and α-tubulin immunorective nets are present, the primary function of the α-tubulin-IR net is motor while the RFamide-IR net is sensory and modulatory, and co-labelling of neurons with both substances is not observed (Eichinger and Satterlie, 2014). Given these descriptions, “multiple parallel conducting systems” as it is applied to scyphomedusae and cubomedusae seems to denote nerve nets that are immunohistochemically distinct and physically separate except at key neural centers.

The hydromedusa *Aequorea victoria* has a physically continuous subumbrellar network of neurons composed of overlapping populations of tubulin and FMRFamide immunoreactive neurons, which was described as “two distinct nerve nets” (Satterlie, 2008). The subumbrella of the hydromedusa *Neoturris* similarly co-labels with α-tubulin and FMRFamide antibodies and was described as having “two plexuses” (Mackie and Meech, 2008). Mackie and Meech (2008) infer that the subumbrellar network of *Neoturris*, which is continuous with the inner nerve ring, is responsible for innervating the smooth subumbrellar radial muscles; the nerve net associated with the striated muscle is α-tubulin-IR but not FMRFamide-IR. Tubulin and FMRFamide -IR neurons apparently represent only a small portion of the neural infrastructure of hydromedusae, and physically distinct nets are present which fulfill the criterion of ‘multiple parallel

conducting systems' as described above for scypho- and cubomedusae (Passano, 1973; Satterlie and Spencer, 1987; Satterlie 2008; Mackie and Meech, 2008).

If the definition above is accepted for 'multiple parallel conducting systems', then having more than one 'distinct nerve net' alone is not sufficient to fulfill it. Furthermore, by the above definition of 'distinct nerve nets', many polyps have more than one nerve net. Differential tubulin and RFamide immunoreactivity were found in the anthozoan *Eunicella cavolini* (Girosi *et al.*, 2005). Tyrosinated tubulin and RFamide antibodies label diffuse nerve nets in the epidermis of the hydropolyp *Phodocoryne carnea*; it is not clear if some neurons were co-labelled, but the orientation and localization of the nets differed (Groger and Schmid, 2000). In the hydropolyp *Coryne*, sensory cells label only with RFamide antibodies, while all other neurons co-label with tubulin and RFamide antibodies (Golz, 1994). Double labelling experiments have not been performed for scyphopolyps and cubopolyps. What constitutes a significant enough difference to be considered a separate net? The RFamide and FMRFamide antibodies commonly used in cnidarian immunolabelling studies are usually not specific to the species or even classes that they are applied to: more specific RFamide antibodies tailored to the species being labelled might reveal more extensive networks than those visualized with nonspecific ones (Grimmelikhuijzen *et al.*, 2002). Antibodies may be devised that label all neurons in an animal (Marx, 1997; Lin *et al.*, 2001), or that label only one kind of sensory cell (Hobmayer *et al.*, 1990). Although minute immunohistochemical distinctions may be found between neurons, at what level is differentiating between them functionally useful for general purposes? Electrophysiologically and behaviourally, scyphopolyps have a single nerve net (Chapman, 1965; Schwab, 1977). Thus the best interpretation for the nervous system of polyps and the subumbrellar plexus of hydromedusae, is probably that there is a *single* net or plexus (as all of the neurons are physically continuous with each other) with regional specialization.

By these definitions, the neuromorphology of staurozoans has more in common with polyps than medusae; although their neurons label with at least two different antibodies, there is no physical separation of these populations and co-labelling is extensive. The innervation associated with the gastrodermis might be considered a distinct nerve net; it is both immunohistochemically distinct from the epidermal network

in that it labels exclusively with FMRFamide antibodies, and physically separate in that it is only continuous with the epidermal network at the lip of the manubrium. The exumbrellar network is also distinct from the subumbrellar network in that it is much more diffuse and predominantly labels with α-tubulin antibodies. However, as the subumbrellar network is continuous with the exumbrellar network at the margin, and with the gastrodermal network at the lip of the manubrium, the nervous system of staurozoans consists of a single continuous, regionally differentiated net.

4.2.3 Sensory neurons and structures

Sensory structures are associated with increased density of neurons, and label strongly with antibodies to known cnidarian neuropeptides (*e.g.* Anderson *et al.*, 2004; Plickert and Schneider, 2004; Nakanishi *et al*., 2009; Satterlie and Eichinger, 2014). While the neurons of nerve nets ("ganglion cells") generally lie parallel to the epithelial surface, sensory neurons are perpendicular to the epithelium, and have a peripheral cell body and sometimes a fine process extending to the surface of the epithelium (Kassianow, 1901; Westfall, 1973; Hobmayer *et al.*, 1990; Golz, 1994; Anderson *et al.*, 2004).

In medusae of all classes, RFamide immunoreactivity is associated with smooth muscle, sensory structures such as rhopalia, and concentrations of sensory cells in the manubrium and tentacles (Mackie *et al.*, 1985; Carlberg *et al.*, 1995; Groger and Schmid, 2000; Jacobs *et al.*, 2007; Satterlie and Eichinger, 2014; Koizumi *et al*., 2015). RFamide immunoreactive nerve nets are interpreted as having a sensory function with some secondary motor function, and usually innervate smooth muscle (Mackie *et al.*, 1985; Anderson *et al.*, 1992; Mackie and Meech, 2008; Eichinger and Satterlie, 2014; Satterlie and Eichinger, 2014). The RFamide-IR network is never associated with striated swim muscles (Mackie *et al.*, 1985; Groger and Schmid, 2000; Satterlie, 2008; Eichinger and Satterlie, 2014; Satterlie and Eichinger, 2014). The primary orientation of the RFamide-IR nerve net differs between species, but is generally oriented parallel to the muscle fibers it overlies or is arranged radially (Anderson *et al.*, 1992; Satterlie and Eichinger, 2014; Groger and Schmid, 2000), as it is in the staurozoans, *H. 'sanjuanensis'* and *M. handi*. The close association of FMRFamide-IR neurons with the smooth muscles in *H.*

'sanjuanensis' and *M. handi* suggest that as in other cnidarians, a primary function of the FMRFamide-IR network is to innervate the smooth muscle.

As sensory and muscular structures tend to be concentrated at the oral end, immunoreactivity tends to increase towards the oral end of polyps (Anthozoa: Pernet *et al.*, 2004; Girosi *et al.*, 2005; Scyphozoa: Sakaguchi, 1999; Hydrozoa: Golz, 1994; Groger and Schmid, 2000). The concentration of sensory cells on the tentacles and manubrium is such that some consider these true "sense organs" (Jacobs *et al.*, 2007). FMRFamide immunoreactivity is also associated with sensory cells in some polyps (Golz, 1994). This pattern holds true for staurozoans: sensory cells were either exclusively or much more strongly labelled by FMRFamide than by α-tubulin antibodies, and were concentrated on the manubrium, tentacles and specialized sensory structures.

4.2.3.1 Pigment spots of *Manania handi*

During development, primary tentacles of scyphozoans and cubozoans transform into rhopalia, which incorporate a statocyst and one or more ocelli, whereas primary tentacles of staurozoans usually transform into anchors or other adhesive structures. However, the transformed primary tentacles of staurozoans do not act as pacemakers or as initiators of spontaneous activity as do the rhopalia of scyphomedusae and cubomedusae. Removal of the anchors or even the entire margin does not inhibit spontaneous activity in *H. 'sanjuanensis'* (Gwilliam, 1960). However, the concentration of FMRFamide-IR cell bodies and neurites at the base of the anchors of *H. sanjuanensis* and primary tentacles of *M. handi* (Fig. 38) suggests that transformed primary tentacles of staurozoans and other medusozoans may share a sensory role. Kassianow (1901) did not find neurons concentrated in the anchors and thought that investigators who claimed ocelli were associated with the anchors were mistaken. However, he did note a distinct concentration of neurons at the base of the anchors in *H. octoradiatus*, which he considered consistent with their use in locomotion and concluded that this concentration acted as a nerve-center to coordinate locomotion. His illustration of this concentration of neurons corresponds exactly to the location of the pigment spot in *M. handi* and the corresponding concentration of neuronal cell bodies and neurites in both *M. handi* and *H. 'sanjuanensis'*.

Reliable accounts of the members of the genus *Manania* indicate that a pigment spot at the base of each primary tentacle is characteristic of the genus (Berrill 1962, *M. atlantica*; Kishinouye 1910, *M. distincta*; Uchida and Hanaoka 1933, Naumov 1961, *M. uchidai*; Gwilliam 1956, Larson and Fautin 1989: *M. handi, M. gwilliami*). Pigment spots are not mentioned in descriptions of *M. auricula* (Clark, 1863b) and *M. hexaradiata* (Broch, 1907), but these descriptions were made from preserved material that had lost pigmentation, and the validity of these species is questionable as they have no features that clearly distinguish them from other *Manania*. *Manania hexaradiata* (Broch, 1907) was described from a single abnormal (hexaradiate) specimen. Although its geographic location in the Canadian Arctic distinguishes it from other *Manania, M. uchidai* is also known from circumpolar waters (Barents sea; Naumov, 1961). *M. auricula* is found in Maine, and as described by Clark (1863), who apparently did not take sections of the animal, cannot be distinguished from *M. atlantica* (Berrill, 1962), which is found in the same location.

Kishinouye (1910) and Uchida and Hanaoka (1933) hypothesized that the pigment spots of *Manania* were light-sensitive organs, and Berrill (1962) described the spot as a "small spherical ocellus". Clark (1878) found that a small pigment spot, which he interpreted as an ocellus, was present at the base of the primary tentacles in juvenile *H. auricula*, but further pigmentation obscured the spot once the animal reached about 6 mm in diameter. *Stylocoronella reidlii* and its congener *S. variabilis* have pigmented spots on the edge of the calyx at the base of the tentacles (Kikinger and Salvini-Plawen, 1995); histology supports the hypothesis that in *S. reidlii* these spots are light-sensitive, although the animal did not show distinct reactions to light stimuli (Blumer *et al.* 1995). Likewise, *M. handi* did not appear to modify its behaviour under varying light conditions. Light sensitivity has been reported for some staurozoans (*H. salpinx, L. quadricornis, M. atlantica*) but these animals were treated very roughly, and movements that were interpreted as initiated by light may have been in response to distress (Berrill, 1962). Other authors have specifically noted that staurozoans do not respond to light stimuli (Lamouroux, 1815).

The concentration of FMRFamide immunoreactive cell bodies and neurites around the pigment spots in *M. handi* supports an interpretation of these spots as sensory

structures (Nakanishi *et al*., 2009; Satterlie and Eichinger, 2014); photoreceptive organs in particular are associated with RFamide immunoreactivity in cniarians (Plickert and Schneider 2004). Pigments are frequently, but not always (Martin, 2002), associated with light-sensitive organs in cnidarians and other metazoans. The presence of pigment in conjunction with strong FMRFamide immunoreactivity strongly argues for a light receptive function of the pigment spots in *Manania.*

Light is a common spawning cue for many cnidarians and various other invertebrates (Anthozoa: Sweeny *et al.* 2011; Staurozoa: Otto, 1976; Hydrozoa: Ballard, 1942; Martin, 2002 Other invertebrates: Purcell, 2005). Some staurozoans also spawn in response to light (Otto, 1976). Thus, ocelli in staurozoans may detect light to trigger synchronous spawning, rather than to modify immediate behaviour. Although *H. 'sanjuanensis'* does not have pigment spots, a similar concentration of neurons is present in a corresponding location. This suggests that despite a lack of pigment spots in many staurozoan genera, they may regardless have a knot of light-sensitive neurons at the base of each primary tentacle that is used to co-ordinate spawning. Alternatively, a concentration of pigment may be present but is obscured by surrounding pigmentation, as noted by Clark (1978). The species that Otto (1976) observed spawning in response to light has no distinguishable ocelli, and yet must have a sensory structure that responds to light. Wietrzykowsky (1912) also observed predictable synchronous spawning in three genera of staurozoans, which may have been co-ordinated by light levels.

The numerous pigment spots in *Stylocoronella reidlii* and *S. variabilis* are associated with the bases of the primary and secondary tentacles. There is evidence that these are light-sensitive structures in juveniles (Blumer *et al.*, 1995). In adult *S. reidlii,* many pigment spots are present at the base of the secondary tentacles and a pigment spot is present in each marginal perradius, although the primary tentacles migrate during development to join the secondary tentacle bunches (Kikinger and Salvini-Plawen, 1995). As the pigment spot remains even when the primary tentacle relocates, this indicates that even genera that lack primary tentacles as adults (*Craterolophus, Lucernaria, Lipkea*) may retain light-sensitive spots at the margin in the interradii and perradii. It would be interesting to see if the pigment spots associated with the base of the secondary tentacles, and the interradial margins that no longer bear distinct pigment spots in *S. reidlii* and *S.*

variabilis, are associated with a knot of concentrated neurons as are the pigment spots of *M. handi*.

The concentration of neurons associated with the pigment spots at the base of the primary tentacles in *M. handi*, and similar concentration present at the base of the tentacles in *H. 'sanjuanensis'*, supports the hypothesis that the transformed primary tentacles of staurozoans are homologous to the rhopalia of cubo- and scyphomedusae (Clark, 1865; Hornell, 1893; Hurst, 1893; Kassianow, 1901; Wietrzykowsky 1910, 1912; Thiel, 1966; Marques and Collins, 2004; Nakanishi *et al*., 2009) and perhaps the marginal sensory structures of hydromedusae (Jacobs *et al.*, 2007; Nakanishi *et al*., 2009). In addition, the same genes involved in patterning rhopalial sensory structures in scyphozoans are expressed in the tentacles of the anthozoan *Nematostella vectensis* during development (Mazza *et al.*, 2007), suggesting that medusozoan tentacle-derived sensory structures may have evolved from pathways that existed in the common ancestor of cnidarians (Jacobs *et al.*, 2007; Nakanishi *et al.*, 2010). This finding supports the hypothesis that the common ancestor of Medusozoa had simple sensory organs associated with the base of the tentacles (Fig. 48); these were probably photoreceptive and may have functioned to detect changes in light levels as a spawning cue or to avoid predators. Further study is needed to determine whether light-sensitive spots associated with the base of the primary tentacles is characteristic of Staurozoa.

4.2.4 Gastrodermal innervation

Gastrodermal nerve nets appear to be typical of cnidarians. The characteristics of gastrodermal nerve nets vary and little attempt has been made to identify the functional significance of the differences, or indeed of the gastrodermal network itself. A gastrodermal network of neurons is probably typical of staurozoans; Kassianow (1901) also found a gastrodermal network of neurons in three staurozoan genera.

An RFamide-IR gastrodermal nerve net lines the subumbrellar and exumbrellar surfaces of the gastric cavity in some scyphomedusae (Passano 1982; Anderson *et al.*, 1992), while Carlberg *et al.* (1995) found that the gastrodermal nerve net of the scyphomedusa *Cyanea* was RFamide-IR in young medusae but switched to taurine-IR in older animals, suggesting a change of function with age. RFamide-IR gastrodermal nerve nets have also been found in anthozoans (Grimmelikhuijzen *et al.*, 2002; Pernet *et al.,*

2004; Girosi *et al.,* 2005), where they may innervate the gastrodermal musculature (Pernet *et al.,* 2004). Both RFamide-IR and serotonergic neurons have been found in the gastrodermis of hydropolyps (Grimmelikhuijzen, 1985; Mayorova and Kosevich, 2013). RFamide immunoreactivity has been found in the gastrodermis of developing hydromedusae (Groger and Schmid, 2000). Mackie and Meech (2008) found that the gastrodermal canals and stomach of the hydromedusae *Aglantha* and *Neoturris* were lined with a tubulin-IR plexus that inhibited swimming during feeding in response to chemosensory cues; in one of these two medusae this gastrodermal nerve net also initiated contraction of the radial smooth muscles that bring food to the manubrium. The gastrodermal nerve plexus of *Neoturris* was only found on the subumbrellar side of the gastrodermal canals (Mackie and Meech, 2008). Similarly, the gastrodermal nerve net of *M. handi* and *H. 'sanjuanensis'* occurs only on the subumbrellar surface, while the exumbrellar gastrodermis including taenioles is devoid of FMRFamide-IR neurons. If the exumbrella of the gastric cavity is innervated in staurozoans, it is immunologically distinct and perhaps performs a different function from the subumbrellar gastrodermis.

The main function of the gastric cavity in cnidarians is digestion and in cnidarians other than hydrozoans the gastrodermis is also the source of gametes, so it is reasonable to assume the neurons found in the gastrodermis are involved in coordinating processes related to digestion or gamete maturation. As the gastrodermal network of staurozoans is continuous with the epidermal, subumbrellar network at the manubrial lip, it is possible that the gastrodermal network influences behaviours related to feeding, as described for the hydrozoans *Aglantha* and *Neoturris* (Mackie and Meech, 2008). Sensory cells present on the gastric filaments may detect the presence of prey in the gastric cavity and trigger processes that aid in digestion such as enzyme release and nematocyst discharge. Marx (1997) found that the gastric filaments of *Aurelia* ephyrae were also innervated and bore sensory cells. Satiation inhibits nematocyst discharge (Smith *et al.*, 1974), prey capture and ingestion in many cnidarians (Thorington *et al.*, 2010). The cilia on the inner surface of the manubrium or hypostome in cnidarians presumably accept food from the tentacles and move prey into the gastrodermis for digestion (Larson, 1980), and are known to reverse direction in order to eliminate indigestible particles (Chapman, 1972). The gastrodermis may monitor satiation levels and inhibit feeding when the gastrovascular

cavity is full, or control the cilia that cover the gastrodermis to coordinate feeding and release of indigestible waste.

4.2.5 Possible significance of features of staurozoan neuromorphology

Studying the characteristics of nerve nets, such as interconnectedness and orientation, can provide clues to their function. In cnidarians, diffuse networks of nonpolarized neurons facilitate co-ordination of the radial body plan as stimuli can be received at any point and be transmitted in all directions (Satterlie, 2011; Eichinger and Satterlie, 2014). Long, parallel neurons oriented along effectors increase conduction speed by taking the shortest distance to their targets. Nerve nets that are below the epithelial surface and embedded between muscle fibers are implicated in innervating musculature, whereas superficial neurons suggest a sensory or modulatory function (Eichinger and Satterlie, 2014).

In the sea anemone *Calamactis praelongus*, conduction velocity is higher in the upper portion of the retractor muscles where neurons are long, dense and parallel to the muscle fibers (Pickens, 1969). In Staurozoa, the FMRFamide-IR network is selectively concentrated over and parallel to the smooth muscle fibers. Therefore it is likely that a primary function of neurites containing FMRFamide is to innervate the muscles as these features increase conduction velocity. The more extensive and interconnected network labelled by α-tubulin antibodies may connect the FMRFamide-IR neurons and transmit stimuli from one location to another, coordinating function.

Increased neuronal density and orientation along some muscle bands may indicate an ability and need for those muscles to contract more swiftly than their diffusely-innervated counterparts. The strong bands of longitudinal muscle and tentacle muscles in *M. handi* and *H. 'sanjuanensis'*, and the marginal muscle of *H. 'sanjuanensis',* best fit this description. Although the marginal muscle of *M. handi* is densely innervated, neurites are not typically parallel to the muscle fibers, and may indicate a need for even spread of excitation rather than speed.

In *M. handi* there are two distinct sets of neurons associated with the interradii; the neurites embedded in and parallel to the longitudinal muscles which presumably function in innervating them, and the long, superficial neurites of the calyx (Fig. 40). The thick bundle of neurites running up the centre of each longitudinal muscle probably

serves to conduct impulses quickly along the longitudinal muscles and into the branches on either side, which may aid in co-ordinating protective responses. The superficial network does not appear to directly interact with the underlying muscular network, and is composed of long, parallel, longitudinally oriented neurons. This suggests that these neurons may serve to quickly conduct sensory information from the base of the calyx to the lip (or *vice versa*). *H. 'sanjuanensis'* also possesses both superficial and embedded neurites, but they are not organized into distinct layers as they are in *M. handi*.

Punctate immunolabelling of neurites in *H. 'sanjuanensis'* and *M. handi* suggests, as it does in other cnidarians, that many peptide-releasing sites (synaptic sites) are present along the length of the neurites (Parkefelt and Ekstrom, 2009), indicating that neurites are synaptically connected to many other cells. These usually represent en-passant synapses with other neurons, epitheliomuscular cells, and nematocytes (Westfall, 1973).

4.2.6 Behavioural corroboration of nerve net properties

Arm bending patterns and spontaneous movements observed in *H. 'sanjuanensis'* and *M. handi* are consistent with the properties suggested by Gwilliam (1960) for the nerve net of *H. 'sanjuanensis'*. My results support Gwilliam's (1960) conclusions that staurozoans have a single nerve net with no pacemaker system. Kassianow (1901) was so impressed with the concentration of neurons at the ends of the arms, around the base of the tentacles that he considered these "nerve centers" and thought they had an integrative or ganglionic role. Although neurites are certainly concentrated around the base of the tentacles (see Figs. 34F, 36G), this may be simply a consequence of the fact that neurites innervating many structures meet in this region: neurites from the margin, perradii and interradii, tentacles and exumbrella are all continuous at the arms.

Gwilliam (1960) inferred from his physiological experiments that the subumbrellar network is through-conducting and requires interneural facilitation to elicit a response, similar to the properties of nerve nets in anemones. Facilitation describes the property of nerve nets where each successive stimulus allows incremental spread of impulses; each impulse facilitates further transmission of the next (Pantin, 1935). Facilitation may be interneural (successive impulses in neurons facilitate the spread of impulses in adjacent neurons) or neuromuscular (successive impulses in neurons facilitate the spread of muscle fiber contraction) (Pantin, 1935). Conduction in staurozoans is

diffuse and decremental, as stimulation of the subumbrella may elicit a response from multiple nearby arms as well as the manubrium, but the further away from the stimulus, the lesser the response (Gwilliam, 1960; present work). The diffuse spread of stimuli suggests that staurozoans possess bidirectional synapses, as other cnidarians do (Satterlie, 2002). Response of the effectors is graded: contraction of the muscles is not an all-or-nothing response and may occur gradually in response to successive stimuli, or suddenly and fully in response to strong stimuli (Gwilliam, 1960).

The exumbrella is less sensitive than the subumbrella and requires high frequency or intense stimuli to produce a response; Gwilliam (1960) interpreted this as adaptive to an environment where the exumbrella is constantly buffeted. In support of this hypothesis, I found a very diffuse exumbrellar network of neurons with no obvious sensory cells save on the basal disc. Insensitivity to stimulation by benign environmental factors, particularly on the exumbrella, would be advantageous to the animal as it is constantly stimulated as wave action moves its seaweed substrate in the intertidal; if it responded to these stimuli, it would rarely assume the relaxed posture with extended arms and tentacles used for prey capture.

The calyx and stalk portions of the longitudinal muscles may contract independently of each other (Gwilliam, 1960; present work) and longitudinal muscles may contract asymmetrically to produce rolling. These asymmetrical contractions suggest that facilitation plays a role in these behaviours. Rolling or sweeping behaviours are probably used to sample the environment for prey. Many spontaneous behaviours involved only one quadrant of the animal, suggesting that the impulse for that behaviour initiated in that quadrant and did not spread beyond it. For a spontaneous behaviour to spread to adjacent sections of the animal, contraction would likely have to be strong enough to stimulate adjacent sections. Although Gwilliam's (1960) results suggested the presence of a mesogleal connection between the exumbrella and subumbrella, but I did not see any evidence of mesogleal nerve fibers.

Although Gwilliam's (1960) results did not exclude the possibility of epithelial conduction, my results suggest that such a system is unnecessary; all behaviours may be explained by the nerve nets observed. Chapman (1965) considered *Aurelia* scyphistoma similar to *H. auricula* in that the epidermis of the calyx and stalk are insensitive, there is

no pacemaker activity, and there is no nervous pathway connecting the longitudinal muscles below the oral disc.

4.2.7 Direct association of neurites with nematocysts

The neurites of the exumbrellar tubulin-IR network appear to be closely associated with the exumbrellar nematocyst batteries (Fig. 45), and may innervate them. Kassianow (1901) also noted the presence of an exumbrellar network of neurons in his study of staurozoans. Direct innervation of nematocytes has been demonstrated in many cnidarians (Westfall, 1973; Anderson *et al.*, 2004; Anderson and Bouchard, 2009). Innervation is not necessary for the discharge of nematocysts (Aerne *et al.*, 2005), but can allow chemosensory cues to modulate sensitivity of the nematocysts, either inhibiting (Smith *et al.*, 1974) or enhancing discharge (Giebel *et al.*, 1988) in response to mechanical stimulation. Nematocysts have a cnidocil, a small spine projecting from the apex of the nematocyst often surrounded by a cone of sensory cilia (Marsical and Bigger, 1976) which acts as a mechanosensory trigger for the nematocyst. Control of nematocyst discharge is desirable as they are single-use cells, and must be continually produced for effective prey capture and defense (Anderson and Bouchard, 2009). RFamide innervation of nematocysts is apparently ubiquitous in cnidarians; RF-amide-IR neurites form a plexus around the base of the cnidocytes that they innervate (Anderson *et al*., 2004).

The exumbrellar nematocysts of medusae are thought to function in defense and do not typically form complexes with other cell types, such as sensory neurons (Anderson and Bouchard, 2009). Exumbrellar innervation varies within and between classes. Eichinger and Satterlie (2014) suggest that the tubulin-IR network in the cubozoan *Tripedalia* may coordinate and stimulate the firing of the exumbrella nematocyst batteries; no FMRFamide immunoreactivity was found associated with the exumbrellar complexes. Scyphomedusae typically have both a FMRFamide-IR and tubulin-IR exumbrellar net (Satterlie and Eichinger, 2014). Tyrosinated tubulin-IR neurites which appear to innervate nematocysts (Groger and Schmid, 2000) and sensory-nematocyst complexes immunoreactive to RFamide (Mackie *et al.*, 1985) have been found on the exumbrella of hydromedusae, while some hydromedusae appear to lack an exumbrellar net (Lin *et al.*, 2001). Although occasional neurons in the exumbrellar plexus of *M. handi* and *H. 'sanjuanensis'* labelled with FMRFamide, these were not as a rule associated with

the nematocyst batteries. However the extensive α-tubulin-IR network, which frequently intersected underneath the batteries, may innervate them.

Anderson *et al.* (2004) demonstrated a nerve plexus at the base of the tentacle epithelium in Anthozoa, Cubozoa, Scyphozoa and Hydrozoa that was directly involved in innervating the nematocysts of the tentacles. This plexus gave rise to many sensory cells that most likely have a role in regulating nematocyst discharge; even cnidocytes that are not directly innervated may be indirectly controlled through association with neighbouring cnidocytes (Anderson *et al.*, 2004). A similar RF-amide-IR plexus with radiating sensory cells was found at the base of the tentacle capita epithelium in *M. handi* and *H. 'sanjuanensis'* (Fig. 36E) and is probably similarly involved in innervating the nematocysts. The epithelium of the tentacle capita in *M. handi* and *H. 'sanjuanensis'* is very thick and may contain several layers of nematocytes (Fig. 24A), such that the surface nematocytes are quite removed from the plexus at the base of the epithelium that presumably innervates them. However, Anderson *et al.* (2004) found that the tentacle plexus may innervate nematocytes that are some distance away if the cnidocyte is greatly elongated to contact the nerve net (Anderson *et al.*, 2004). As neuro-nematocyst synapses were found by Kassianow (1901) in *Craterolophus tethys*, it is likely that some staurozoan nematocysts are innervated as in other cnidarians.

The phalloidin and α-tubulin labelled projections on the tentacle capita (Figs. 13C; 24A; 36F) do not appear to represent cnidocils. Although cnidocils would likely label with both phalloidin and α-tubulin antibodies, given that they contain both microfilaments (actin) and microtubules (composed of tubulin) (Cormier and Hessinger, 1980), there are far more nematocysts than there are projections. These projections may represent cilia of dedicated mechanosensory cells that are responsible for stimulating the discharge of many associated nematocysts.

4.3. Morphological Features of Interest

4.3.1. Nematocyst Clusters

The nematocyst clusters (often erroneously called 'batteries') are found in all genera and appear to be unique to Staurozoa. They are formed either by invagination of the subumbrella (Weill, 1925; Kassianow, 1901) or by delamination (Wietrzykowsky, 1912; Uchida and Hanaoka, 1933) of subumbrellar epidermal cells and appear early in

development of the stauropolyp, well before the gonads differentiate (Wietrzykowsky, 1912). The clusters appear as bubbles sandwiched between the subumbrellar epidermis and gastrodermis, surrounded by a thin layer of mesoglea except at the apex where the wall of the cluster is continuous with the subumbrellar epidermis (Fig. 22C). The nematocysts in the lumen of the clusters are all of the same size, and are loose and disorganized within the pocket (Wietrzykowsky, 1912; Kassianow, 1901; Weill, 1925; Fig. 25A), spilling out freely when the cluster is pierced (Weill, 1925; present work). The nematocysts in the clusters are produced by the epithelium of the pocket and move to the interior when mature (Uchida and Hanaoka, 1933; Kassianow, 1901; Miranda *et al.*, unpublished).

Proposed functions for the clusters include: 1) a reservoir for nematocysts that will be used to replenish tentacle nematocysts when they are depleted (Weill, 1925; Leuschel, 1932), or 2) organs for defence and/or attack (Kassianow, 1901; Uchida and Hanaoka, 1933; Keferstein, 1862; Kling, 1879; Berrill, 1962), specifically for protecting the gonads (Kassianow, 1901; Uchida and Hanaoka, 1933). Weill (1925) believed that all nematocysts were produced in the infundibula and the clusters simply served as a staging area for the nematocysts prior to moving to the tentacles, while Leuschel (1932), Kassianow (1910) and Wietrzykowsky (1912) thought they were produced *in situ*. Uchida and Hanaoka (1933) reportedly observed nematocysts migrating from the clusters into the gastrodermis and epidermis. However, I found that the nematocysts of the clusters were distinct in size and shape from all other nematocysts; the only nematocysts similar in shape to those of the clusters were borne on the gastric filaments, where they appear to be independently produced (see below) and even at their largest were smaller than those of the clusters. The cluster nematocysts could not represent immature subumbrellar or tentacle nematocysts, as they were as a rule much larger and differed in shape.

The epithelium around the apex of each cluster is thickened, producing a raised bump over the solid pack of cells, which in *H. 'sanjuanensis'* (and presumably in *M. handi,* which was not sectioned), connected each cluster to the subumbrellar epidermis (Fig. 22C). Kassianow (1901) also noted thickened epithelium over the apex of the clusters in *Lucernaria campanulata, Craterolophus tethys* and *Haliclystus octoradiatus*,

but instead of a plug of cells he found permanent pores connecting the interior of the cluster to the exterior of the subumbrella. Miranda *et al.* (unpublished) sectioned the clusters of 10 species of staurozoan from 5 genera, and found an aperture connecting the clusters to the subumbrellar surface in only *Lucernaria bathyphila* and *Craterolophus convolvulus*. The wall of each cluster in *M. handi* has muscle fibers running meridionally from the apex to the base of the cluster (Fig. 18B, C); although no muscle fibers were distinguished around the nematocyst clusters of *H. 'sanjuanensis'*, they did label with phalloidin, and it is likely that presence of the muscle fibers was obscured by the overlying perradial muscle fibers and epithelium. Kassianow (1901) also found meridional muscle fibers in the walls of the clusters in the three genera that he studied. Kassianow (1901) assumed that upon stimulation the nematocysts were ejected through the pore by muscular contractions of the cluster walls for defense or attack. Berrill (1962) reported that *Artemia* were killed immediately when they came into contact with the clusters of *L. quadricornis*. Although I pipetted *Artemia* on to the subumbrellar surface, I never observed a similar effect. In both *M. handi* and *H. 'sanjuanensis'* fibers of the various muscle groups adjacent to the clusters deviated around their apices (Figs. 14D; 16C, D; 18; also noted by Kassianow [1901]), which suggests a need for the apex of the cluster to remain unobstructed.

The apices of the clusters are uniquely innervated; in both *M. handi* and *H. 'sanjuanensis'* a ring of putative sensory neurons is borne on the raised epithelium and surrounds the center of the apex (Figs. 42C; 43D, E). Kassianow (1901) also found a ring of neurites and a concentration of sensory neurons encircling the pore in the three genera he studied. The loose nematocytes in the clusters would be easily expelled through a pore by muscular contractions of the cluster walls upon reception of a stimulus by the sensory cells surrounding the aperture. It escapes me how the loose nematocytes would be functional in defense or prey capture, as there is no guarantee that they would be oriented in a direction appropriate to piercing prey or predators. If this behaviour does occur, it is also of interest what triggers the firing of the nematocyst capsules as they lack a cnidocil (Weill, 1925; present work) and are not connected to any cells which could function in triggering them except the nematocyte that contains them. Since the presence of the clusters and the shape of the nematocysts within them are highly conserved in

staurozoans (Miranda, pers. comm.), it is likely that they serve some important function. That of defense or prey capture seems most supported by evidence.

Why then does the exit pore appear to be present in only some species? The pore may only be present following a certain stage of development, or it may be transient. There are examples of orifices in cnidarians that are only created when needed. For example, the microhydrula stage of staurozoans ingests food without a mouth by disrupting the epithelium and engulfing prey when captured (Wietrzykowsky, 1912; Spoon and Blanquet, 1978; Bouillon and Deroux, 1967), and many hydropolyps including *Hydra* spp. do not have a permanent mouth (Campbell, 1987). Campbell (1987) discusses a mechanism for the quick opening of a mouth orifice in *Hydra* spp., which may also be relevant to the nematocyst clusters of staurozoans. When the 'mouth' of *Hydra* spp. is closed, the epithelium of the hypostome is continuous and cells are joined by septate junctions. During feeding, the radial muscles of the hypostome stretch the mouth region, the cell attachments break and a mouth opens. Closure is slow and resembles wound healing (Campbell, 1987). In *M. handi* and *H. 'sanjuanensis'*, the pack of cells that connects each cluster to the subumbrellar surface labels strongly with α-tubulin and phalloidin, indicating that microtubules and microfilaments may be concentrated in these cells. This might be associated with cell movement involved in opening the pore.

Alternatively, if the clusters function primarily in defence of the gonad tissue, the pores may only develop once the gonad tissue reaches a certain level of maturity. The level of development of the specimens in which pores were and were not found by Kassianow (1901) and Miranda *et al.* (unpublished) are unknown. However, if the pore does not open until sexual maturity, it is curious that the nematocyst clusters begin to develop before the gonads do.

It seems unlikely that the presence or absence of a pore would be a species-specific feature as the presence of the clusters themselves is apparently so conserved, and without a way for the nematocysts to exit the cluster, they seem rather useless.

The nematocyst clusters may be a synapomorphy of Staurozoa (Fig. 48); no other group of cnidarians has comparable nematocyst structures, and the nematocyst clusters are prominent morphological features in all genera of staurozoans.

4.3.2 Other features of nematocysts

That nematocytes are produced in one location and migrate to a final destination (usually the tentacles) before use has been observed in many cnidarians and is an accepted characteristic of nematocytes (*e.g.* Wietrzykowsky, 1912; Weill, 1925; Hyman, 1947). Nevertheless, cnidogenesis and migration has only been closely studied in *Hydra* (Burnett and Lentz, 1960; Campbell and Marcum, 1980; Kass-Simon and Scappaticci, 2002). In *Hydra,* nematocytes are produced in the epithelium of the body column and migrate as ameboid cells to the tentacles for use (Campbell and Marcum, 1980). Campbell and Marcum (1980) found that muscle tails acted as guides for the movement of nematocytes, which could move biaxially along the muscle tails and were often seen to reverse direction, but movement was primarily towards the tentacles. The nondischarging end of the capsule always pointed in the direction of migration, so migrational direction was easily deduced without observing movement. If the orientation of the muscle fibers was distorted by grafting, the nematocytes reoriented themselves along the fibers, rather than along the axis of the animal (Campbell and Marcum, 1980). Nematocytes may migrate away from the muscle fibers, but move much more slowly when they do so, and the capsules lose their regular orientation. In *H. 'sanjuanensis'* and *M. handi*, many nematocysts were oriented parallel to the muscle fibers (Figs. 21B; 22A; 24D), suggesting that the nematocytes move along the muscle fibers as they do in *Hydra* (Campbell and Marcum, 1980). On the tentacle stalks, the nondischarging end of the nematocyst capsules pointed towards the capita (Fig. 21B), indicating that the nematocytes were migrating towards the capita to replenish nematocytes there.

Although many nematocysts are produced in a single source location and migrate before use, others are produced *in situ.* Schmidt and Moraw (1982) studied the migration of nematocytes in an anthozoan and found that nematocytes were produced in the epidermis of the body wall and matured as they migrated in an ameboid fashion to the tentacles. All nematocytes were produced in the body wall epidermis except sparse nematocysts in the oral disc which were generated *in situ* (Schmidt and Moraw, 1982). In *Haliclystus octoradiatus,* Wietrzykowsky (1912) noted maturing nematocytes below the infundibula in the stalk muscles, but did not observe migration and therefore was puzzled by their presence in such a useless location. Weill (1925) observed migration of

nematocytes from the base of the infundibula towards the margin in *H. octoradiatus* and inferred that all nematocytes were produced at the base of the infundibula, and were used exclusively in the tentacles. The orientation of the nematocyst capsules along the longitudinal muscles in *H. 'sanjuanensis'* and *M handi* supports the hypothesis that in staurozoans, nematocysts of the tentacles are produced at the base of the infundibula and migrate towards the tentacles. However, the nematocysts of the exumbrella, gastric filaments and gonads are of different sizes and shapes to those in the tentacles and embedded in the musculature (Table 1), so they may be produced *in situ*.

The nematocytes of the clusters are produced *in situ* (see above). Although the nematocysts of the gastric filaments are the same shape as the cluster nematocysts, the cluster nematocysts are much larger than the largest euryteles found in the gastric filaments (Table 1). In addition, the range of nematocyst sizes found in the gastric filaments of *H. 'sanjuanensis'* (Fig. 23B) suggest that these nematocysts are also produced *in situ*.

Heterotrichous microbasic euryteles are spiked toxin-delivering nematocysts that are found in all medusozoan classes, but are absent in Anthozoa. Atrichous isorhizas are ubiquitous in Cnidaria; they have a closed tip, do not deliver toxins, and are used primarily in adhesion (Kass-Simon and Scappaticci, 2002). In *Hydra* these nematocysts are only used in locomotion and their discharge is inhibited in the presence of prey (Ewer, 1947). The presence of these two nematocyst types and no others is characteristic of Staurozoa (Reft, 2012; Miranda *et al.*, 2009; Fautin 2009; Collins and Daly 2005; Larson and Fautin 1989; Gwilliam, 1956). Presence of both isorhizas and euryteles on the tentacles appears to be typical of Staurozoa (Kassianow, 1901; Miranda *et al.*, 2009).

When the types of nematocysts are not useful in identifying species, sometimes the sizes and distribution of the nematocyst types can be informative (Calder, 1977). Nematocyst distribution in *H. 'sanjuanensis'* differed from that of *M. handi* in having nematocysts embedded over the gonads and in the distribution of the nematocyst clusters, which is already known to be species-specific (*e.g.* Hirano, 1997). Specific nematocyst features such as the distinctly eggplant-shaped exumbrellar nematocysts in *H. 'sanjuanensis'* may also prove to be useful in identification if they are sufficiently

unique. Further studies must be done to determine the characteristics of nematocysts in a greater range of staurozoans.

FMRFamide labelling of the expanded portion of the filament of the euryteles over the gonads may indicate that these nematocysts contain a toxin that incorporates the FMRFamide sequence; most cnidarian toxins are proteins or polypeptides (Suput, 2011).

4.3.3 Periderm

Manania handi and *H. 'sanjuanensis'* probably possess a periderm, a proteinaceous sheath secreted by the epidermis which often has a fibrillar structure, may contain chitin or collagen, and encases some part of the organism (Chapman, 1978; Tidball, 1984). The staurozoan periderm is a thin, transparent cup that encases the basal disc and is left behind when the staurozoan moves. A new periderm is produced when the animal reattaches. Gwilliam (1956) also noted that these species (as *M. prasinus* and *H. auricula*) produced peridermal cups; a similar structure has been mentioned by many other authors for a variety of staurozoans (Johnston, 1835; Clark, 1878; Wietrzykowsky, 1912; Migot, 1922). Migot (1922) thought that this sheath was essential to adhesion, and Johnston (1835) thought that the animal was damaged by removing it from the seaweed, and the material left behind was some of its tissue. Some scyphopolyps are able to regrow their peridermal sheath when it is removed, while in others removal results in the death of the polyp (Chapman and Werner, 1972); it is possible that removal does damage some staurozans, but no ill effects were observed when *M. handi* or *H. 'sanjuanensis'* were removed from their periderm.

The structure of the staurozoan periderm was studied by Singla (1976) who found that the sheath contained fibrillar material similar to the periderm of scyphopolyps (Singla, 1976; Chapman, 1968). It is also similar to the small periderm encasing the basal disc of cubopolyps (Chapman, 1978). Marques and Collins (2004) reviewed the presence of periderm in Cnidaria and stated that a periderm or perisarc (the more extensive chitinous cuticle of hydropolyps) is reported for polyp stages of every medusozoan group save staurozoans and is never present in Anthozoa. This assertion that staurozoans lack a periderm has since been used in morphology-based phylogenetic analysis using cladistics (*e.g.* Leme *et al.*, 2008). Given the characteristics outlined above, the basal cup of staurozoans qualifies as a periderm, and contrary to Marques and Collins (2004), all

medusozoan polyps possess a periderm. By this definition many anthozoans also possess a periderm (Tidball, 1984; López-González *et al*., 1995). It is unclear how 'periderm' was used by Marques and Collins (2004).

The periderm may be essential for prolonged adhesion, as suggested by Migot (1922). It may be that those animals that cease to adhere after prolonged time in the lab have lost the ability to produce periderm due to the lack of some essential stimulus or nutrient that is unavailable in lab conditions. In the cubopolyp *Tripedalia cystophora*, the basal disc of the polyp is anchored to the periderm via desmocytes (Chapman, 1978). The periderms of *M. handi* and *H. 'sanjuanensis'* were encrusted with microorganisms, which has been noted previously for staurozoans (Singla, 1976) and other cnidarians (Chapman, 1978). In colonial polyps, the periderm is much more extensive and functions to support long branching portions of the colony.

4.3.4 Anchors

Accessory adhesive structures that function through agglutinants (many cnidarians adhere using nematocysts) are found periodically in members of the Medusozoa. The cubozoan *Copula sivickisi* is unique in having four adhesive pads on the apex of its bell which are used for temporary adhesion to various substrates; similar to the anchors and adhesive pads of staurozoans, adhesion seems to be under nervous control, as accidental adhesion, or adhesion simply due to contact, does not occur (Hartwick, 1991). Also similar to staurozoans, the adhesive pads of *C. sivickisi* contain very few nematocysts and are composed of large columnar cells (Hartwick, 1991). Many hydromedusae also have specialized adhesive organs on the tentacles (Singla, 1977; Hyman, 1947; Honegger, 1984) some of which are composed of glandulomuscular cells, whereas others lack myonemes at the base of the glandular cells. The adhesive pads of staurozoans also lack muscle tails. No evidence of adhesive organs in scyphomedusae has been reported. The accessory adhesive structures described above are used to cling to plants in shallow habitats, and may be used to reduce dispersal or prevent being swept away from rich intertidal waters when the tide goes out (Hartwick, 1991; Hyman, 1947).

A common theme for the glandular cells composing cnidarian adhesive structures is the presence of microtubules that are anchored to the mesoglea and extend to the apex in a parallel orientation to the axis of the secretory cells (Singla, 1976, 1977; Honegger,

1984). Honegger (1986) infers that these microtubules are involved in transport of adhesive material to the cell apex, while Singla (1976, 1977) believes they are contractile and allow the adhesive epithelium to conform to the contour of the substrate. I observed longitudinally oriented α-tubulin-IR filaments in the glandular cells of the adhesive pads of both *M. handi* and *H. 'sanuanensis',* which probably represent microtubules similar to those described above.

I observed extensive use of anchors in *H. 'sanjuanensis'* of all sizes, particularly when roughly handled or when stalk adhesion was disrupted. Spontaneous stalk detachment and reattachment was also observed. When the animal was jostled, the anchors apparently adhered to perform a stabilizing or securing function. Swift adhesion of the anchors to the first thing to come in contact with them when the stalk was detached is probably a functional response to prevent being swept out to sea if they become detached from their substrate, and allow movement from one substrate to another. These observations support the hypothesis that the anchors are used to prevent being swept away in the event that the pedal disc becomes detached (Larson, 1980). Authors that did not observe a function for the anchors (e.g. Hyman, 1940) may not have been working with healthy animals, as evidenced by other observations such as an inability to reattach once removed from seaweed, and lack of feeding.

Although I did not directly observe anchors being used for active locomotion, *H. 'sanjuanensis'* shifted position overnight and showed a preference for substrates in motion. Movement to a new substrate was presumably accomplished in the manner described for other species, where adhesion of the basal disc and tentacles or various adhesive structures (anchors, pads, cushions) is alternated to produce a somersaulting type of movement similar to that of *Hydra*. This behaviour has been reported for *Kishinouyea corbini* (Larson, 1980), *Haliclystus salpinx* and *Lucernaria quadricornis* (Berrill, 1962), *Haliclystus auricula* (Clark, 1878; Couch, 1878), *Haliclystus octoradiatus* (Kassianow, 1901), *Depastrum cyathiforme* (Mayer, 1910), *Stenoscyphus inbai* (Kishinouye, 1902) and *Stylocoronella* (Kikinger and Salvini-Plawen, 1995). When the basal disc was manually detached from the substrate, re-adhesion occurred as it would have during locomotion, the anchors providing adhesion until the basal disc twisted around to adhere to a new substrate.

M. handi were never observed to spontaneously detach the stalk from the substrate and it is therefore unlikely that they routinely move in the somersaulting fashion described above. Use of the adhesive pads was not frequently observed in the still lab environment unless provoked, but presumably they serve a stabilizing function in its turbulent intertidal habitat. Berrill (1962) noted that *Thaumatoscyphus atlanticus* (=*Manania atlantica*) was relatively inactive and while it adhered using its adhesive pads, it never detached from the substrate. It seems likely that *M. handi* might periodically detach from its substrate and move to a new perch, as it was always found on healthy blades of *Phyllospadix* with sparse *Smithora naiadum* growth.

Larson (1980) described a feeding behaviour in *Kishinouyea corbini* where the staurozoan adhered to the substrate using anchors, and then by detaching its stalk flipped over such that the oral surface was pressed against the substrate, trapping prey such as small crustaceans in order to ingest them. I also observed this behaviour in *H. 'sanjuanensis'* (Fig. 29C), although a substantial stimulus was required to initiate it (a large prey item, or many small prey) and prey was more frequently captured by the tentacles and brought to the mouth through arm movement. It is curious that the anchors of *H. 'sanjuanensis'* are so sensitive, as labelling with FMRFamide and α-tubulin antibodies showed that they were conspicuously lacking in innervation. Although sensory neurons were occasionally observed in the distal adhesive pad (Fig. 37B), anchors were often devoid of any apparent innervation. Kassianow (1901) did not find sensory cells in the anchors of *H. octoradiatus*, but did not offer an explanation as to how they could then be used in locomotion. This may suggest the presence of an additional network of neurons that was not immunoreactive to FMRFamide or α-tubulin; as FMRFamide is not a Staurozoa-specific peptide, it is possible that not all RFamide-like immunoreactivity was visualized. Alternatively labelling may have been obscured by the thick epithelium or pigmentation of the anchors; the thick epithelium of the basal disc often obscured the rich network of neurites at its base, which was present regardless. A third interpretation is that the adhesive cells act independent of neuronal innervation. However, this seems unlikely since adhesion behaviour is modulated according to whether or not the medusa is currently attached to something: adhesion is swift if the animal is floating freely, but does not routinely occur if it is attached by the basal disc.

4.3.5 Basal disc

The presence of a small depression at the center of the basal disc in some species of staurozoans led to the hypothesis that suction plays a part in adhesion (Migot, 1922; Berrill, 1962). This does not seem to be the case in *H. 'sanjuanensis'* or *M. handi* as neither species has a depression at the center of the basal disc, and effective adhesion is maintained when only a small portion of the basal disc is in contact with the substrate. Adhesion is most likely accomplished through sticky glandular secretions.

Singla (1976) studied the ultrastructure of the basal disc of *Haliclystus* and found that a rich nerve plexus with symmetrical and asymmetrical synapses lay at the base of the epithelium near the mesoglea; this is confirmed by my observations (Fig. 42B, C). The sensory cells distributed over the basal disc were not mentioned by Singla (1976), but were found by Kassianow (1901). The basal disc contains few nematocytes, and similar to the anchors, the supporting cells of the basal disc contain both microtubules and microfilaments, which could provide contractile force that allows the epithelium to adjust to the contour of the substrate (Singla, 1976). Singla (1977) inferred that the contractile microtubule and microfilament elements of the basal disc were under nervous control.

4.4 Notes on the neuromusculature of *Aurelia* sp.

Chapman (1965) claimed that the tentacles of *Aurelia* sp. scyphistoma were sheathed in muscle. Chia *et al.* (1984) found that longitudinal muscle fibers ensheathed the tentacles, but were much stronger on the adaxial side, explaining why the tentacles always bend towards the mouth. My investigations using fluorophore-tagged phalloidin showed a flat sheet of longitudinal muscle on the adaxial side of each tentacle; presumably the weak muscle fibers on the abaxial side were not labelled strongly enough to be visualized using conventional fluorescence microscopy. I did not find any pseudo-striated muscle in the tentacles as Chia *et al.* (1984) reported. Neurons were concentrated in the epidermal epithelium of the tentacles and oral disc (Chapman, 1965; Sakaguchi *et al.*, 1999; present work); innervation of the tentacles includes sensory cells (Chia *et al.*, 1984). The fibers of the longitudinal muscles do not quite extend to the basal disc (Chapman, 1965; Chia *et al.*, 1984; present work) and the neurites following them similarly thin out and terminate short of the basal disc (Chapman, 1965; Sakaguchi *et al.*,

1999; present work). Chapman (1965) claimed that the ectodermal body wall and stolons also had thin muscle processes, but Chia *et al.* (1984) found no muscle processes in either the body wall or stolons, although they contained aggregates of microtubules and were contractile. The endoderm does not have neuromuscular elements (Chia *et al.*, 1984; present work).

Although Chia *et al.* (1984) claim that the epidermis of scyphistomae is devoid of innervation, my results show tracts of neurites running down the body wall from the oral disc between pairs of tentacles (Fig. 74C). These tracts were found in several polyps that showed no sign of developing into strobila. Marx (1997) found that in the strobila, distal ephyra were increasingly innervated, as I did. During strobilation, ephyral muscles appear to develop *de novo* while the longitudinal muscles of the scyphistoma degenerate (Marx, 1997; present work; Eggers and Jarms, 2007). In the strobila, I observed that the longitudinal muscle bands ran through the stack of ephyra to the base of the distal ephyra, where the muscle bands abruptly terminate. In contrast, Marx (1997) observed that the longitudinal muscle bands were no longer present in the distal few ephyra, and that regular swellings appeared along the muscle bands in each ephyra. I did not observe swellings along the muscle bands.

Marx's (1997) observations of ephyral smooth muscle agree with mine; smooth muscle lines the distal side of the circular swim muscle and the radial arm muscles, and a knot of smooth muscle is present at the apex of the cleft between each pair of arms (Fig. 20A-C). Nakanishi *et al.* (2009) mentions that the DNN surrounds the striated muscles in ephyrae; according to my observations this concentration of the DNN corresponds to the areas of smooth muscle bordering the striated swim muscle. The DNN primarily innervates smooth muscle, therefore it is unsurprising that concentrations of these elements co-occur. Although Grimmelikhuijzen *et al.* (2002) says that 'fast' neurotransmitters of vertebrates, such as glutamate, are not found in Cnidaria, my findings indicated that glutamate immunoreactivity is present in the GFNN of *Aurelia* sp. ephyra.

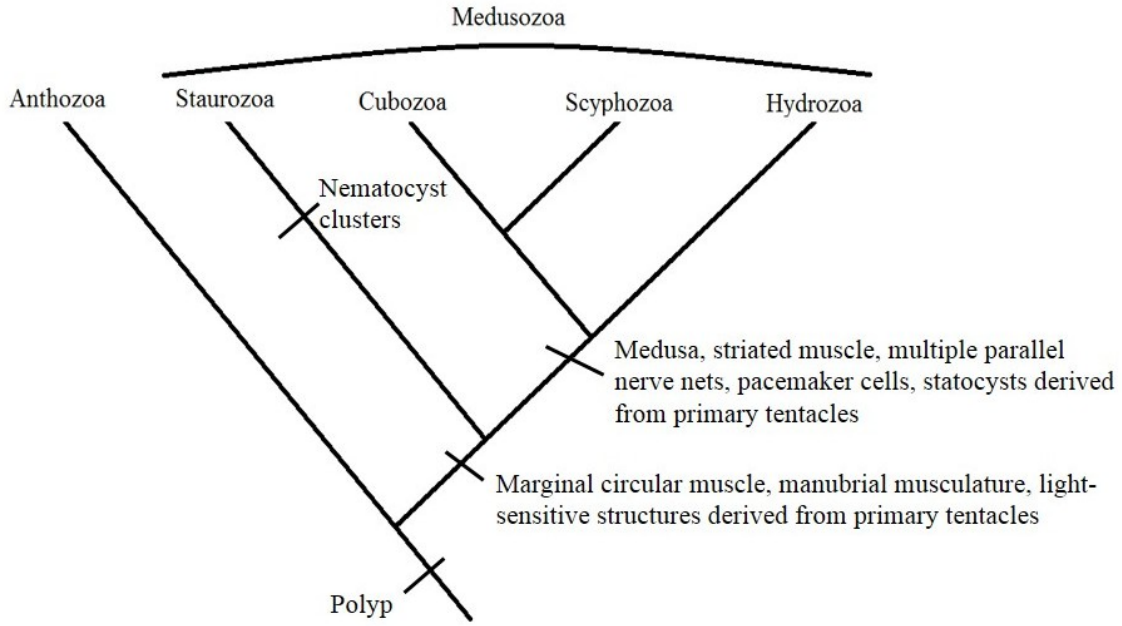


Figure 48. A working hypothesis for relationships among cnidarian classes with hypothesized characteristics suggested by comparative neuromusculature of staurozoans mapped at nodes.

4.5 Conclusions

The neuromusculature of staurozoans is similar to that of other cnidarians in many respects. The arrangement of the marginal and manubrial musculature suggests that the subumbrellar musculature of staurozoans is homologous to muscle groups of medusae, and was present in the common ancestor of Medusozoa (Fig. 48). The apparent lack of striated musculature in members of Staurozoa suggests that it did not arise in Medusozoa until after Staurozoa diverged (Fig. 48). Behavioural and morphological evidence indicate that staurozoans lack the pacemaker system which co-ordinates the swim response in medusae, although *M. handi* is capable of a synchronous marginal contraction, probably due to the physical continuity of the marginal muscle (Fig. 48). Synchronous contraction of marginal muscle fibres in *M. handi* may serve to expel debris from the deep tubular calyx of these staurozoans, or aid in prey capture. A divided or undivided marginal muscle was probably present in the pre-medusa common ancestor of Medusozoa (Fig. 48), and may have served a similar function in this ancestor prior to

modification through the addition of a pacemaker system and striated muscle to produce the swimming dispersive medusa in Scyphozoa, Cubozoa and Hydrozoa. The four longitudinal muscles extending the length of the stalk from the peristomial pits in staurozoans and scyphopolyps may suggest this was a characteristic present in the medusozoan ancestor, which was subsequently modified in Cubozoa, Hydrozoa and some staurozoans lacking stalk musculature, or may indicate convergence between Staurozoa and Scyphozoa.

The musculature of *M. handi* appears to be more specialized than that of *H. 'sanjuanensis'* in that it incorporates strong pennate longitudinal muscles and branches of longitudinal muscle which presumably serve to compress and stabilize, respectively, the tubular calyx during protective contractions.

The nervous system of the staurozoans described in this study is similar to that of cnidarian polyps in that it takes the form of a single diffuse nerve net regionally co-labeled by antibodies against FMRFamide and α-tubulin, indicating that multiple parallel nerve nets in Medusozoa did not arise until after Staurozoa diverged (Fig. 48). FMRFamide-IR neurons probably function primarily in innervating the smooth musculature, sensory systems including ocelli and nematocysts, and co-ordinating gastrodermal function. FMRFamide-IR neurons perform similar functions in Cubozoa and Scyphozoa. In cubomedusae and scyphomedusae α-tubulin-IR neurons usually innervate striated muscle, which is lacking in Staurozoa. Alpha-tubulin-IR neurons in staurozoans may conduct impulses diffusely in order to co-ordinate function between different body regions and co-ordinate exumbrellar nematocyst discharge and sensation. Evidence described here for putative ocelli at the base of the primary tentacles of *M. handi* supports the hypothesis of homology between primary tentacles of staurozoans and rhopalia of other medusozoans (Fig. 48). These putative photoreceptive neurons may facilitate light-induced spawning behaviour, as observed in some staurozoans. Results indicate that a light-sensitive patch of neurons exists even in staurozoans without externally visible pigment patches, and may be characteristic of the Class.

Structure and innervation of the nematocyst clusters suggest that they perform a specialized function triggered by stimuli delivered directly to the clusters. A function in repelling predators or subduing prey is supported by their structure, which is suited to

expelling nematocytes when stimulated. Further study is needed to determine why an exit pore that would permit expulsion of nematocytes is not always present, and how the nematocysts discharge once released. Nematocyst distribution indicates that the nematocytes of the tentacles are probably produced at the base of the infundibula and migrate along muscle fibers to the capita, while nematocysts of the gastric filaments, gonad and exumbrella may be produced *in situ*.

Staurozoans appear to possess a periderm, indicating that this characteristic is common to at least all medusozoans and perhaps all cnidarians. The periderm may play a role in adhesion, and is probably produced by the large glandular cells of the basal disc. The structure of the adhesive primary tentacle modifications of staurozoans is similar to that of the basal disc in other cnidarians. The adhesive pads and anchors probably serve a similar function to adhesive structures found in other cnidarian groups, and aid in locomotion and preventing removal from their preferred shallow habitat by currents. Although the adhesive pads and anchors appear to be under nervous control, they were sparsely innervated; this may indicate the presence of neurons not labelled by FMRFamide or α-tubulin, or another mechanism to modify adhesion.

The findings of this report support the hypothesis that Staurozoa represent a distinct Class of cnidarians and are consistent with their placement as sister group to the remaining medusozoan classes. FMRFamide immunoreactive neurons that innervate smooth muscle and sensory structures appear to be ubiquitous within Cnidaria. Results indicate that multiple parallel nerve nets, pacemaker activity, statocysts and striated muscle are characteristics that arose in the medusozoan line after the divergence of Staurozoa, likely in conjuction with the medusa body plan. A marginal circular muscle, manubrial musculature and light-sensitive structures associated with transformed primary tentacles are present in Staurozoa and were likely present in the common ancestor of Medusozoa. Nematocyst clusters are unique structures whose neuromuscular features admirably equip them for expelling nematocysts upon stimulation, and likely represent a synapomorphy of Staurozoa.

5.0 Literature Cited

Aerne, B.L., Stidwill, R.P, and Tardent, P. 2005. Nematocyst discharge in *Hydra* does not require the presence of nerve cells. J Exp Zool **258**(1): 137-141

Anderson, P.A.V and Bouchard, C. 2009. The regulation of cnidocyte discharge. Toxicon **54**: 1046–1053

Anderson, P.A.V. and Schwab, W.E. 1983. Action potential in neurons of motor nerve net of *Cyanea* (Coelenterata). J Neurophysiol **50**(3): 671-683

Anderson, P.A.V. Thompson, L.F., and Moneypenney, C.G. 2004. Evidence for a common pattern of peptidergic innervation of cnidocytes. Biol Bull **207**(2): 141-146

Anderson, P.A.V., Moosler, A., and Grimmelikuijzen, C.J.P. 1992. The presence and distribution of Antho-RFamide-like material in scyphomedusae. Cell Tissue Res **267**: 67-74

Arai, M.N. 1997. A Functional Biology of Scyphozoa. Chapman & Hall, Boundary Row, London.

Arai, M.N. 2009. The potential importance of podocysts to the formation of scyphozoan blooms: a review. Hydrobiologia **616**: 241-246

Audesirk G. & Audesirk, T. 1980. Complex mechanoreceptors in *Tritonia diomedea*. I. Responses to mechanical and chemical stimuli. J Comp Physiol **141**: 101-109

Azizi, E., Brainerd, E.L., and Roberts, T.J. 2008. Variable gearing in pennate muscles. PNAS **105(**5): 1745–1750

Ballard, W.W. 1942. The mechanism for synchronous spawning in Hydractinia and Pennaria. Biol Bull **82**(3): 329-339

Berrill, M. 1962. The biology of three New England Stauromedusae, with a description of a new species. Can J Zool **40**: 1249-1262

Berrill, M. 1963. Comparative functional morphology of the Stauromedusae. Can J Zool **41**: 741-752

Blumer, M.J.F., Salvini-Plawen, L.v., Kikinger, R., and Büchinger, T. 1995. Ocelli in a Cnidaria polyp: the ultrastructure of the pigment spots in *Stylocoronella riedli* (Scyphozoa, Stauromedusae). Zoomorphology **115**: 221-227

Bocharova, E.S. and Kozevich, I.A. 2011. Modes of reproduction in sea anemones (Cnidaria, Anthozoa). Biol Bull **38**(9): 849-860

Boero, F., Bouillon, J., Piraino, S. and Schmid, V. 2002. Asexual reproduction in the Hydrozoa (Cnidaria). *In* Reproductive biology of invertebrates. *Edited by* R.N. Hughes. Oxford & IBH Publishing Co., New Delhi. pp. 141-158

Bouillon, J., and Deroux, G. 1967. Remarques sur les Cnidaires du type de *Microhydrula pontica* Valkanov 1965, trouvés à Roscoff. Cah Biol Mar **8**: 253-272

Bridge, D., Cunningham, C.W., DeSalle, R., and Buss, L.W. 1995. Class-level relationships in the phylum Cnidaria: Molecular and morphological evidence. Mol Biol Evol **12**(4): 679-689

Bridge, D., Cunningham, C.W., Schierwater, B., DeSalle, R., and Buss, L.W. 1992. Class-level relationships in the phylum Cnidaria: Evidence from mitochondrial genome structure. Proc Natl Acad Sci USA **89**: 8750-8753

Bridge, D.M., Ha, C.R., Nemir, A., Renden, A., Rorick, M.M., Shaffer, A., Underkoffler, D.M., Wills, A.E., and Martínez, D.E. 2004. Variations on a theme? Polyp and medusa development in *Podocoryna carnea*. Hydrobiologia **530/531**: 299-307

Broch, H. 1907. Hydroiden und Medusen. Report of the second Norwegian Arctic expedition in the "Fram" 1898-1902, Vol. II, No. 12.

Browne, E.T. 1910. Coelentera. V. Medusae. Reports of the National Antarctic Expedition, 1901-1904 of Natural History **5**: 1–62

Burnett, A. L. and Lentz, T. 1960. The Nematocyst of *Hydra* (Part III). The migration pathways of Nematocysts in *Hydra*. Ann Soc Roy Zool Bel **902**: 281-293

Burton, P.M. 2008. Insights from diploblasts; the evolution of mesoderm and muscle. J Exp Zool (Mol Dev Evol) **310B:** 5-14

Cairns, S.D., Gershwin, L., Brook, F.J., Pugh, P., Dawson, E.W., V, O. Ocana., Vervoort, W., Williams, G., Watson, J.E., Opresko, D.M., Schuchert, P., Hine, P. Michael., Gordon, D., Campbell, H.J., Wright, A.J., Sanchez, J.A. and Fautin, D.G. 2009. Phylum Cnidaria: corals, medusae, hydroids, myxozoans. *In* New Zealand inventory of biodiversity. *Edited by* D. P. Gordon. Christchurch, New Zealand: Canterbury University Press pp. 59-101

Calder, D.R. 1977. Nematocysts of the ephyra stages of *Aurelia, Chrysaora, Cyanea*, and *Rhopilema* (Cnidaria, Scyphozoa). T Am Microsc Soc **96**(1): 13-19

Calder, D.R. 1983. Nematocysts of stages in the life cycle of *Stomolophus meleagris*, with keys to scyphistomae and ephyrae of some western Atlantic Scyphozoa. Can J Zool **61**: 1185-1192

Campbell, R.D. 1987. Structure of the mouth of *Hydra* spp. A breach in the epithelium that disappears when it closes. Cell Tissue Res **249**:189-197

Campbell, R.D. and Marcum, B.A. 1980. Nematocyte migration in *Hydra*: Evidence for contact guidance *in vivo*. J Cell Sci **41**: 33-51

Carlberg, M., Alfredsson, K., Nielsen, S. and Anderson, P.A.V. 1995. Taurine-like immunoreactivity in the Motor Nerve Net of the jellyfish *Cyanea capillata.* Biol Bull **188**(1): 78-82

Carlgren O. 1935. Über eine neue Südafrikanische Lucernariide, *Depastromorpha africana*, n. gen, n. sp., nebst Bemerkungen über den Bau und die Systematik dieser Tiergruppe. Kungl Sv Vet. Akademiens Handlingar **15**:1–24

Carlgren, O. 1938. Eine neue südafrikanische Lucernariidae, *Lucernariopsis capensis*. Kungliga Fysiografiska Sällskapets I Lund Förhandlingar **8**: 1–6

Chapman, D. M. 1999. Microanatomy of the bell rim of *Aurelia aurita* (Cnidaria: Scyphozoa). Can J Zool **77**(1): 34-46

Chapman, D.M. 1965. Co-Ordination in a scyphistoma. Am Zool **5**(3): 455-464

Chapman, D.M. 1968. Structure, histochemistry and formation of the podocyst and cuticle of *Aurelia aurita.* J Mar Biol Ass UK **48**: 187-208

Chapman, D.M. 1972. Behavior and flagellar currents in coronate polyps (Scyphozoa) and comparisons with semaeostome polyps. Helgoländ Meeresun **25**: 214-227

Chapman, D.M. 1978. Microanatomy of the cubopolyp, *Tripedalia cystophora* (class Cubozoa). Helgoländ Meeresun **31**: 128-168.

Chapman, D.M. and Werner, B. 1972. Structure of a solitary and a colonial species of *Stephanoscyphus* (scyphozoa, Coronatae) with observations on periderm repair. Helgoländ Meeresun **23**(4): 393-421

Chapman, D.M., Pantin, C.F.A. and Robson, E.A. 1962. Muscle in coelenterates. Rev Can Biol **21**: 267-278

Chia, F.S., Amerongen, H.M. and Peteya, D.J. 1984. Ultrastructure of the neuromuscular system of the polyp of *Aurelia aurita* L., 1758 (Cnidaria, Scyphozoa). J Morphol **180**: 69-79

Clark, H.J. 1863a. Lucernaria the coenotype of Acalephae. J Boston Soc Nat Hist **9**:47-54

Clark, H.J. 1863b. Prodromus of the history, structure, and physiology of the order Lucernariae. J Boston Soc Nat Hist **7**: 531–567

Clark, H.J. 1878. Lucernaria and their allies: A memoir on the anatomy and physiology of *Haliclystus auricula* and other Lucernarians. Smithsonian Contributions to Knowledge.

Collins, A.G. 2000. Towards understanding the phylogenetic history of Hydrozoa: Hypothesis testing with 18S gene sequence data. Sci Mar **64**(Supl. 1): 5-22

Collins, A.G. 2002. Phylogeny of Medusozoa and the evolution of cnidarian life cycles. J Evol Biol **15**: 418–432

Collins, A.G., and Daly, M. 2005. A new deepwater species of Stauromedusae, *Lucernaria janetae* (Cnidaria, Staurozoa, Lucernariidae), and a preliminary investigation of stauromedusan phylogeny based on nuclear and mitochondrial rDNA data. Biol Bull **208**: 221–230

Collins, A.G., Lipps, J.H., Valentine, J.W. 2000. Modern mucociliary creeping trails and the bodyplans of neoproterozoic trace-makers. Paleobiology **26**(1): 47-55

Collins, A.G., Schuchert, P., Marques, A.C., Jankowski, T., Medina, M., and Schierwater, B. 2006. Medusozoan phylogeny and character evolution clarified by new large and small subunit rDNA data and an assessment of the utility of phylogenetic mixture models. Syst Biol **55**(1): 97-115

Corbin, P.G. 1978. A new species of the stauromedusan genus *Lucernariopsis* (Coelenterata: Scyphomedusae). J Mar Biol Ass UK **58**: 285–290

Corbin, P.G. 1979. The seasonal abundance of four species of Stauromedusae (Coelenterata: Scyphomedusae) at Plymouth. J Mar Biol Ass UK **59**: 385-391

Cormier, S.M. and Hessinger, D.A. 1980. Cnidocil apparatus: sensory receptor of *Physalia* nematocytes. J Ultra Mol Struct R **72**: 13-19

Couch, J. 1878. A Cornish Fauna. Lake & Lake, Truro pp. 83-84

Dabiri, J.O., Colin S.P., and Costello J.H. 2006. Fast-swimming hydromedusae exploit velar kinematics to form an optimal vortex wake. J Exp Biol **209**: 2025–2033

Daly, M. 2004. Anatomy and taxonomy of three species of sea anemones (Cnidaria: Anthozoa: Actiniidae) from the Gulf of California, including *Isoaulactinia hespervolita* Daly, n. sp. Pac Sci **58**(3): 377–390

Daly, M., Brugler, M.R., Cartwricht, P., Collins, A.G., Dawson, M.N., Fautin, D.G., France, S.C., McFadden, C.S., Opresko, D.M., Rodriguez, E., Romano, S.L., and Stake, J.L. 2007. The phylum Cnidaria: A review of phylogenetic patterns and diversity 300 years after Linnaeus. Zootaxa **1668**: 127–182

Davenport, J. 1998. Note on the trophic relationships of the stauromedusa *Haliclystus antarcticus* from subantarctic South Georgia. J Mar Biol Ass UK **78**: 663-664

Dawson, M.N. 2004. Some implications of molecular phylogenetics for understanding biodiversity in jellyfishes, with emphasis on Scyphozoa. Hydrobiologia **530/531**: 249-260

Dawson, M.N. and Jacobs, D.K. 2001. Molecular evidence for cryptic species of *Aurelia aurita* (Cnidaria, Scyphozoa). Biol Bull **200**: 92-96

Eales, N.B. 1938. *Lucernaria discoidea*, a new species from the Channel Islands. J Mar Biol Ass UK **23**: 167–170

Eckelbarger, K.J. and Larson, R.J. 1993. Ultrastructural study of the ovary of the sessile Scyphozoan, *Haliclystus octoradiatus* (Cnidaria: Stauromedusae). J Morphol **218**: 225-236

Eggers, N., and Jarms, G. 2007. The morphogenesis of ephyra in Coronatae (Cnidaria, Scyphozoa). Mar Biol **152**:495–502

Eichinger, J.M. and Satterlie, R.A. 2014. Organization of the ectodermal nervous structures in medusae: cubomedusae. Biol Bull **226**: 41–55

Ellis, V.L., Ross, D.M. and Sutton, L. 1969. The pedal disc of the swimming sea anemone *Stomphia coccinea* during detachment, swimming, and resettlement. Can J Zool **47**(3): 333-342

Ewer, R.F., 1947. On the functions and mode of action of the nematocysts of hydra. Proc Zool Soc Lond **117**: 365-376

Falconer, A. 2013. A stalked jellyfish *Stenoscyphus inabai* (Kishinouye, 1893) (Stauromedusae), found at The Jawbone, Port Phillip Bay, Victoria. The Victorian Naturalist **130**(5): 202-207

Fautin, D.G. 2002. Reproduction in Cnidaria. Can J Zool **80**: 1735-1754

Fautin, D.G. 2009. Structural diversity, systematics, and evolution of cnidae. Toxicon **54**: 1054-1064

Fautin, D.G. and Mariscal, R.N. 1991. Cnidaria: Anthozoa. *In* Microscopic anatomy of invertebrates, Vol. 2: Placozoa, Porifera, Cnidaria, and Ctenophora. *Edited by* F. W. Harrison and J. A. Westfall. Wiley-Liss, Inc., New York. pp. 267-358

Gellerman, M .P. 1926. Medusae of the San Juan archipelago. Masters thesis, University of Washington, Seattle, Washington.

Giebel, G.E.M., Thorington, G.U., Lim, R.Y. and Hessinger, D.A. 1988. Control of cnida discharge: ii. microbasic p-mastigophore nematocysts are regulated by two classes of chemoreceptors. Reference: Biol Bull **175**: 132-136.

Girosi, L., Ramoino, P., Diaspro, A., Gallus, L., Ciarcia, G., and Tagliafierro, G. 2005. FMRFamide-like immunoreactivity in the sea-fan *Eunicella cavolini* (Cnidaria: Octocorallia). Cell Tissue Res **320**: 331–336

Gladfelter, W.G. 1972. Structure and function of the locomotory system of the Scyphomedusa *Cyanea capillata*. Mar Biol **14**: 150-160

Gladfelter, W.G. 1973. A comparative analysis of the locomotory systems of medusoid Cnidaria. Helgoländ Meeresun **25**: 228-272

Golz, R. 1994. Occurrence and distribution of RFamide-positive neurons within the polyps of *Coryne* sp. (Hydrozoa, Corynidae). Biol Bull **186**: 115-123

Govindarajan, A.F., Boero, F. and Halanych, K.M. 2006. Phylogenetic analysis with multiple markers indicates repeated loss of the adult medusa stage in Campanulariidae (Hydrozoa, Cnidaria). Mol Phyl Evol **38**: 820-834.

Grassé, P.P. 1997. Traité de zoologie, anatomie, systématique, biologie. Tome III, Fascicule 2: Cnidaires (Hydrozoaires, Scyphozoaires et Cubozoaires), Cténaires. Masson.

Grassle, J.F. 1985. Hydrothermal vent animals: distribution and biology. Science, New Series **229**(4715): 713-717

Grimmelikhuijzen, C.J.P. 1985. Antisera to the sequence Arg-Phe-amide visualize neuronal centralization in hydroid polyps. Cell Tissue Res **241**: 171-182

Grimmelikhuijzen, C.J.P., Williamson, M. and Hansen, G.N. 2002. Neuropeptides in cnidarians. Can J Zool **80**: 1690–1702

Gröger, H. and Schmid, V. 2000. Nerve net differentiation in medusa development of *Podocoryne carnea*. Sci Mar **64**(Supl. 1): 107-116

Grohmann, P.A., Magalhães, M.P., and Hirano, Y.M. 1999. First record of the Order Stauromedusae (Cnidaria, Scyphozoa) from the tropical Southwestern Atlantic, with a review of the distribution of Stauromedusae in the Southem Hemisphere. Species Diversity **4**: 381-388

Guberlet, M.L. 1936. Animals of the Seashore. Binsford and Mort, Portland, OR. pp. 46-47

Gwilliam, G.F. 1956. Studies on Western North American Stauromedusae (PhD Dissertation). University of California.

Gwilliam, G.F. 1960. Neuromuscular physiology of a sessile Scyphozoan. Biol Bull **119**(3): 454-473

Haeckel, E. 1882. Report on the deep-sea medusae dredged by H.M.S. Challenger during the years 1873-1876. **4**: 48-62, Pl. 15-17

Hamner, W.M. Jones, M.S. and Hamner, P.P. 1995. Swimming, feeding, circulation and vision in the Australian box jellyfish, *Chironex fleckeri* (Cnidaria:Cubozoa). Mar Freshwater Res **46**(7): 985-990

Hanaoka, K. 1934. Notes on the early development of a stalked medusa. Proceedings of the Imperial Academy **10**(2): 117-120

Hanaoka, K. 1935. Experiments on the polarity of a stalked medusa *Thaumatoscyphus distinctus* Kishinouye (with 23 Text-figures). Journal of the faculty of science Hokkaido Imperial University Series VI. Zoology **4**(3): 159-181

Hartwick, R.F. 1991. Observations on the anatomy, behaviour, reproduction and life cycle of the cubozoan *Carybdea sivickisi*. Hydrobiologia **216/217**: 171-179

Hirano Y.M. 1997. A review of a supposedly circumboreal species of stauromedusa, *Haliclystus auricula* (Rathke, 1806). *In* Proceedings of the 6th International Conference on Coelenterate Biology. *Edited by* J.C. den Hartog. Noordwijkerhout, The Netherlands. pp 247-252

Hirano, Y.M. 1986. Species of Stauromedusae from Hokkaido, with notes on their metamorphosis (with 12 text-figures). Journal of the faculty of science Hokkaido University Series VI. Zoology **24**(3): 182-201

Hobmayer, E., Holstein, T.W. and David, C.N. 1990. Tentacle morphogenesis in hydra II. Formation of a complex between a sensory nerve cell and a battery cell. Development **109**: 897-904

Honegger, T.G. 1984. Ultrastructure of the adhesive tentacles of the limnomedusa *Vallentinia gabriella* (Hydrozoa, Olindiadidae). Zoomorphology **104**: 26-32

Hornell, J. 1893. The Lucernarians as degenerate Scyphomedusae. A note upon the phylogeny of the Order. Preliminary. Natural Science: A Monthly Review of Scientific Progress **3**: 204-208

Horridge, A. 1956a. The nervous system of the ephyra larva of *Aurellia aurita*. Quarterly Journal of Microscopical Science **97**(1): 59-74

Horridge, G.A. 1956b. The nerves and muscles of medusae V. Double innervation in Scyphozoa. J Exp Biol **33**: 366-383

Hündgen, M. 1984. Cnidaria: Cell Types. *In:* Biology of the integument volume 1: Invertebrates. *Edited by*: J. Bereiter-Hahn, A.G. Matoltsy and K. Sylvia Richards. Springer-Verlag, Germany.

Hurst, C.H. 1893. Biological Theories. VI – The phylogeny of Lucernrians. Natural Science: A Monthly Review of Scientific Progress **3**: 209-217

Hyman, L.H. 1940. Observations and experiments on the physiology of medusae. Biol Bull **79**(2): 282-296

Hyman, L.H. 1947. Two new hydromedusae from the California Coast. T Am Microsc Soc **66**(3): 262-268

Jacobs, D.K. Nakanishi, N., Yuan, D., Camara, A., Nichols, S.A., and Hartenstein, V. 2007. Evolution of sensory structures in basal metazoa. Integrative and Comparative Biology **47**(5): 712–723

Jahnel, S.M., Walzl, M., and Technau, U. 2014. Development and epithelial organisation of muscle cells in the sea anemone *Nematostella vectensis*. Frontiers in Zoology **11**(44)

Jarms, G., and Tiemann, H. 1966. On a new hydropolyp without tentacles, *Microhydrula limopsicola* n. sp., epibiotic on bivalve shells from the Antarctic. Sci Mar **60**(1): 109-115

Johnston, G. 1835. *Lucernaria convolvulus.* The Magazine of Natural History, and Journal of Zoology, Botany, Mineralogy, Geology and Meteorology pp. 59-61

Josephson, R.K. and March, S.C. 1966. The swimming performance of the sea-anemone *Boloceroides.* J Exp Biol **44**: 493-506

Kahn, A.S., Matsumoto, G.I., Hirano, Y.M, and Collins, A.G. 2010. *Haliclystus californiensis*, a "new" species of stauromedusa (Cnidaria: Staurozoa) from the northeast Pacific, with a key to the species of *Haliclystus*. Zootaxa **2518**: 49-59

Kassianow, N., 1901: Studien über das Nervensystem der Lucernariden nebst sonstigen histologischen Beobachtungen über diese Gruppe. Zeitschrift fur Wissenschaftliche Zoologie. **69**: 287-377

Kass-Simon, G. and Pierobon, P. 2007. Cnidarian chemical neurotransmission, an updated overview. Comp Biochem Phys A **146**: 9–25

Kass-Simon, G., and Scappaticci Jr., A.A. 2002. The behavioural and developmental physiology of nematocysts. Can J Zool **80**: 1772-1794

Kayal, E., Bentlage, B., Collins, A.G., Kayal, M., Pirro, S., and Lavrov. D.V. 2012. Evolution of linear mitochondrial genomes in medusozoan cnidarians. Genome Biol Evol **4**(1):1-12

Kayal, E., Roure, B., Philippe, H., Collins, A.G., and Lavrov, D.V. 2013. Cnidarian phylogenetic relationships as revealed by mitogenomics. BMC Evolutionary Biology. **13**(5): 1-18

Keferstein, W. 1862. Untersuchung über niedere Seethiere. Zeit Wiss Zool **12**: 1-26, Pl. 1-11.

Kikinger, R., and Salvini-Plawen, L.v. 1995. Development from polyp to stauromedusa in *Stylocoronella* (Cnidaria: Scyphozoa). J Mar Biol Ass UK **75**: 899-912

Kishinouye, K. 1910. Some medusae of Japanese waters. Journal of the college of science, Imperial University, Tokyo, Japan. **27**: 1-35

Kling, O. 1879. Ueber *Craterolophus tethys.* Ein Beitrag zur Anatomie und Histologie der Lucernarien. Morph Jahrb **5**: 141-166.

Koizumi, O., Hamada, S., Minobe, S., Hamaguchi-Hamada, K., Kurumata-Shigeto, M., Nakamura, M., and Namikawa, H. 2015. The nerve ring in cnidarians: its presence and structure in hydrozoan medusae. Zoology **118**: 79–88

Kowalevsky, A. 1884. Entwicklungsgeschichte der *Lucernaria*. Zoologischer Anzeiger **7**: 712-717.

Kramp, P.L. 1961. Synopsis of medusae of the world: Stauromedusae. J Mar Biol Ass UK **40**: 293-303

Lamouroux, M. 1815. Mémoire sur la Lucernaire campanulée. Memoires du Muséum D'histoire Naturelle **2**: 460-473

Larson, R.J. 1980. A new stauromedusa, *Kishinouyea corbini* (Scyphozoa, Stauromedusae) from the tropical western Atlantic. B Mar Sci **30**(1): 102-107

Larson, R.J. 1988. *Kyopoda lamberti* gen.nov., sp.nov., an atypical stauromedusa (Scyphozoa, Cnidaria) from the eastern Pacific, representing a new family. Can J Zool **66**: 2301-2303

Larson, R.J. and Fautin, D.G. 1989. Stauromedusae of the genus *Manania* (= *Thaumatoscyphus*) (Cnidaria, Scyphozoa) in the northeast Pacific, including descriptions of new species *Manania gwilliami* and *Manania handi*. Can J Zool **67**: 1543-1549

Leme, J.M., Simões, M.G., Marques, A.C., and Van Iten, H. 2008. Cladistic analysis of the suborder Conulariina Miller and Gurley, 1896 (Cnidaria, Scyphozoa; Vendian-Triassic). Palaeontology **51**(3): 649–662

Leuschel, H. 1932. Beiträge zur Histologie und Physiologie der Lucernariden. Zool Jahrb **52**: 338-388, Pl. 3-4.

Lin, Y.J, Gallin, W.J. and Spencer, A.N. 2001. The anatomy of the nervous system of the hydrozoan jellyfish, *Polyorchis penicillatus*, as revealed by a monoclonal antibody. Invert Neurosci **4**: 65-75

López-González, P.J., Ocaña, O., García-Gómez, J.C., and Núñez, J. 1995. North-eastern Atlantic and Mediterranean species of *Cornulariidae* Dana, 1846 (Anthozoa: Stolonifera) with the description of a new genus. Zool Med Leiden **69**: 261-272

Lutz, R.A., Desbruyères, D., Shank, T.M and Vrijenhoek, R.C. 1998. A deep-sea hydrothermal vent community dominated by Stauromedusae. Deep-Sea Res Pt II **45**: 329-334

Mackie, G.O. and Meech, R.W. 2008. Nerves in the endodermal canals of hydromedusae and their role in swimming inhibition. Invert Neurosci **8**:199–209

Mackie, G.O., and Passano, L.M. 1968. Epithelial conduction in hydromedusae. J Gen Physiol **52**: 600-621

Mandal, F.B. 2012. Invertebrate zoology. PHI Learning, New Delhi.

Margnum, D.C. 1970. Burrowing behavior of the sea anemone *Phyllactis*. Biol Bull **138**(3): 316-325

Marques, A.C., and Collins, A.G. 2004. Cladistic analysis of Medusozoa and cnidarian evolution. Invertebr Biol **123**(1): 23–42

Marsical, R.N. 1974. Nematocysts. *In* Coelenterate biology: Reviews and new perspectives. *Edited by* L. Muscatine and H.M. Lenhoff. Academic Press, New York. pp. 129-178

Marsical, R.N. and Bigger, C.H. 1976. A comparison of putative sensory receptors associated with nematocysts in the anthozoan and scyphozoan. *In* Coelenterate ecology and behavior. *Edited by* G.O. Mackie. Plenum Press, New York. pp. 559-568

Martin, V.J. 1988. Development of nerve cells in hydrozoan planulae: I. Differentiation of ganglionic cells. Biol Bull **174**: 319-329

Martin, V.J. 2002. Photoreceptors of cnidarians. Can J Zool **80**(10): 1703-1722

Marx, R.M. 1997. Dissertation: The development of the nervous system of *Aurelia aurita* (Scyphozoa, Coelenterata). University of Victoria, Victoria, BC.

Mayer, A.G. 1910. Medusae of the world. III. Scyphomedusae. Carnegie institution of Washington, Washington, D.C.

Mayorova, T.D., and Kosevich, I.A. 2013. Serotonin-immunoreactive neural system and contractile system in the hydroid *Cladonema* (Cnidaria, Hydrozoa). Invert Neurosci **13**: 99-106

Mayorova, T.D., Kosevich, I.A., and Melekhova, O.P. 2012. On some features of embryonic development and metamorphosis of *Aurelia aurita* (Cnidaria, Scyphozoa). Russian Journal of Developmental Biology **43**(5): 271–285

Mazza, M.E., Pang, K., Martindale, M.Q. and Finnerty, J.R. 2007. Genomic organization, gene structure, and developmental expression of three Clustered otx genes in the sea anemone *Nematostella vectensis*. J Exp Zool **308B**(4): 494–506

McFarlane, I.D. 1969. Co-ordination of pedal-disk detachment in the sea anemone *Calliactis parasitica*. J Exp Biol **51**: 387-396

McInnes, D.E. 1989. A stalked jellyfish (Stauromedusae) found at Black Rock, Port Phillip Bay. A first recording in Australia. Victorian Naturalist. **106**(3): 86-92

Migot, A. 1922. Sur le mode de fixation des Lucernaires a leur support. Comptes rendus des Séances de la Société de Biologie **86**(15)

Mills, C.E. 1999-present. Stauromedusae: list of all valid species names. Electronic internet document available at http://faculty.washington.edu/cemills/Staurolist.html. Published by the author, web page established October 1999, last updated March 2012

Mills, C.E. and Hirano, Y.M. 2007. Stauromedusae. *In* Encyclopedia of tidepools and rocky shores. *Edited by* M.W. Denny and S.D. Gaines. University of California Press, Berkeley. pp. 541-543

Mills, C.E., Marques, A.C., Migotto, A.E., Calder, D.R., Hand, C., Rees, J.T., Haddock, S.H.D., Dunn, C.W., Pugh, P.R., Larson, R.J., Fautin, D.G., and Williams, G.C. 2007. Cnidaria. *In* The Light and Smith manual: Intertidal invertebrates from Central California to Oregon. *Edited by* J.T. Carlton. University of California Press, Oakland, California. pp. 118-188

Miranda, L.S. Morandini, A.C., and Marques, A.C. 2012. Do Staurozoa bloom? A review of stauromedusan population biology. Hydrobiologia **690**(1): 57-67

Miranda, L.S., Collins, A.G. and Marques, A.C. 2013. Internal anatomy of *Haliclystus antarcticus* (Cnidaria, Staurozoa) with a discussion on histological features used in Staurozoan taxonomy. J Morphol **274**(12): 1-19

Miranda, L.S., Collins, A.G., and Marques, A.C. 2010. Molecules clarify a cnidarian life cycle – The ‘‘hydrozoan’’ *Microhydrula limopsicola* is an early life stage of the staurozoan *Haliclystus antarcticus.* PLoS ONE **5**(4): 1-9

Miranda, L.S., Collins, A.G., Hirano, Y.M and Mills, C.E. Unpublished. Evolution of the body plan in Staurozoa (Cnidaria): a comparative histological study.

Miranda, L.S., Morandini, A.C., and Marques, A.C. 2009. Taxonomic review of *Haliclystus antarcticus* Pfeffer, 1889 (Stauromedusae, Staurozoa, Cnidaria), with remarks on the genus Haliclystus Clark, 1863. Polar Biol **32**:1507-1519

Moroz, L.L., Kocot, K.M., Citarella, M.R., Dosung, S., Norekian, T.P., Povolotskaya, I.S., Grigorenko, A.P., Dailey, C., Berezikov, E., Buckley, K.M., Ptitsyn, A., Reshetov, D., Mukherjee, K., Moroz, T.P., Bobkova, Y., Yu, F., Kapitonov, V.V., Jurka, J., Bobkov, Y.V., Swore, J.J., Girardo, D.O., Fodor, A., Gusev, F., Sanford, R., Bruders, R., Kittler, E., Mills, C.E., Rast, J.P., Derelle, R., Solovyev, V.V., Kondrashov, F.A., Swalla, B.J., Sweedler, J.V., Rogaev, E.I., Halanych, K.M. and Kohn, A.B. 2014, The ctenophore genome and the evolutionary origins of neural systems. Nature **510**(7503): 109-114

Muller, W.A., and Leitz, T. 2002. Metamorphosis in Cnidaria. Can J Zool **80**: 1755-1771

Nakanishi, N., Hartenstein, V., and Jacobs, D.K. 2009. Development of the rhopalial nervous system in *Aurelia* sp.1 (Cnidaria, Scyphozoa). Dev Genes Evol **219**: 301–317

Nakanishi, N., Yuan, D., Hatenstein, V., and Jacobs, D.K. 2010. Evolutionary origin of rhopalia: insights from cellular-level analyses of Otx and POU expression patterns in the developing rhopalial nervous system. Evolution and Development **12**(4): 404–415

Nakanishi, N., Yuan, D., Jacobs, D.K., and Hartenstein, V. 2008. Early development, pattern and reorganization of the planula nervous system in Aurelia (Cnidaria, Scyphozoa). Dev Genes Evol **218**: 511-524

Naumov, D.V. 1961. Scyphomedusae of the seas of the USSR. Marine Biological Association of the United Kingdom, Plymouth pp. 77-95

Östman, C. 1987. New techniques and old problems in Hydrozoan systematics. *In* Modern trends in the systematics, ecology, and evolution of hydroids and

hydromedusae. *Edited by* J. Boullion, F. Boero, F. Cicogna and P.F.S. Cornelius. Clarendon Press, Oxford.

Östman, C. A guideline to nematocyst nomenclature and classification, and some notes on the systematic value of nematocysts. Sci Mar **64**(Supl. 1): 31-46

Ostman, C. and Hydman, J. 1997. Nematocyst analysis of *Cyanea capillata* and *Cyanea lamarckii* (Scyphozoa, Cnidaria). Sci Mar **61**(3): 313-344

Otto, J.J. 1976. Early development and planula movement in *Haliclystus* (Scyphozoa: Stauromedusae). *In:* Coelenterate ecology and behavior. *Edited by:* G.O. Mackie. Pleanum Press, New York. pp. 319-329

Otto, J.J. 1978. The settlement of *Haliclystus* planulae. *In* Settlement and metamorphosis of marine invertebrate larvae. *Edited by* F.S. Chia and M. Rice. Elsevier, New York. pp. 13-22

Panikkar, N.K. 1944. Occurrence of a stauromedusa on the Indian coast. Current Science, Bangalore **13**: 238–239

Pantin, C.F.A. 1935. The nerve net of the Actinozoa: II. Plan of the nerve net. J Exp Biol **12**: 139-155

Parkefelt, L. and Ekstrom, P. 2009. Prominent system of RFamide immunoreactive neurons in the rhopalia of box jellyfish (Cnidaria: Cubozoa). J Comp Neurol **516**: 157–165

Passano, L.M. 1973. Behavioral control systems in meduae; a comparison between hydro- and scyphomedusae. Publications of the Seto Marine Biological Laboratory, **20:** 615-645

Passano, L.M. 1982. Scyphozoa and Cubozoa. *In* electrical conduction and behaviour in "simple" invertebrates. *Edited by* G.A.B. Shelton. Clarendon Press, Oxford. pp. 149-202

Pernet, V., Anctil, M., Grimmelikhuijzen, C.J.P. 2004. Antho-RFamide-containing neurons in the primitive nervous system of the anthozoan *Renilla koellikeri*. J Comp Neurol **472**: 208–220

Petie, R., Garm, A., Nilsson, D. 2013. Velarium control and visual steering in box jellyfish. J Comp Physiol A **199**(4): 315-324

Piatigorsky, J. and Koszmik, Z. 2004. Cubozoan jellyfish: an Evo/Devo model for eyes and other sensory systems. Int J Dev Biol **48**: 719-729

Pickens, P.E. 1969. Rapid contractions and associated potentials in a sand-dwelling anemone. J Exp Biol **51**: 513-528

Piraino, S., De Vito, D., Schmich, J., Bouillon, J., and Boero, F. 2004. Reverse development in Cnidaria. Can J Zool **82**(11): 1748-1754

Pisani, V., Otero-Ferreri, F., Lottto, S., Maurel, P. and Goy, J. 2007. *Lipkea rusopoliana* (Stauromedusa, Scyphozoa, Cnidaria) dans les aquariums du Musée Océanographique de Monaco. Bull Soc Zool Fr **132**(3): 183-190

Plickert, G. and Schneider, B. 2004. Neuropeptides and photic behavior in Cnidaria. Hydrobiologia **530/531**: 49-57

Prell, H. 1909. Beitrage zur Kenntnis der Lebensweise einiger Pantopoden. Bergens Mus Aarbok **10**: 1-30

Purcell, J.E. 2005. Climate effects on formation of jellyfish and ctenophore blooms: a review. J Mar Biol Ass UK **85**: 461-476

Quaglia, A. 1981. The muscular system of coelenterates. Bolletino di zoologia **48**:(1): 51-56

Reft, A.J. 2012. Dissertation: Understanding the morphology and distribution of nematocysts in sea anemones and their relatives. Ohio State University, Ohio.

Richardson, K.C., Jarrett, L. and Finke, E.H. 1960. Embedding in epoxy resins for ultrathin sectioning in electron microscopy. Stain Technol **35**: 313-323

Rodriguez, C.S., Marques, A.C., Stampar, S.N., Morandini, A.C., Christiansen, E., Genzano, G.N., and Mianzan, H.W. 2011. The taxonomic position of the pelagic 'staurozoan' *Tessera gemmaria* as a ceriantharian larva. Zootaxa **2971**: 49–58

Rodriguez, E., Barbeitos, M.E., Brugler, M.R., Crowley, L.M., Grajales, A., Gusma, L., Häussermann, V., Reft, A., and Daly, M. 2014. Hidden among sea anemones: the first comprehensive phylogenetic reconstruction of the order Actiniaria (Cnidaria, Anthozoa, Hexacorallia) reveals a novel group of hexacorals. PLoS ONE **9**(5): 1-17

Romanes, G.J. 1885. Jellyfish, starfish and sea urchins, being a research on primitive nervous systems. D. Appleton, New York.

Sakaguchi, M., Imai, Y., and Nomoto, S. 1999. The presence and distribution of RFamide-like immunoreactive nerve fibers in scyphistomae of *Aurelia aurita*. Comp Biochem Phys A **122**: 261–266

Salvini-Plawen, L.v. 1978. On the origin and evolution of the lower Metazoa. Z Zool Syst Evolut **16**: 40-88

Salvini-Plawen, L.v. 2006. First record of a mature stauromedusa *Stylocoronella* (Cnidaria) in nature. Cah Biol Mar **47**(2): 219-222

Sanyal, S. and Mookerjee, S. 1960. Experimental dissociation of cells from *Hydra*. Wilhelm Roux' Archiv für Entwicklungsmechanik der Organismen. **152**: 131-136

Satterlie, R.A. 1979. Central control of swimming in the cubomedusan jellyfish *Carybdea rastonii*. J Comp Physiol **133**: 357-367

Satterlie, R.A. 2002. Neuronal control of swimming in jellyfish: a comparative story. Can J Zool **80**: 1654-1669

Satterlie, R.A. 2008. Control of swimming in the hydrozoan jellyfish *Aequorea victoria*: subumbrellar organization and local inhibition. J Exp Biol **211**: 3467-3477

Satterlie, R.A. 2011. Commentary: Do jellyfish have central nervous systems? J Exp Biol **214**: 1215-1223

Satterlie, R.A. 2014. Multiple conducting systems in the cubomedusa *Carybdea marsupialis*. Biol Bull **227**(3): 274-284

Satterlie, R.A. and Eichinger, J.M. 2014. Organization of the ectodermal nervous structures in jellyfish: scyphomedusae. Biol Bull **226**: 29–40

Satterlie, R.A. and Spencer, A.N. 1987. Organization of conducting systems in "simple" invertebrates: Porifera, Cnidaria and Ctenophora. *In* Nervous systems of invertebrates. *Edited by* M.A. Ali. Plenum Press, New York. pp. 213-264

Satterlie, R.A., Thomas, K.S., and Gray, G.C. 2005. Muscle organization of the cubozoan jellyfish *Tripedalia cystophora* Conant 1897. Biol Bull **209**(2): 154-163

Scemes, E. and McNamara, J.C. 1991. The ultrastructure of the radial neuromuscular system of the jellyfish *Liriope tetraphylla* (Hydrozoa, Trachymedusae): Implications in Crumpling Behavior. Biol Bull **181**: 474-483

Schlater, G. 1891. Die Sinneskolben bon *Haliclystus auricula* var. Zeitschrift fuer Wissenschaftliche Zoologie. **52:** 580-592

Schlesinger, A., Zlotkin, E., Kramarsky-Winter, E., and Loya, Y. 2009. Cnidarian internal stinging mechanism. Proc R Soc B **276**: 1063-1067

Schmidt, H. and Moraw, B. 1982. Die Cnidogenese der Octocorallia (Anthozoa, Cnidaria): II. Reifung, Wanderung und Zerfall von Cnidoblast und Nesselkapsel. Helgoländ Meeresun **35**: 97-118

Schuchert, P. 1993. Phylogenetic analysis of the Cnidaria. Z Zool Syst Evolut **31**: 161-173

Schwab, W.E. 1977. The ontogeny of swimming behavior in the scyphozoan, *Aurelia aurita*. I. Electrophysiological analysis. Biol Bull **152**: 233-250

Seipel, K. and Schmid, V. 2005. Review: Evolution of striated muscle: Jellyfish and the origin of triploblasty. Dev Biol **282**: 14-26

Seipel, K. and Schmid, V. 2006. Mesodermal anatomies in cnidarian polyps and medusae. Int J Dev Biol **50**: 589-599

Singla, C.L. 1976. Ultrastructure and attachment of the basal disc of *Haliclystus*. *In* Coelenterate ecology and behavior. *Edited by* G.O. Mackie. Plenum Press, New York and London pp. 533-540

Singla, C.L. 1977. Fine structure of the adhesive pads of *Gonionemus vertens*. Cell Tissue Res **181**: 395-402

Slautterback, D.B. 1967. The cnidoblast-musculoepithelial cell complex in the tentacles of *Hydra*. Zeitschrift für Zellforschung **79**: 296-318

Smith, S., Oshida, J. and Bode, H. 1974. Inhibition of nematocyst discharge in *Hydra* fed to repletion. Biol Bull **147**(1): 186-202

Spoon, D.M. and Blanquet, R.S. 1978. Life cycle and ecology of the minute hydrozoan *Microhydrula*. Trans Amer Micros Soc **97**(2): 208-216

Stake, J.L. and Sammarco, P.W. 2003. Effects of pressure on swimming behavior in planula larvae of the coral *Porites astreoides* (Cnidaria, Scleractinia). J Exp Mar Biol Ecol **288**(2): 181-201

Stangl, K., Salvini-Plawen, L.v., and Holstein, T.W. 2002. Staging and induction of medusa metamorphosis in *Carybdea marsupialis* (Cnidaria, Cubozoa). Vie et Milieu **52**(4): 131-140

Steinmetz, P.R.H., Kraus, J.E.M., Larroux, C., Hammel, J.U., Amon-Hassenzahl, A., Houliston, E., Wörheide, G., Nickel, M., Degnan, B.M., and Technau, U. 2012. Independent evolution of striated muscles in cnidarians and bilaterians. Nature **487(**7406): 231-234

Straehlr-Pohl, I., and Jarms, G. 2005. Life cycle of *Carybdea marsupialis* Linnaeus, 1758 (Cubozoa, Carybdeidae) reveals metamorphosis to be a modified strobilation. Mar Biol **147**: 1271-1277

Suput, D. 2011. Interactions of cnidarian toxins with the immune system. Inflammation & Allergy - Drug Targets. **10**: 429-437

Swain, T.D., Schellinger, J.L., Strimaitis, A.M., and Reuter, K.E. 2015. Evolution of anthozoan polyp retraction mechanisms: convergent functional morphology and evolutionary allometry of the marginal musculature in order Zoanthidea (Cnidaria: Anthozoa: Hexacorallia). BMC Evolutionary Biology **15**(123)

Sweeny, A.M., Boch, C.A., Johnsen, S., and Morse, D.E. 2011. Twilight spectral dynamics and the coral reef invertebrate spawning response. J Exp Biol **214**: 770-777

Tardent, P. 1978. Coelenterata, Cnidaria. *In*: Morphogenese der Tiere. *Edited by:* F. Seidel Gustav Fischer Verlag, Jena, pp. 83-289.

Thiel, H. 1966. The evolution of scyphozoa: a review. *In* The Cnidaria and their evolution. *Edited by* W.J. Rees, Academic, London, pp 77–117

Thomas, M.B. and Edwards, N.C. 1991. Cnidaria: Hydrozoa. *In* Microscopic anatomy of invertebrates, Vol. 2: Placozoa, Porifera, Cnidaria, and Ctenophora. *Edited by* F. W. Harrison and J. A. Westfall. Wiley-Liss, Inc., New York. pp. 91-183

Thorington, G.U., Mcauley, V., Hessinger, D.A. 2010. Effects of satiation and starvation on nematocyst discharge, prey killing, and ingestion in two species of sea anemone. Biol Bull **219**: 122–131

Tidball, J.G. 1984. Cnidaria: Secreted surface. *In:* Biology of the integument volume 1: invertebrates. *Edited by*: J. Bereiter-Hahn, A.G. Matoltsy and K. Sylvia Richards. Springer-Verlag, Germany.

Toshino, S. Miyake, H. and Iwanaga, S. 2014. Development of *Copula sivickisi* (Stiasny, 1926) (Cnidaria: Cubozoa: Carybdeidae: Tripedaliidae) collected from the Ryukyu Archipelago, southern Japan. Plankton Benthos Res **9**(1): 32–41

Tsai, P.S., Kaufhold, J.P., Blinder, P., Friedman, B., Drew, P.J., and Karten, H.J. 2009. Correlations of neuronal and microvascular densities in murine cortex revealed by

direct counting and colocalization of nuclei and vessels. J Neurosci **29**(46): 14553–14570

Tunnicliffe, V., Embley, R.W., Holden, J.F., Butterfield, D.A., Massoth, G.J. and Juniper, S.K. 1997. Biological colonization of new hydrothermal vents following an eruption on Juan de Fuca Ridge. Deep-Sea Res I, **44**(9-10): 1627-1644

Uchida, T. 1929. Studies on the Stauromedusae and cubomedusae, with special reference to their metamorphosis. Japanese Journal of Zoology **2**: 103-193

Uchida, T., and Hanaoka, K. 1933. On the morphology of a stalked medusa, *Thaumatoscyphus distinctus* Kishinouye. Journal of the Faculty of Science Hokkaido Imperial University Series VI. Zoology, **2**(3): 135-153

Vagelli, A.A. 2007. New observations on the asexual reproduction of *Aurelia aurita* (Cnidaria, Scyphozoa) with comments on its life cycle and adaptive significance. Invertebrate Zoology **4**: 111-127

Van Iten, H., Leme, J.M., Simões, M.G., Marques, M.C., and Collins, A.G. 2006. Reassessment of the phylogenetic position of conulariids (?Ediacaran-Triassic) within the subphylum medusozoa (phylum cnidaria). Journal of Systematic Palaeontology. **4**(2): 109-118

Vogt, C. 1886. Zoologie et physiologie. Arch Sci Genève **3**(16): 356-362

Vogt, C. 1887. Sur un nouveau genre de médusaire sessile *Lipkea ruspoliana* c.v. Mémoires de l'Institut national Genevois **17**: 7-53.

Watanabe, H., Fujisawa, T. and Holstein, T.W. 2009 Cnidarians and the evolutionary origin of the nervous system. Develop Growth Differ **51**: 167–183

Weill, M.R. 1925. Foyers de formation et voies de migration des nématocystes de *Halyclistus octoradiatus* Clark. Existence, sur leur parcours, de reservoirs sélectifs. Comptes rendus hebdomadaires des séances de l'académie des sciences **180**

Werner, B. 1973. New investigations on systematics and evolution of the class Scyphozoa and the phylum Cnidaria. Publications of the Seto Marine Biological Library **20**: 35-61

Werner, B. 1975. Bau und Lebensgeschichte des Polypen von *Tripedalia cystophora* (Cubozoa, class, nov., Carybdeidae) und seine Bedeutung für die Evolution der Cnidaria. Helgoländ Meeresun **27**: 461-504

Werner, B. 1983. Die Metamorphose des Poypen von *Tripedalia cystophora* (Cubozoa, Carybdeidae) in die Meduse. Helgoländ Meeresun **36**: 257-276

Werner, B., Chapman, D.M. and Cutress, Ch. E. 1976. Muscular and nervous systems of the cubopolyp (Cnidaria). Experientia **32**(8): 1047-1049

Westfall, J.A. 1973. Ultrastructural evidence for neuromuscular systems in coelenterates. Am Zool **13**(2): 237-246

Wietrzykowski, W. 1910. Recherches sur le dévelopment des Lucernaridés. Arch Zool Exp Gen **5**: 10-27

Wietrzykowski, W. 1911. Seconde note sur dévelopment des Lucernaires. Arch Zool Exp Gen **5**(2): 50-51

Wietrzykowsky, W. 1912. Recherches sur le développement des Lucernaires. Arch Zool Exp Gen **5**(10): 1-95

Yuan, D., Nakanishi, N., Jacobs, D.K., and Hartenstein, V. 2008. Embryonic development and metamorphosis of the scyphozoan *Aurelia*. Dev Genes Evol **218**: 525-539

Zagal, C.J. 2004a. Population biology and habitat of the stauromedusa *Haliclystus auricula* in southern Chile. J Mar Biol Ass UK **84**: 331-336

Zagal, C.J. 2004b. Diet of the stauromedusa *Haliclystus auricula* from southern Chile. J Mar Biol Ass UK **84**: 337-340

Zagal, C.J. 2008. Morphological abnormalities in the stauromedusa *Haliclystus auricula* (Cnidaria) and their possible causes. J Mar Biol Ass UK **88**(2): 259–262

Zagal, C.J., Hirano, Y.M., Mills, C.E., Edgar, G.J., and Barrett, N.S. 2011. New records of Staurozoa from Australian coastal waters, with a description of a new species of *Lucernariopsis* Uchida, 1929 (Cnidaria, Staurozoa, Stauromedusae) and a key to Australian Stauromedusae. Marine Biology Research **7**: 651-666

6.0 Appendix

6.1 Additional behavioural and morphological notes

Many of the behaviours I observed in *H. 'sanjuanensis'* were also observed by Hyman (1940), although her animals appear to be less responsive than mine, perhaps due to poor condition. My observations also largely agree with those of Gwilliam (1960). Previous researchers have invariably reported *H. 'sanjuanensis'* from *Zostera* substrates (Gellerman, 1926; Gwilliam, 1956), but I found them on a much greater variety of algae even on San Juan Island, where those records are from. *Zostera* was not present in the Chinese Cemetery habitat where I collected *H. 'sanjuanensis'*. Although *Phyllospadix* fulfills a similar ecological role to *Zostera*, *H. 'sanjuanensis'* were much more common on other algal substrates.

It is unclear how contraction of the tentacles results in a circling motion. They appear to possess only longitudinal musculature and yet may bend at any point along the shaft before whipping in a circle (Fig. 29A). The circling motion may be produced by differential or sequential contraction of longitudinal filaments around the shaft of the tentacle (Fig. 13C). Although the ensheathing longitudinal musculature of the hollow tentacles has been recorded for many staurozoans (e.g. Clark, 1863a), few observations have been made on their movements save for their use in prey capture and locomotion. Undulation of the tentacles as described by Clark (1878) was never observed.

The tentacles appear to be able to distinguish between metal and glass probes and a potential food source. This indicates that chemosensation plays a role in responding to mechanical stimuli. *H. 'sanjuanensis'* also appear to be capable of distinguishing between different types of animal matter: *Idotea* and protists were not recognized as food items (Fig. 29B), whereas various amphipods, zoea, copepods, nauplii, nematodes and human fingers elicited feeding responses, even when they were much too large to ingest and caused harm to the animal. *Idotea* may be chemically camouflaged with respect to *H. 'sanjuanensis'*, and lack chemical cues that trigger the feeding response.

M. handi may be behaviourally as well as visually camouflaged. Although violent jostling initiates the protective response, the animal relaxes quickly when stimulation ceases. Gentle jostling causes complete relaxation of the stalk, which allows passive, seaweed-like movement.

6.2 Description of *Manania handi*

My observations of *Haliclystus 'sanjuanensis'* and *Manania handi* generally agree with those that have been noted previously.

The length of the stalk in *M. handi* has been variably described as shorter, longer or as long as the calyx (Larson and Fautin, 1989; Gwilliam, 1956). Although I found that stalk length of *M. handi* was generally equal to the length of the calyx, the stalk was proportionally longer in smaller animals, an observation also made by Uchida and Hanaoka (1933), Naumov (1961) and Berrill (1962) for other species of *Manania*. Berrill (1962) concluded that the stalk and calyx have differential growth rates during ontogeny, as the stalk and calyx are of equal length in adults. Gwilliam (1956) stated that the stalk was sharply differentiated from the calyx in *M. handi*, while Larson and Fautin (1989) indicate that there is no sharp differentiation. I found that in small animals the stalk was not sharply differentiated from the calyx, whereas in mature animals they were more clearly differentiated.

Gwilliam (1956) indicates that the outermost 3-6 secondary tentacles of each bunch have adhesive pads, while the primary tentacles are smaller and similar in morphology to the outer secondary tentacles. I found that the tentacles in the abaxial row of secondary tentacles developed adhesive pads, which occurred in variable odd numbers according to the size of the animal, the central pad being smaller than subsequent flanking pairs (Fig. 11B). The smallest animal had a single central pad, while the largest had five per arm. The primary tentacles were smaller and bent towards the calyx while the secondary tentacles stand upright, but they are otherwise similar.

6.3 Age-specific substrate selection in *H. 'sanjuanensis'*

Other authors have noted as I did that juvenile staurozoans tend to be present only on filamentous algae (Wietrzykowsky, 1912; Zagal, 2004a). Wietrzykowsky (1912) hypothesized that this was due to a 'net effect' of the filamentous algae: the sticky eggs are much more likely to adhere to the filamentous algae than other alga due to the increased surface area and density of the filaments. He tested this hypothesis by allowing spawned eggs to be carried past *Zostera* blades and filamentous red algae by a gentle

current, and found that eggs adhered to the filamentous algae but not the *Zostera*. Most eggs were retained by neither alga and sank to the substrate. Despite extensive searching, I did not find microhydrulid stages on algal substrates. We expect to find microhydrula on the same substrates as the youngest polyp stages, as the planulae have limited mobility and are immobile after settlement. The microhydrulid stages of other species have been found in diatomaceous mats or algal films on various substrates (Bouillon and Deroux, 1967), or incorporated into sediments (Jarms and Tiemann, 1966; Spoon and Blanquet, 1978), but it is unknown which species these represented and whether the juveniles of these species are found on the same substrates. Where the settled planulae are and, if they do not occur on the same substrates as the juveniles, how the juveniles end up on the filamentous algae, is a puzzle that yet needs to be solved.

6.4 Dispersal

Many staurozoan populations undergo seasonal fluctuation in abundance, and may have a yearly population cycle (Corbin, 1979). Many species are most abundant in the spring and summer, and may disappear entirely over the winter (Berrill, 1962; Corbin, 1979; Zagal, 2004a; Miranda *et al.*, 2012). This has led some to infer that staurozoans overwinter in a resting or encysted stage (Otto, 1976, 1978; Zagal, 2004a). Gwilliam (1956) noted that the *Zostera* beds where *Haliclystus* were found in his study area were largely destroyed every winter by storms, yet staurozoans were present again in the spring when the *Zostera* re-established. He hypothesized that there is a permanent subtidal population that supplies the intertidal bed with planulae. However, he does not propose a mechanism for migration of the non-ciliated creeping planulae between habitats.

Hydrothermal vent staurozoans have been found at several locations along the East Pacific Rise (Lutz *et al.*, 2006). Although these populations are morphologically and genetically similar, it is not clear whether they are conspecific (Lutz *et al.*, 2006). If they are conspecific, how do these widely separated populations maintain gene flow given their apparent limited dispersive potential? Even if they are not conspecific, individual hydrothermal vents are short-lived, lasting several decades at most (Grassle, 1985) and periodic colonization of new vents is necessary. Rapid colonization of new habitats from

source populations is important for the success of hydrothermal vent communities (Tunnicliffe *et al.*, 1997).

Evidence thus suggests that staurozoans have greater dispersive potential than is currently known and may have an inconspicuous resting stage which allows apparent seasonal disappearance and reestablishment of populations. Our lack of developmental knowledge is a great disadvantage in solving these problems.

There is evidence that some staurozoan life cycles include a resting stage; researchers who have investigated staurozoan development have usually failed to achieve development past the settled planula or 'microhydrula' stage (Kowalevsky, 1884; Hanaoka, 1934; Otto, 1976, 1978). However, some cultures of microhydrula have persisted in culture for months to decades without further development (Otto, 1976, 1978; Jarms and Tiemann, 1966; Spoon and Blanquet, 1978; Bouillon and Deroux, 1967; see Miranda *et al.*, 2010), indicating that some specific cue is needed to initiate further development, and that the animals may stall development and reproduce asexually indefinitely (Jarms and Tiemann, 1966; Spoon and Blanquet, 1978; Bouillon and Deroux, 1967) until the appropriate cue is received. The microhydrula stage has also been found year-round in the wild (Bouillon and Deroux, 1967).

Spoon and Blanquet (1978) provide a possible mechanism for increased dispersal of staurozoans: they observed planuliform buds from microhydrula attached to the caudal setae of actively swimming copepods. If this type of "hitchhiking" is common in staurozoans, it may serve to increase their dispersive potential. The only other apparent potential dispersive mechanism is opportunistic transport of adults or larvae on pieces of seaweed carried by currents, which may serve to maintain gene flow between separate populations of a single species or to establish new populations.

6.5 Reproduction and Development

The collapse of the gonadal vesicles following spawning in *H. 'sanjuanensis'* (Fig. 27B) was also noted by Clark (1878) in '*H. auricula*'. He demonstrated that there is a pore in each vesicle near where it connects to the subumbrella through which eggs or sperm are expelled into the gastric cavity (Clark, 1878). Although spawning was observed in *M. handi*, a similar depletion was not noted, perhaps because the gonads of *M. handi* are in the form of folded bands rather than discrete vesicles.

Developmental stages of *H. 'sanjuanensis'* found in the wild (Fig. 9) match descriptions of *H. octoradiatus* development by Wietrzykowsky (1912), except that a two-tentacle stage was never found for *H. 'sanjuanensis'*; the smallest polyps had four equally developed bumps representing the beginnings of the first four primary tentacles. This may represent a difference in development between species, as many cnidarian polyps have an initial two tentacles (Salvini-Plawen, 1978), or development may vary according to environmental conditions. The fact that many polyps begin with an initial two tentacles is one of the lines of evidence used to infer that cnidarians are descended from bilateral ancestors (Marques and Collins, 2004).